Appendix F
3D Model Predictions of the Worst-Case Response of the Mowi Canada East - Northern Harvest Smolt Ltd. Freshwater Aquifer to Long Term Withdrawals, Stephenville, NL

Fracflow Consultants Inc.
Environmental, Hydrogeological and
Geotechnical Engineering Consultants

MOWI®

3D Model Predictions of the Worst-Case Response of the Mowi Canada East – Northern Harvest Smolt Ltd. Freshwater Aquifer to Long Term Withdrawals, Stephenville, NL

(FFC File 3113)

Prepared by:

Fracflow Consultants Inc.
154 Majors Path
St. John's, NL
A1A 5A1

LICENSED PROFESSIONAL GEOSCIENTIST
08452
EUNJEONG SEOK
SIGNATURE
27. Mar 2023
DATE
NEWFOUNDLAND & LABRADOR

Submitted to:

Mowi Canada East Inc.
P.O. Box 430
St. Alban's, NL
A0H 2E0

PROVINCE OF NEWFOUNDLAND
PERMIT HOLDER
CLASS "A"
This Permit Allows
FRACFLOW CONSULTANTS INC.
To practice Professional Engineering
in Newfoundland and Labrador.
Permit No. as issued by APEGN D0169
which is valid for the year 2023.

March 27, 2023

REGISTERED PROFESSIONAL ENGINEER
JOHN E. GALE
SIGNATURE
27 Mar. 2023
DATE
PROVINCE OF NEWFOUNDLAND

Executive Summary

Fracflow Consultants Inc. (Fracflow) conducted an initial hydrogeological assessment of the area adjacent to the Port of Stephenville (Port Harmon) to determine the potential for developing a water supply for a proposed fish hatchery in 2009 (Northern Harvest Sea Farms (NHSF) – now Mowi Canada East Inc. (MOWI)) - which was subsequently constructed. NHSF started operating the water supply well field for its fish hatchery in Stephenville in 2011 with three production wells. One more production well was added to the original well field and placed into production in 2019. In order to accommodate an increase in water demand and to provide a backup water supply, a new water supply well field with three new production wells was constructed and connected to the fish hatchery in 2021. These production wells in two well fields have been operating since 2011, the original well field, and since 2021 for both well fields at combined flowrates that ranged from approximately70,000 m^3/month from the original well field at the early stage of the hatchery operation to 300,000 m^3/month after adding the new well field.

The Department of Environment and Climate Change (DECC) required that a worst-case scenario (WCS) or a worst case aquifer response be analyzed to determine the aquifer response over the long-term to ensure that the aquifer is not dewatered or the water quality is not degraded because of the water production at the MOWI hatchery site in Stephenville and climate change impacts. DECC also requested that the 3D model be compared to field measurements after an additional five years (in 2026) to determine how well the 3D model predicted the response of the aquifer to the actual well field withdrawal rates and to predict future aquifer response to the expected well field groundwater withdrawal rates. Since those model simulations will provide a range of computed responses (similar to a limited probability assessment) for the proposed future climatic conditions and groundwater withdrawals, Fracflow proposed that if the measured aquifer drawdowns in 2026 fall within the range predicted by the model for the 2026 time period, there would be no need to rerun the 3D model at that time since this agreement would confirm that the model predictions are a reasonable prediction of future aquifer response to pumping.

For the prediction model, to be conservative to the aquifer dewatering issue, a sustained period of 10 years or more of no precipitation would be the worst case scenario that would result in depleting a large volume of the aquifer and lowering the water levels significantly. However, that is neither an acceptable nor realistic scenario in the real world. Instead, Fracflow proposed an alternate approach, based on the historical annual and monthly precipitation data and the historical temperature data, along with one standard deviation above and one standard deviation below the base numbers, be used as the basic data set for computing and assigning future recharge values to the 3D model along with the withdrawal rates for each production well based on MOWI's expected pattern of water usage throughout each year.

The monthly precipitation data collected at the station *Stephenville A* were used to calculate the monthly recharge values for the project site/model area. Then the historical climate data were used to set up two 25-year precipitation data sets for the prediction models. The first data set was chosen from the years between 1997 and 2021 to reflect the recent precipitation trend and

quantity. The second data set was chosen from 1949 to 1973. The two data sets were used for projecting the yearly total precipitation from 2022 onwards for the next 25-year prediction, 2022 - 2046 for the 3D prediction model. Each of the two data sets was fitted with the second order polynomial trendline to extract a representative precipitation for each year. Then each 25-year precipitation data set was distributed to monthly recharge data for the corresponding years. The withdrawal records of the historical and current production wells were provided by the Client and compiled to determine how water usage for the MOWI hatchery site has changed over time and to estimate the future water usage/demand for the next 25 years.

The 3D finite element model mesh is based on the mesh that was constructed in 2018 as part of the initial assessment that was requested by MAE (now DECC) for the granular aquifer. The original model mesh has been modified to accommodate the update of the well field configuration and the site activities. The previous models for the project site were calibrated under steady-state conditions. Therefore, the existing model was updated by replacing the constant input parameters with time-dependent parameters. The measured recharge rates and water withdrawal rates were distributed to monthly data sets for each corresponding year. Then the new transient model was simulated using the known input parameters and calibrated under a transient condition prior to the prediction model simulations by comparison to the measured hydraulic heads in the monitoring wells.

As part of the 3D numerical model for predicting long term aquifer response and worst case response, the basic transient model simulations were started for the year 2011 when the operation of the first well field started (November 2011). The transient simulations were conducted for the period of January 2011 to December 2021 using the known withdrawal rates from the production wells and known climatic data. The simulations also included new activities at the project site such as installation and operation of the new well field in July 2021 and the new drain system at the new building in October 2019. The prediction model simulations were continued as an extension of the model simulation results as of December 2021.

For the 25-year prediction model, six sub-data sets were generated from the two 25-year data sets that were selected form the historical data. Two main sub-data sets, *Main 1 and Main 2,* used the trend line values from the 25-year period data sets. For the two upper limit sets, *Upper Limit 1 and Upper Limit 2*, the recharge values were increased by one standard deviation of the corresponding data set. With these calculations, the monthly recharge values were increased between 27% and 58%, so these data sets were used to simulate the upper extreme cases. For simulation of the lower extreme cases, two lower limit sets, *Lower Limit 1 and Lower Limit 2,* were created by subtracting one standard deviation from the monthly total precipitation values, which resulted in decreases in the monthly recharge values of between 27% and 58%.

Five drawdown contour maps for *Main 1* show the location of the 2.0 m contour lines around the production wells in 2036 when the highest drawdowns were observed among the five reference years, 2026, 2031, 2036, 2041 and 2046. The 2.0 m drawdown contour lines plot close to or at each production well. The area enclosed by the 2 m contour line increased in 2031 to form a

circular shape around the production wells at the new well field. The area enclosed by the 2 m contour line expanded further in 2036. The drawdown contour maps for the *Main 2* simulations show the 1.2 m contour lines around the production wells in the existing well field and 1.8 m to 2.0 m contour lines in the new well field after five years of withdrawal simulations in 2026. The drawdown cones expanded with time and, in 2046, the drawdown in the two well fields increased to greater than 1.6 m in the existing well field and greater than 2.6 to 2.8 m in the new well field. Comparison of the steady state hydraulic head contour map for non-pumping conditions with the hydraulic head contour maps for the various pumping simulations shows how the hydraulic head contour lines have been shifted up-gradient by the well field operation.

The recovery of the water elevations under the simulations of the *Upper Limit 1* model was readily noticeable on the drawdown contour maps. Compared to the drawdown contour map in December 2021, it was obvious that the capture area as defined by the 0 m contour line in 2026 decreased and was limited to the two well fields and its surrounding areas including the building drainage. The capture area was increased slightly in 2031 but decreased again in 2036. The shrinkage or reduction of the capture area continued until 2046 when the capture areas were limited to the existing well fields and the building drainage. At the new well field, the capture areas are only around the production wells. The capture area of the 0 m contour line for the *Upper Limit 2* model was limited to the area near the two well fields and the building drainage in 2026 and the capture area expanded with time. The drawdown contour map at the end of the current simulation in 2046 was similar to that of the model results in December 2021.

The drawdown contour maps for *Lower Limit 1* do not show the typical circular shape of the drawdown contour lines as shown in the previous models. Instead, the contour lines bend around the two well fields and each of the five production wells. The general drawdown values in 2026 were 1.6 m around the existing well field and 2.8 m around the new well field. The drawdowns increased with time and the drawdowns in 2036 were approximately 2.0 m around the existing well field and 3.6 m around the new well field. With the recovery of the water elevations, the drawdown contours around the two well fields in 2046 were 1.6 m at the existing well field and 3.2 m at the new well field. The monitoring well at the far-field site showed a drawdown of 3.1 m in 2026, 4.0 m in 2036 and 3.5 m in 2046. The drawdown contour maps for *Lower Limit 2* simulations also show contour lines bent around the two well fields. The general drawdowns were approximately 1.6 m around the existing well field and 2.8 m around the new well field in 2026. The drawdowns increased with time and dropped to about 2.4 m around the existing well field and 4.4 m around the new well field in 2046. The drawdown in a well at the far-field site was approximately 3.4 m in 2026 and 5.4 m in 2046.

The water elevations were highly correlated with the recharge rate to the aquifer system in the model area. Based on the simulations using the two 25-year precipitation/recharge data sets, the drawdown increased when the recharge values were decreased and the drawdown decreased or the capture area shrunk when the recharge increased. This observation was more obvious for the data set with continuous reduction in recharge. With no recovery to the aquifer system, the depletion of the aquifer continued throughout the 25-year simulation period. However, when the

recharge increased after a period of decrease, the two well fields responded to the increasing recharges, so the water elevations recovered and the capture area decreased.

The decreased water elevations (drawdowns) for the current simulations were attributed not only to the pumping of the production wells but also to the reduced recharge values. With the recharge and withdrawal rates changing at the same time, it is difficult to identify which was the controlling factor for the drawdown in the aquifer system. When the withdrawal rates are the main factor in the change of the water elevations and the recharge rates oscillate around their average values with time, the drawdown contours form circular shapes. However, when the water elevation changes are mainly due to the changes in recharge rates over the area, the drawdown contours do not form closed circular shapes. The impact of the withdrawal rates in those models was shown as bent contour lines around the production wells. Bigger drawdowns in the far-field area than those in the well fields indicate that the drawdowns in the far-field were largely affected by the differences in the overall recharge values in different areas.

The model simulations, utilizing the various estimates of precipitation rates and well field withdrawal rates, do not show excessive drawdowns in the aquifer that could be described as aquifer dewatering. Also, the model shows that the water levels in the aquifer will recover if several years of low precipitation are followed by several years of higher precipitation that corresponds to increased recharge.

The model simulations predict a range of computed responses (essentially a limited probability assessment) for the proposed/predicted future climatic conditions and expected groundwater withdrawals. Therefore, Fracflow proposes that if the measured aquifer drawdowns in 2026 fall within the range predicted by the six prediction models for the 2026 time period, then there would be no need to conduct additional 3D model simulations at that time since this would confirm that the model predictions area a reasonable prediction of the future aquifer responses to pumping/production of the two well fields. For the purposes of comparing measured and computed changes in water levels and determining if the 2026 model simulations match the measured drawdowns, Fracflow proposes that this comparison be based on the two nested deep piezometers in each well field and the two adjacent shallow piezometers for each well field – five reference points for each well field with the comparison being based on the average precipitation data for both 2025 and 2026 and the recorded withdrawal rates for that two year period that most closely match the precipitation and climate data that were used for the relevant model input data.

Table of Contents

List of Figures

List of Tables

List of Appendices

1.0 INTRODUCTION

1.1 Background

Fracflow Consultants Inc. (Fracflow) conducted an initial hydrogeological assessment of the area adjacent to the Port of Stephenville (Port Harmon) to determine the potential for developing a water supply for a proposed fish hatchery in 2009 (Northern Harvest Sea Farms (NHSF) – now Mowi Canada East Inc. (MOWI)) which was subsequently constructed. NHSF started operating the water supply well field for its fish hatchery in Stephenville in 2011 with three production wells. One more production well was added to the existing well field and initiated its production in 2019. In order to meet an increasing water demand, a new water supply well field with three new production wells was constructed approximately 1 km north of the original well field and its water supply to the fish hatchery was commissioned with all three production wells in 2021. These production wells from two well fields have been operating since 2011 at combined flowrates that range from approximately70,000 m^3/month at the early stage of the operation to 300,000 m^3/month after adding the new well field.

The Department of Environment and Climate Change (DECC) required that a worst-case scenario (WCS) be analyzed to determine the aquifer response over the long-term to ensure that the aquifer is not dewatered or the water quality is not degraded because of the water production at the MOWI hatchery site in Stephenville and climate change impacts. DECC also requested that the 3D model be calibrated or the simulations be repeated after an additional five years (in 2026) to determine how well the 3D model predicted the response of the aquifer to the actual well field withdrawal rates and to predict future aquifer response to the expected well field groundwater withdrawal rates. Since the current model simulations provide a range of computed responses (a limited type of probability assessment) for the proposed future climatic conditions and groundwater withdrawals, Fracflow proposes that if the measured aquifer drawdowns in 2026 fall within the range predicted by the model for the 2026 time period, there would be no need to rerun the 3D model at that time since this agreement between measured and predicted aquifer response would confirm that the model predictions are a reasonable prediction of future aquifer response to pumping. For the purposes of comparing measured and computed changes in water levels and determining if the 2026 model simulations match the measured drawdowns, Fracflow proposes that this comparison be based on the two nested deep piezometers in each well field and the two adjacent shallow piezometers for each well field – five reference points for each well field.

There are five main factors that impact the long-term aquifer performance and water quality; (1) annual and seasonal changes in precipitation, (2) changes in recharge, (3) changes in withdrawal rates by MOWI, (4) new withdrawals by other parties, and (5) release of contaminants that sterilize or strand part of the aquifer water supply. Withdrawal by other parties can be controlled by DECC and the Town of Stephenville and will not be addressed in this analysis. Release of contaminants such as a truck-load of fuel can be addressed by an immediate remedial response by the polluter since the depth to the water table is between 16 and 20 m

below ground surface (bgs). Therefore, the major impacts on the long-term aquifer response that were considered in this WCS analysis are the climatic change impacts on precipitation and recharge along with changes in the withdrawal rates.

For the prediction model, to be conservative to the aquifer dewatering issue, a sustained period of 10 years or more of no precipitation would be the worst case scenario that would result in depleting a large volume of the aquifer and lowering the water levels significantly. However, that is neither an acceptable nor realistic scenario in the real world. Instead, Fracflow proposed an alternate approach, based on the historical annual and monthly precipitation data and the historical temperature data, be used as the basic data set for computing and assigning future recharge values to the 3D model along with the withdrawal rates for each production well based on the MOWI's expected pattern of water usage throughout each year.

1.2 Objectives and Scope of Work

For the WCS model, a 3D transient numerical model was simulated in two steps:

1) The first step was to update and calibrate the existing 3D steady-state model to a 3D transient model. The starting point of the updated 3D transient model was the January month of the year in which the operation of the existing/old well field started (November 2011). Then the simulation continued until December 31, 2021 using the historical climatic data and the known/measured withdrawal rates including the installation and operation of the new well field and the drain system at the new building site.
2) The second step was to prepare the input parameters and to run the prediction models for the 25-year period starting in 2022 (January 2022 – December 2046). The input parameters for the prediction models were estimated using the historical climate data and the anticipated/predicted withdrawal rates for each production well by MOWI. The prediction model simulations were continued or extended by using the simulation results produced by the C*urrent Model* as of December 31, 2021.

The model results are recorded and presented as five-year water elevation contour maps and drawdown contour maps for December 31 in 2026, 2031, 2036, 2041, and 2046. However, all of the monthly and annual aquifer response data plots are available for review.

In addition, one transient contaminant transport simulation was completed using particle tracking in order to assess if any known or assumed source of contaminants at the surrounding area would travel to the well fields and to the production wells.

2.0 CLIMATE AND HYDROGEOLOGY

2.1 Precipitation Data - Historical

The historical climatic data for the model area were downloaded from the *Stephenville A* station at the Environment and Climate Change Canada (ECCC) website (ECCC, 2022). The climatic data are available in hourly, daily and monthly formats between 1942 and 2022 (current). The monthly data sets were mainly used for analyzing the overall trend of the yearly precipitation over the project area. However, only the hourly and daily data are available from ECCC, not the monthly data, for the recent years from September 2014 to current time. Therefore, the daily precipitation data were used to calculate the total precipitation for each corresponding month. Then the monthly total precipitations between November 1941 and June 2022 were used to calculate the yearly total precipitations that were used to derive the yearly precipitation trend for those years.

According to the ECCC data set, the monthly data are flagged as 'M' when there are any missing daily data for the corresponding month. If the same rule is applied in calculating the monthly and yearly total precipitations, that is flagging as 'M' with any missing data points within the corresponding days for monthly data or corresponding months for yearly data, the total number of yearly data points available for trend analyzing was 65 out of 80 from 1942 to 2021. The 1941 and 2022 data were not included in the data set because all 12 months of the data were not available for those years. The available data using this calculation method are plotted in **Figure 2.1a** showing no data points after 2014 due to missing data. The other data gaps are shown as disconnected data lines. This could result in misinterpretation of the overall precipitation trend especially for the recent years. To overcome this issue, it was to allow a few missing data points in the monthly precipitation data set.

To find a reasonable number of allowable missing data points, options of one to five point(s) were applied in the calculation and three allowable missing points/days in a month were chosen to maximize the available monthly data points with minimum impact on the data trend. Therefore, any monthly data with more than three daily missing data points were flagged as 'M'. For each yearly total precipitation, a year with any missing monthly data points were flagged as 'M' and excluded from the yearly total precipitation data set. This provided 76 years of data points as shown in **Figure 2.1b** in comparison to the data set in **Figure 2.1a**. The latter data set was chosen for analyzing the trend of the yearly total precipitation.

The total yearly precipitation data between 1942 and 2021 that satisfied the calculation criteria mentioned above are presented in **Table 2.1** and **Figure 2.2** with its second order polynomial trendline. Based on the data set and its trendline, the yearly total precipitation shows increasing trend from 838 to 1,661 mm between 1943 and 1982 with annual variations, and then levelling off between approximately 1,176 and 1,632 mm for the next 11 years until 1993. Then the precipitation decreased to 1,017 mm/year in 2010 and then annual trend changed its direction again and increased to 1,624 mm/year in 2021.

2.2 **Withdrawal Rates - Historical**

The other main variable in the 3D prediction model was the withdrawal rates from the aquifer that were controlled by the water demand from the MOWI fish hatchery in Stephenville. The first well field of the MOWI hatchery started its operation in 2011 and the second well field was added to the production line in 2021. **Figure 2.3** shows the locations of the two MOWI hatchery well fields with the production and monitoring wells. The withdrawal records of the historical and current production wells were provided by the Client and compiled to determine how water usage for the MOWI hatchery site changed over time and to estimate the future water usage/demand for the next 25 years. The compiled data between 2011 and 2021 were organized by monthly data for each individual production well and are presented in **Table 2.2** and **Figure 2.4**. The combined monthly withdrawals from the well fields are plotted in **Figure 2.5**.

The first well field started its operation in 2011 with three production wells, HW1, HW2 and PW1. Most of the water was supplied by the two main production wells, HW1 and HW2 and the third production well, PW1, was operated only when extra water was required due to its smaller size (150 mm diameter) and production capacity. The location map of the production wells at the MOWI site is provided in **Figure 2.3**. Based on the water usage records starting November 2011, the two original production wells were pumped alternately until April 2018 with 1 to 17 months of continuous pumping period at one time. The average combined monthly withdrawal from the three production wells between 2011 and 2018 was approximately 77,000 m^3; 37,000 m^3 each from HW1 and HW2, and 2,600 m^3 from PW1. In April 2018, both main production wells, HW1 and HW2, were in production simultaneously with the combined monthly withdrawal increasing to 106,000 m^3 in April 2018, followed by additional increases in the combined withdrawal to approximately 133,000 m^3 (61,000 m^3 each from HW1 and HW2 and 11,000 m^3 from PW1) until a new production well, HW3, was added to the first well field in December 2019. PW1 was disconnected from the supply line at the same time. After HW3 was brought on-line, the combined monthly withdrawal was increased to 167,000 m^3; 47,000 m^3 each from HW1 and HW2, and 73,000 m^3 from HW3.

The second/new well field started operation in July 2021 with three production wells. MHPW2 and MHPW4 were added to the production line in July 2021 and MHPW1 in August 2021. The average monthly withdrawal between July and December 2021 was 43,000 m^3 for MHPW1 and 42,000 m^3 for each of MHPW2 and MHPW3. After the second well field was brought on-line, the combined monthly withdrawal from both well fields increased by up to 28,000 m^3 in December 2021 with the average monthly withdrawal being 220,000 m^3 (**Figure 2.5**).

As of December 2021, among the six production wells that were connected to the water production line at the MOWI hatchery site, five wells, HW1 and HW3 from the first well field, and MHPW1, MHPW2 and MHPW4 from the second well field, were running as production wells. One remaining production well, HW2, was reserved as a back-up well in case of an emergency.

2.3 Hydraulic Head Data

As part of the annual groundwater sampling event, the LTC (Level, Temperature and Conductivity) logger units were installed in the monitoring wells for both well fields in June 2019. The data in the logger units were downloaded at least twice a year during the groundwater sampling events and the data between June 2019 and December 2021 are plotted in **Figure 2.6** for the wells (near-field) on or near the two well fields and **Figure 2.7** for the wells (far-field) off/away from the well fields.

In addition to monitoring the water levels using the logger units, continuous groundwater monitoring systems were installed and operated by DECC in three monitoring wells, MW6, FMW10 and FMW12, starting November 2019. The well data for the three monitoring wells were obtained from DECC and plotted in **Figure 2.8** as provided.

Table 2.1 Historical yearly total precipitation from 1942 to 2021 at the *Stephenville A* climate station (ECCC, 2022).

Year	Yearly Total Precipitation (mm/year)	Year	Yearly Total Precipitation (mm/year)	Year	Yearly Total Precipitation (mm/year)	Year	Yearly Total Precipitation (mm/year)
1942	N/A	1962	1219	1982	1661	2002	1417
1943	838	1963	1039	1983	1483	2003	1131
1944	1122	1964	1097	1984	1352	2004	1281
1945	977	1965	1122	1985	1248	2005	1154
1946	N/A	1966	N/A	1986	1203	2006	1288
1947	1119	1967	1204	1987	1250	2007	1369
1948	N/A	1968	1301	1988	1308	2008	1187
1949	1091	1969	1115	1989	1588	2009	1351
1950	915	1970	1196	1990	1632	2010	1017
1951	1015	1971	1203	1991	1288	2011	1173
1952	992	1972	1237	1992	1176	2012	1176
1953	1061	1973	1362	1993	1624	2013	1590
1954	996	1974	1207	1994	1573	2014	1252
1955	1095	1975	1227	1995	1412	2015	1314
1956	979	1976	1144	1996	1232	2016	1347
1957	1145	1977	1358	1997	1350	2017	1286
1958	1246	1978	1263	1998	1371	2018	1576
1959	1247	1979	1504	1999	1383	2019	1480
1960	871	1980	1366	2000	1474	2020	1148
1961	1264	1981	1252	2001	1127	2021	1624

* N/A: data not available due to missing monthly data.

Table 2.2 Monthly withdrawal rates from the historical and current production wells at the MOWI hatchery site in Stephenville (page 1 of 3).

Year	Month	1st Well Field (m^3)					2nd Well Field (m^3)				Total (m^3)
		HW1	HW2	HW3	PW1	Sub-total	MHPW 1	MHPW 2	MHPW 4	Sub-total	
2011	11	13,093	0		0	13,093					13,093
	12	68,045	0		0	68,045					68,045
2012	01	69,097	0		0	69,097					69,097
	02	63,188	0		0	63,188					63,188
	03	57,552	0		0	57,552					57,552
	04	22,003	0		0	22,003					22,003
	05	44,496	0		0	44,496					44,496
	06	52,864	0		11,224	64,087					64,087
	07	50,623	8,858		13,290	72,771					72,771
	08	0	63,886		14,761	78,647					78,647
	09	0	64,556		15,841	80,397					80,397
	10	0	73,687		17,509	91,195					91,195
	11	0	74,466		14,598	89,064					89,064
	12	0	82,310		8,182	90,492					90,492
2013	01	48,247	27,598		0	75,845					75,845
	02	76,287	0		0	76,287					76,287
	03	76,663	0		0	76,663					76,663
	04	65,848	0		0	65,848					65,848
	05	78,969	0		1,357	80,326					80,326
	06	74,902	0		13,896	88,798					88,798
	07	76,412	0		0	76,412					76,412
	08	90,977	0		0	90,977					90,977
	09	78,587	0		0	78,587					78,587
	10	81,280	0		0	81,280					81,280
	11	78,598	0		0	78,598					78,598
	12	80,255	0		0	80,255					80,255
2014	01	79,775	0		11,545	91,320					91,320
	02	71,860	0		10,297	82,157					82,157
	03	81,830	0		1,968	83,798					83,798
	04	80,293	0		0	80,293					80,293
	05	83,542	0		0	83,542					83,542
	06	67,794	26,748		4,263	98,805					98,805
	07	0	84,005		6,765	90,770					90,770
	08	8,607	83,842		1,041	93,490					93,490
	09	12,434	68,961		0	81,394					81,394
	10	84,087	0		0	84,087					84,087
	11	84,392	0		0	84,392					84,392
	12	84,272	0		0	84,272					84,272
2015	01	84,321	0		0	84,321					84,321
	02	72,356	0		3,549	75,905					75,905
	03	84,251	0		0	84,251					84,251
	04	81,394	0		0	81,394					81,394
	05	65,428	0		0	65,428					65,428
	06	0	77,126		0	77,126					77,126
	07	0	74,564		0	74,564					74,564
	08	0	81,950		0	81,950					81,950
	09	37,301	32,172		142	69,615					69,615
	10	44,208	35,720		0	79,928					79,928
	11	0	75,682		0	75,682					75,682
	12	0	77,262		0	77,262					77,262

Table 2.2 Monthly withdrawal rates from the historical and current production wells at the MOWI hatchery site in Stephenville (page 2 of 3).

Year	Month	1st Well Field (m^3)					2nd Well Field (m^3)				Total (m^3)
		HW1	HW2	HW3	PW1	Sub-total	MHPW 1	MHPW 2	MHPW 4	Sub-total	
2016	01	0	78,009		0	78,009					78,009
	02	0	74,739		0	74,739					74,739
	03	0	81,552		0	81,552					81,552
	04	0	74,052		0	74,052					74,052
	05	0	71,969		0	71,969					71,969
	06	0	68,050		3,347	71,397					71,397
	07	0	53,801		16,484	70,285					70,285
	08	3,140	59,230		7,473	69,844					69,844
	09	839	72,972		4,884	78,696					78,696
	10	0	73,234		6,710	79,944					79,944
	11	0	72,160		6,639	78,800					78,800
	12	6,536	71,795		2,954	81,285					81,285
2017	01	1,101	74,302		0	75,404					75,404
	02	0	71,631		0	71,631					71,631
	03	0	79,748		0	79,748					79,748
	04	0	78,276		0	78,276					78,276
	05	0	76,069		0	76,069					76,069
	06	0	78,587		0	78,587					78,587
	07	4,328	66,464		0	70,792					70,792
	08	6,743	61,198		0	67,941					67,941
	09	6,514	63,635		0	70,149					70,149
	10	0	77,622		0	77,622					77,622
	11	75,251	13,191		698	89,140					89,140
	12	82,528	0		0	82,528					82,528
2018	01	14,527	67,183		0	81,710					81,710
	02	72,858	0		0	72,858					72,858
	03	10,842	73,774		0	84,616					84,616
	04	28,345	71,081		6,519	105,945					105,945
	05	40,539	56,892		14,756	112,187					112,187
	06	41,864	52,215		11,044	105,122					105,122
	07	55,338	51,506		0	106,845					106,845
	08	68,775	64,545		1,668	134,988					134,988
	09	52,766	50,536		0	103,302					103,302
	10	51,697	47,620		4,099	103,416					103,416
	11	70,318	69,745		7,822	147,885					147,885
	12	72,220	71,130		15,508	158,858					158,858
2019	01	65,543	69,745		13,524	148,812					148,812
	02	57,808	58,838		15,579	132,225					132,225
	03	68,933	68,230		17,498	154,661					154,661
	04	61,106	58,991		16,097	136,193					136,193
	05	62,261	66,055		18,561	146,877					146,877
	06	64,502	64,823		18,032	147,357					147,357
	07	50,378	49,375		6,999	106,752					106,752
	08	66,213	64,932		9,588	140,734					140,734
	09	67,690	67,478		17,727	152,895					152,895
	10	71,604	70,699		15,988	158,291					158,291
	11	70,917	70,590		6,955	148,463					148,463
	12	45,799	60,980	55,028	0	161,807					161,807

Table 2.2 Monthly withdrawal rates from the historical and current production wells at the MOWI hatchery site in Stephenville (page 3 of 3).

Year	Month	1st Well Field (m^3)					2nd Well Field (m^3)				Total (m^3)
		HW1	HW2	HW3	PW1	Sub-total	MHPW 1	MHPW 2	MHPW 4	Sub-total	
2020	01	54,712	55,300	80,838	0	190,850					190,850
	02	58,091	57,165	75,404	0	190,659					190,659
	03	59,928	59,612	78,800	0	198,340					198,340
	04	48,089	48,607	73,654	0	170,349					170,349
	05	56,838	56,985	77,235	0	191,057					191,057
	06	44,164	45,625	69,364	0	159,153					159,153
	07	25,772	39,460	76,990	0	142,222					142,222
	08	27,696	43,297	72,580	0	143,574					143,574
	09	38,059	12,292	65,281	0	115,632					115,632
	10	46,819	29,283	69,140	0	145,242					145,242
	11	41,302	37,846	66,382	0	145,531					145,531
	12	54,875	51,114	72,700	0	178,689					178,689
2021	01	56,211	51,997	74,591	0	182,799					182,799
	02	50,400	42,910	60,653	0	153,963					153,963
	03	50,144	42,163	72,956	0	165,263					165,263
	04	35,055	44,725	79,252	0	159,033					159,033
	05	53,120	52,406	83,847	0	189,373					189,373
	06	51,681	52,640	85,281	0	189,602					189,602
	07	37,797	25,674	66,796	0	130,268	0	16,353	16,353	32,706	162,974
	08	34,047	0	51,615	0	85,662	27,359	45,848	47,217	120,423	206,086
	09	40,561	0	55,284	0	95,845	40,392	39,629	40,817	120,838	216,682
	10	38,975	0	48,187	0	87,161	40,942	40,937	41,689	123,569	210,730
	11	46,606	0	56,581	0	103,187	47,696	47,696	47,696	143,089	246,276
	12	44,262	0	57,508	0	101,770	59,906	59,443	58,822	178,171	279,941

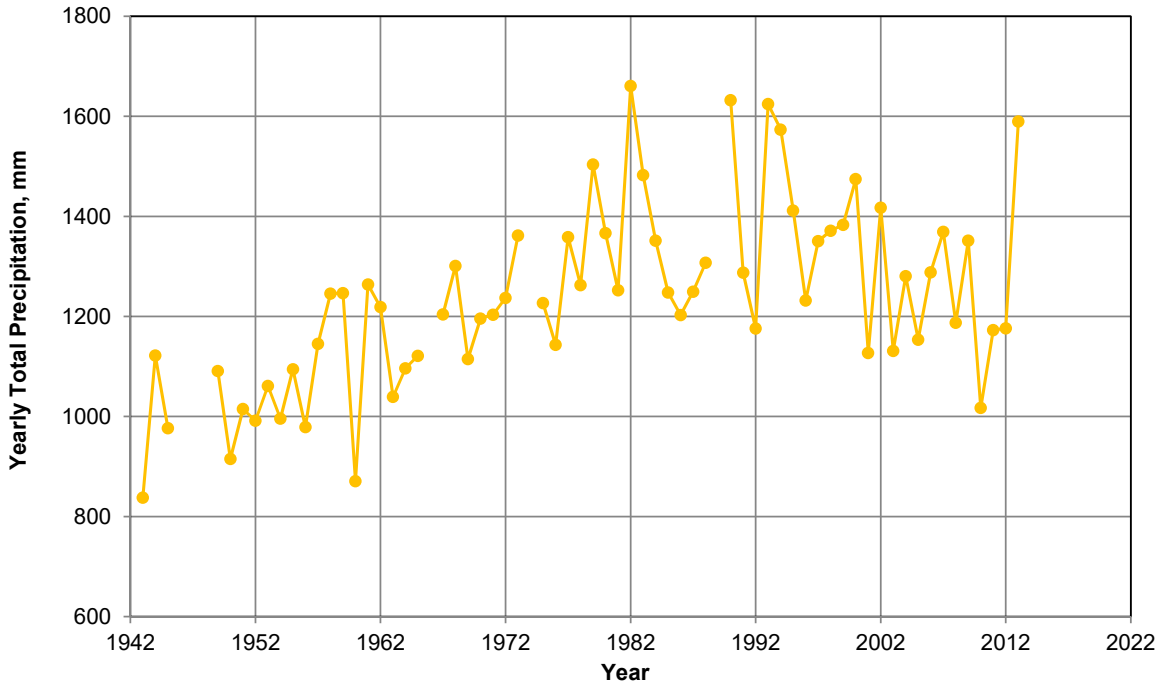

Figure 2.1a Yearly total precipitation excluding any missing data points from 1942 to 2021 at the *Stephenville A* climate station (ECCC, 2022).

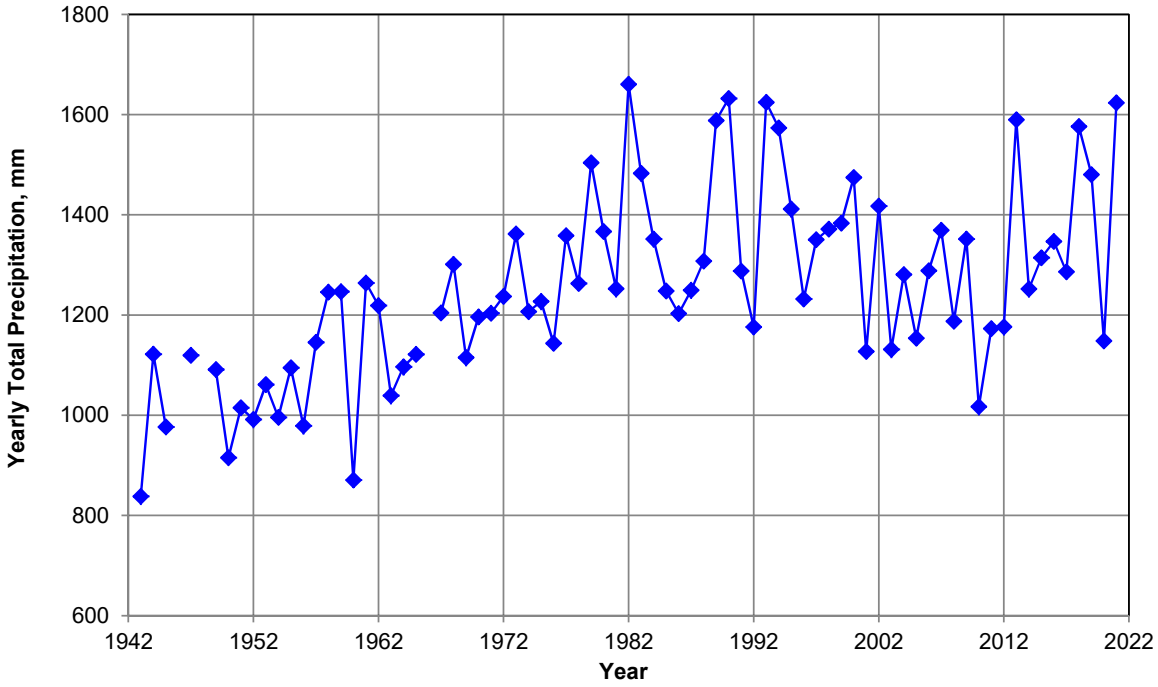

Figure 2.1b Yearly total precipitation allowing up to three daily missing data points from 1942 to 2021 at the *Stephenville A* climate station (ECCC, 2022).

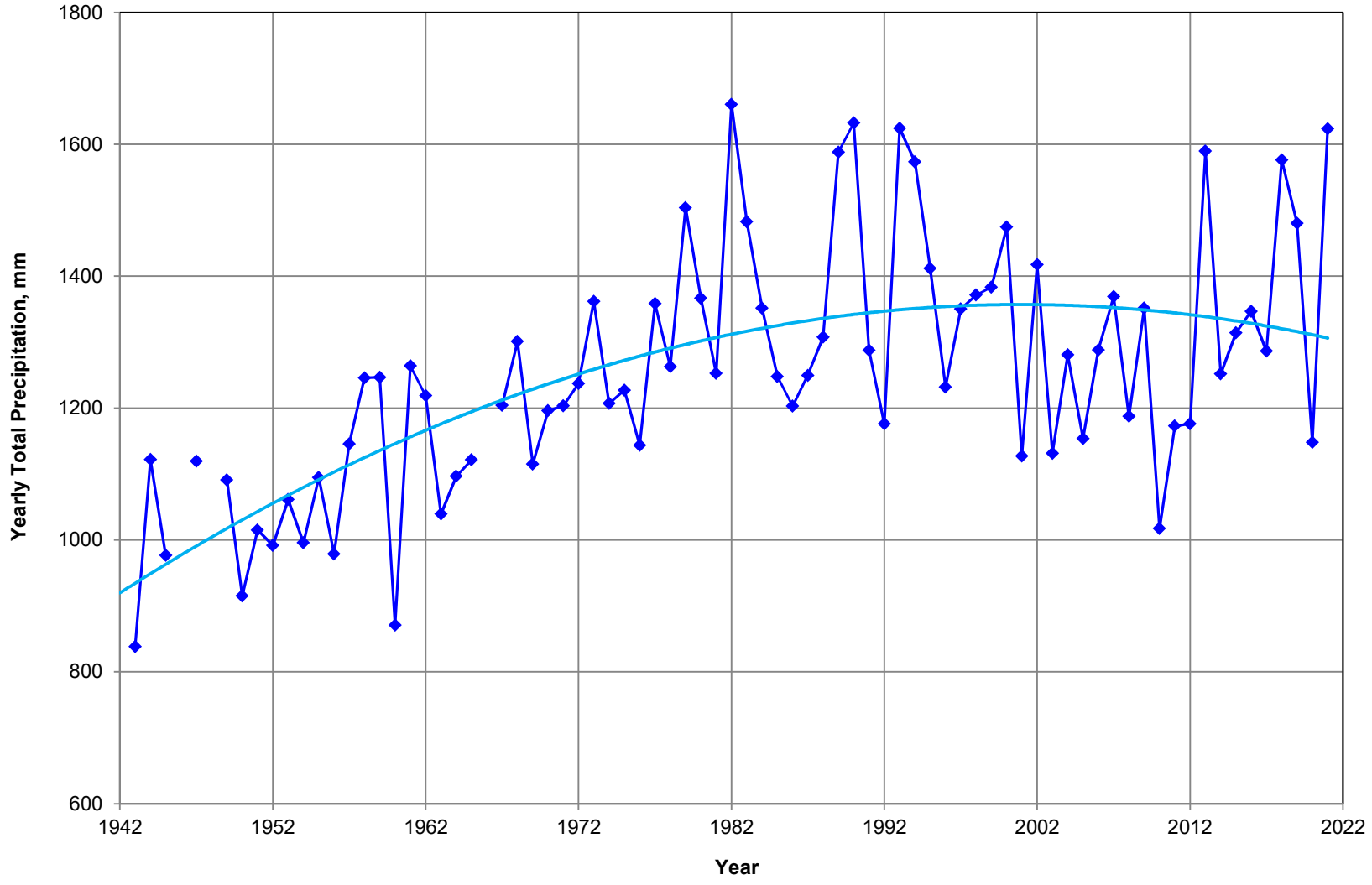

Figure 2.2 Yearly total precipitation data set and its trendline from 1942 to 2021 at the *Stephenville A* climate station (ECCC, 2022).

Project No.	Document Reference
3113	FFC-NL-3113-057b
Location	Date
Stephenville, NL	December 2022

FFC

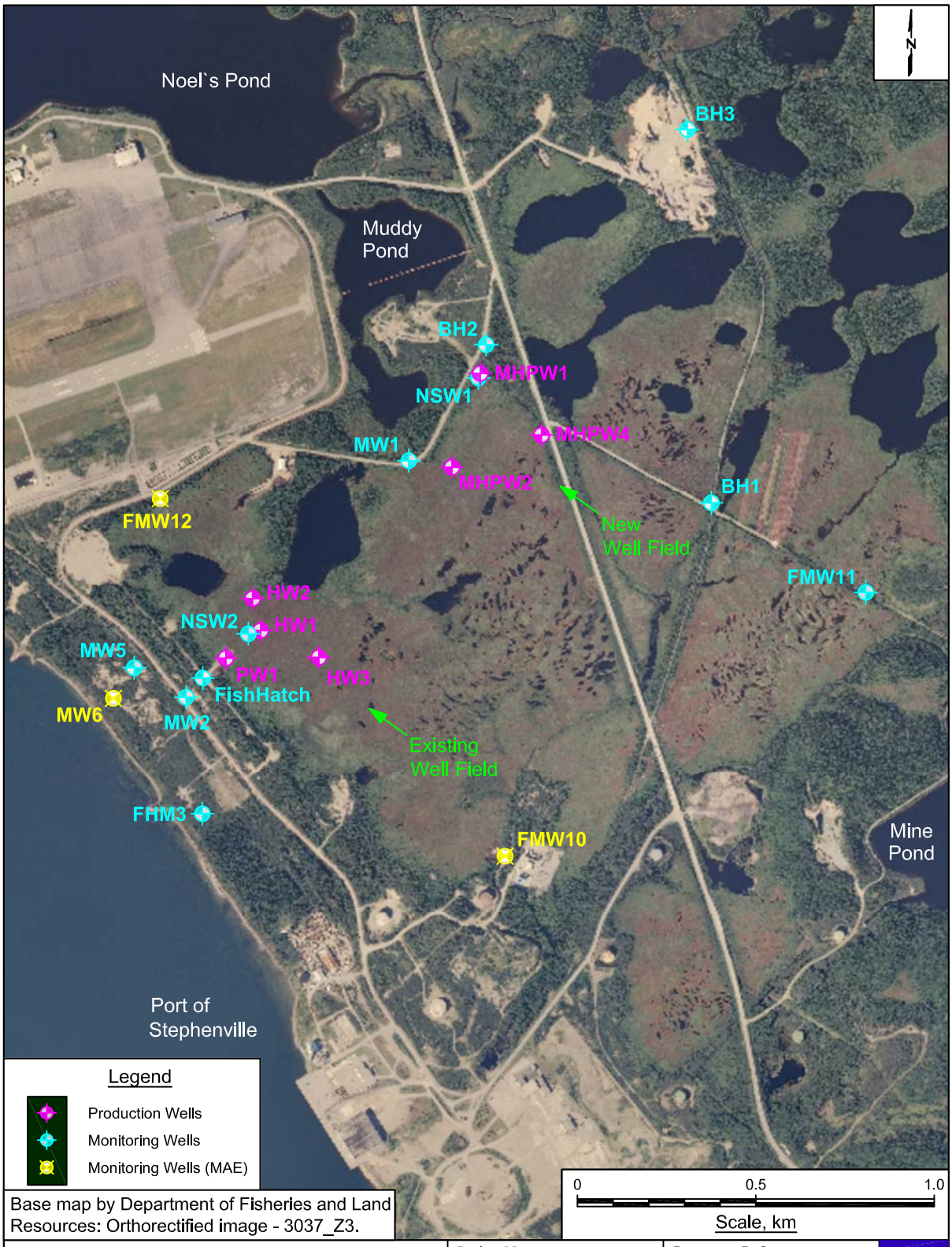

Figure 2.3 Location map of monitoring and production wells and two well fields at the MOWI fish hatchery site.

Project No.	Document Reference
3113	FFC-NL-3113-057b
Location	Date
Stephenville, NL	December 2022

FFC

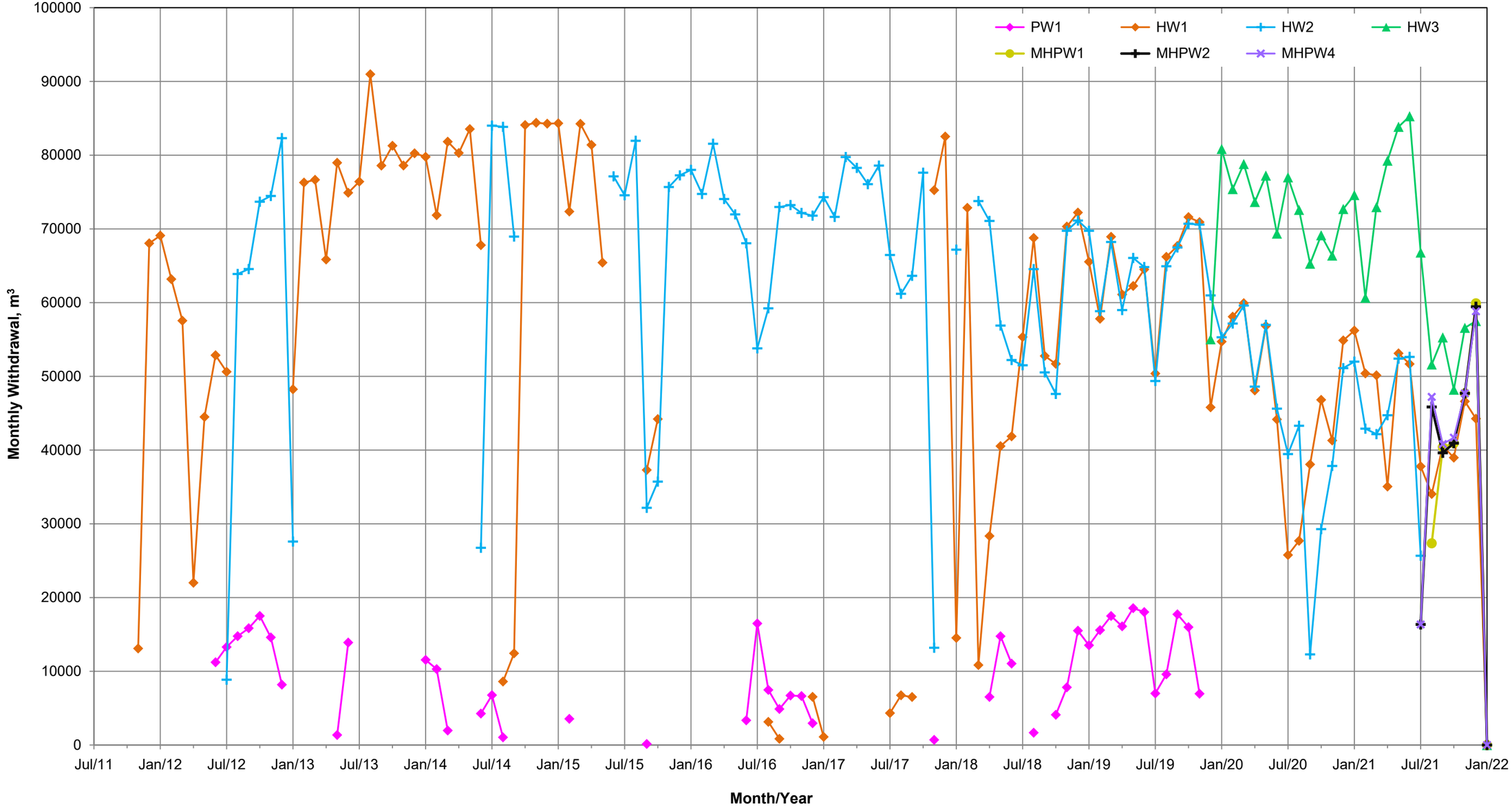

Figure 2.4 Monthly withdrawal from November 2011 to December 2021 for production wells, PW1, HW1, HW2 and HW3 from the existing well field, and MHPW1, MHPW2 and MHPW4 from the new well field.

Project No.	Document Reference
3113	FFC-NL-3113-057b
Location	Date
Stephenville, NL	December 2022

FFC

Figure 2.5 Combined monthly withdrawals of the production wells from the two well fields between November 2011 and December 2021.

Project No.	Document Reference
3113	FFC-NL-3113-057b
Location	Date
Stephenville, NL	December 2022

FFC

Figure 2.6 Plot of hydraulic head versus time for the near-field monitoring wells from June 2019 to June 2022.

Project No.	Document Reference
3113	FFC-NL-3113-057b
Location	Date
Stephenville, NL	December 2022

FFC

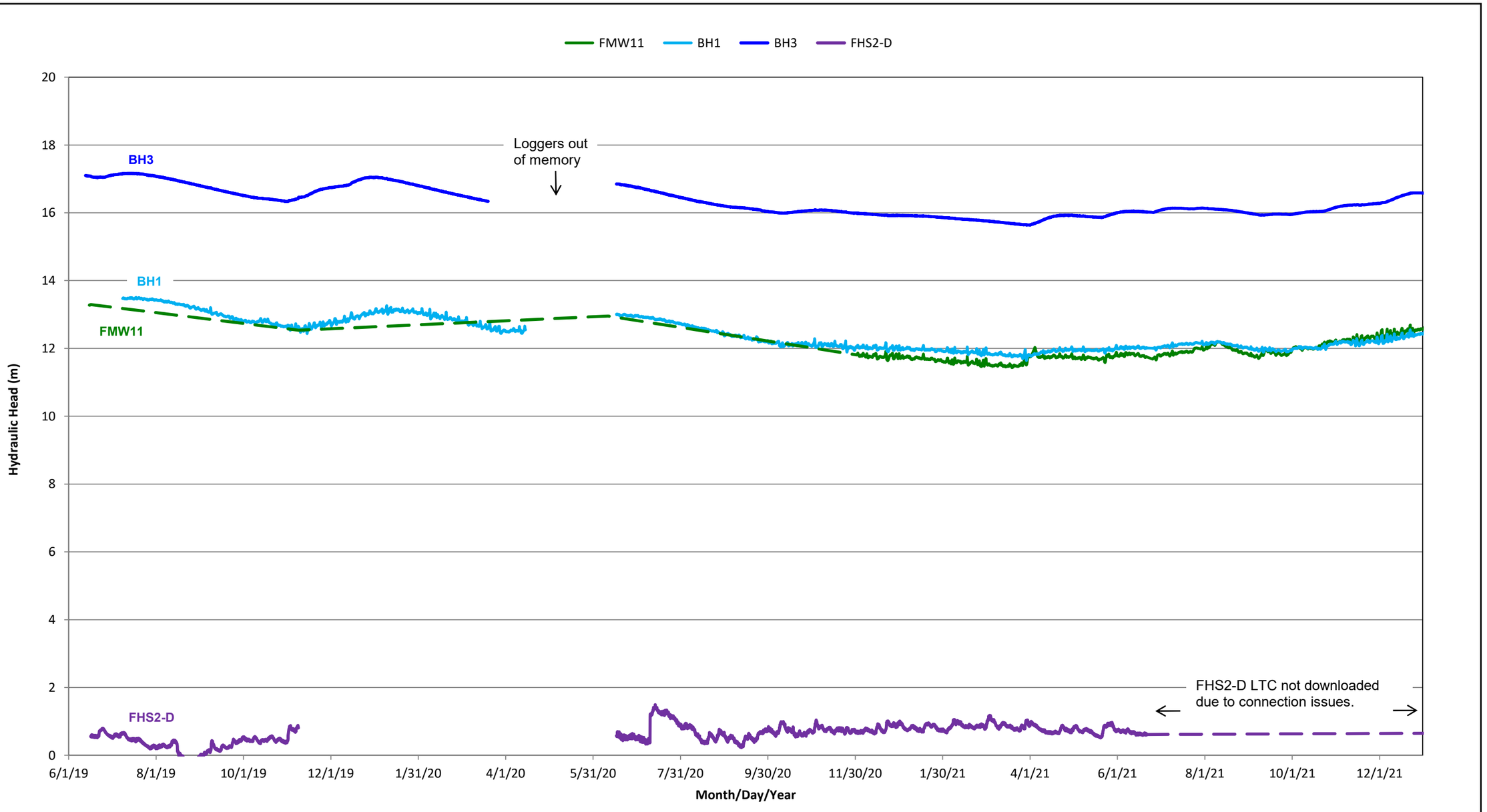

Figure 2.7 Plot of hydraulic head versus time for the far-field monitoring wells from June 2019 to June 2022.

Project No.	Document Reference
3113	FFC-NL-3113-057b
Location	Date
Stephenville, NL	December 2022

FFC

Figure 2.8 Plot of hydraulic head versus time for the DECC/MAE monitoring wells from November 2019 to December 2021.

Project No.	Document Reference
3113	FFC-NL-3113-057b
Location	Date
Stephenville, NL	December 2022

FFC

3.0 MODEL INPUT PARAMETERS FOR PREDICTION MODEL

3.1 Precipitation – 25-Year Prediction

For the prediction of the yearly total precipitation for the future, two data sets of 25-year periods were chosen from the historical precipitation data from 1942 to 2021. The first data set, *Data Set 1*, was chosen from the years between 1997 and 2021 to reflect the recent precipitation trend and quantity. The historical data for the corresponding period are plotted with green symbols in **Figure 3.1**. This 25-year period data set presents an example of a change in the trend direction. The data set started at 1,350 mm in 1997 with overall decreasing trend to 1,017 mm in 2010 and then changed its trend to an upward direction to reach 1,624 mm in 2021.

The second data set, *Data Set 2*, was chosen from 1949 to 1973 and the corresponding data set is plotted as red symbols in **Figure 3.1.** This data set was selected to satisfy three criteria; (1) the interval would be selected between 1942 and 1982 when the general trend of the yearly total precipitation was increasing with time, (2) the yearly total precipitation would be in relatively low range such as below 1,400 mm, and (3) majority of the missing yearly data points would be out of the selected interval. The missing yearly data points between 1942 and 1982 existed in 1942, 1946, 1948 and 1966 data (**Table 2.1**). The yearly total precipitation for this period ranged from 871 to 1,362 mm with an overall increasing trend. This second 25-year period data set presents an example of a continuous change in one direction. In addition, the overall range of the yearly total precipitation (871 – 1,362 mm) was lower than that of the first data set (1,017 - 1,624 mm).

The two data sets were fitted with the second order polynomial trendlines as shown in **Figure 3.1**. The trendline for *Data Set 1* is the green curved line starting at 1,398 mm/year and then decreasing to 1,238 mm/year at Year 12. The trend then changed its direction and the precipitation increased to 1,495 mm/year at the last year, Year 25. The red/orange line represents the trendline of *Data Set 2* showing continuous increasing in the yearly total precipitation from 1,004 mm in Year 1 to 1,265 mm/year in Year 25. The calculated yearly total precipitation using the trendline equations from the two 25-year period data sets are presented in **Table 3.1**.

The two data sets were used for projecting the yearly total precipitation from 2022 onwards for the next 25-year prediction, 2022 - 2046 for the 3D prediction model. The projected precipitation data that were assigned to corresponding years in the prediction model simulations are indicated under ‘Projected Year’ column in **Table 3.1**. It should be noted that *Data Set 2*, from 1949 to 1973, was flipped over, reversed, for projection to the future years, so that the precipitation value in Year 1 will be applied to 2046 and Year 25 to 2022. Flipping of the data set was necessary to keep the predictive model more conservative with decreasing precipitation values with time (depleting condition of the aquifer) for the purpose of the worst-case scenario and to avoid a sudden and unrealistic drop in recharge rates in 2022.. **Table 3.2** and **Figure 3.2** present the yearly total precipitation values that were used as the basic data set for the input parameters in

the 3D transient model. The average, minimum and maximum precipitation values for each data set are summarized in **Table 3.3**.

Table 3.3 Summary of the precipitation data for the measured and predicted data sets.

	Current Model	**Prediction Model**	
Precipitation (mm/year)	**Measured**	**Data Set 1**	**Data Set 2**
	2011 - 2021	**2022 - 2046**	**2022 - 2046**
Average	1,361	1,315	1,128
Minimum	1,148	1,238	1,004
Maximum	1,624	1,495	1,265

3.2 Withdrawal – 25-Year Prediction

To predict the future water usage of the next 25 years (2022 - 2046), the historical water withdrawal records up to December 2021 were examined to identify yearly and monthly trends/patterns in the water usage at the MOWI hatchery site. As shown in the previous sections, the monthly withdrawal was maintained at a constant rate since the start of operations and until April 2018 and then increased steadily during the next three years until July 2020 when the new well field was brought on-line (**Figure 2.5**). **Figure 3.3** shows the yearly total withdrawal between 2012 and 2021 by MOWI in Stephenville. The 2011 data are not shown in this graph because only two months of data were available for the corresponding year. Whereas the increments in the years between 2018 and 2020 were due to the higher water demand, the increment in 2022 was mainly caused by adding the new/second well field to the production line and its related work activities for the hatchery expansion. The abnormality of the increment during this period is more readily noticeable in the individual yearly plot of the combined monthly withdrawals from all production wells. As shown in **Figure 3.4**, the changes (increases) in the monthly withdrawals for November and December 2021 are much higher than the general changes (increases or decreases) in the other years. Fracflow was informed by the Client that during this period the new wells were operated without the SCADA system, so the water usage was slightly more than normal due to filling new tanks and flushing old tanks. Therefore, those data were not included for estimation of both the yearly and monthly withdrawal trends.

The future withdrawals depend largely on the production cycles of the biomass at the hatchery. Therefore, the future water demand was outlined based on consultation with MOWI personnel in March 2022. The summary of the consultation is (1) a 2% to 3% yearly increase would be an acceptable prediction for the future water demand barring any future facility expansion, (2) the water usage would be slightly reduced for 2022, (3) the water usage would be increased in 2023 to the usage level at the beginning of 2022, and (4) the future production cycles on which the

withdrawals would depend were not confirmed at the time of communication. Based on the summary, it seemed to be a reasonable assumption to apply a 2.5% increase to the yearly withdrawals. However, the withdrawal increment would apply for the first 10 years (2022 - 2031) of the 25-year prediction modeling, and then the withdrawal would be maintained at the level of 2031 for the next 15 years (2032 - 2046). **Figure 3.5** and **Table 3.4** present the historical/measured (2012 - 2021) and predicted (2022 - 2046) yearly total withdrawals that was used as a basic data set for the input parameters in the 3D transient model.

Table 3.1 Historical yearly total precipitation and corresponding precipitation predicted based on the trendlines of the two selected 25-year periods.

Data Set 1: 1997 - 2021				
Historical/Measured		Predicted/Trendline		
Year	Yearly Total Precipitation (mm/year)	Model Year	Yearly Total Precipitation (mm/year)	Projected Year
1997	1350	1	1398	**2022**
1998	1371	2	1369	**2023**
1999	1383	3	1343	**2024**
2000	1474	4	1320	**2025**
2001	1127	5	1299	**2026**
2002	1417	6	1282	**2027**
2003	1131	7	1267	**2028**
2004	1281	8	1256	**2029**
2005	1154	9	1247	**2030**
2006	1288	10	1241	**2031**
2007	1369	11	1238	**2032**
2008	1187	12	1238	**2033**
2009	1351	13	1240	**2034**
2010	1017	14	1246	**2035**
2011	1173	15	1254	**2036**
2012	1176	16	1265	**2037**
2013	1590	17	1279	**2038**
2014	1252	18	1296	**2039**
2015	1314	19	1316	**2040**
2016	1347	20	1339	**2041**
2017	1286	21	1364	**2042**
2018	1576	22	1393	**2043**
2019	1480	23	1424	**2044**
2020	1148	24	1458	**2045**
2021	1624	25	1495	**2046**

Data Set 2: 1949 - 1973				
Historical/Measured		Predicted/Trendline		
Year	Yearly Total Precipitation (mm/year)	Model Year	Yearly Total Precipitation (mm/year)	Projected Year
1949	1091	1	1004	**2046**
1950	915	2	1013	**2045**
1951	1015	3	1022	**2044**
1952	992	4	1032	**2043**
1953	1061	5	1041	**2042**
1954	996	6	1051	**2041**
1955	1095	7	1061	**2040**
1956	979	8	1071	**2039**
1957	1145	9	1081	**2038**
1958	1246	10	1092	**2037**
1959	1247	11	1102	**2036**
1960	871	12	1113	**2035**
1961	1264	13	1124	**2034**
1962	1219	14	1135	**2033**
1963	1039	15	1146	**2032**
1964	1097	16	1157	**2031**
1965	1122	17	1168	**2030**
1966	N/A	18	1180	**2029**
1967	1204	19	1192	**2028**
1968	1301	20	1203	**2027**
1969	1115	21	1215	**2026**
1970	1196	22	1228	**2025**
1971	1203	23	1240	**2024**
1972	1237	24	1252	**2023**
1973	1362	25	1265	**2022**

* N/A: data not available due to missing monthly data.

Table 3.2 Measured (2011 - 2021) and predicted (2022 - 2046) yearly total precipitation as the input parameters for the 3D transient model.

Year		Yearly Total Precipitation (mm/year)	
		Data Set 1	Data Set 2
Historical/Measured	2011	1173	
	2012	1176	
	2013	1590	
	2014	1252	
	2015	1314	
	2016	1347	
	2017	1286	
	2018	1576	
	2019	1480	
	2020	1148	
	2021	1624	
Predicted/Trendline	2022	1398	1265
	2023	1369	1252
	2024	1343	1240
	2025	1320	1228
	2026	1299	1215
	2027	1282	1203
	2028	1267	1192
	2029	1256	1180
	2030	1247	1168
	2031	1241	1157
	2032	1238	1146
	2033	1238	1135
	2034	1240	1124
	2035	1246	1113
	2036	1254	1102
	2037	1265	1092
	2038	1279	1081
	2039	1296	1071
	2040	1316	1061
	2041	1339	1051
	2042	1364	1041
	2043	1393	1032
	2044	1424	1022
	2045	1458	1013
	2046	1495	1004

Table 3.4 Measured (2011 - 2021) and predicted (2022 - 2046) yearly total withdrawals as the input parameters for the 3D transient model.

Year		Yearly Total Withdrawal (m^3)
Historical/Measured	2011	81,138 for Nov. & Dec.
	2012	822,988
	2013	949,875
	2014	1,038,321
	2015	927,426
	2016	910,572
	2017	917,887
	2018	1,317,734
	2019	1,735,067
	2020	1,971,297
	2021	2,362,722
Predicted/Trendline	2022	2,291,840
	2023	2,349,136
	2024	2,407,865
	2025	2,468,061
	2026	2,529,763
	2027	2,593,007
	2028	2,657,832
	2029	2,724,278
	2030	2,792,385
	2031	2,862,195
	2032	2,862,195
	2033	2,862,195
	2034	2,862,195
	2035	2,862,195
	2036	2,862,195
	2037	2,862,195
	2038	2,862,195
	2039	2,862,195
	2040	2,862,195
	2041	2,862,195
	2042	2,862,195
	2043	2,862,195
	2044	2,862,195
	2045	2,862,195
	2046	2,862,195

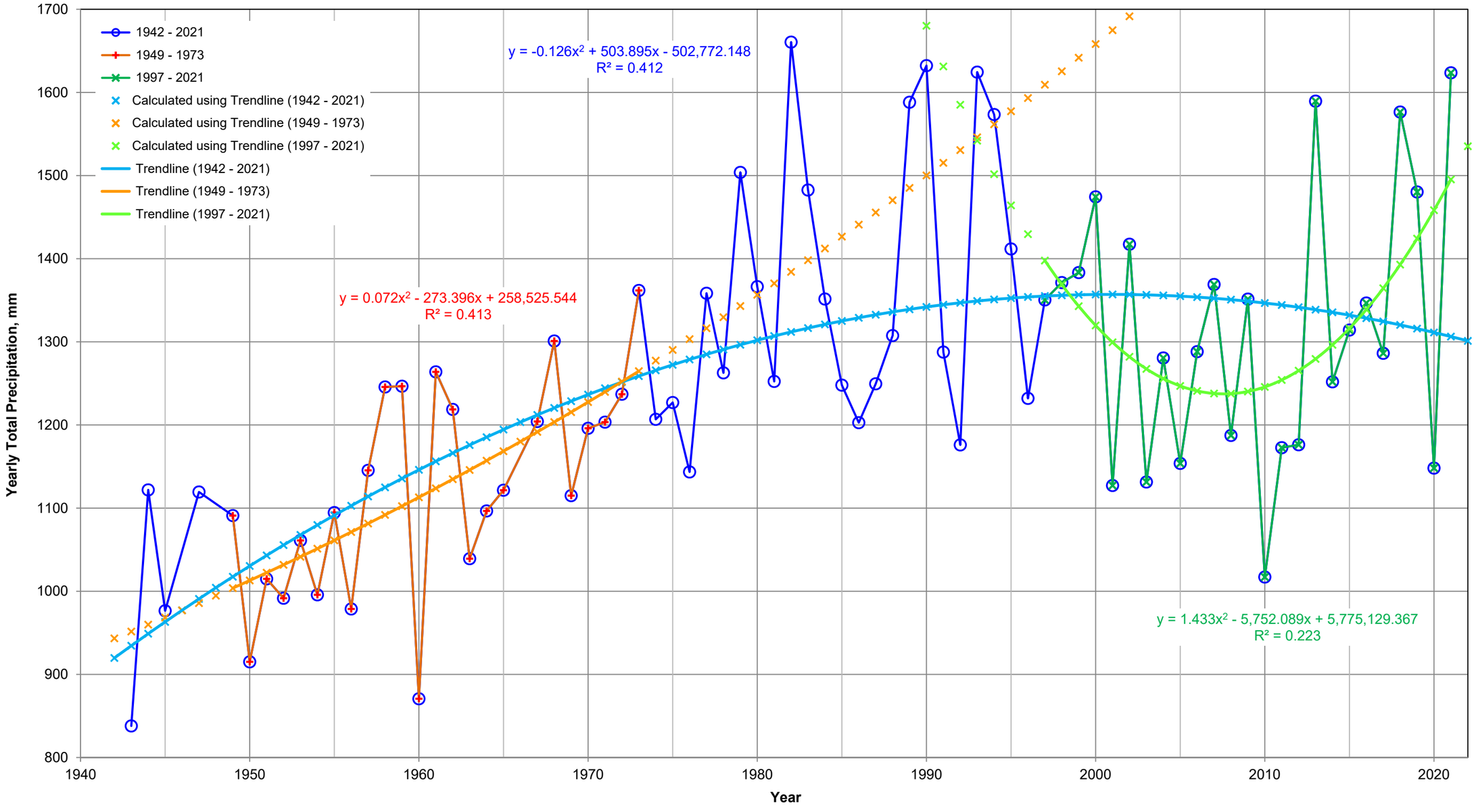

Figure 3.1 Yearly total precipitation data for the entire data period (1942 - 2021) and two 25-year periods (1949 - 1973 and 1997 - 2021) and their trendlines.

Project No.	Document Reference
3113	FFC-NL-3113-057b
Location	Date
Stephenville, NL	December 2022

FFC

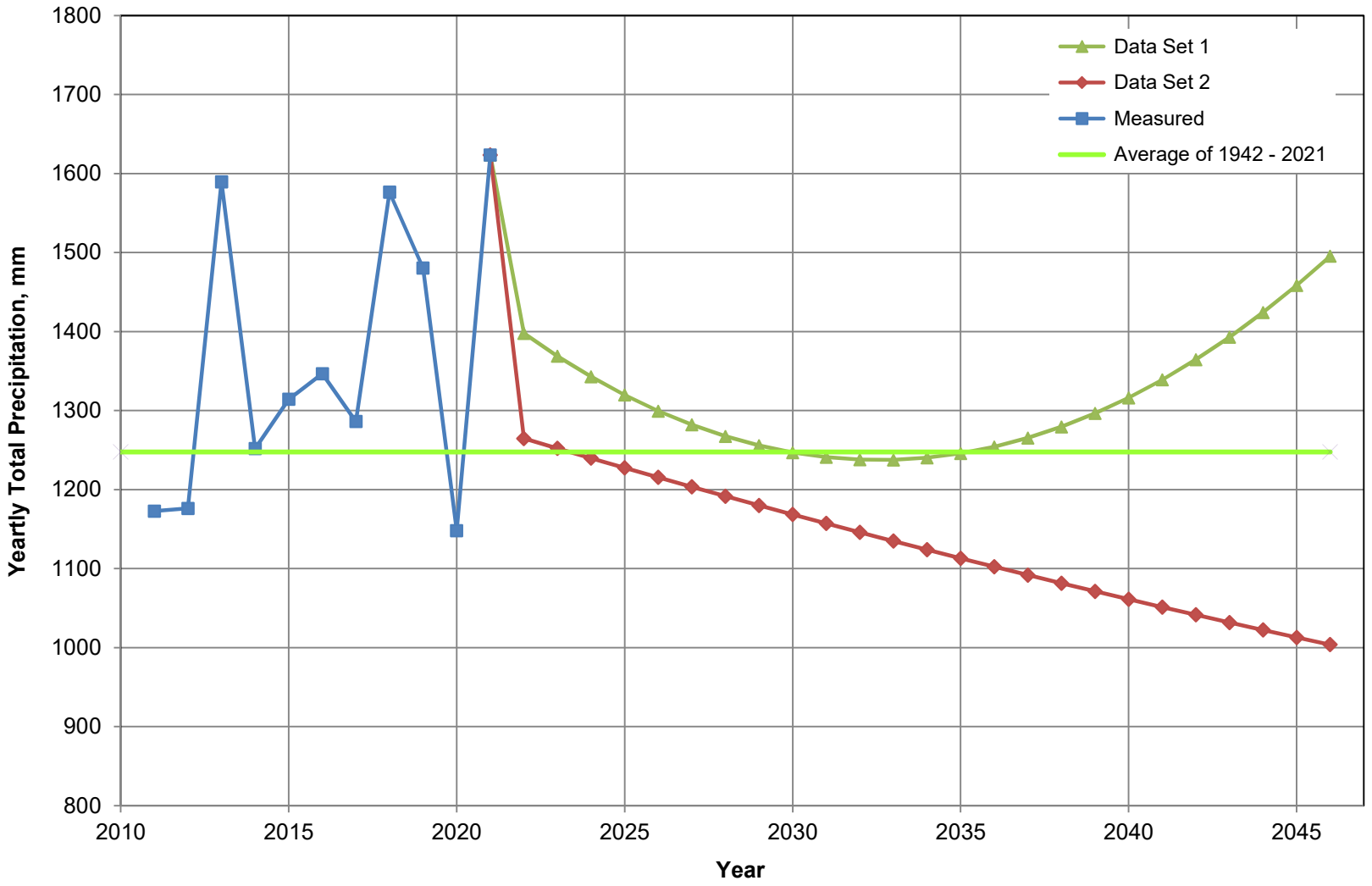

Figure 3.2 Yearly total precipitation for the measured data from 2011 to 2021 and two predicted data sets from 2022 to 2046 for the 3D transient model for the MOWI Site, Stephenville, NL.

Project No.	Document Reference
3113	FFC-NL-3113-057b
Location	Date
Stephenville, NL	December 2022

FFC

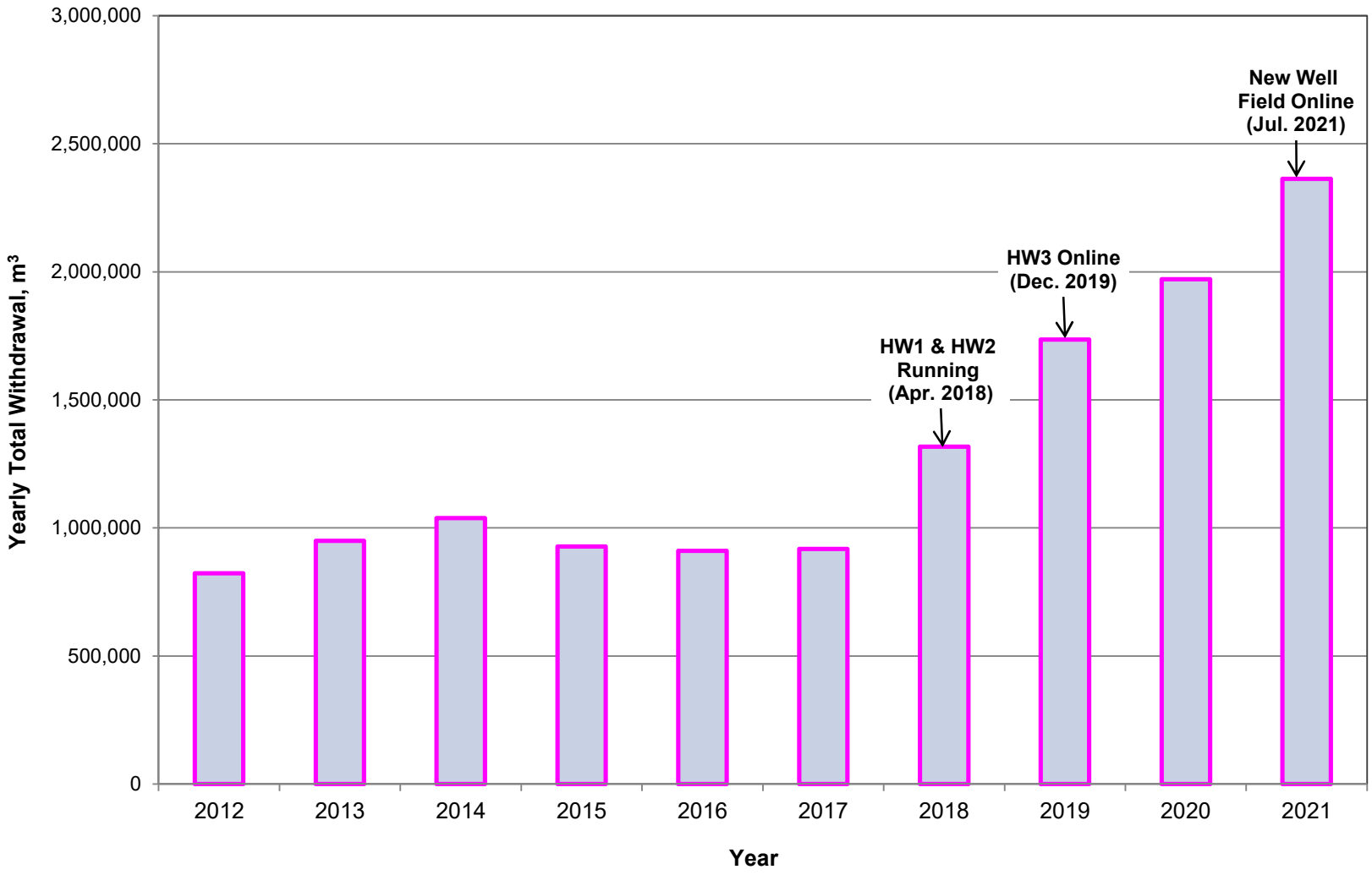

Figure 3.3 Yearly total withdrawal between 2012 and 2021 at the MOWI hatchery site in Stephenville, NL.

Project No.	Document Reference
3113	FFC-NL-3113-057b
Location	Date
Stephenville, NL	December 2022

FFC

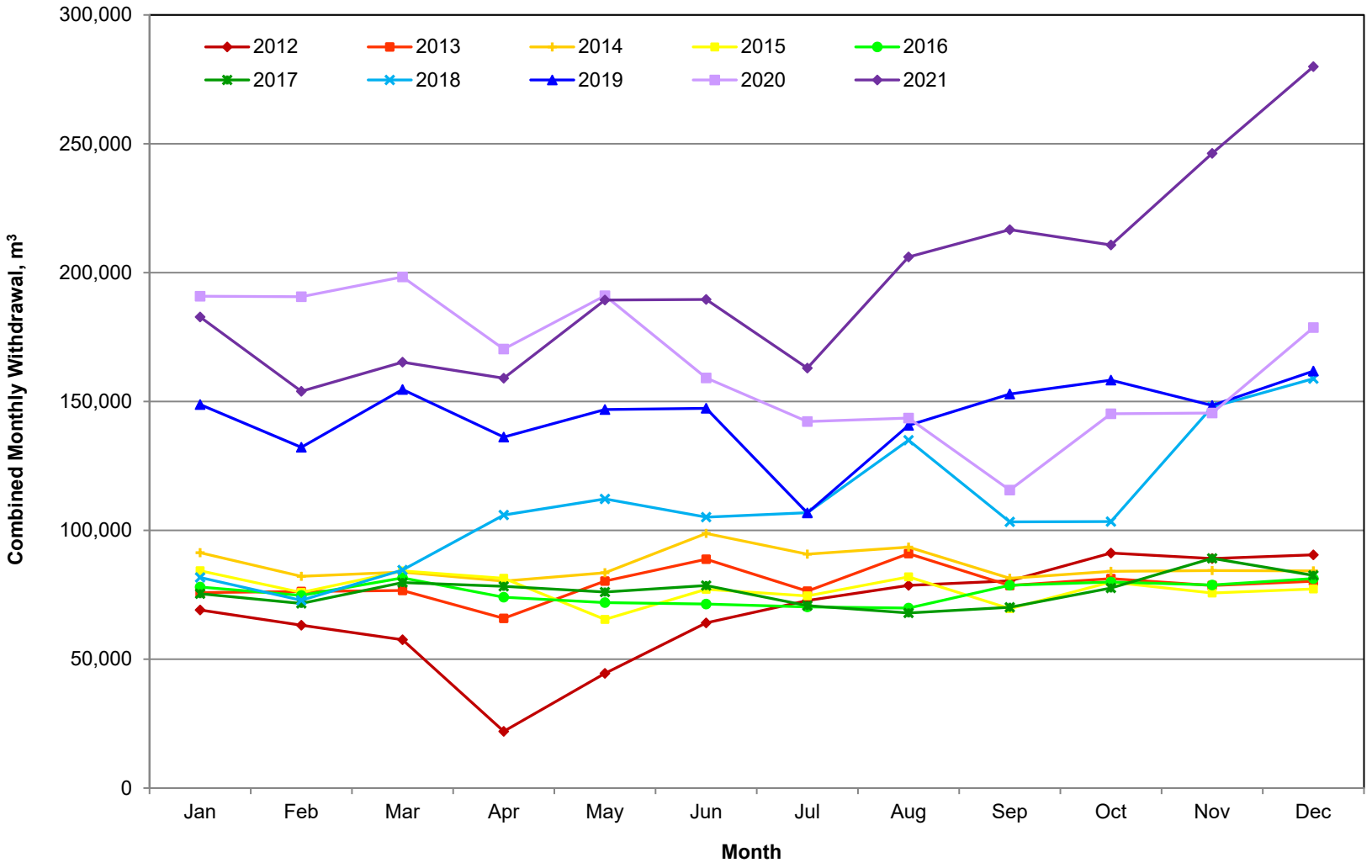

Figure 3.4 Individual yearly plot of the combined monthly withdrawal from all production wells of both well fields between 2012 and 2021.

Project No.	Document Reference
3113	FFC-NL-3113-057b
Location	Date
Stephenville, NL	December 2022

FFC

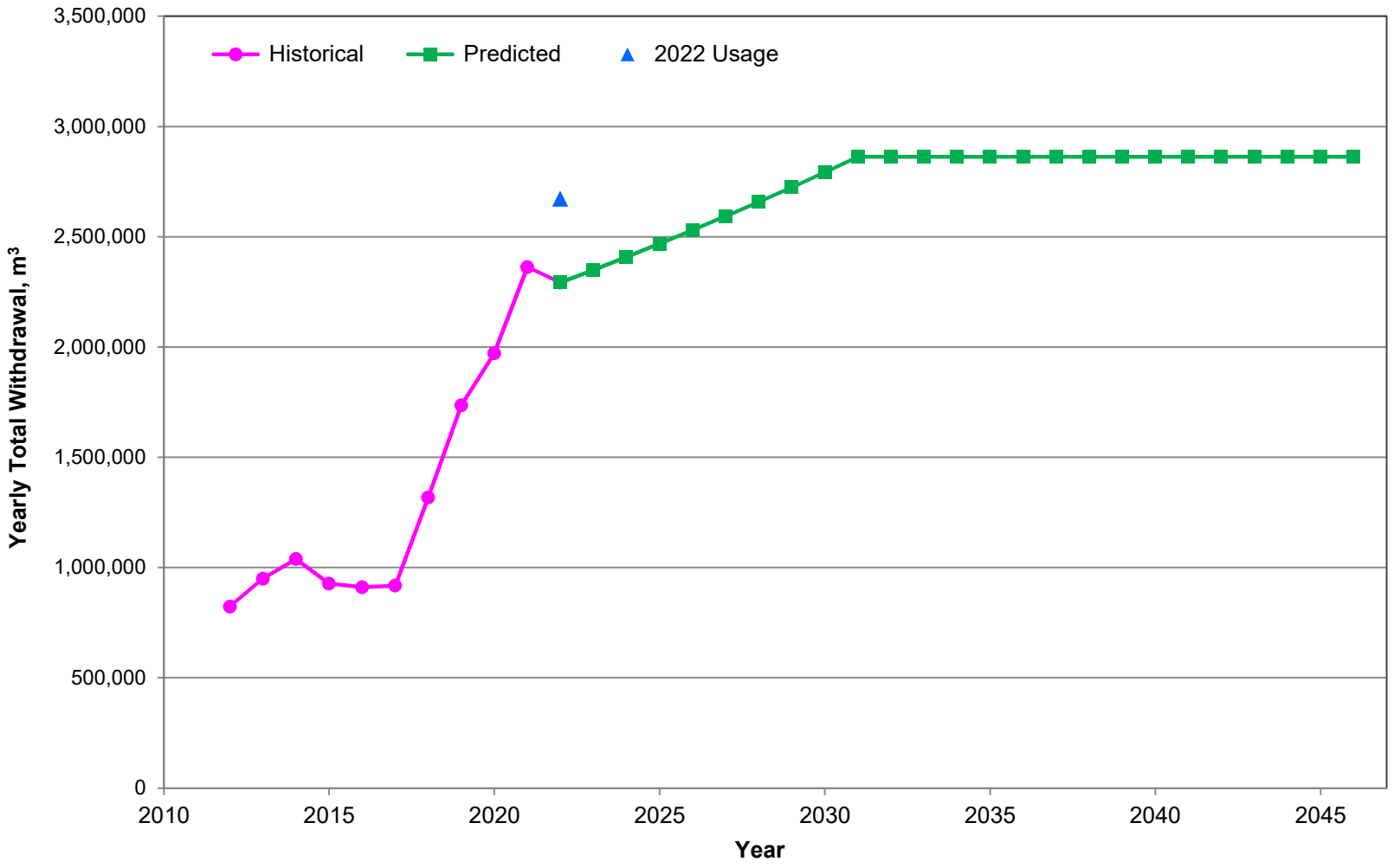

Figure 3.5 Yearly total withdrawal for the historical period between 2012 and 2021 and for the predicted period between 2022 and 2046 at the MOWI hatchery site in Stephenville, NL.

Project No.	Document Reference
3113	FFC-NL-3113-057b
Location	Date
Stephenville, NL	December 2022

FFC

4.0 NUMERICAL MODELING - PREDICTING LONG-TERM AQUIFER RESPONSE AND WORST CASE RESPONSE

As part of the 3D numerical model for predicting long term aquifer response and worst case response, the basic transient model simulations were started for the year 2011 when the operation of the first well field started (November 2011). These basic simulations were conducted for the period of January 2011 to December 2021 using the known withdrawal rates from the production wells and known climatic data. The simulations also included new activities at the project site such as installation and operation of the new well field in July 2021 and the new drain system at the new building in October 2019.

The computer modelling software code that has been used for this groundwater simulation is FEFLOW (Finite Element subsurface Flow System). FEFLOW (Diersch, H. -J. G., 2005) is an advanced, finite element code that is used to model groundwater flow and transport in both porous media and fractured-bedrock systems. The transport portion of the FEFLOW code allows the user to track the movement of particles, or tracers, along discrete flow lines to map the direction of movement and travel time of water and conservative as well as non-conservative ions between points of interest. Unlike the finite difference code, the finite element approach is more suited to simulate multiple production and observation wells because the mesh around the production wells can be refined locally resulting in a significantly smaller number of grid points and simulation time than that required by the finite difference code.

A simplified conceptual hydrogeological model of the aquifer and well field capture area plus adjacent hydrogeological buffer areas was developed for use in modelling the groundwater flow and the potential impacts of changes and variations in recharge on the groundwater withdrawals. The conceptual hydrogeological model was constructed based on a combination of the available hydrogeological data and informed judgement. Every attempt was made to incorporate field measurements collected at the site during this study and previous studies. However, assumptions were still required in most locations since the data coverage is sparse in some areas, especially in the central bog area where access for a drill rig is limited.

The 3D finite element model mesh for the current modeling was based on the mesh that was constructed in 2018 as part of the initial assessment that was requested by MAE (now DECC) for the granular aquifer. The original model mesh has been modified to accommodate the overall update well field configuration and the site activities such as (1) adding the new production well HW3 in the existing well field, (2) updating the exact locations of the three new production wells in the new well field based on the as-built locations, and (3) updating the elevations of the new hatchery expansion building drains based on their reported final locations and depths. In addition, the four new test wells that were constructed as part of the saltwater supply investigation were also added to the model.

The previous model for the project sites was calibrated under steady-state conditions. Therefore, the existing model was updated by replacing the constant input parameters with time-dependent

parameters, where required. The measured recharge rates and water withdrawal rates were distributed to monthly data sets for each corresponding year. Then the new transient model flow system was simulated using the known input parameters and calibrated under a transient condition prior to the prediction model simulations.

4.1 Current Model – Year 2011 to 2021

The starting point of the updated 3D transient model was the January month of the year in which the operation of the existing/old well field started (November 2011). Then the simulation continued until the recent time (December 31, 2021) using the recorded historical climatic data and the known/measured withdrawal rates, including the installation and operation of the new well field and the drain system at the new building site. The *Current Model* is the updated transient model for a period of 2011 to 2021 that was simulated using the measured precipitation data and the recorded well field withdrawal rates.

4.1.1 Current Model – Input Parameters

The monthly precipitation data collected at the station *Stephenville A* was used to calculate the monthly recharge values for the project site/model area. The recharge rates to the aquifer and the regional groundwater system from precipitation are generally determined by several factors such as runoff, infiltration, evapotranspiration, etc. To accommodate the variation in those factors, the model area was divided into three zones for assigning the recharge rates as shown in **Figure 4.1**; the marsh covered area of the granular aquifer (Bog Area), areas that are not predominantly covered by marsh (Non-Bog Area), and the Intermediate Area. In general, the ground was frozen in the winter months and there was little to no recharge occurring across the frozen ground layer. However, at the Bog Area, the bog acts as a buffer zone and the water stored in the bog layer is released to the underlying aquifer during the winter months. Therefore, the recharge would occur throughout the entire year through the Bog Area. However, in the Non-Bog Area, the recharge to the groundwater decreased or stopped during the winter months depending on the air temperatures and the thickness of the frozen ground. The recharge rate then gradually increased with the increasing temperatures in the next spring when the ground surface thawed and the snow was melting. During this time of the year, significant run off occurred where the amount of snow melt was exceeding the recharge capacity of the subsurface layers (overburden) of the area. In addition, the relative steep slopes on the high elevation area outside of the two well fields also show a higher volume of runoff. Therefore, the overall recharge rates of the Non-Bog Area were smaller than that of the Bog Area. The Intermediate Area is a mixture of the other two ground types for recharge rates.

Based on the range of the recharge rates that were assigned to the previously calibrated steady-state model, a range between 24% and 30% of the total yearly precipitation was set as starting input parameters for the calibration of the transient model. Then the yearly recharge rate was

distributed over 12 corresponding months based on the controlling factors, such as runoff, infiltration, evapotranspiration, etc., that were mainly affected by the monthly temperatures. During the calibration process, the recharge value for each recharge area was adjusted for a better match between the measured and simulated hydraulic heads.

The other major input parameter for the model was the withdrawal rate. The measured monthly total withdrawal data were provided by the Client, which were used as the monthly input data for the transient model simulation. The input parameter data sets for the six production wells are shown in **Figures 4.2a to 4.2d**.

4.1.2 Current Model – Simulation and Calibration

Using the known values as input data, the transient model was simulated for a period of 2011 to 2021. The simulation results of the *Current Model*, computed hydraulic head data, were compared to the hydraulic head data that were measured in the available production and monitoring wells during the corresponding period (**Figures 2.6 to 2.8**). For the calibration process, the recharge values were adjusted until better matches were achieved between the measured and calculated/simulated hydraulic heads. When there was a choice to make between simulation results, the criteria was (1) to choose a simulation that provided a better match in the monitoring wells from the two well fields, and (2) to choose a simulation where the calculated heads were lower than the measured heads to be consistent as Worse Case Scenario model simulations.

Since the withdrawal rates were fixed values from the well field operation, and the original model had been calibrated to various hydraulic properties of the aquifer under steady state conditions, the recharge values were used as the main and only factor to be adjusted for the transient model calibration. The final yearly total recharge values used in the *Current Model* were 30%, 22% and 20% of the yearly total precipitation for the Bog Area, the Intermediate Area, and the Non-Bog Area, respectively. The final monthly total recharge values for the three zones used in the transient simulation between 2011 and 2021 are shown in **Figure 4.3**.

Plots of measured hydraulic heads versus the computed hydraulic head data from the 3D transient simulations in selected monitoring wells are shown in the next four figures. **Figure 4.4** plots the hydraulic head data in September 30, 2019 prior to the construction of the building drain. The hydraulic head data in **Figures 4.5 to 4.7** show the results of the *Current Model* in April, August and December, 2021. Note that from October 2019, the model simulations include additional activities on and around the two well fields, such as the operation of the new well field (July 2021) and the construction of the drainage system at the new building site (October 2019). For a perfect match between measured and computed hydraulic heads, the data points would plot on a 45-degree line – the solid line in **Figures 4.4 to 4.7**. The dashed lines on either side of the solid line indicate a +/- difference of 1.0 m between the measured and computed values. For data points that plot below the solid line, the measured values are higher than the computed values.

For data points that plot above the solid line, the model heads are higher than the measured heads. The R^2 term of the plot indicates the degree of fit between the measured and computed heads. A few monitoring wells plot outside of the 1.0 m dash lines such as FMW11 in **Figure 4.4** and FMW10 and FMW11 in **Figure 4.5 to 4.7**. However, the *Current Model* was considered to be well calibrated based on the high R^2 (0.99 and 0.96) between the measured and computed hydraulic heads as shown in **Figures 4.4 and 4.7.**

The measured (logger data) versus computed (3D model simulations) hydraulic head data for the simulation period (January 2011 to December 2021) of the *Current Model* are presented in **Figures 4.8 to 4.10** for selected wells. Data for the selected monitoring wells within the two wells fields, NSW2-I, FishHatch, MW2 and FHM3 from the existing well field and NSW1-I, BH2 and MW1 from the new well field, are plotted in **Figures 4.8a to 4.8g.** The hydraulic head data for the wells from the far-field, BH1, BH3 and FMW11, are shown in **Figures 9a to 9c** and for the three DECC/MAE wells, FMW10, FMW12 and MW6, in **Figures 10a to 10c**. The results of the wells within the two well fields (**Figures 4.8a to 4.8g**) showed approximately less than 1 m of the difference between the measured and computed heads. In general, the wells within the immediate well field areas show a better match than the wells outside of the immediate well field areas. The results from wells in the far-field area such as BH1, BH3 and FMW11 showed head differences of up to approximately 2 m with the calculated heads being higher than the measured heads at the selected wells.

4.1.3 Current Model – Results

The hydraulic heads from the steady-state model simulation under a non-pumping condition was used as the initial heads for the transient model simulation as described in the previous sections. **Figures 4.11 and 4.12** present two contour maps of the groundwater elevation/hydraulic head data at the depth of the water table level and the pumping level, respectively. The contour maps indicated that the general flow direction of the ground water under the steady-state condition was from northeast to southwest toward Port Harmon/Port of Stephenville and the two well fields lay between the 4.2 and 7.3 m contour lines for the existing well field and between 10.3 and 13.3 m contour lines for the new well field.

The two groundwater contour maps of the *Current Model* simulation (2011 - 2021) under pumping conditions are presented in **Figures 4.13 and 4.14** at the water table level and the pumping level, respectively. The overall flow direction of the ground water was in the same direction as those of the non-pumping condition under the steady-state simulation. However, the groundwater contour lines were shifted toward the northeast direction (up-gradient) indicating that the groundwater elevations decreased in and around the two well fields. Since flow occurs in the direction perpendicular to the contour lines, the bended contour lines around wells indicate flow toward the corresponding wells, i.e., pumping conditions for each production well. At the end of the simulations for the *Current Model* in December 2021, the water elevations were

between 3.5 and 6.5 m in the existing well field and between 9.3 and 12.2 m in the new well field.

Comparison of the hydraulic head data from the transient simulation results to the initial head data under non-pumping condition produces the capture areas/drawdown contours. The capture area and the drawdown contour map at the end of the *Current Model* (December 31, 2021) are shown in **Figures 4.15 and 4.16**.with 0.2 m contour lines at the water table level and the pumping level, respectively. Drawdown of 1.0 m contour lines were plotted around the production wells at the existing well field and 1.2 m contour lines at the new well field. The majority of the monitoring wells were located within the 0.4 m drawdown contour line.

The water elevation contour maps and the drawdown contour maps at the pumping levels are presented here and the maps at the water table level for the prediction models are presented in **Appendices A and B**, respectively.

4.2 Prediction Model – Year 2022 to 2046

The next step in the Worst-Case modeling was to predict the aquifer responses to the long term withdrawal for the next 25 years (January 2022 to December 2046). The two main parameters that would have an impact on the hydraulic heads in the prediction models were the recharge (precipitation) rates and the withdrawal rates. The recharge rates that were determined for the *Current Model* were used in the prediction models. The future withdrawal rates from the production wells within the two well fields were set by the Client based on the predicted future demands as shown in the previous chapter (**Figure 3.5**). The prediction model simulations (2022 - 2046) were continued using the simulation results of the *Current Model* in December 31, 2021.

4.2.1 Prediction Models – Input Parameters

Two recharge data sets that were proposed for the Worst-Case scenarios, and the two data sets were adopted from the historical precipitation data as shown in **Figure 3.1**. The first data set, *Data Set 1*, reflected the last 25 years of the historical precipitation data as shown in the green trend line in **Figure 3.1**. The second data set, *Data Set 2*, of 25-year precipitation data were extracted from an earlier period of the historical data when the overall precipitation rates were lower than *Data Set 1*.

Based on the two *Data Sets*, six sub-data sets, two main sets, two upper limit sets and two lower limit sets, were created for the prediction models. The two main sets, *Main 1 and Main 2*, were determined using the trend line of the corresponding 25-year period data set. Then the upper and lower limit sets were generated by adding or subtracting the one standard deviation of the corresponding data set to each of the 25 data points. **Table 4.1** summarizes the six sub-data sets

for the prediction models and their recharge values as the input parameters. The assigned recharge values for the six sub-data sets are plotted in **Figures 4.17 to 4.22**.

Table 4.1 Summary of the six sub-data sets for the prediction model simulations and their recharge scheme as input parameters.

Data Set	Sub-Data Set	Input Parameter
Data Set 1	Main 1	Trend line value of 1997 - 2021
	Upper Limit 1	Main 1 + Standard Deviation
	Lower Limit 1	Main 1 - Standard Deviation
Data Set 2	Main 2	Trend line value of 1949 - 1973
	Upper Limit 2	Main 2 + Standard Deviation
	Lower Limit 2	Main 2 - Standard Deviation

4.2.2 Prediction Model Results – Main Models

The two main sub-data sets, *Main 1 and Main 2*, used the trend line values from the 25-year period data sets as summarized in the previous sections. The simulation results were extracted for every five years for presentation.

Data Set 1 – Main 1

The five groundwater elevation (hydraulic head) contour maps for *Main 1* are plotted in **Figures 4.23 to 4.27** with five year intervals from 2026 to 2046. Compared to the results of the *Current Model* (**Figure 4.14**), the contour lines in the groundwater contour maps generally shifted in the northeast direction as the simulation time increased until 2036 (**Figure 4.25**) which indicated that the water levels were decreasing in the area with time. The contour lines then shifted backward in a southwest direction from 2041 to 2046 (**Figures 4.26 and 4.27**) indicating that the water tables were recovering during this period. It was also noted that the contour lines were bent around the production wells which was produced by the pumping condition in the wells showing the groundwater flow direction toward the wells. After five years of simulation, the water elevations were between 3.5 and 6.2 m at the existing well field and between 8.8 and 11.5 m at the new well field in 2026. The water elevations decreased and were between 3.5 and 6.0 m at the existing well field and between 8.5 and 11.0 m at the new well field in 2036. The water elevations recovered by 2046 and the existing well field lay between 3.5 and 6.3 m and the new well field was between 9.0 and 11.5 m. Compared to the water elevation contour map provided by the initial condition (**Figure 4.12**), the water elevations at the outside area of the well fields (far-field area) near BH3 also dropped by approximately 1.4 m between 2021 and 2036.

Five drawdown contour maps for *Main 1* during the 25-year simulation are presented in **Figures 4.28 to 4.32** with a five year interval. The deep red coloured areas in the drawdown contour maps represent drawdowns greater than 2.0 m. These contour lines were limited to the area around each production well. In 2026, for example, these lines are plotted as a dot for each production well (**Figure 4.28**). Then the area increased in 2031 (**Figure 4.29**) to form a circular shape around the production wells at the new well field. The area was further expanded in 2036 (**Figure 4.30**), and then decreased with time in 2041 and 2046 as shown in **Figures 4.31 and 4.32**.

Data Set 2 – Main 2

The other main input data set is based on *Data Set 2*, whose recharge values were continuously decrease approximately 1% each year throughout the 25 years. The water elevation contour maps at the pumping level for *Main 2* are presented in **Figures 33 to 37**. The overall groundwater elevation contour lines moved toward the northeast direction gradually for the entire 25-year simulation period at both well fields. At the far-field site near BH3, the water elevation dropped about 2.4 m between 2021 and 2046 (**Figure 4.37**). After a five year prediction with the *Main 2* simulation in 2026, the existing well field lay between the 3.5 and 6.2 m contour lines and the new well field between 8.7 and 11.3 m (**Figure 4.33**). Then, by 2046, the final water elevations decreased to between 3.0 and 5.5 m at the existing well field and between 8.0 and 10.3 m at the new well field (**Figure 4.33**).

The drawdown contour maps for *Main 2* are shown in **Figures 4.38 to 4.42**. The drawdown around the production wells was approximately 1.2 m in the existing well field and 1.8 to 2.0 m in the new well field after the five year prediction simulation in 2026 (**Figure 4.38**). The drawdown cones expanded with time and, in 2046, the drawdown in the two well fields increased to greater than 1.6 m in the existing well field and greater than 2.6 to 2.8 m in the new well field (**Figure 4.42**). The drawdown cones are typically formed as a circular shape around the pumping wells as shown in **Figure 4.16**. However, the drawdown contours for the current simulation, the circular shaped contours disappeared to form bent contour lines. The decreased water elevations (drawdowns) for the current simulations were attributed not only to the pumping of the production wells but also to the reduced recharge values.

4.2.3 Prediction Model Results – Upper Limit Models

Two upper limit models, *Upper Limit 1 and Upper Limit 2*, were simulated as the upper extreme cases. The recharge values were increased by one standard deviation of the corresponding data set. With these calculations, the monthly recharge values were increased between 27% and 58%.

Data Set 1 – Upper Limit 1

In comparison to the two main data sets, *Main 1 and Main 2*, the simulation results of *Upper Limit 1*, showed the increased water elevation in the overall modeled area. The five water elevation maps are presented in **Figures 4.43 to 4.47**. The contour lines at both well fields were shifting slightly toward northeast from 2026 (**Figure 4.43**) to 2031 (**Figure 4.44**) indicating of decreasing in water elevations. Then the water elevations recovered from 2036 (**Figure 4.45**) to 2046 (**Figure 4.47**). At the lowest levels in 2031, the water elevations at the existing well field lay between 3.7 and 6.7 m 2031, and then changed to between 4.0 and 7.0 m in 2046. The water elevations at the new well field lay between 9.8 and 12.8 m in 2031 and between 10.3 and 13.5 m in 2046. By comparing these contour maps to the water elevation contour maps from the initial conditions, the water elevations at the well fields were approximately 0.5 m lower in 2031 and similar in 2041 to those of the initial conditions. The water elevation in BH3 at the far-field site was 17.6 m at the initial condition (**Figure 4.12**) and down to 17.1 m in 2021. However, the water elevation recovered to 17.9 m in 2031 and 18.9 m in 2046 in these simulations.

The recovery of the water elevations under the current simulations was readily noticeable on the drawdown contour maps (**Figures 4.48 to 4.52**). Comparing the simulation hydraulic head maps to the drawdown contour map in December 2021 (**Figure 4.16**), it was obvious that the capture area at the 0 m contour line in 2026 shrunk and was limited to the two well fields and its surrounding areas including the building drainage (**Figure 4.48**). The capture area was slightly increased in 2031 but shrunk again in 2036. The shrinkage of the capture area continued until 2046 when the capture areas were limited to the existing well field and the building drainage. At the new well field, the capture areas were located primarily around the production wells.

Data Set 2 – Upper Limit 2

The water elevation contour maps for the simulations of *Upper Limit 2* are presented in **Figures 4.53 to 4.57**. With gradually decreasing recharge values, the water elevations decreased with time. However, because the assigned recharge values represents the upper extreme cases, the water elevations at both well fields did not drop significantly. The water elevation contour map in 2026 (**Figure 4.53**) plot the existing well field between 3.7 and 6.5 m contour lines and the new well field between 9.7 and 12.7 m contour lines, which was approximately 0.5 to 0.8 m below the water elevations of the initial conditions but approximately 0 to 0.5 m above the water elevations in December 2021. With continuous decrease in water elevation, the water elevation of the existing well field in 2046 (**Figure 4.57**) lay between 3.5 and 6.5 m and the new well field between 9.3 and 12.2 m. Among the five *Upper Limit 2* simulation results, the lowest water elevations were found in 2046. However, the water elevation contour map in 2046 was similar to that of *Current Model* in December 2021.

Figures 4.58 to 4.62 show the drawdown contour maps for *Upper Limit 2*. The capture area of the 0 m contour line was limited to the area near the two well fields and the building drainage in 2026 (**Figure 4.58)** and the capture area expanded with time. The drawdown contour map at the

end of the current simulation in 2046 (**Figure 4.62**) was similar to that of the *Current Model* in 2021 (**Figure 4.16**).

4.2.4 Prediction Model Results – Lower Limit Models

The two prediction models, *Lower Limit 1 and Lower Limit 2*, were simulated as the lower extreme cases. The input parameters determined by subtracting one standard deviation from the monthly total precipitation values resulted in decreases in the monthly recharge values between 27% and 58%.

Data Set 1 – Lower Limit 1

The water elevation contour maps for *Lower Limit 1* (**Figures 4.63 to 4.67**) showed a similar pattern to the previous two models for *Data Set 1*. The contour lines were shifted to the northeast until 2036 and the water elevations recovered in 2041 and 2046. The water elevations for the two well fields were between 3.0 and 5.3 m at the existing well field and between 7.3 and 9.5 m at the new well field in 2036 (**Figure 4.65**). The water elevations were recovered in 2046 and were between 3.0 and 5.5 m and between 7.5 and 9.8 m at the old and new well field, respectively (**Figure 4.67**).

The drawdown contour maps for *Lower Limit 1* in **Figures 4.68 to 4.72** do not show the typical circular shape of the contour lines as shown in the previous models. Instead, the contour lines bent around the two well fields and each of the five production wells. The general drawdown values in 2026 (**Figure 4.68**) were 1.6 m around the existing well field and 2.8 m around the new well field. The monitoring well at the far-field site, BH3, showed a drawdown of 3.1 m in 2026. The drawdowns increased with time and the drawdowns in 2036 were approximately 2.0 m around the existing well field and 3.6 m around the new well field (**Figure 4.70**). After recovering the water elevation, the drawdown contours around the two well fields in 2046 were 1.6 m at the existing well field and 3.2 m at the new well field. The drawdown in BH3 was approximately 3.5 m in 2046.

Data Set 2 – Lower Limit 2

The five water elevation contour maps for the *Lower Limit 2* model are shown in **Figures 4.73 to 4.77**. The water elevations at the existing well field after the first five years of the prediction model simulation was between 3.0 and 5.3 m at the existing well field and between 7.7 and 10.3 m at the new well field (**Figure 4.73**). The water elevations in the current simulation decreased continuously with the simulation time. The water elevations at the end of the simulation time in 2046 were between 2.7 and 4.8 m at the existing well field and between 6.5 and 8.8 m at the new well field (**Figure 4.77**). The water elevations in BH3 at the far-field area were 14.2 m in 2026 (**Figure 4.73**) but it dropped to 12.2 m in 2046 (**Figure 4.77**).

The five drawdown contour maps are presented in **Figures 4.78 to 4.82**. The drawdown contour maps for the *Lower Limit 2* simulations also show bent contour lines around the two well fields. The general drawdowns were approximately 1.6 m around the existing well field and 2.8 m around the new well field in 2026 (**Figure 4.78**). The drawdowns increased with time and dropped to approximately 2.4 m around the existing well field and 4.4 m around the new well field in 2046 (**Figure 4.82**). The drawdowns in BH3 were approximately 3.4 m in 2026 and 5.4 m in 2046.

4.2.5 Particle Tracking

The computed pathways and travel times for the six production wells are presented in **Figures 4.83 to 4.88** using the backward tracking method with a porosity of 30%. Each pathway shows the travel time symbols ranging from 1 year to 25 years. Based on the particle tracking results, the main groundwater source for the two well fields is Long Gull Pond and the area in between Long Gull Pond and the well fields. When the computed groundwater elevations increase, such as produced by the recharge input values for the *Upper Limit 1 and Upper Limit 2* simulations (**Figures 4.85 and 4.86**), the groundwater can be traced from the recharge areas at the topographically higher locations to the well fields without drawing significant quantities of water from known areas of groundwater impacts from former industrial and military activities. As such the model predicts that, other than flow system induced changes in water chemistry produced by increased recharge rates or by changes in water quality in the recharge areas, there should be no impact on the current well field water quality over the time. The main source of changes in water quality at the well fields is expected to be caused by any induced upwelling of groundwater from the underlying bedrock. Regular sampling of the deep piezometers in each well field is expected to give an adequate warning of any impending changes in water quality over time.

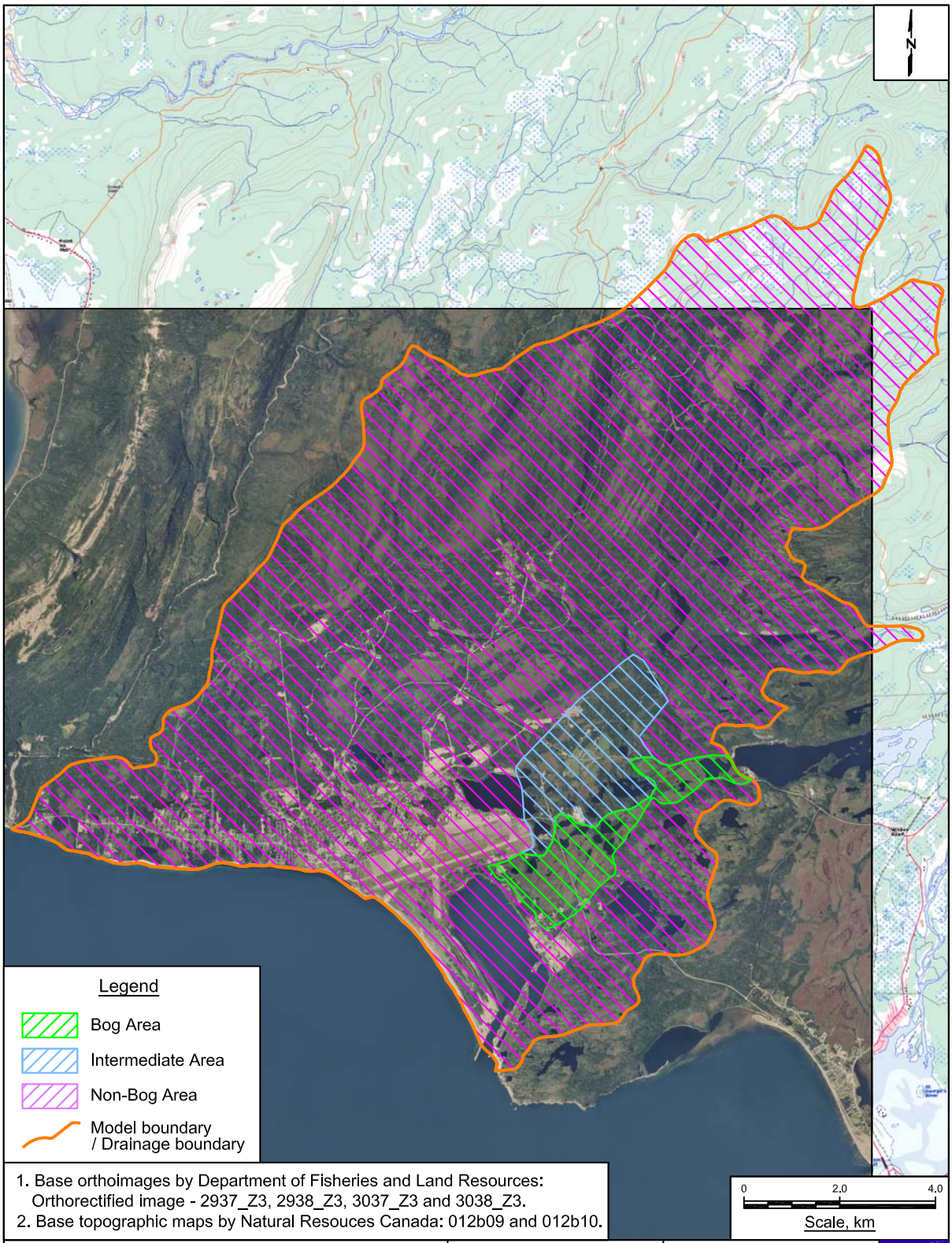

Figure 4.1 The pattern of recharge assigned to the 3D model for model calibration.

Project No. 3113	Document Reference FFC-NL-3113-057b
Location Stephenville, NL	Date December 2022

FFC

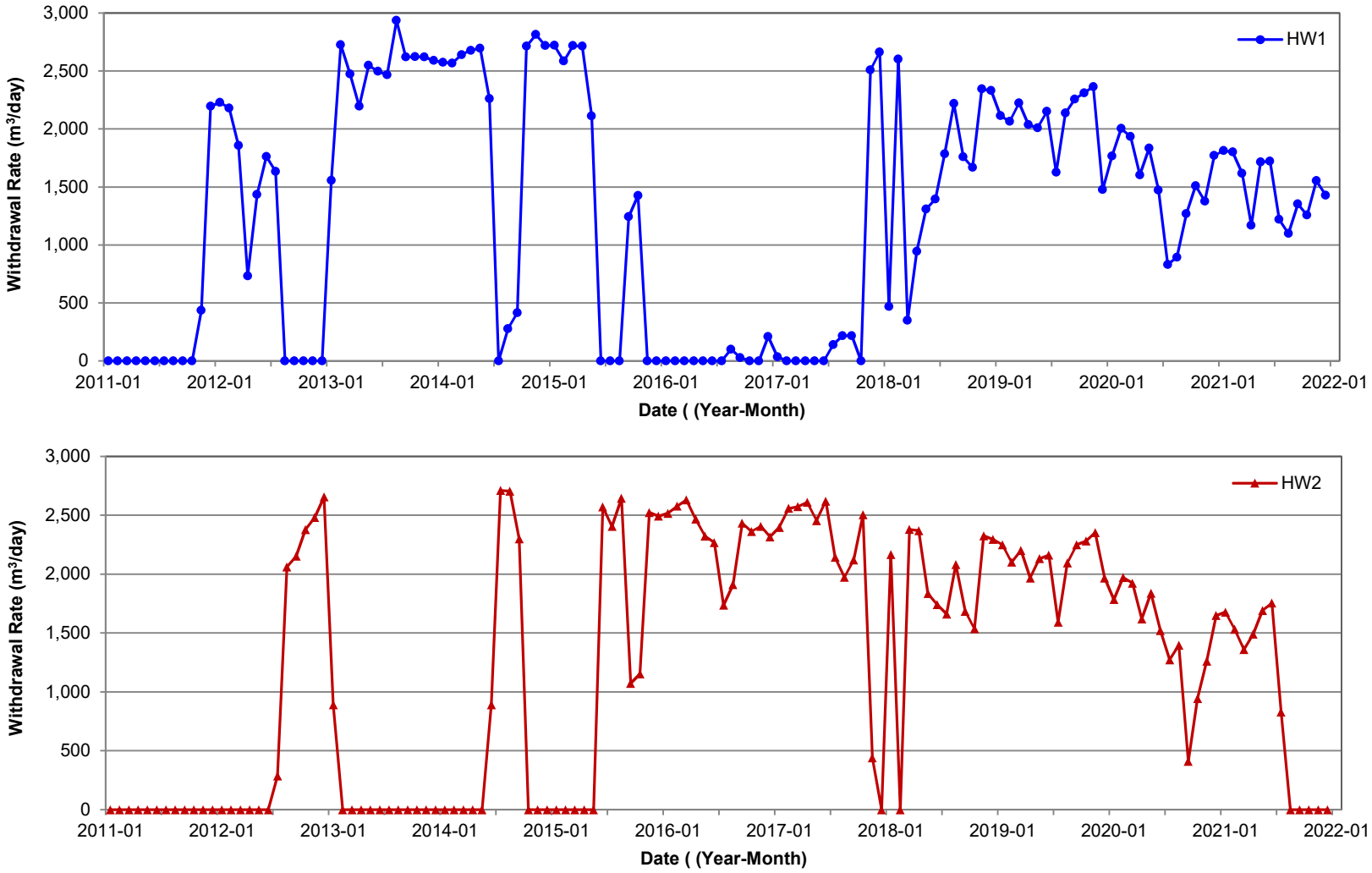

Figure 4.2a Withdrawal rates in cubic metre per day as the source/sink input parameters in the 3D model for HW1 and HW2 between 2011 and 2021.

Project No.	Document Reference
3113	FFC-NL-3113-057b
Location	Date
Stephenville, NL	December 2022

FFC

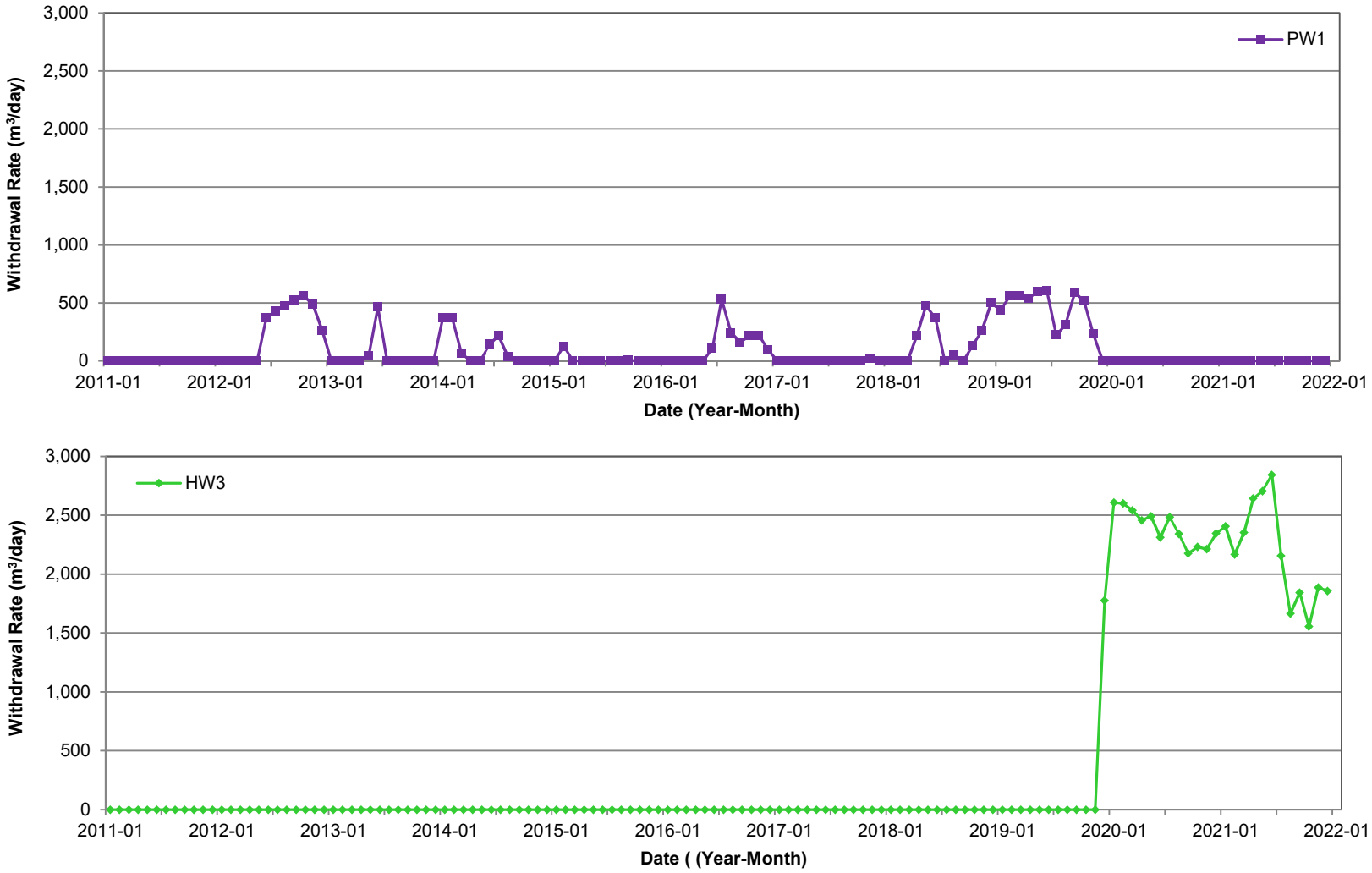

Figure 4.2b Withdrawal rates in cubic metre per day as the source/sink input parameters in the 3D model for PW1 and HW3 between 2011 and 2021.

Project No. 3113	Document Reference FFC-NL-3113-057b
Location Stephenville, NL	Date December 2022

FFC

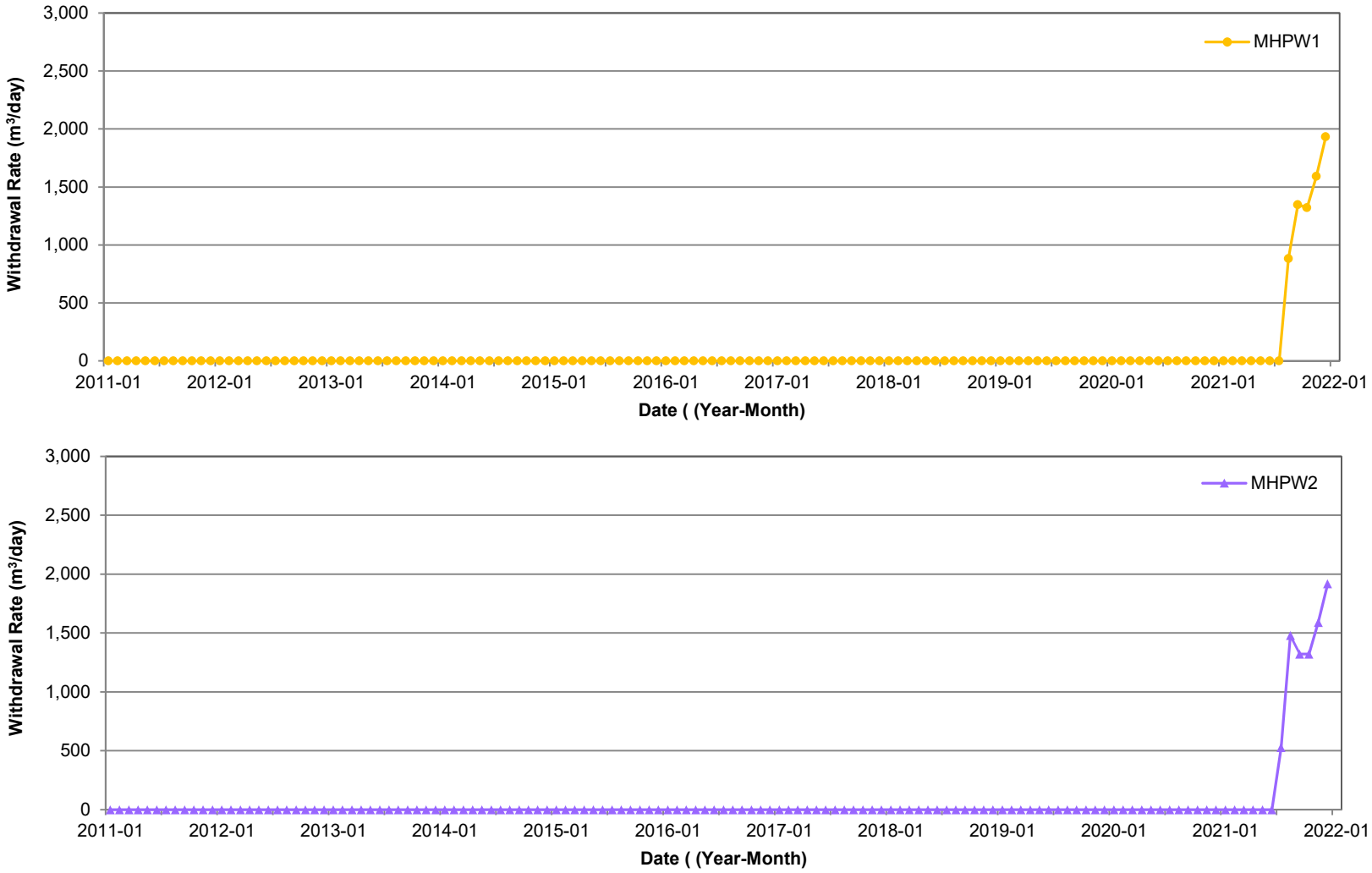

Figure 4.2c Withdrawal rates in cubic metre per day as the source/sink input parameters in the 3D model for MHPW1 and MHPW2 between 2011 and 2021.

Project No. 3113	Document Reference FFC-NL-3113-057b
Location Stephenville, NL	Date December 2022

FFC

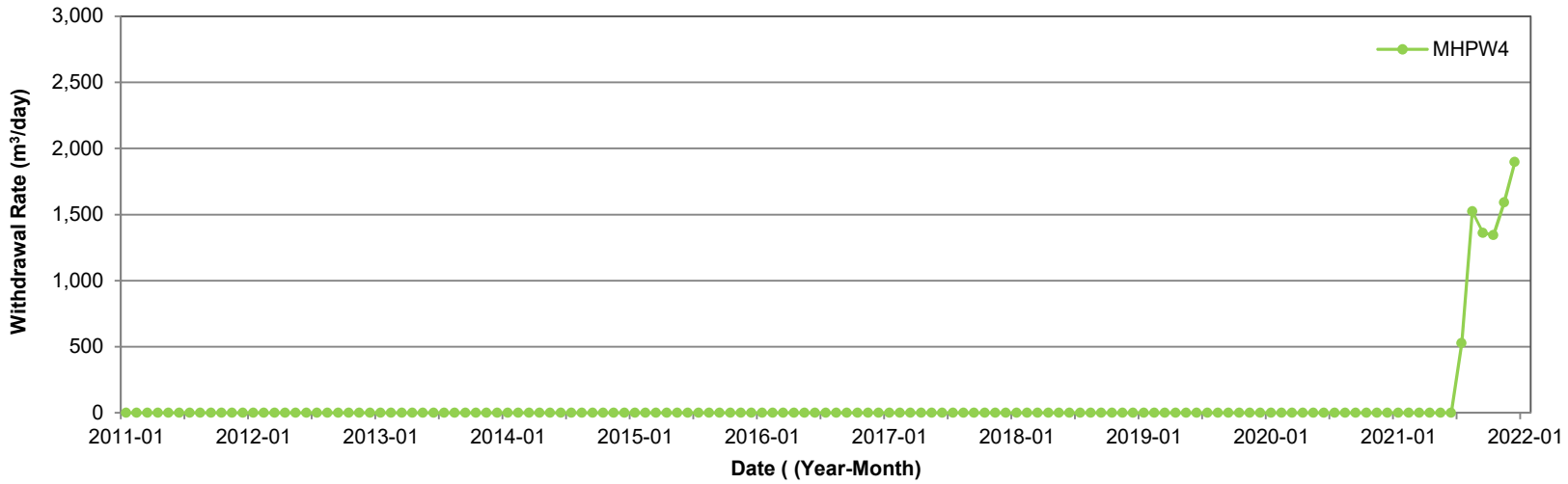

Figure 4.2d Withdrawal rates in cubic metre per day as the source/sink input parameters in the 3D model for MHPW4 between 2011 and 2021.

Project No. 3113	Document Reference FFC-NL-3113-057b
Location Stephenville, NL	Date December 2022

FFC

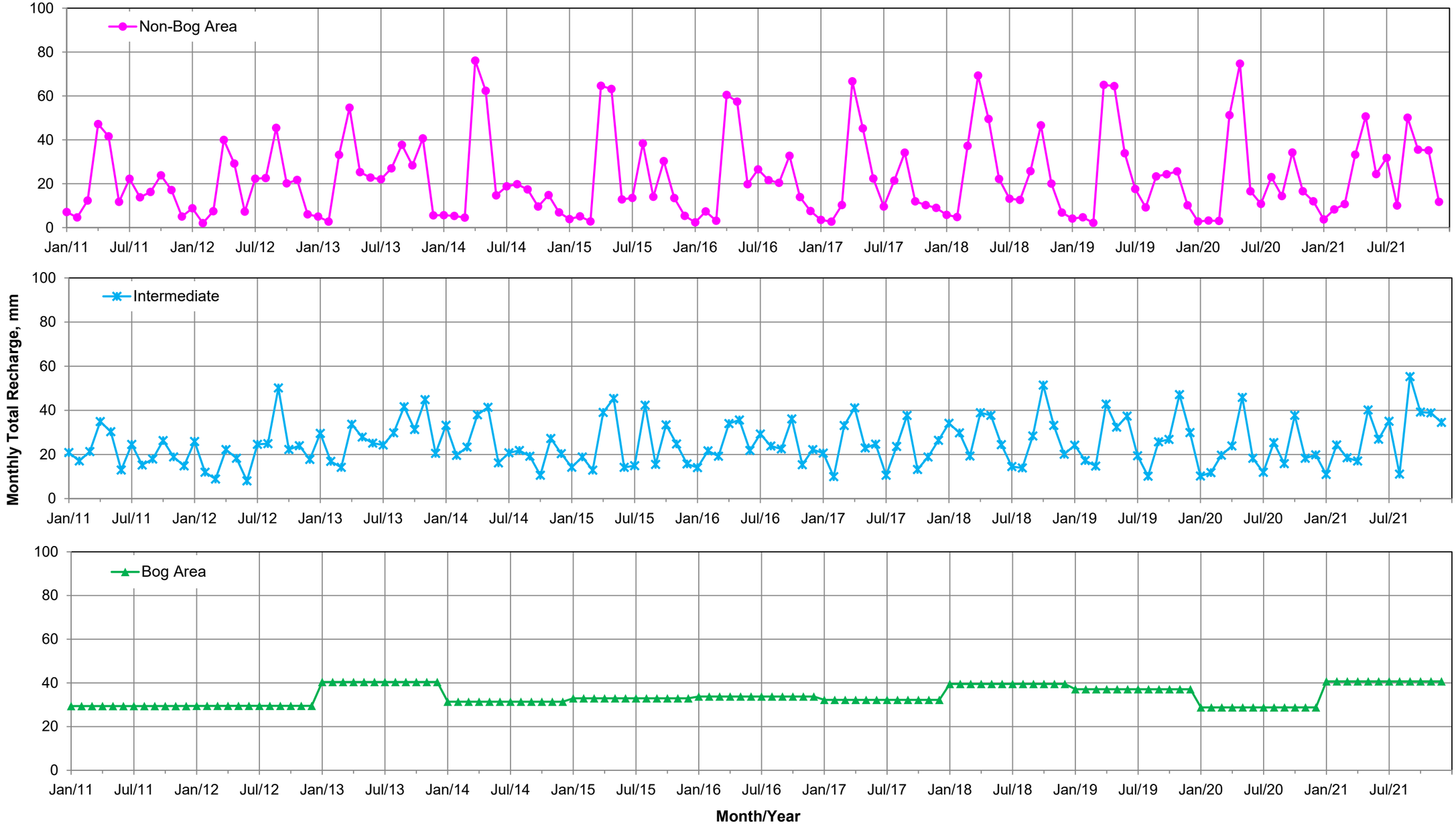

Figure 4.3 Monthly total recharge assigned for the 3D hydrogeological model. The recharge values are calculated based on the climate data from *Stephenville A* station (ID 8403800).

Project No.	Document Reference
3113	FFC-NL-3113-057b
Location	Date
Stephenville, NL	December 2022

FFC

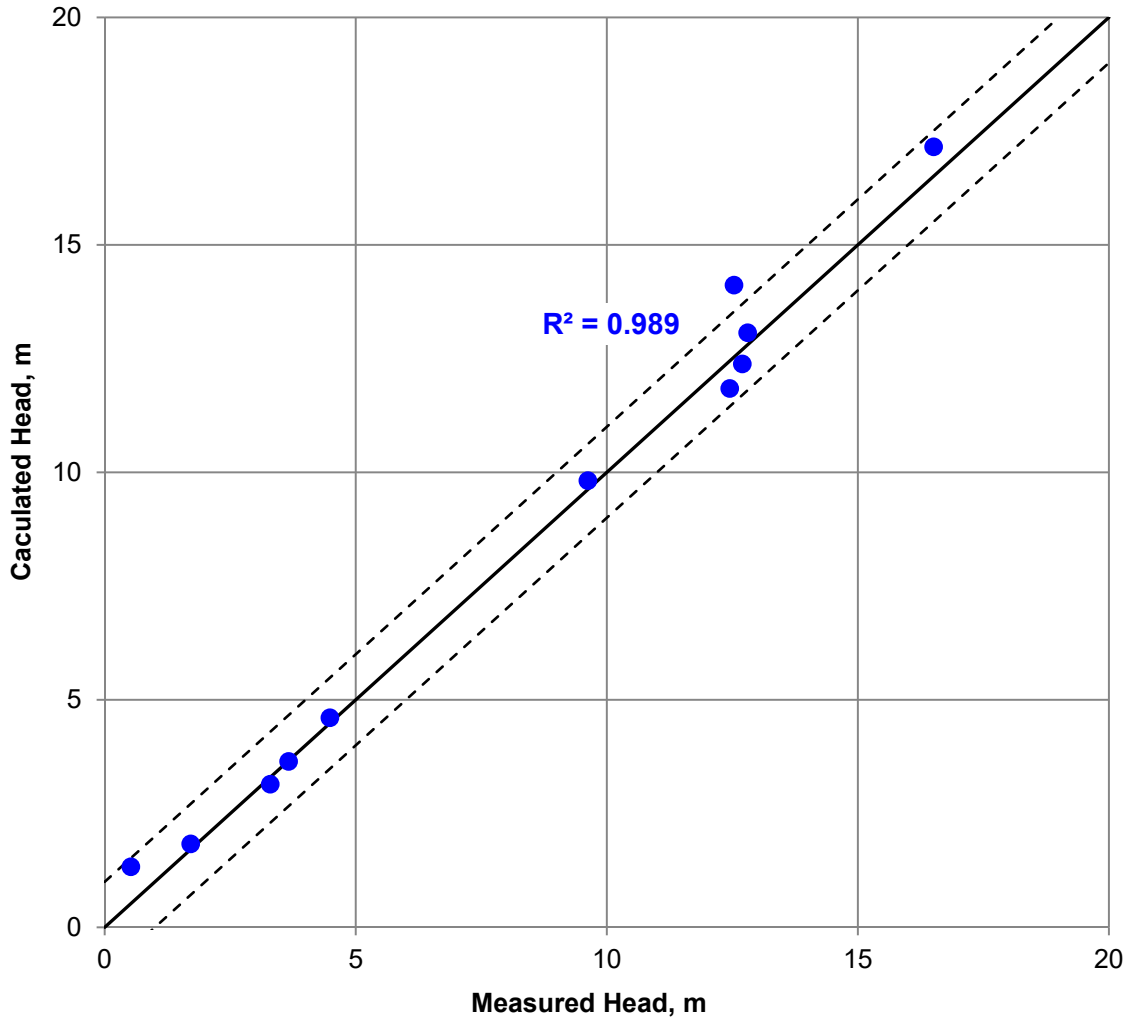

Figure 4.4 Plot of measured versus hydraulic heads that were computed by the 3D model at the available locations for September 30, 2019.

Project No.	Document Reference
3113	FFC-NL-3113-057b
Location	Date
Stephenville, NL	December 2022

FFC

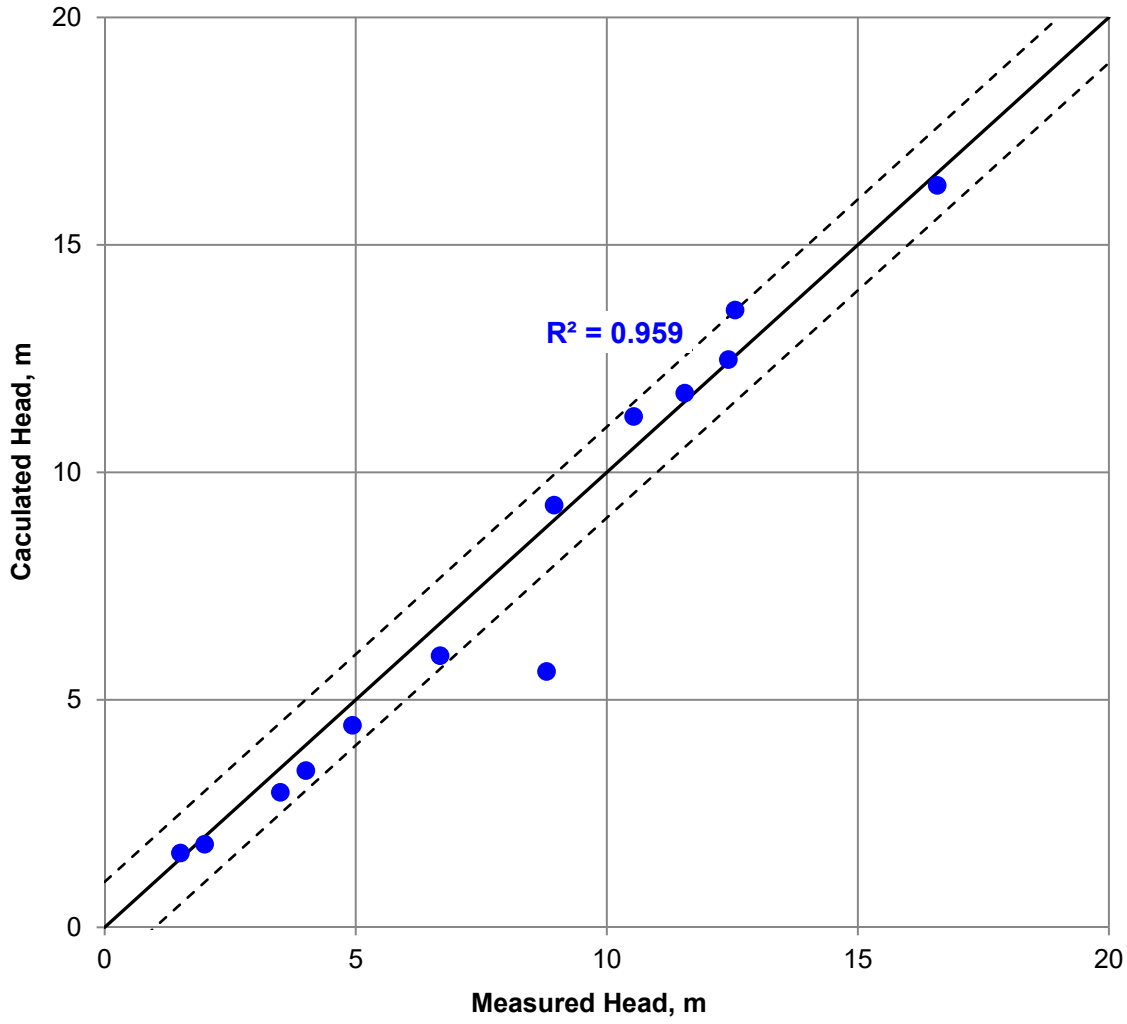

Figure 4.5 Plot of measured versus hydraulic heads that were computed by the 3D model at the available locations for April 30, 2021.

Project No.	Document Reference
3113	FFC-NL-3113-057b
Location	Date
Stephenville, NL	December 2022

FFC

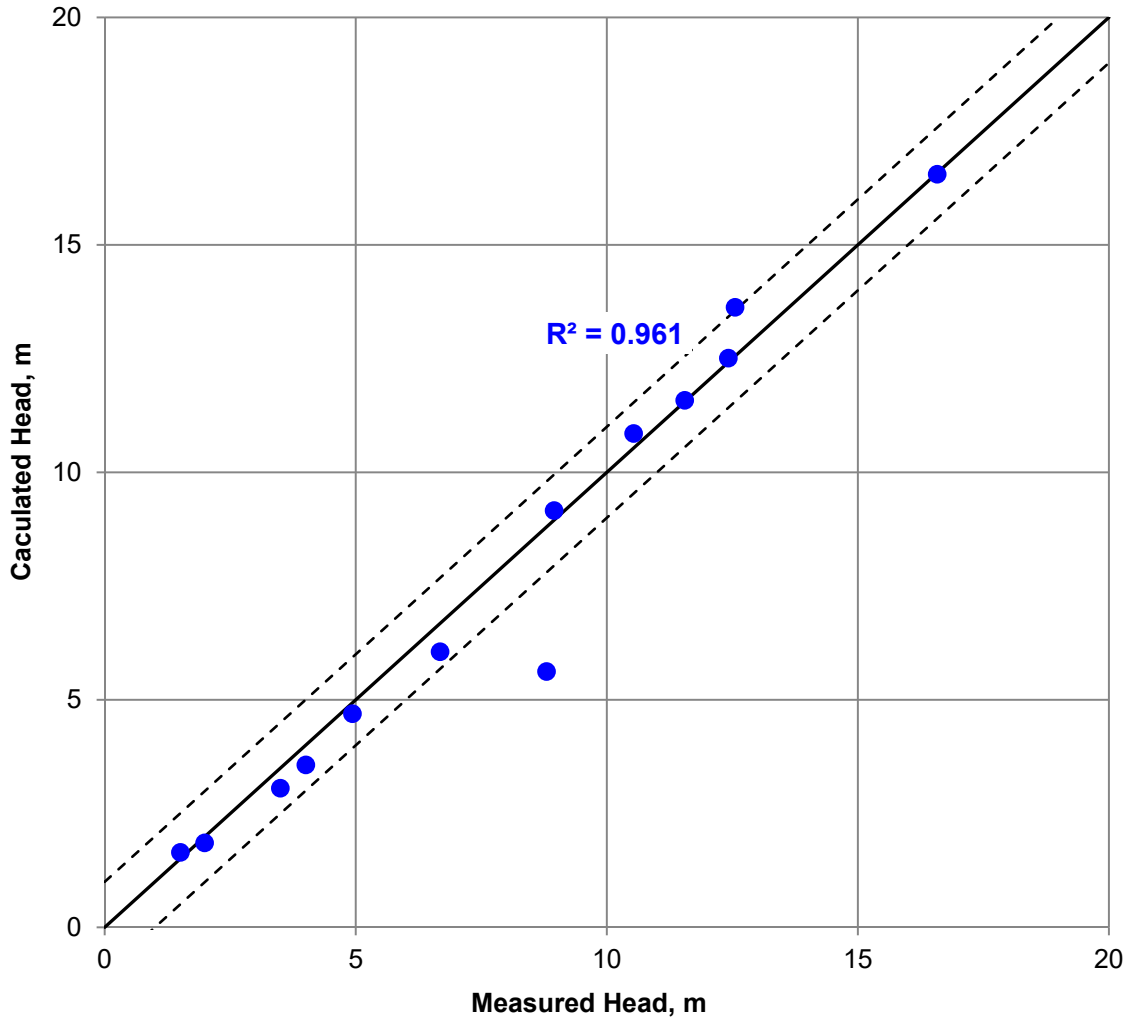

Figure 4.6 Plot of measured versus hydraulic heads that were computed by the 3D model at the available locations for August 31, 2021.

Project No.	Document Reference
3113	FFC-NL-3113-057b
Location	Date
Stephenville, NL	December 2022

FFC

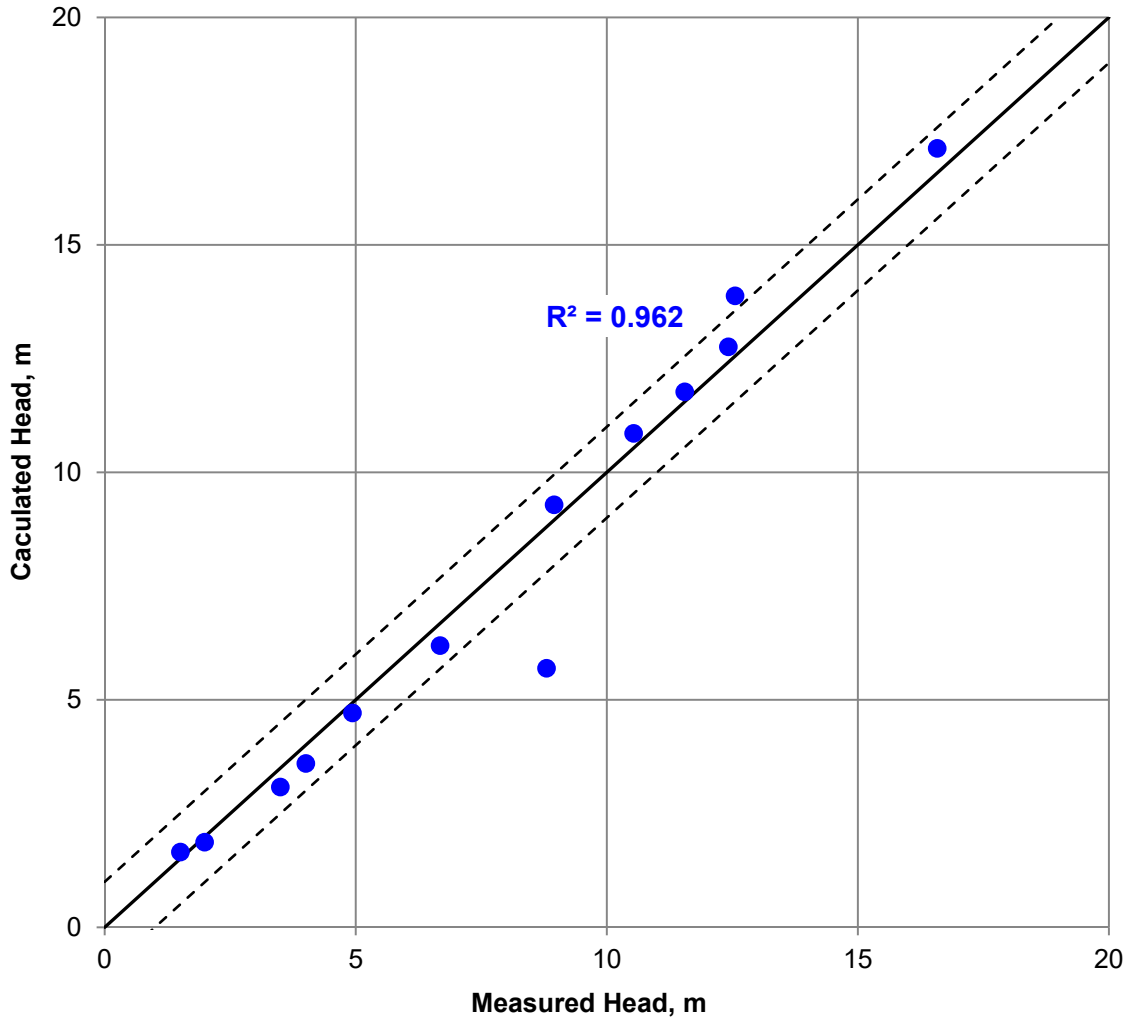

Figure 4.7 Plot of measured versus hydraulic heads that were computed by the 3D model at the available locations for December 31, 2021.

Project No.	Document Reference
3113	FFC-NL-3113-057b
Location	Date
Stephenville, NL	December 2022

FFC

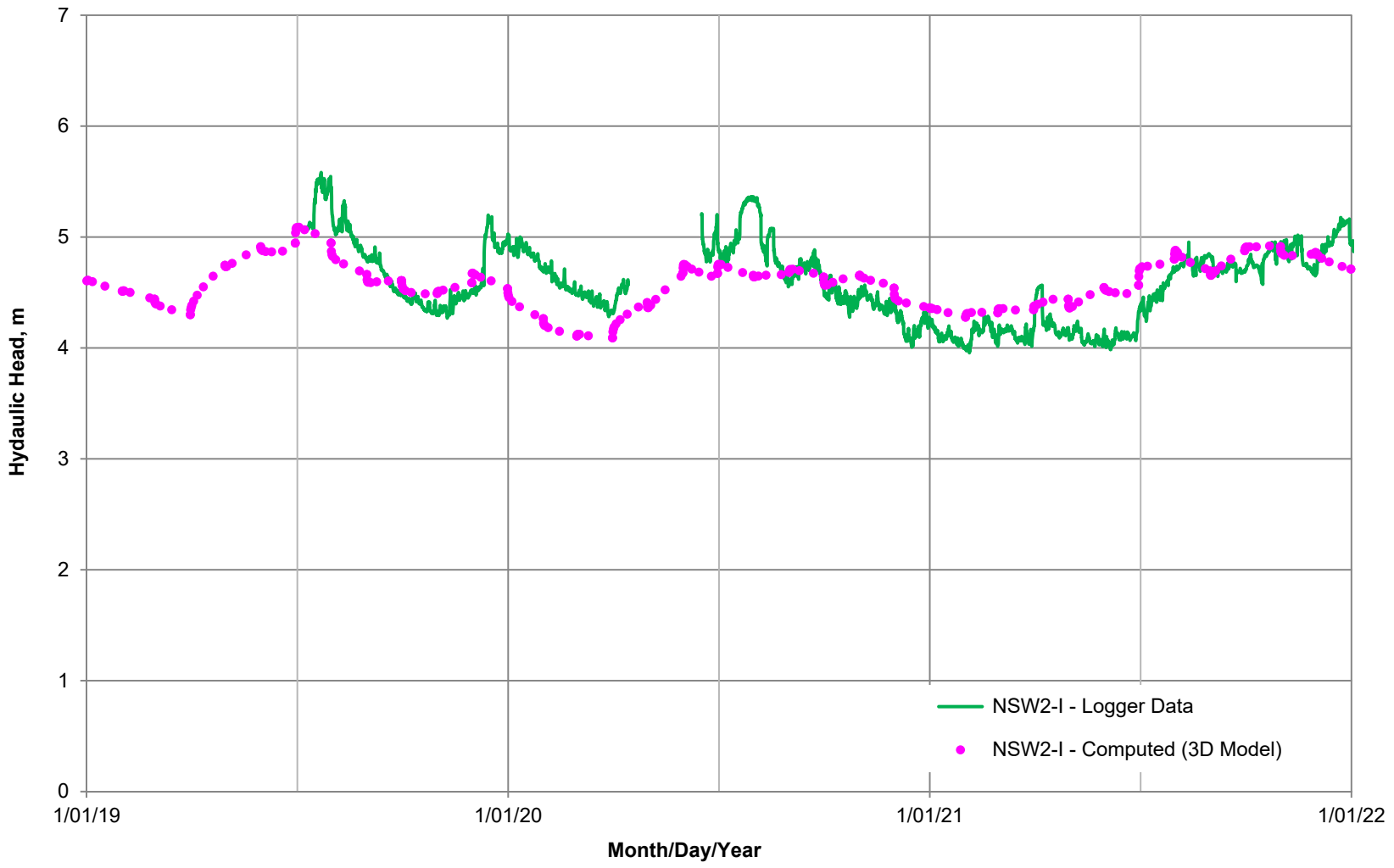

Figure 4.8a Plot of measured (green) versus computed (magenta) hydraulic heads for the near-field monitoring well, NSW2-I, between 2019 and 2021.

Project No. 3113	Document Reference FFC-NL-3113-057b
Location Stephenville, NL	Date December 2022

FFC

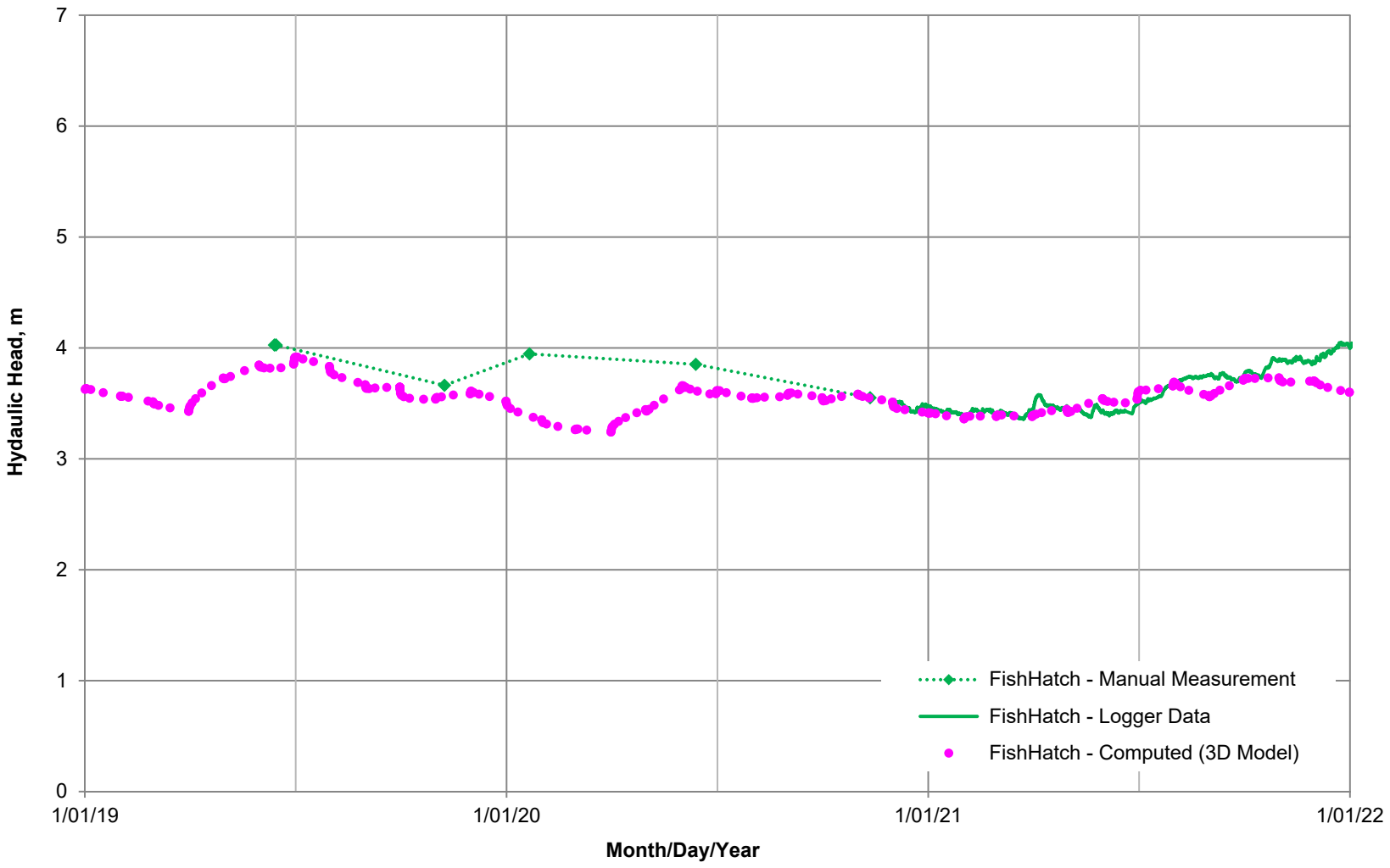

Figure 4.8b Plot of measured (green) versus computed (magenta) hydraulic heads for the near-field monitoringwell, FishHatch, between 2019 and 2021.

Project No. 3113	Document Reference FFC-NL-3113-057b
Location Stephenville, NL	Date December 2022

FFC

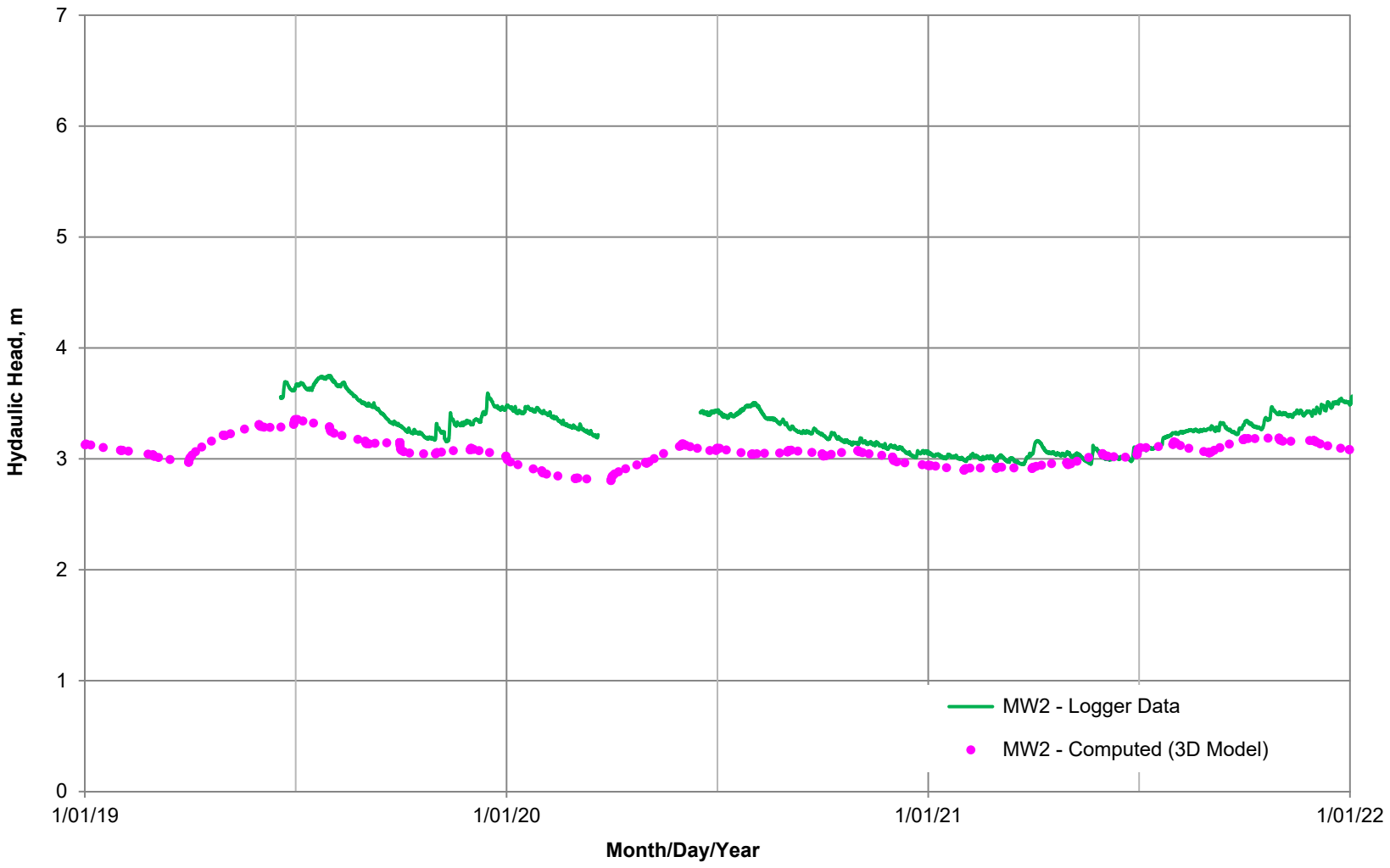

Figure 4.8c Plot of measured (green) versus computed (magenta) hydraulic heads for the near-field monitoring well, MW2, between 2019 and 2021.

Project No. 3113	Document Reference FFC-NL-3113-057b
Location Stephenville, NL	Date December 2022

FFC

Figure 4.8d Plot of measured (green) versus computed (magenta) hydraulic heads for the near-field monitoring well, FHM3, between 2019 and 2021.

Project No. 3113	Document Reference FFC-NL-3113-057b
Location Stephenville, NL	Date December 2022

FFC

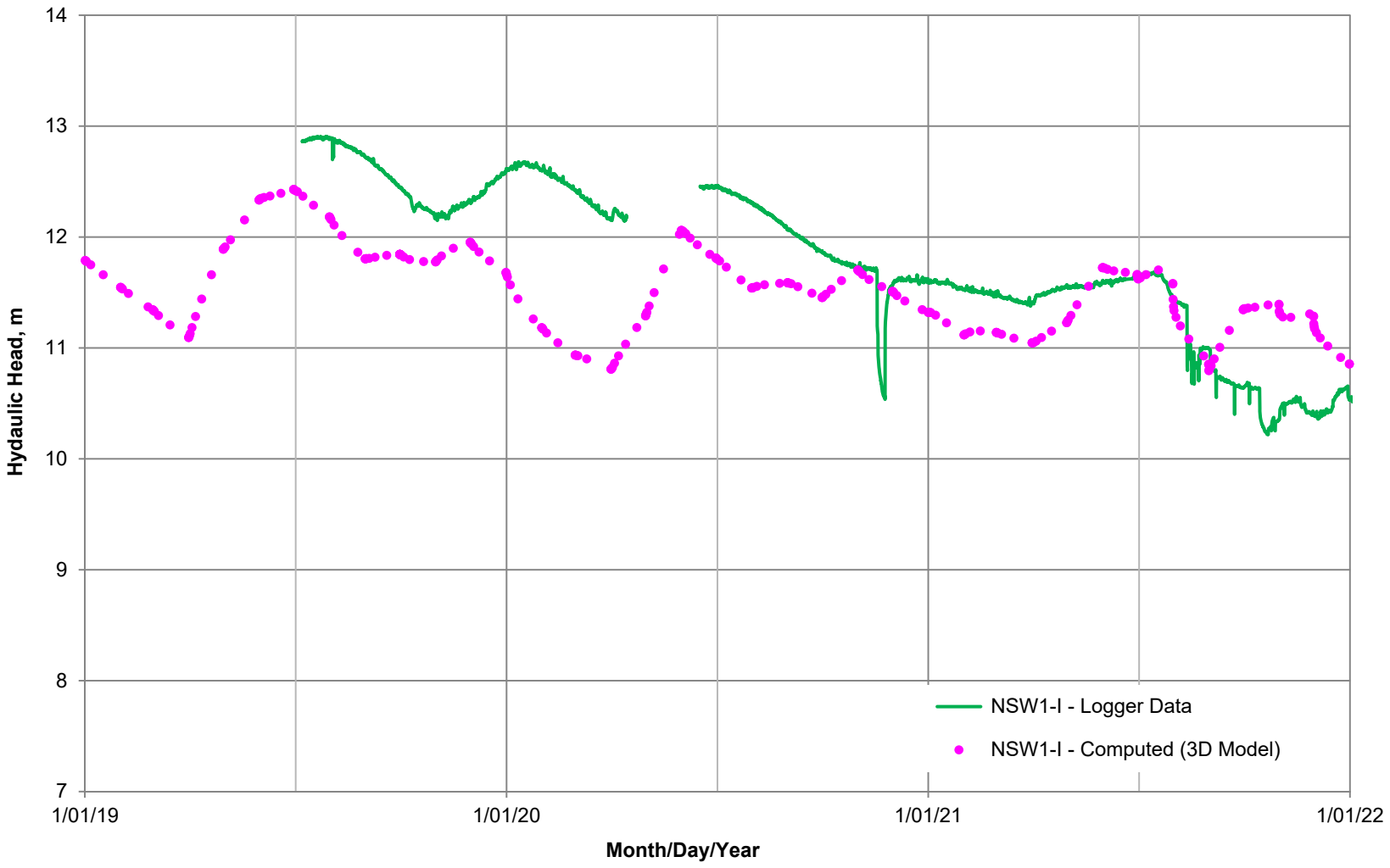

Figure 4.8e Plot of measured (green) versus computed (magenta) hydraulic heads for the near-field monitoring well, NSW1-I, between 2019 and 2021.

Project No. 3113	Document Reference FFC-NL-3113-057b
Location Stephenville, NL	Date December 2022

FFC

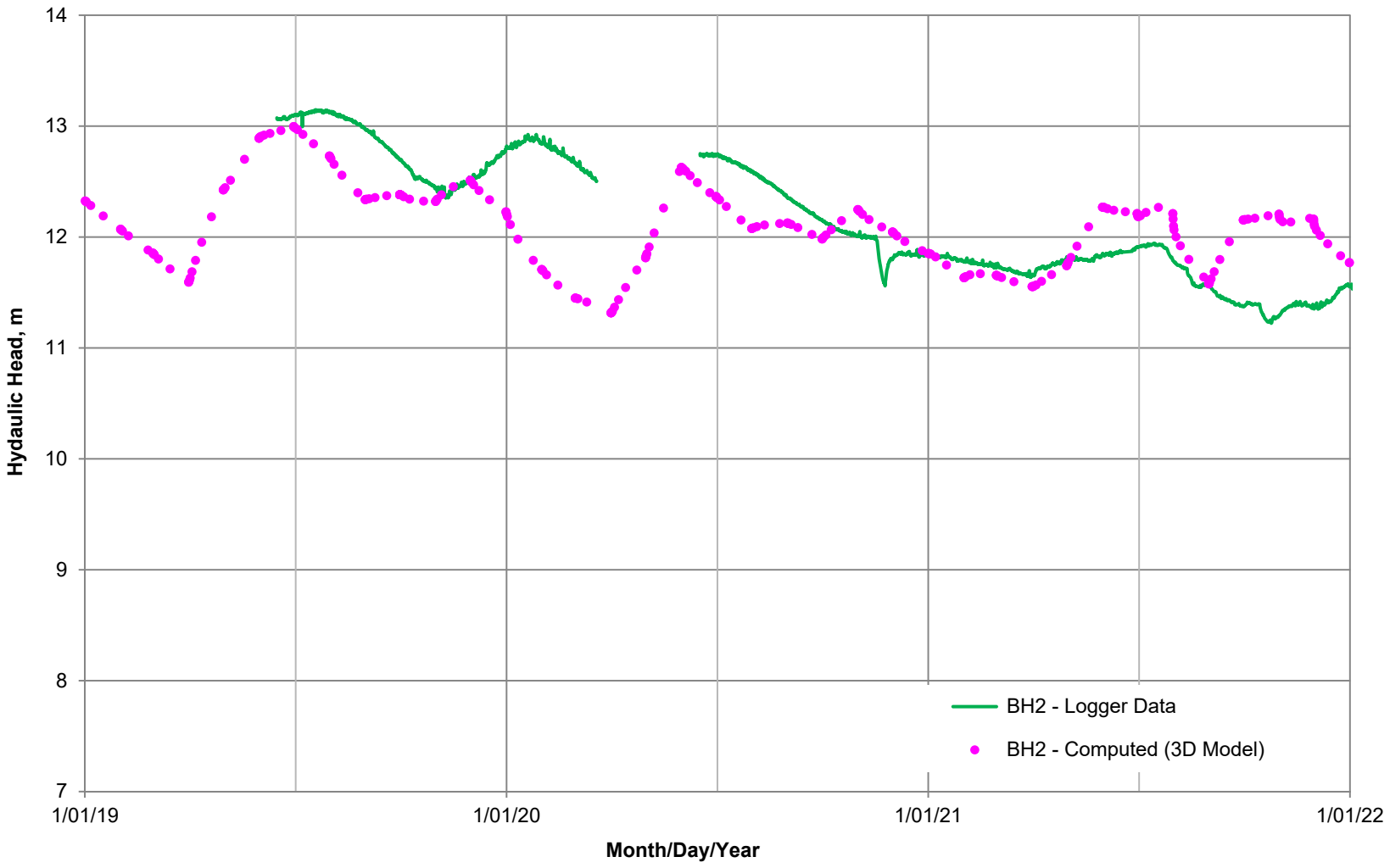

Figure 4.8f Plot of measured (green) versus computed (magenta) hydraulic heads for the near-field monitoring well, BH2, between 2019 and 2021.

Project No. 3113	Document Reference FFC-NL-3113-057b
Location Stephenville, NL	Date December 2022

FFC

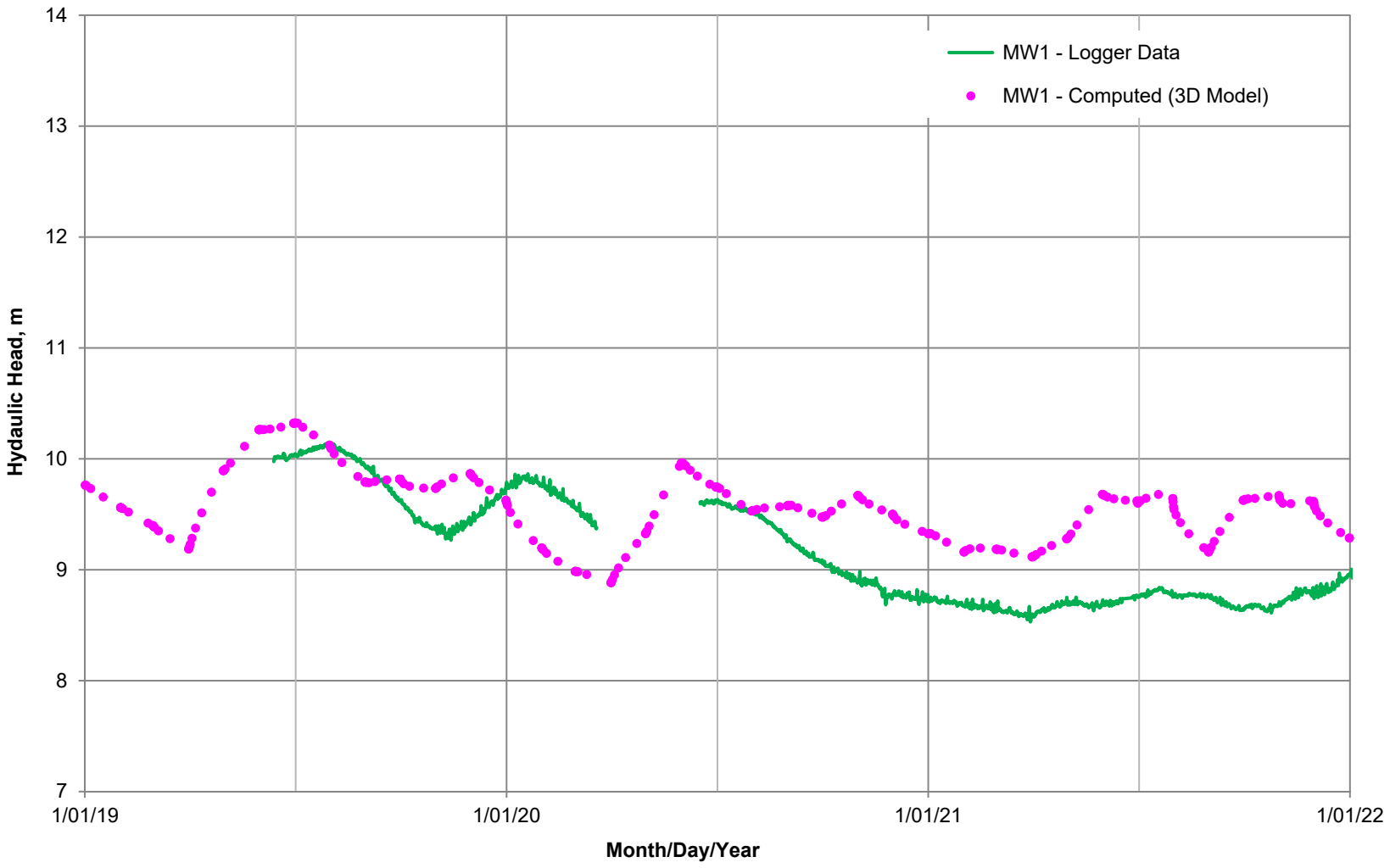

Figure 4.8g Plot of measured (green) versus computed (magenta) hydraulic heads for the near-field monitoring well, MW1, between 2019 and 2021.

Project No. 3113	Document Reference FFC-NL-3113-057b
Location Stephenville, NL	Date December 2022

FFC

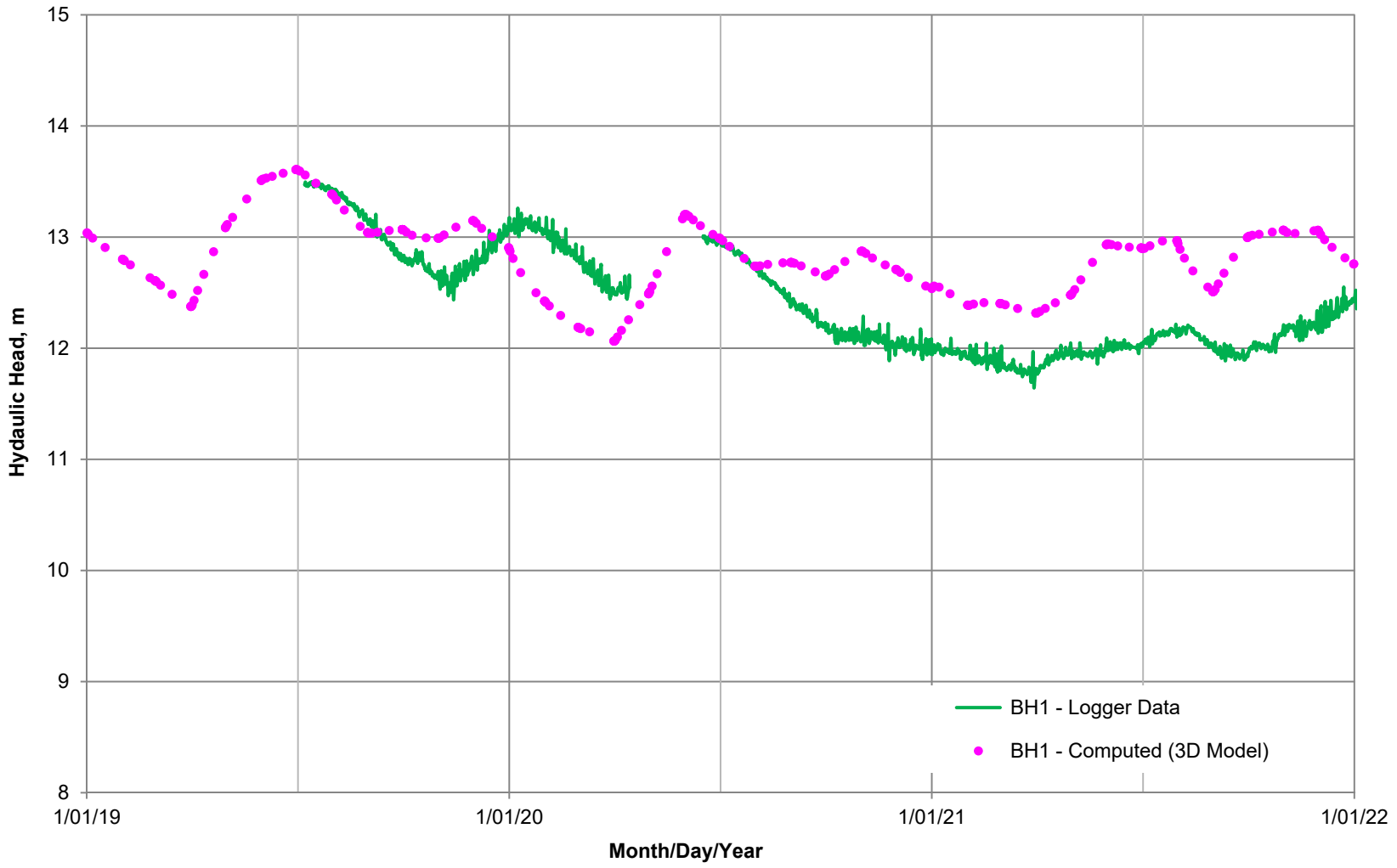

Figure 4.9a Plot of measured (green) versus computed (magenta) hydraulic heads for the far-field monitoring well, BH1, between 2019 and 2021.

Project No. 3113	Document Reference FFC-NL-3113-057b
Location Stephenville, NL	Date December 2022

FFC

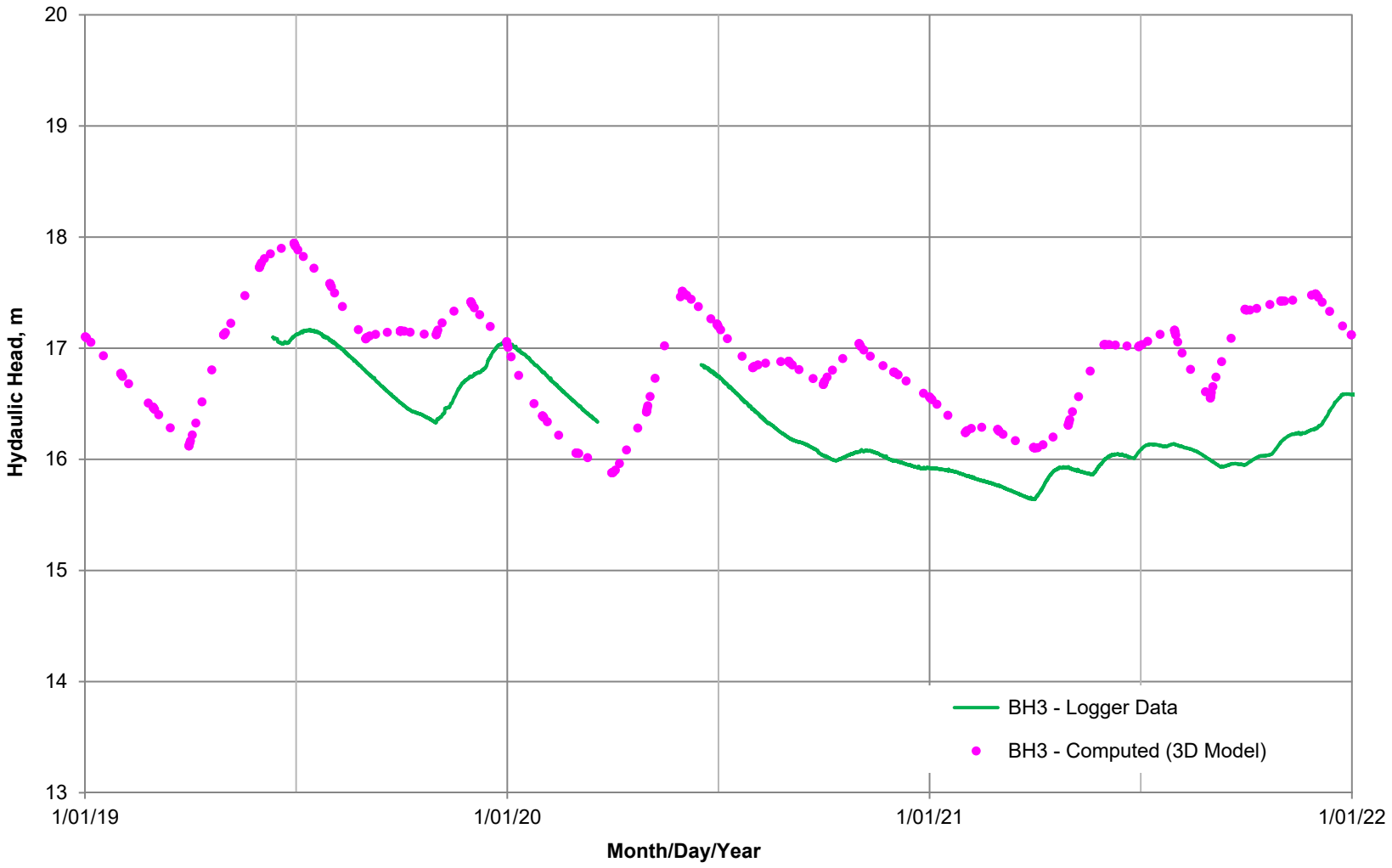

Figure 4.9b Plot of measured (green) versus computed (magenta) hydraulic heads for the far-field monitoring well, BH3, between 2019 and 2021.

Project No. 3113	Document Reference FFC-NL-3113-057b
Location Stephenville, NL	Date December 2022

FFC

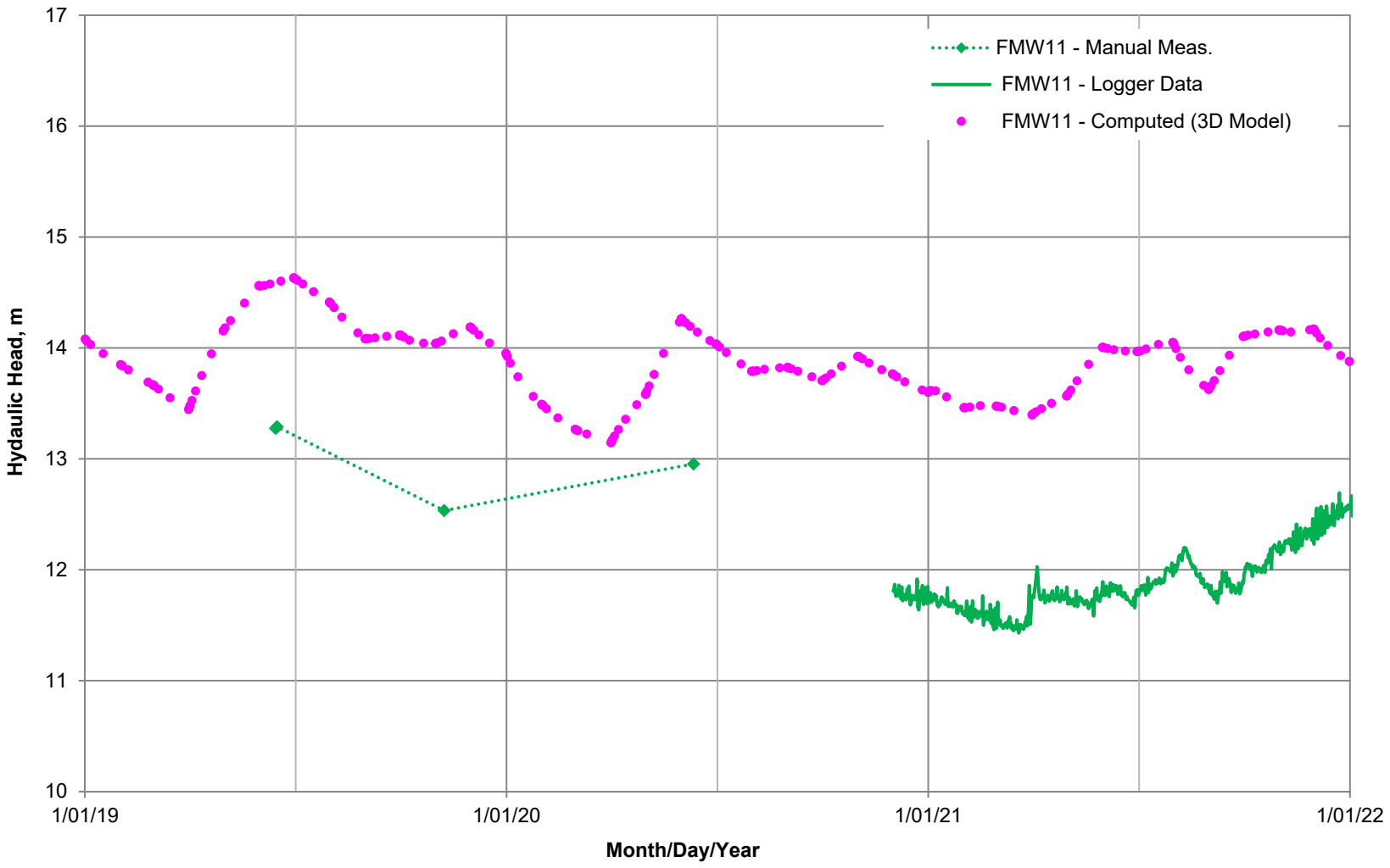

Figure 4.9c Plot of measured (green) versus computed (magenta) hydraulic heads for the far-field monitoring well, FMW11, between 2019 and 2021.

Project No. 3113	Document Reference FFC-NL-3113-057b
Location Stephenville, NL	Date December 2022

FFC

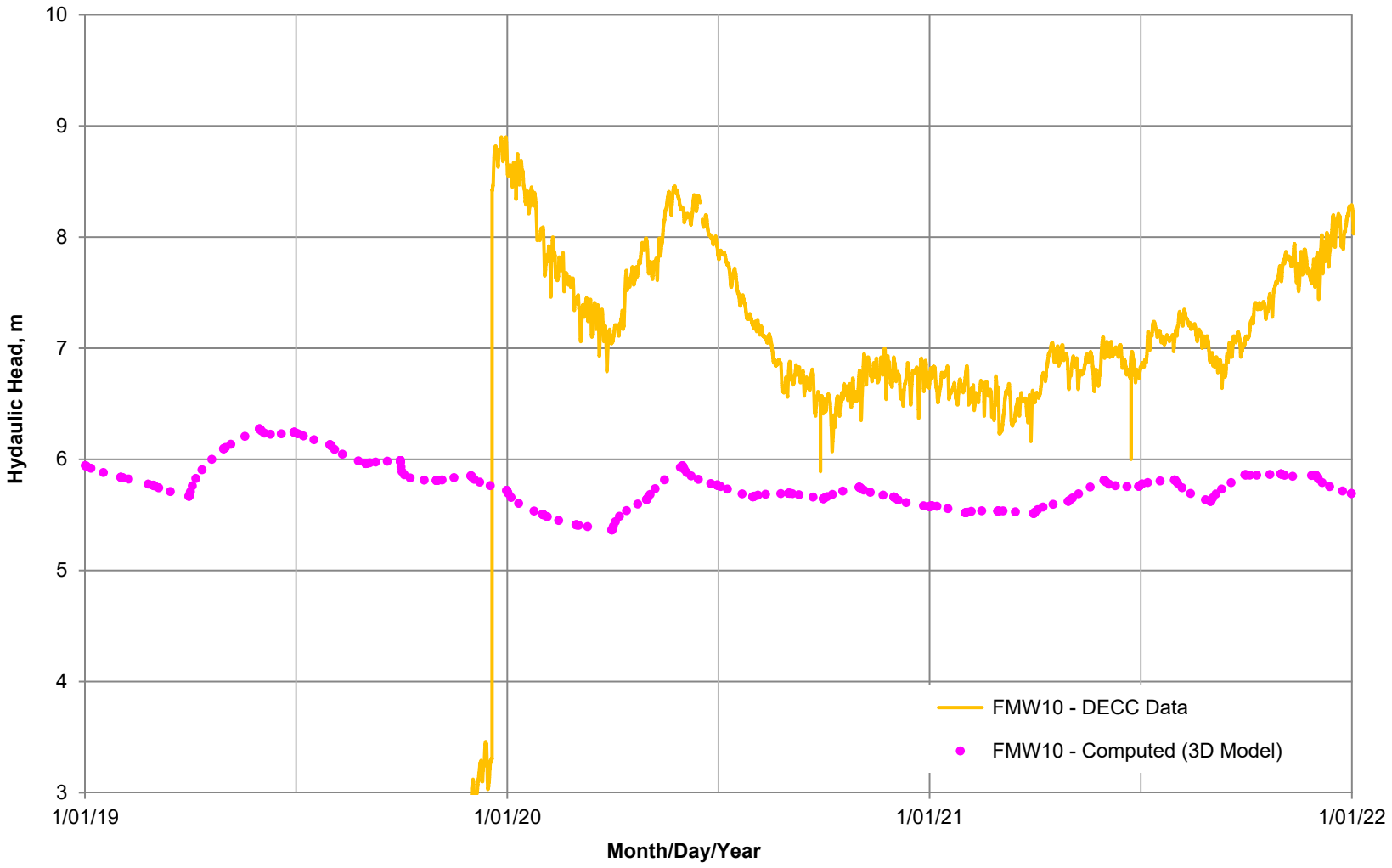

Figure 4.10a Plot of DECC data (yellow) versus computed (magenta) hydraulic heads for the monitoring well, FMW10, between 2019 and 2021.

Project No. 3113	Document Reference FFC-NL-3113-057b
Location Stephenville, NL	Date December 2022

FFC

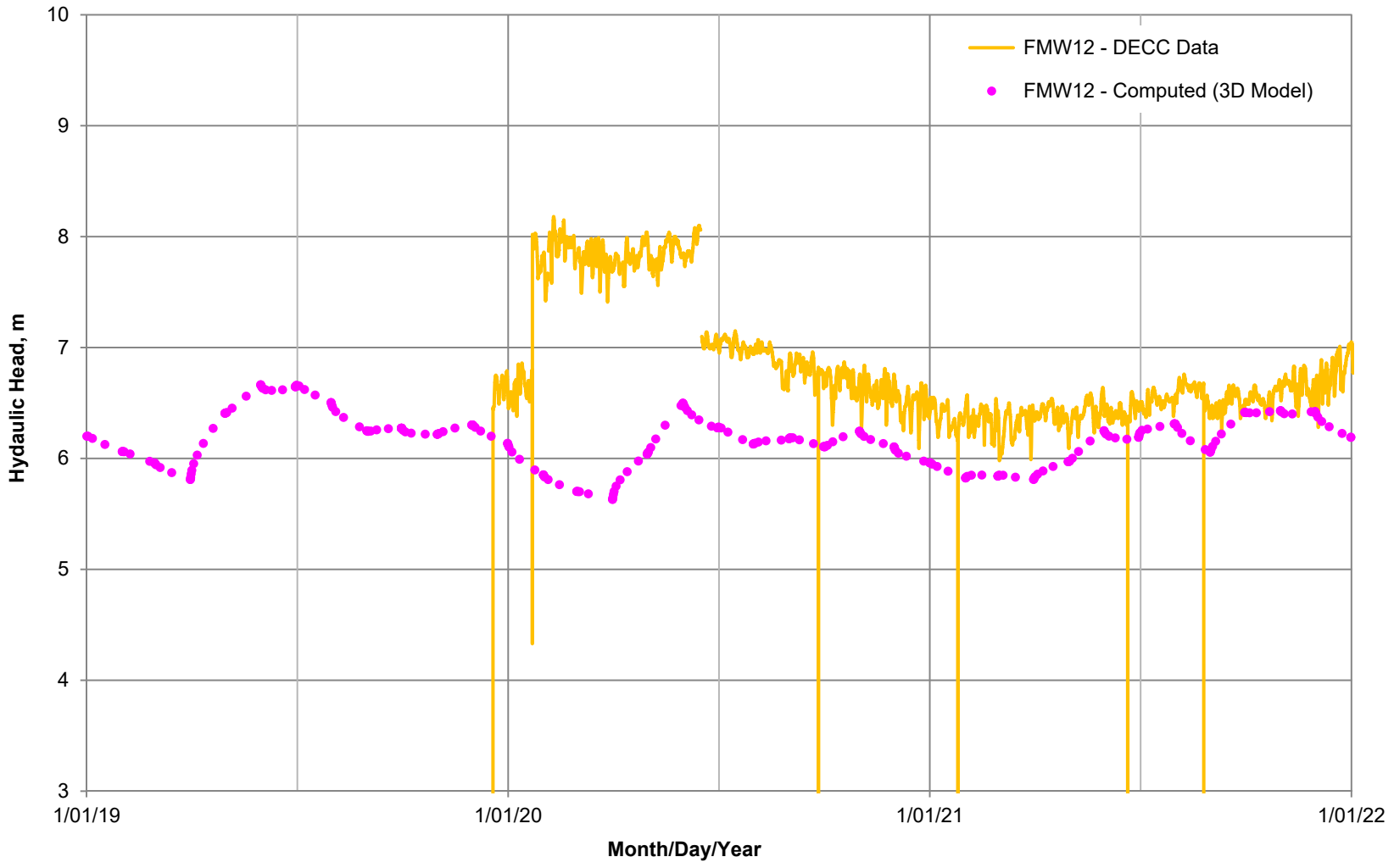

Figure 4.10b Plot of DECC data (yellow) versus computed (magenta) hydraulic heads for the monitoring well, FMW12, between 2019 and 2021.

Project No. 3113	Document Reference FFC-NL-3113-057b
Location Stephenville, NL	Date December 2022

FFC

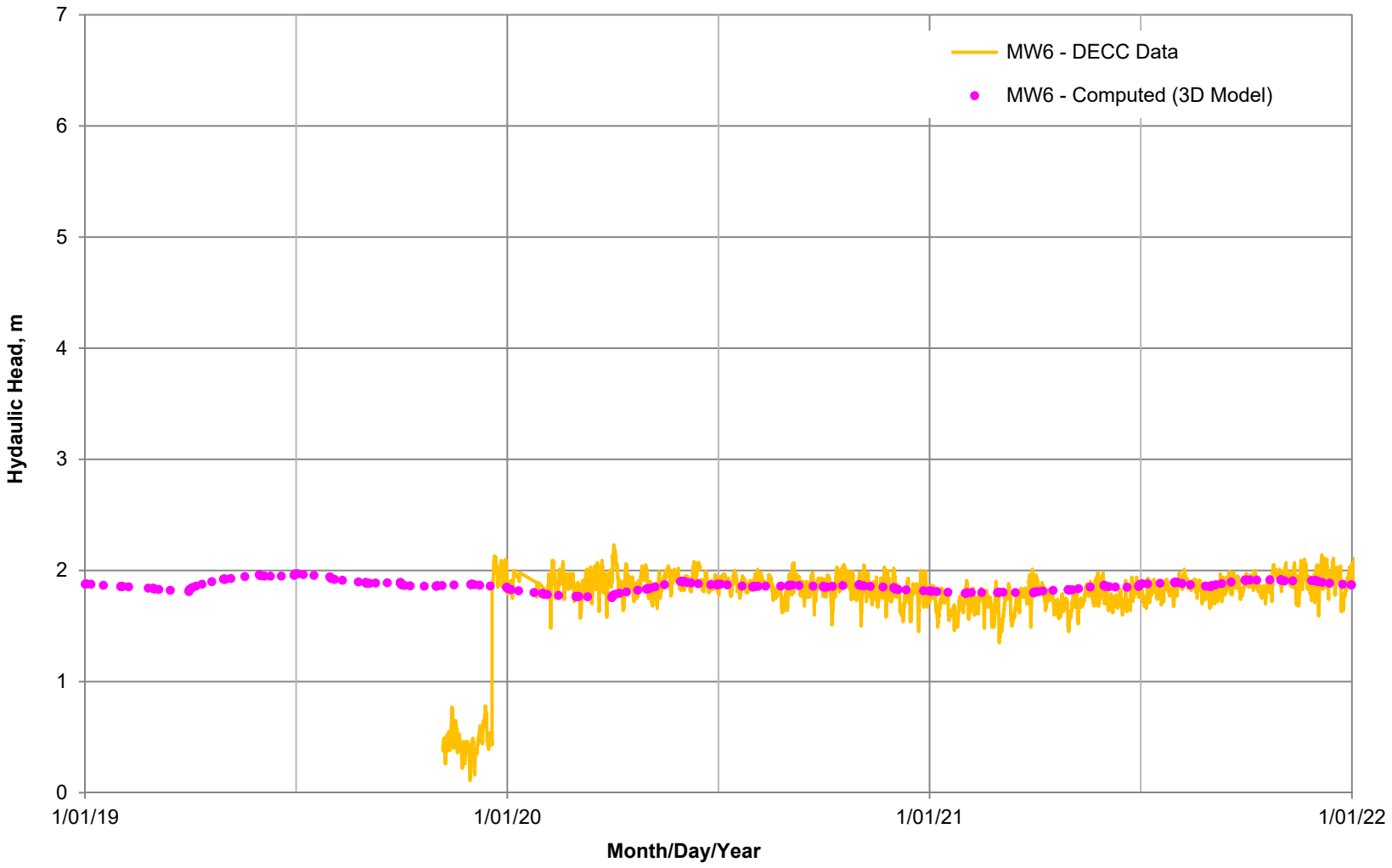

Figure 4.10c Plot of DECC data (yellow) versus computed (magenta) hydraulic heads for the monitoring well, MW6, between 2019 and 2021.

Project No. 3113	Document Reference FFC-NL-3113-057b
Location Stephenville, NL	Date December 2022

FFC

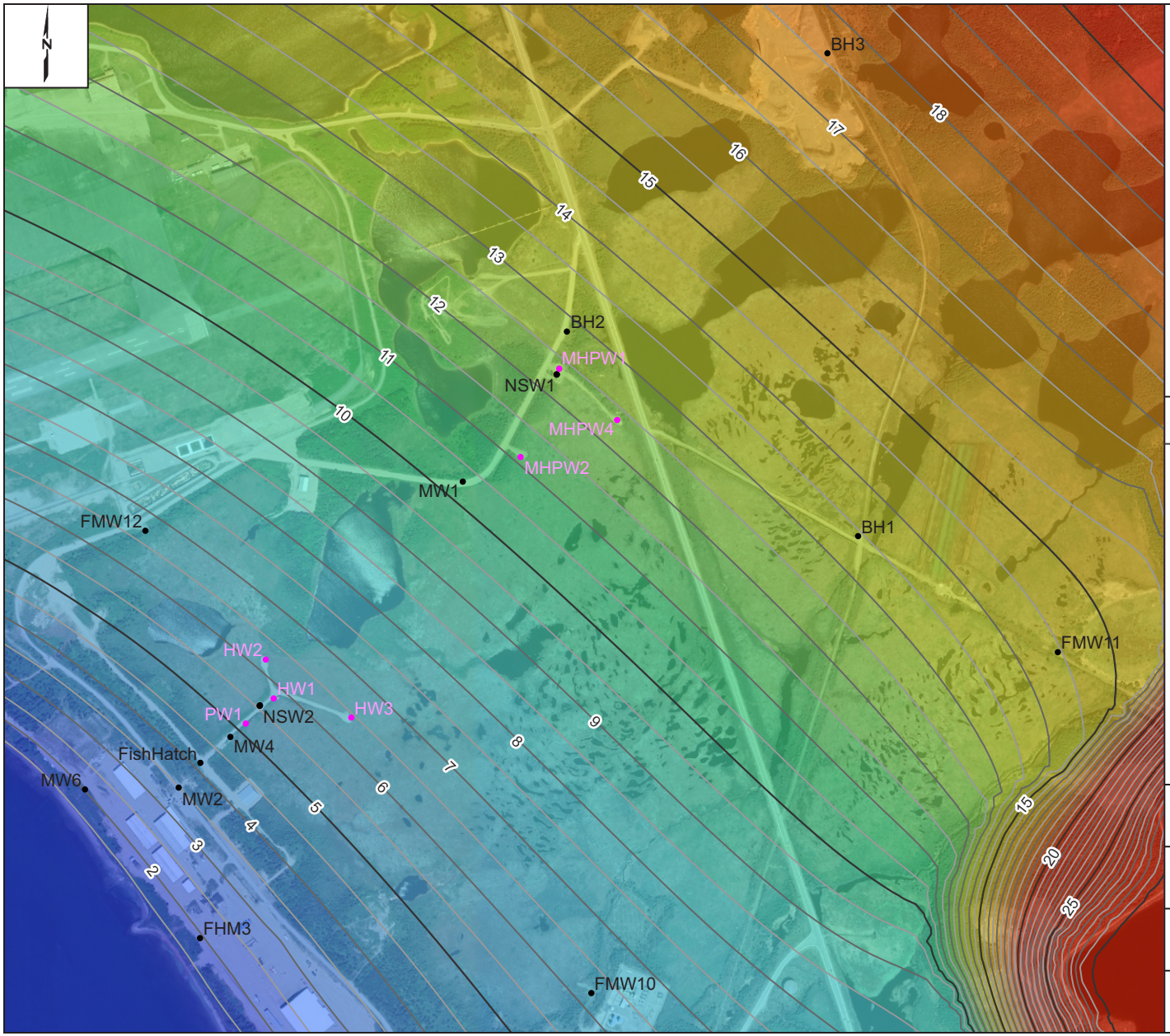

Legend

- Production well location
- Monitoring well location

Legend

Contours, m

1 5 10 15 >20

0 100 200 300 400 500

Scale, m

Note: Base orthorectified image from Google Earth (2022).

Figure 4.11

Contour map of the water elevation (hydraulic head) for the non-pumping condition under steady-state simulation at the water table level.

Document Reference	FFC-NL-3113-057b
Location	Stephenville, NL
Project No.	3113
Date	December 2022

FFC

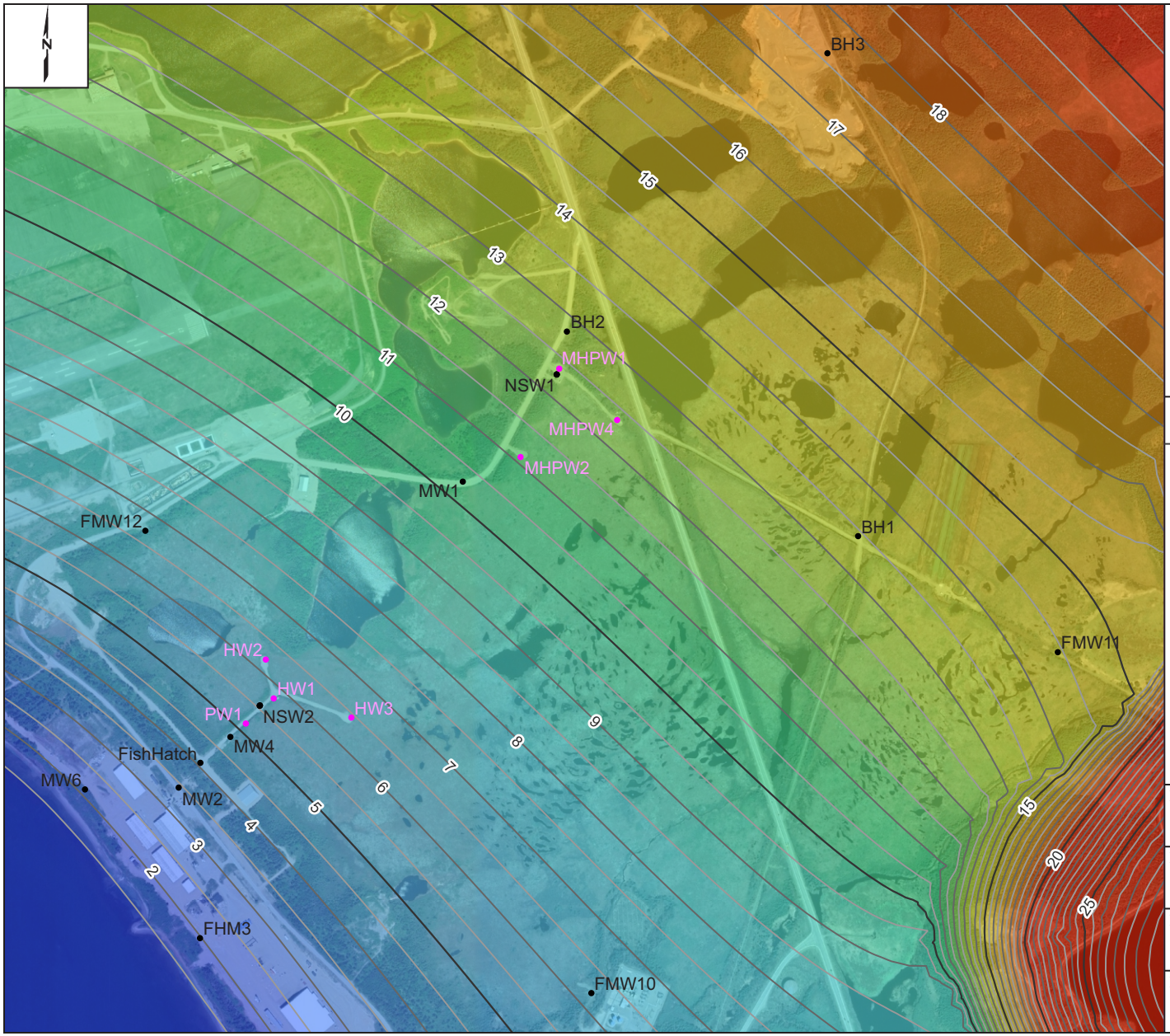

Legend

- Production well location
- Monitoring well location

Legend

Contours, m

1 5 10 15 >20

0 100 200 300 400 500

Scale, m

Note: Base orthorectified image from Google Earth (2022).

Figure 4.12

Contour map of the water elevation (hydraulic head) for the non-pumping condition under steady-state simulation at the pumping level.

Document Reference	FFC-NL-3113-057b
Location	Stephenville, NL
Project No.	3113
Date	December 2022

FFC

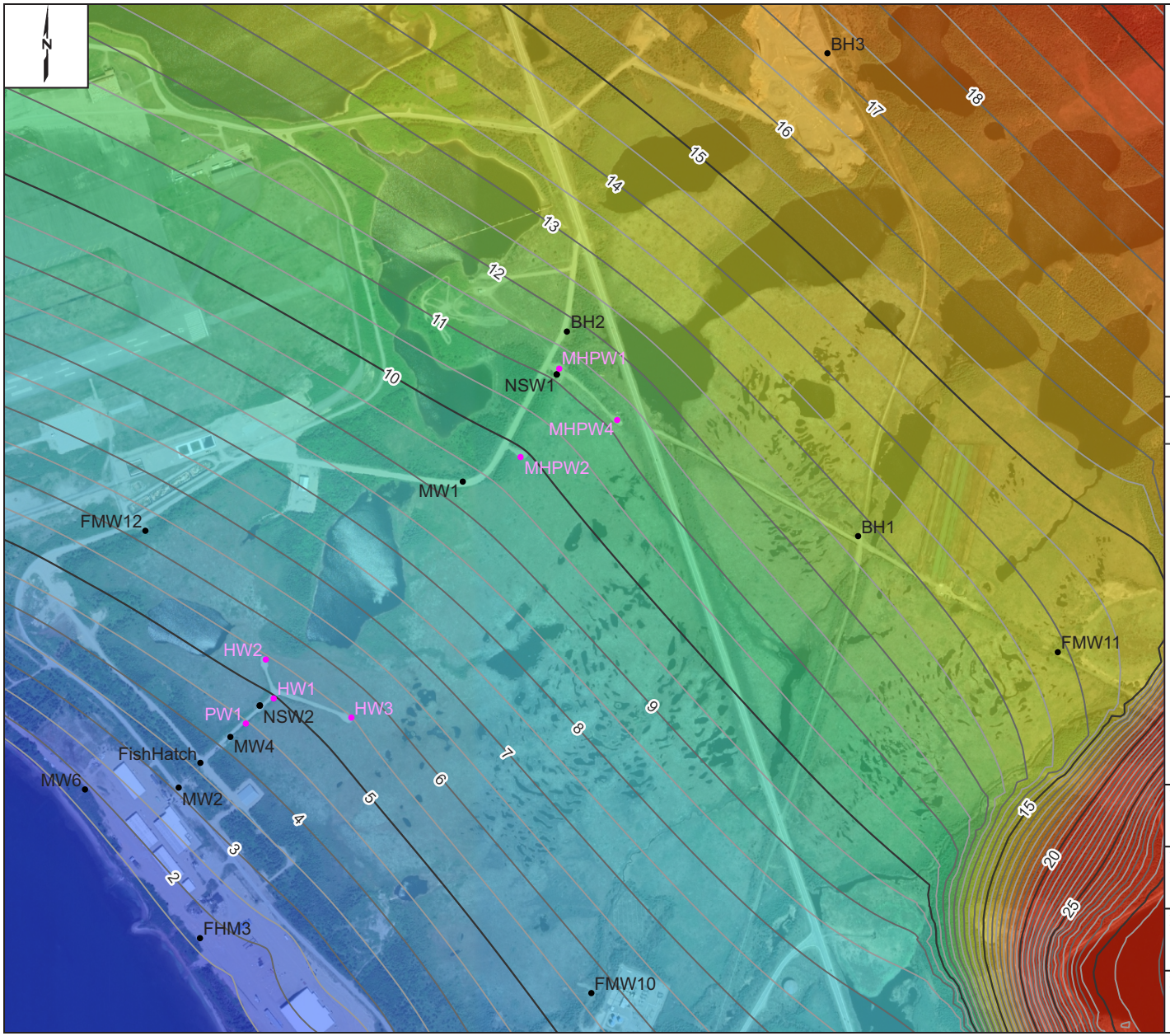

Legend

- Production well location
- Monitoring well location

Legend

Contours, m

1 5 10 15 >20

0 100 200 300 400 500

Scale, m

Note: Base orthorectified image from Google Earth (2022).

Figure 4.13

Contour map of the water elevation (hydraulic head) for the pumping condition under transient simulation at the water table level in December 31, 2021.

Document Reference	FFC-NL-3113-057b
Location	Stephenville, NL
Project No.	3113
Date	December 2022

FFC

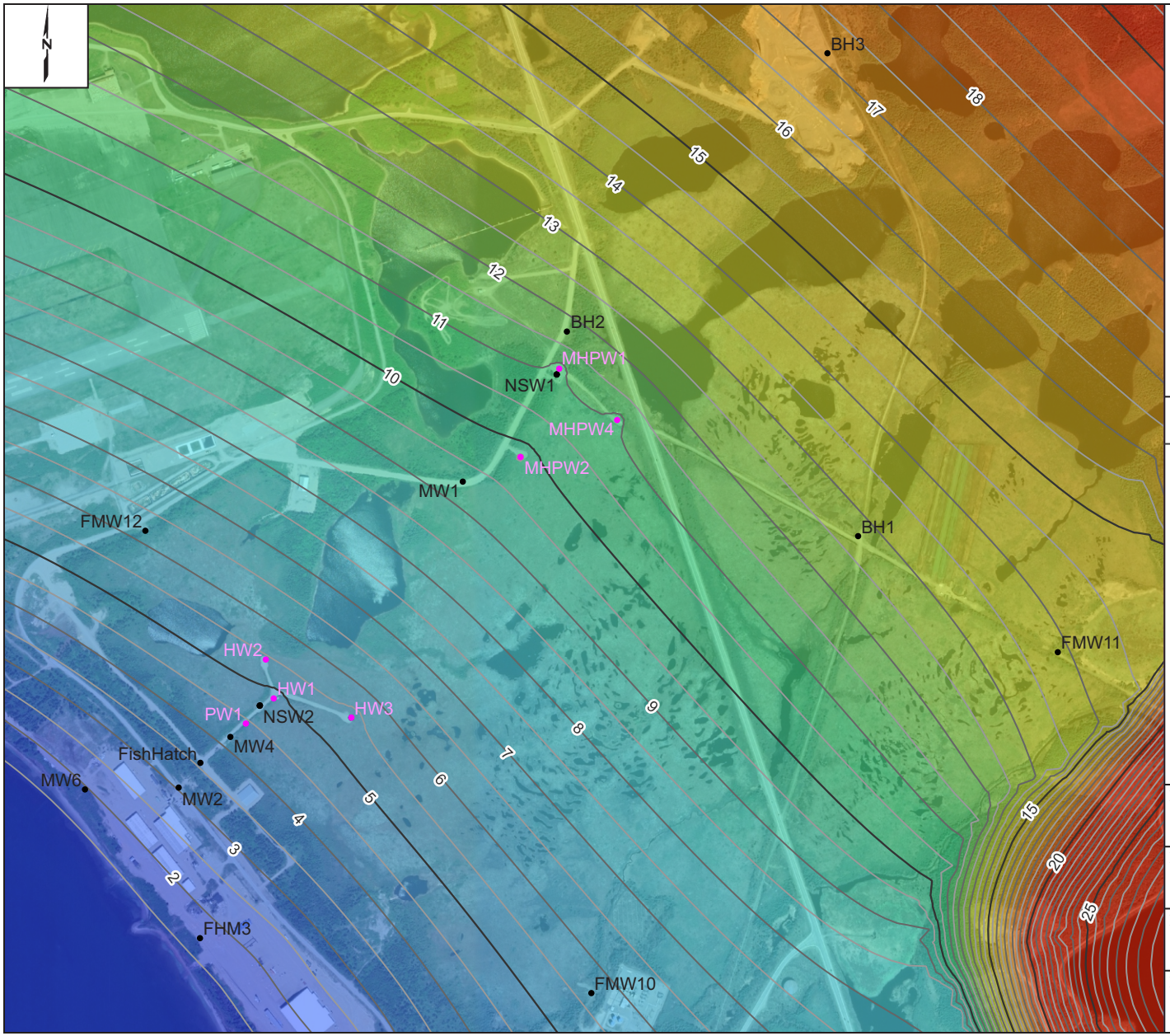

Legend

- Production well location
- Monitoring well location

Legend

Contours, m

1 5 10 15 >20

0 100 200 300 400 500

Scale, m

Note: Base orthorectified image from Google Earth (2022).

Figure 4.14

Contour map of the water elevation (hydraulic head) for the pumping condition under transient simulation at the pumping level in December 31, 2021.

Document Reference	FFC-NL-3113-057b
Location	Stephenville, NL
Project No.	3113
Date	December 2022

FFC

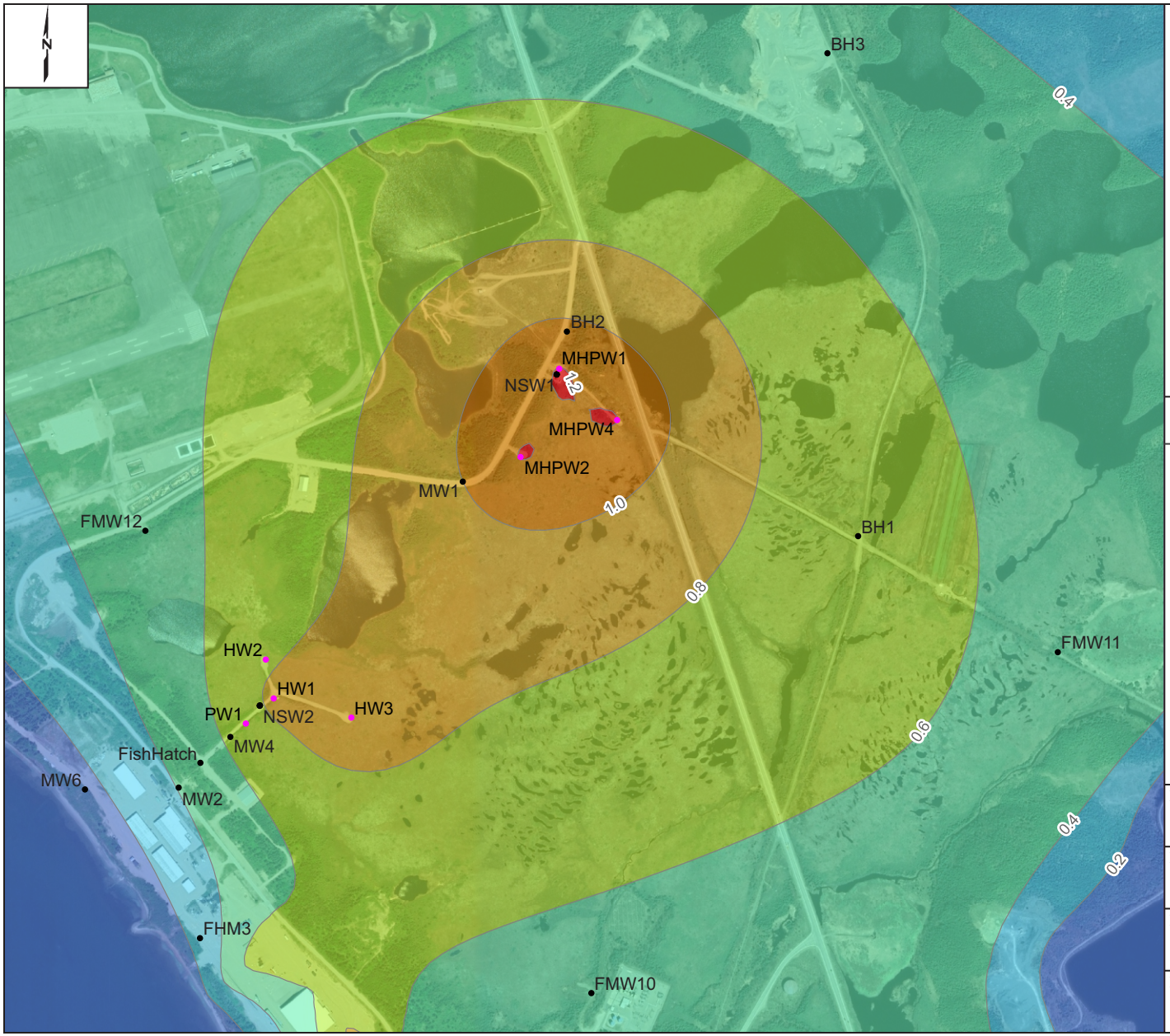

Legend

Production well location

Monitoring well location

Legend

Contours, m

0 0,4 0,8 >1,2

0 100 200 300 400 500

Scale, m

Note: Base orthorectified image from Google Earth (2022).

Figure 4.15

Capture area calculated by the transient model at the water table level under operation of the available production wells in December 31, 2021.

Document Reference	FFC-NL-3113-057b
Location	Stephenville, NL
Project No.	3113
Date	December 2022

FFC

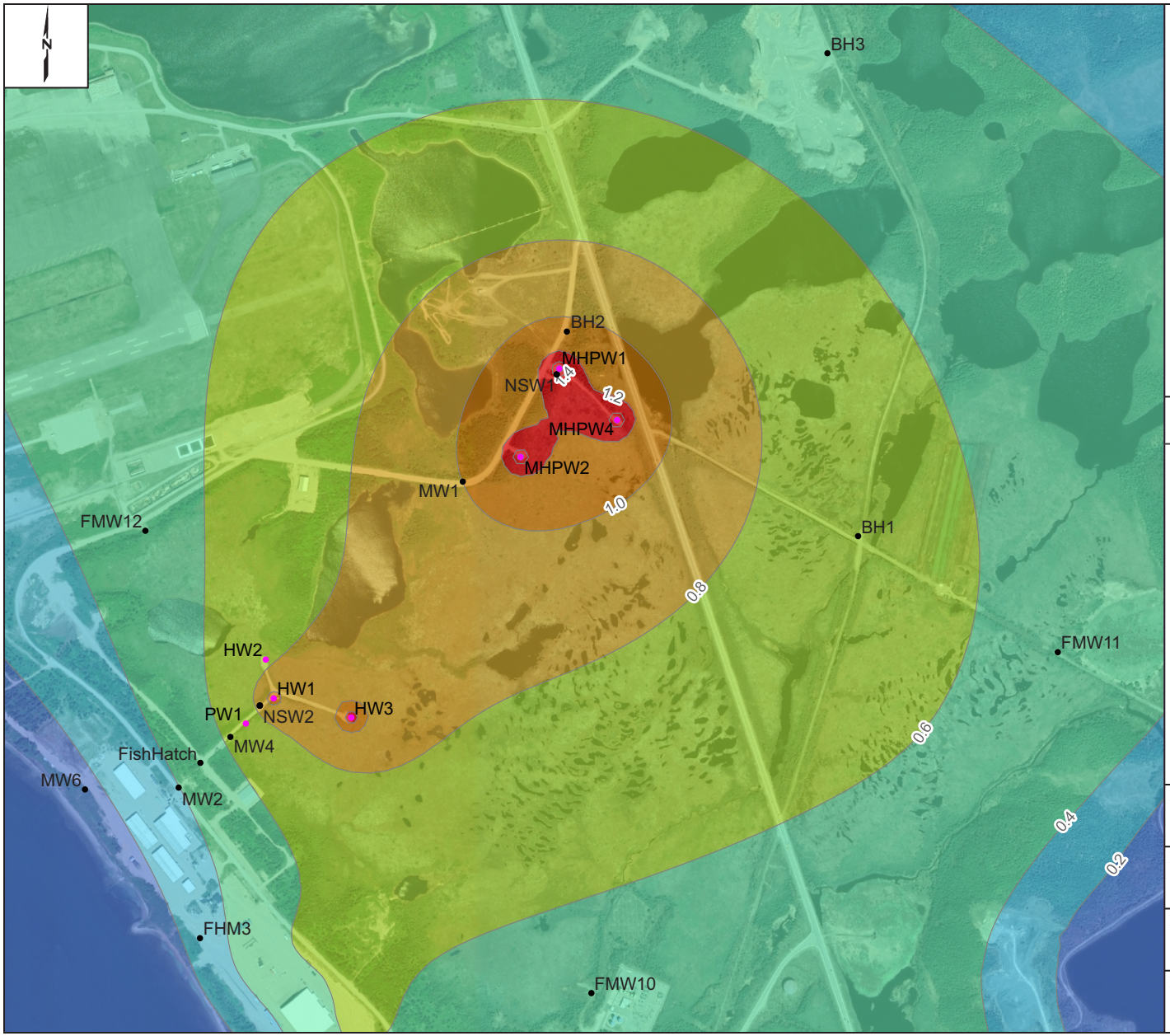

Legend

Production well location

Monitoring well location

Legend

Contours, m

0 0,4 0,8 >1,2

0 100 200 300 400 500

Scale, m

Note: Base orthorectified image from Google Earth (2022).

Figure 4.16

Capture area calculated by the transient model at the pumping level under operation of the available production wells in December 31, 2021.

Document Reference	FFC-NL-3113-057b
Location	Stephenville, NL
Project No.	3113
Date	December 2022

FFC

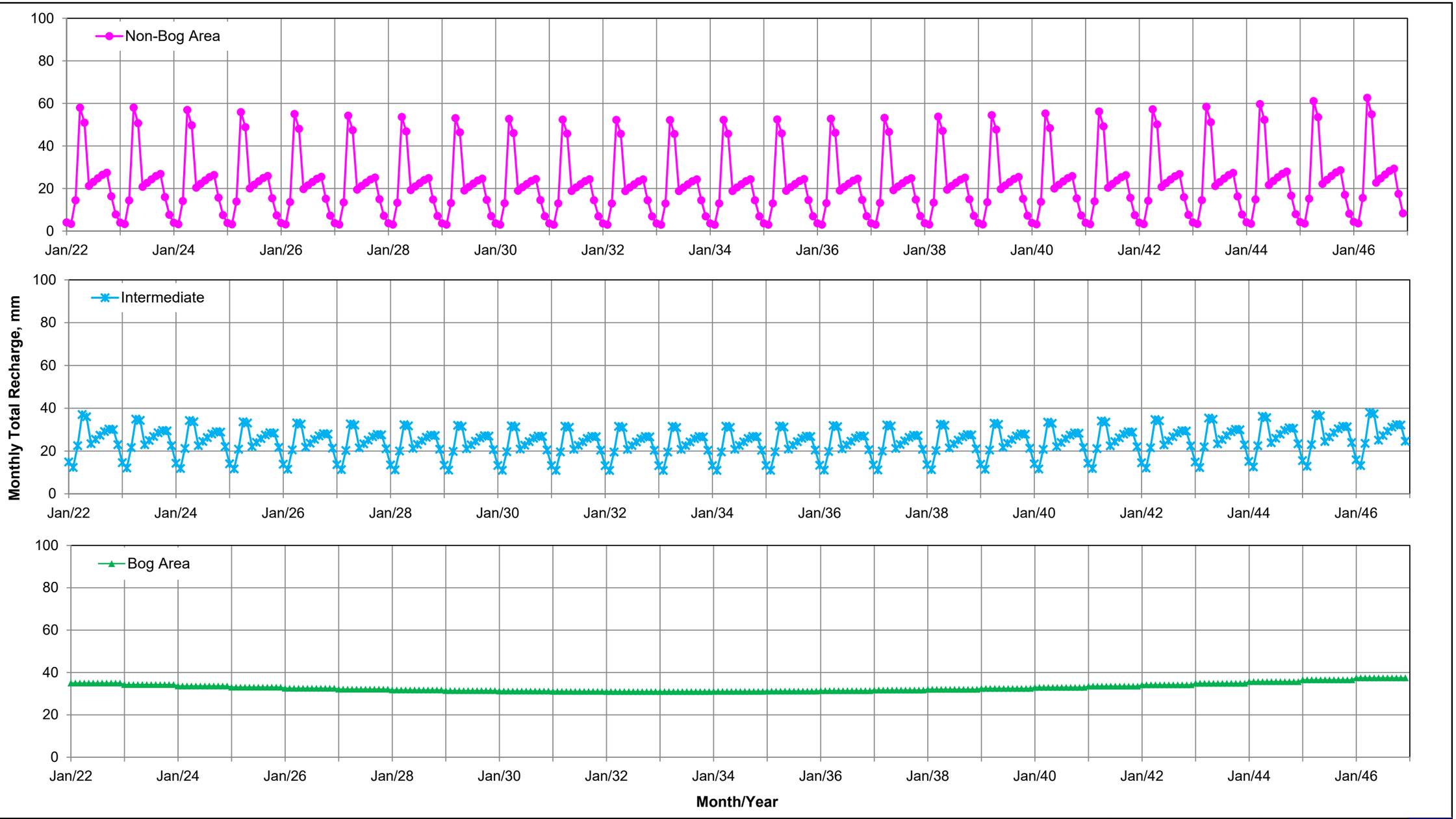

Figure 4.17 Monthly total recharge assigned for the 3D hydrogeological prediction model of the main data set, *Main 1* . The recharge values were determined based on the yearly mean values for the selected 25-year data collected from *Stephenville A* station (ID 8403800).

Project No.	Document Reference
3113	FFC-NL-3113-057b
Location	Date
Stephenville, NL	December 2022

FFC

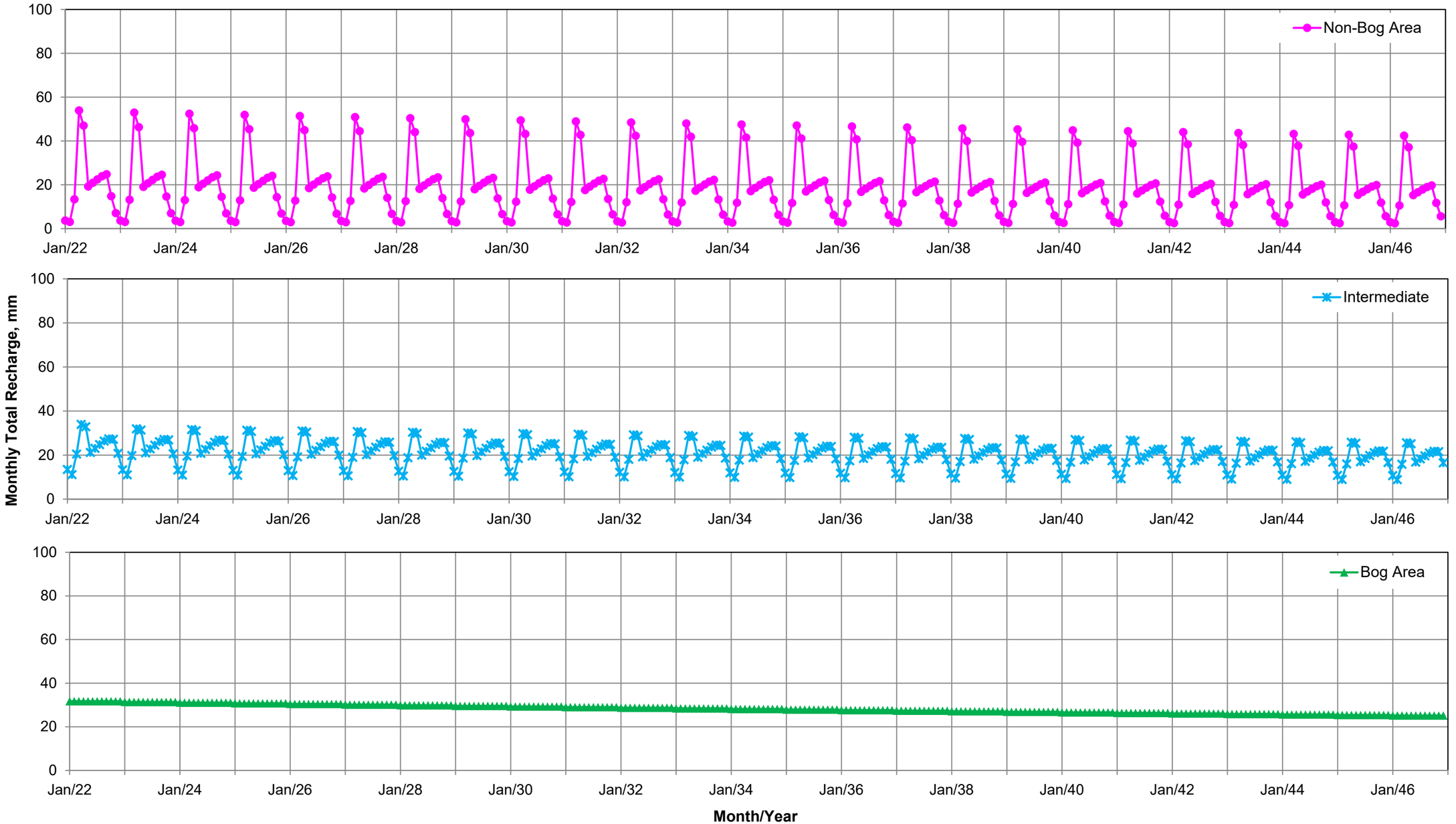

Figure 4.18 Monthly total recharge assigned for the 3D hydrogeological prediction model of the main data set, *Main 2* . The recharge values were determined based on the yearly mean values for the selected 25-year data collected from *Stephenville A* station (ID 8403800).

Project No.	Document Reference
3113	FFC-NL-3113-057b
Location	Date
Stephenville, NL	December 2022

FFC

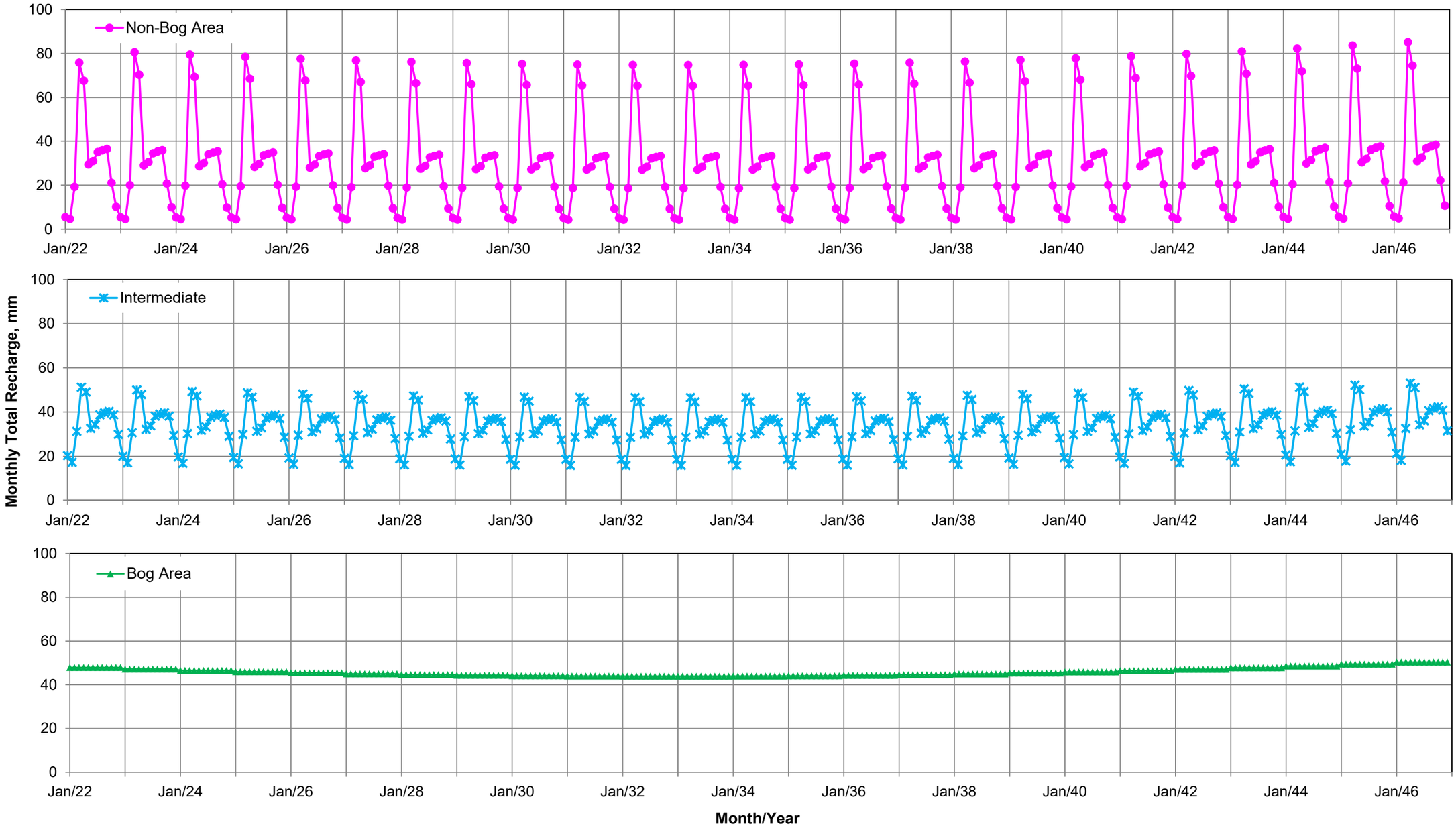

Figure 4.19 Monthly total recharge assigned for the 3D hydrogeological prediction model of the upper limit data set, *Upper Limit 1* . The recharge values were determined by adding the standard deviation to the yearly mean values for the selected 25-year data.

Project No. 3113	Document Reference FFC-NL-3113-057b
Location Stephenville, NL	Date December 2022

FFC

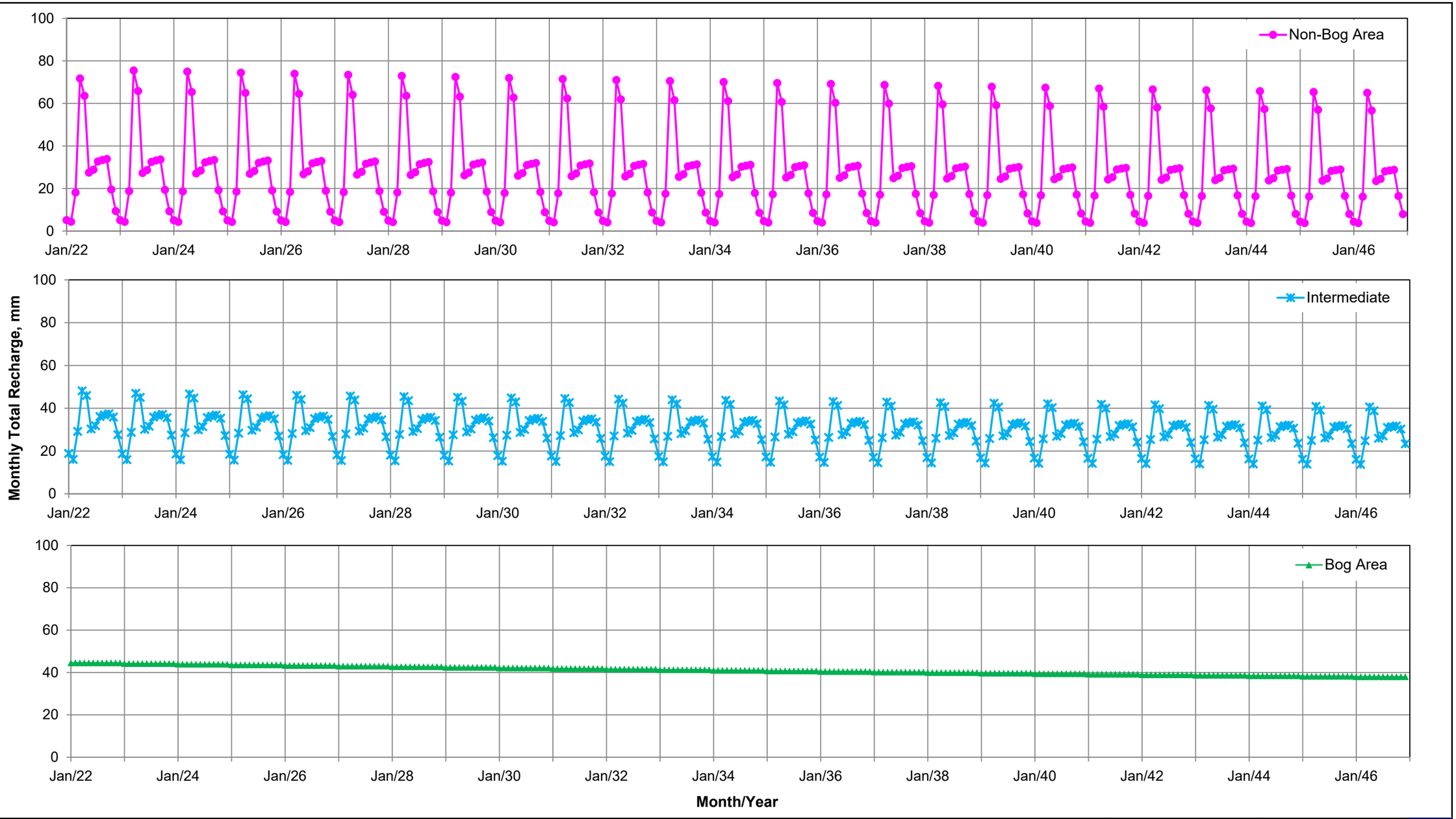

Figure 4.20 Monthly total recharge assigned for the 3D hydrogeological prediction model of the upper limit data set, *Upper Limit 2* . The recharge values were determined by adding the standard deviation to the yearly mean values for the selected 25-year data.

Project No. 3113	Document Reference FFC-NL-3113-057b
Location Stephenville, NL	Date December 2022

FFC

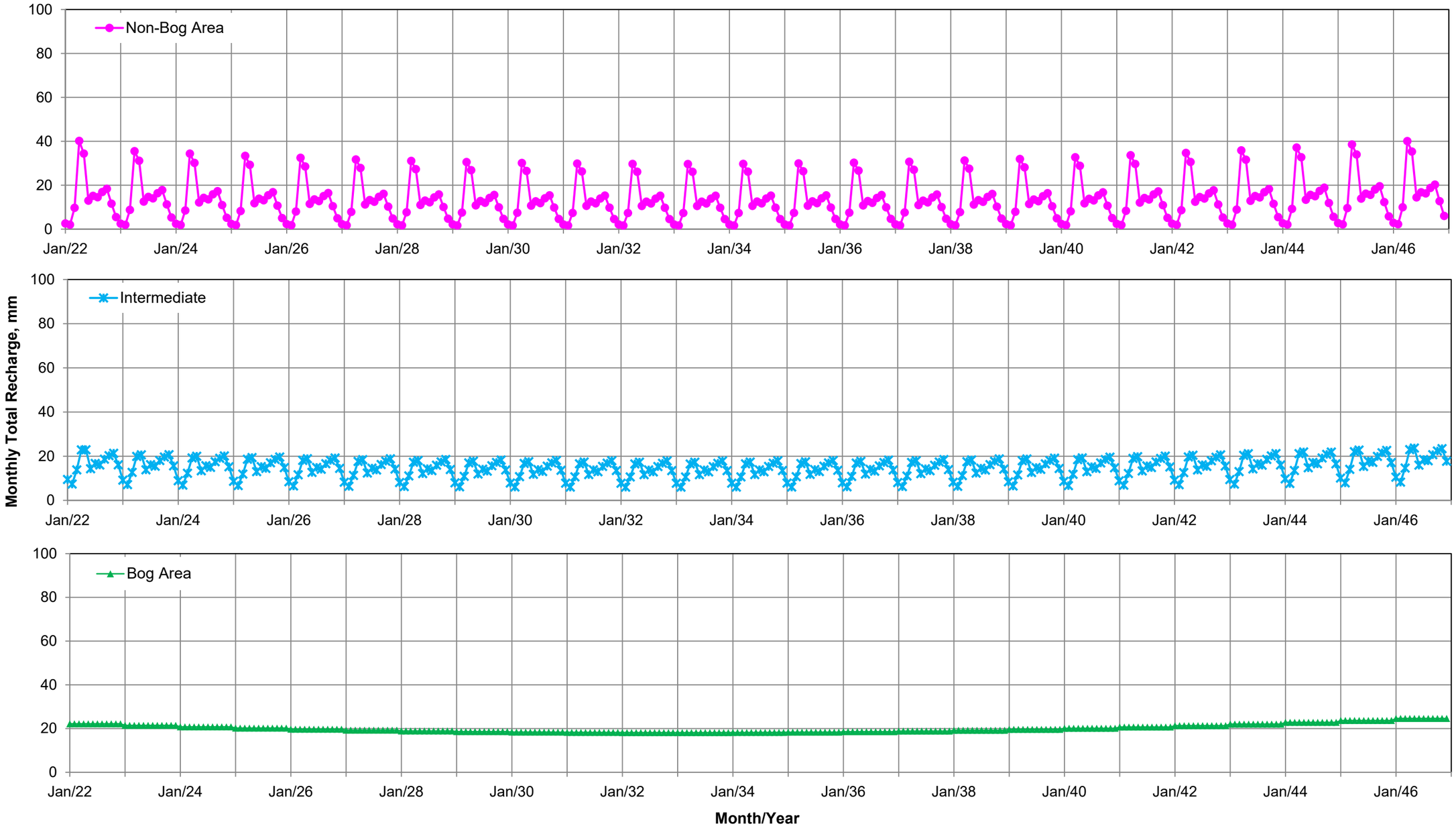

Figure 4.21 Monthly total recharge assigned for the 3D hydrogeological prediction model of the upper limit data set, *Lower Limit 1* . The recharge values were determined by subtracting the standard deviation to the yearly mean values for the selected 25-year data.

Project No.	Document Reference
3113	FFC-NL-3113-057b
Location	Date
Stephenville, NL	December 2022

FFC

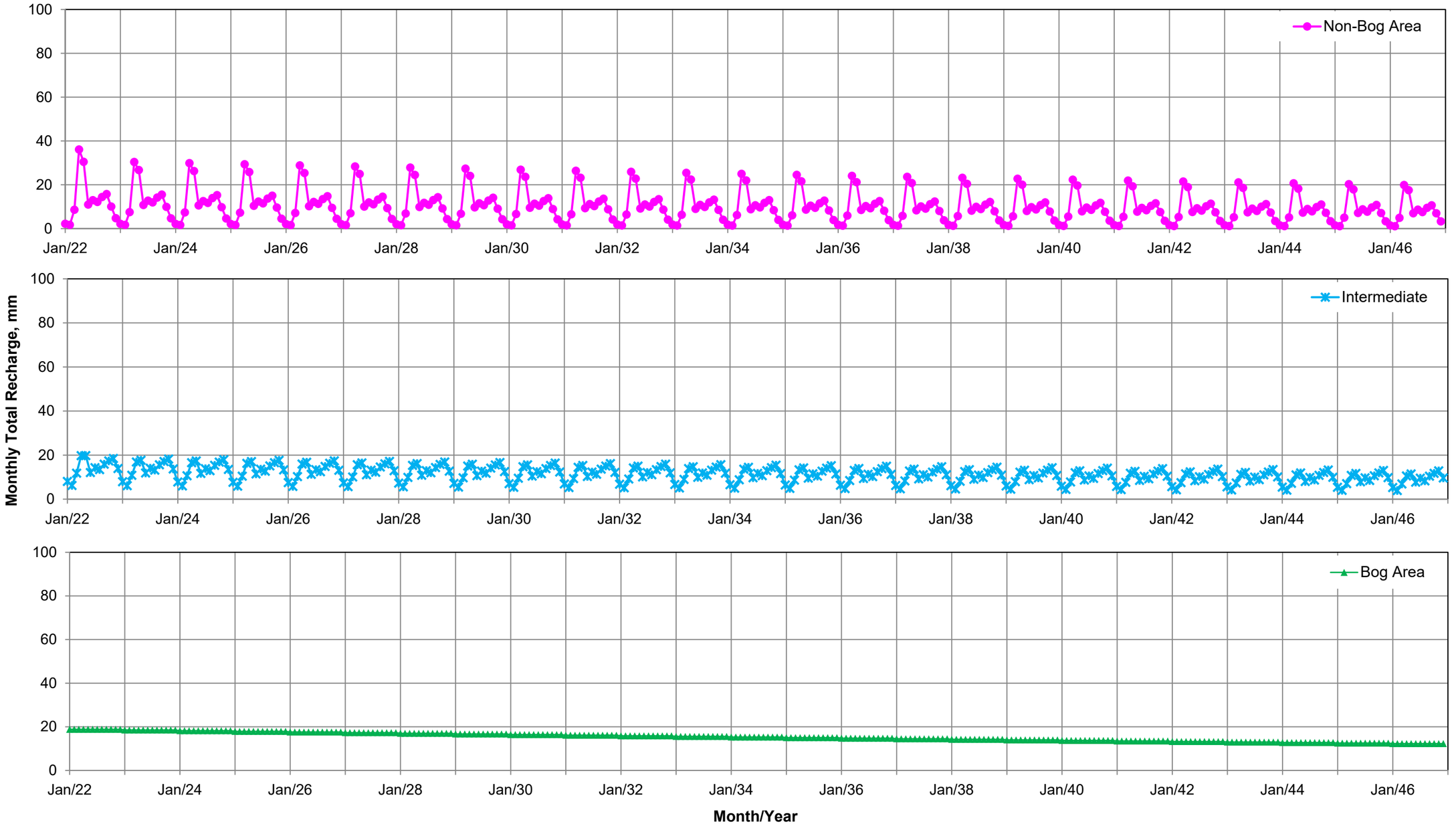

Figure 4.22 Monthly total recharge assigned for the 3D hydrogeological prediction model of the upper limit data set, *Lower Limit 2* . The recharge values were determined by subtracting the standard deviation to the yearly mean values for the selected 25-year data.

Project No.	Document Reference
3113	FFC-NL-3113-057b
Location	Date
Stephenville, NL	December 2022

FFC

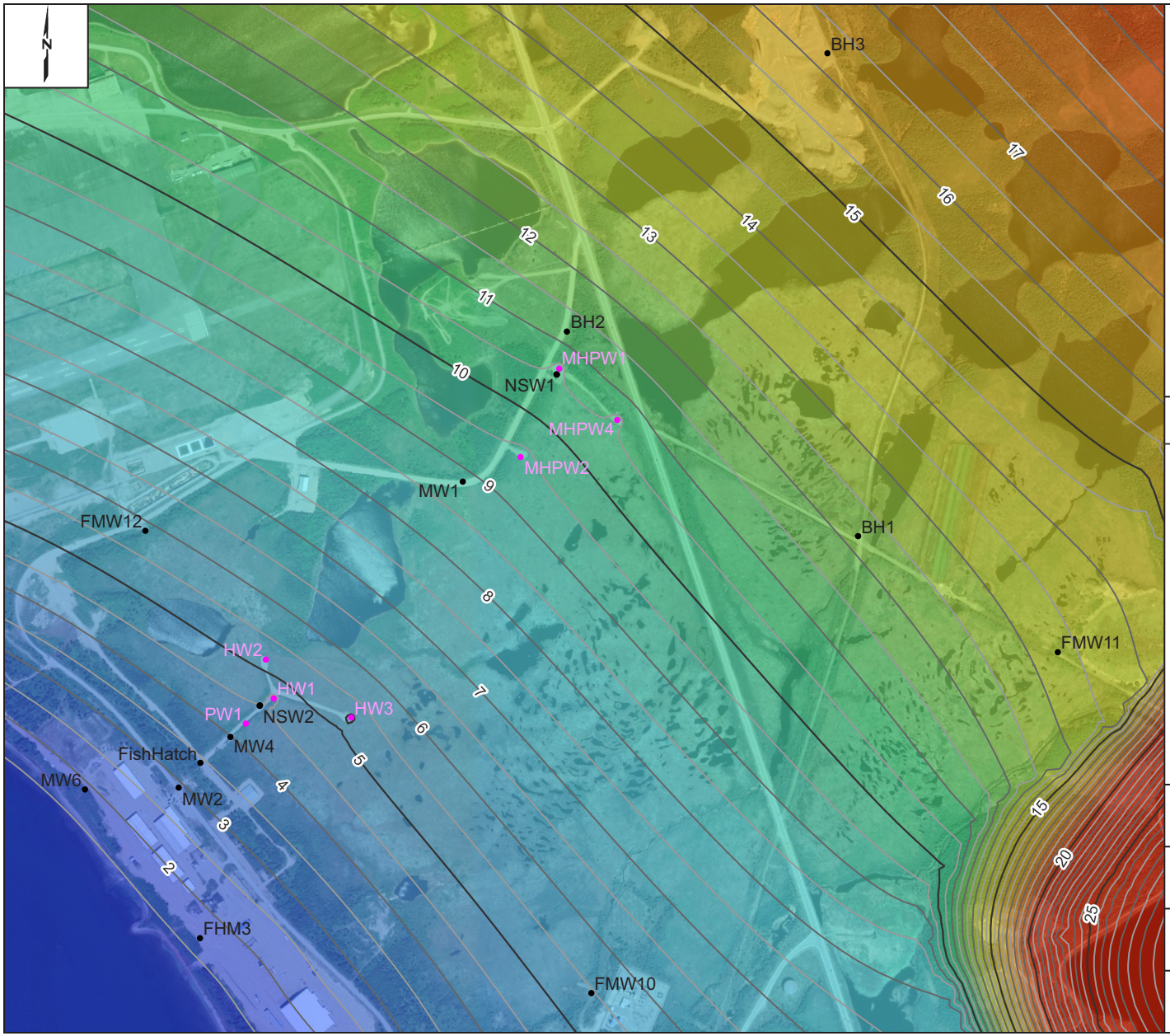

Legend

Production well location

Monitoring well location

Legend

Contours, m

1 5 10 15 >20

0 100 200 300 400 500

Scale, m

Note: Base orthorectified image from Google Earth (2022).

Figure 4.23

Contour map of the calculated water elevation (hydraulic head) at the pumping level with the prediction model, *Main 1,* under operation of the five production wells in December 31, 2026.

Document Reference
FFC-NL-3113-057b

Location
Stephenville, NL

Project No.
3113

Date
December 2022

FFC

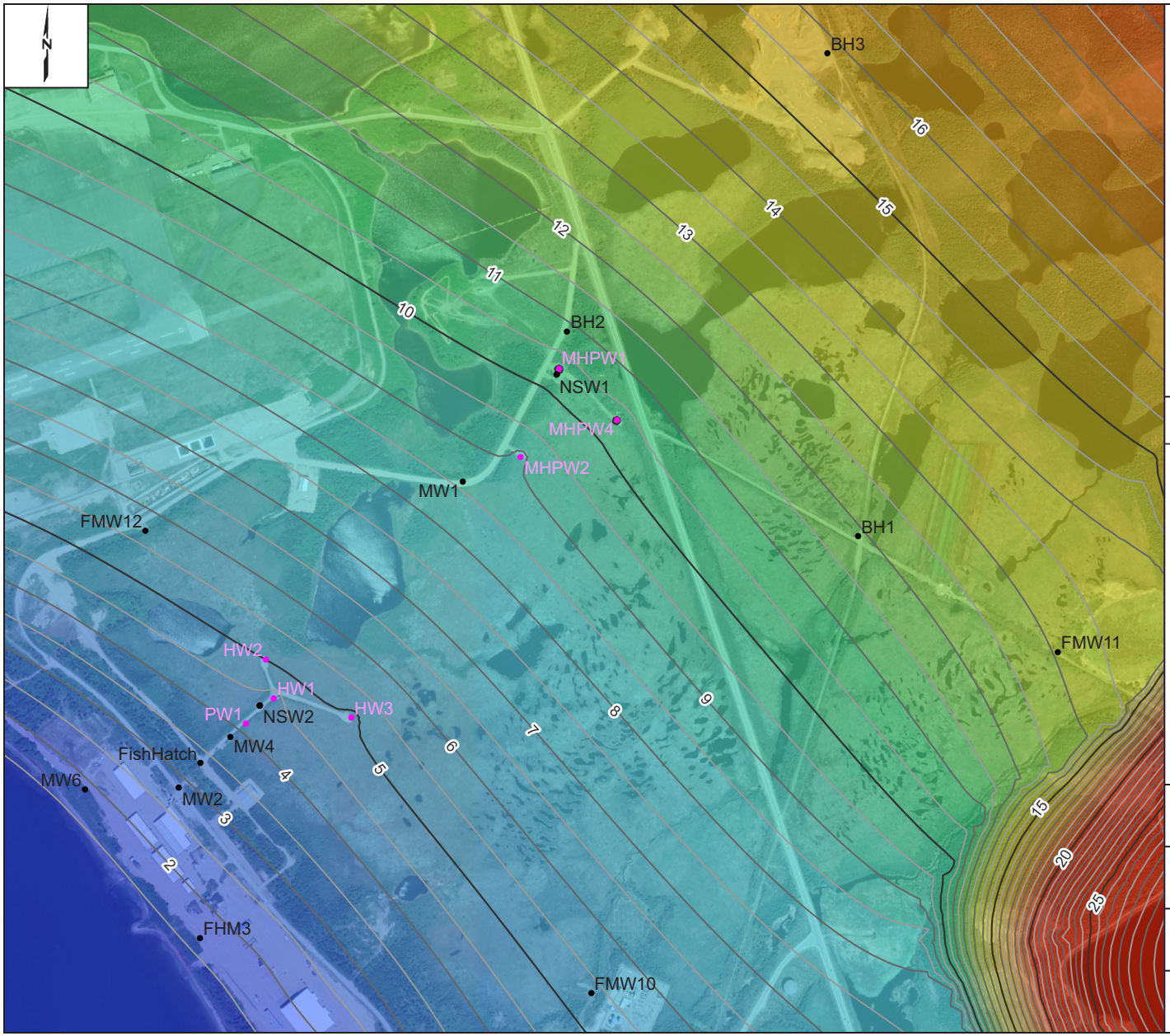

Legend

- Production well location
- Monitoring well location

Legend

Contours, m

1 5 10 15 >20

0 100 200 300 400 500

Scale, m

Note: Base orthorectified image from Google Earth (2022).

Figure 4.24

Contour map of the calculated water elevation (hydraulic head) at the pumping level with the prediction model, *Main 1,* under operation of the five production wells in December 31, 2031.

Document Reference	FFC-NL-3113-057b
Location	Stephenville, NL
Project No.	3113
Date	December 2022

FFC

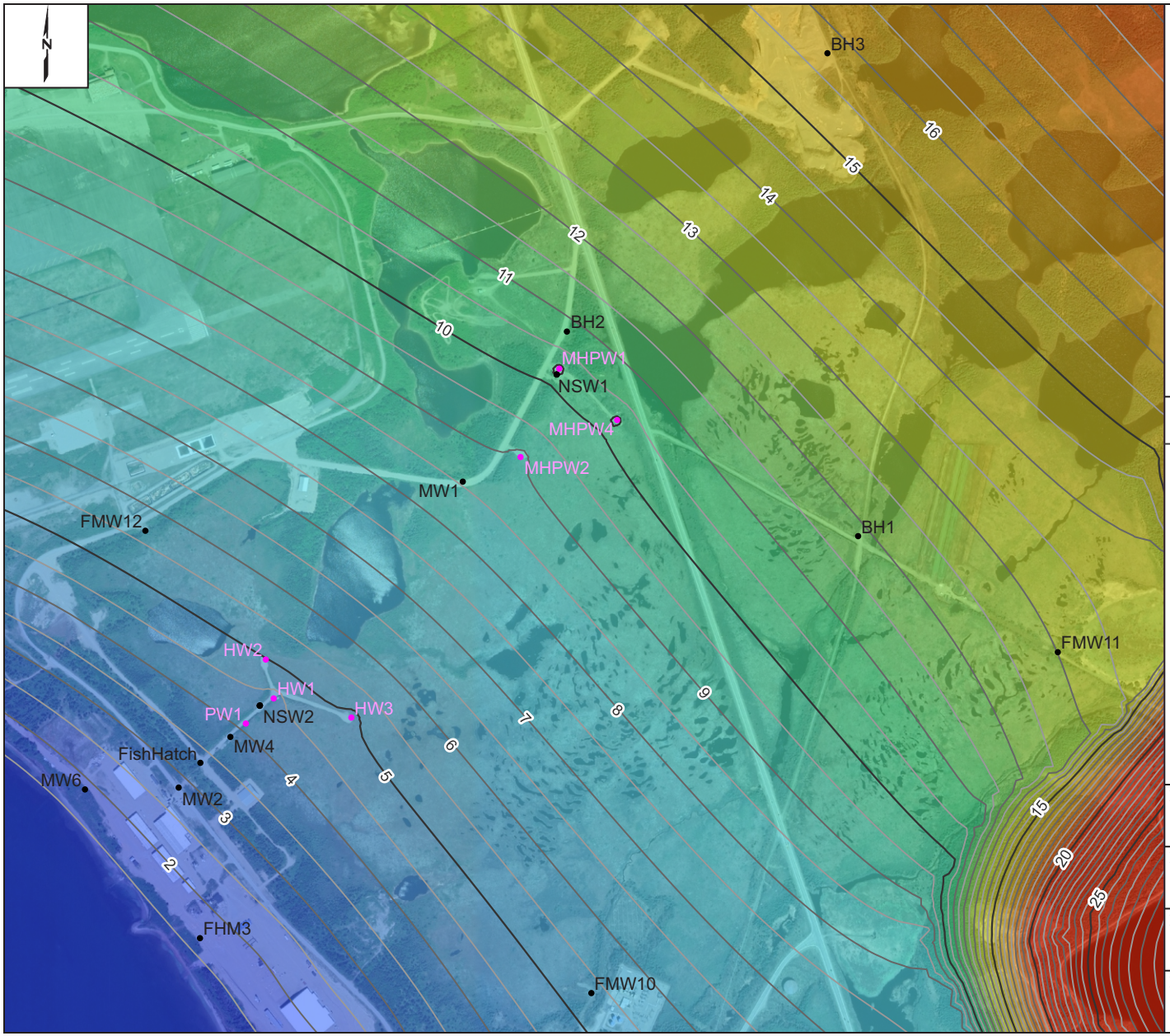

Legend

- Production well location
- Monitoring well location

Legend

Contours, m

1 5 10 15 >20

0 100 200 300 400 500

Scale, m

Note: Base orthorectified image from Google Earth (2022).

Figure 4.25

Contour map of the calculated water elevation (hydraulic head) at the pumping level with the prediction model, *Main 1,* under operation of the five production wells in December 31, 2036.

Document Reference	FFC-NL-3113-057b
Location	Stephenville, NL
Project No.	3113
Date	December 2022

FFC

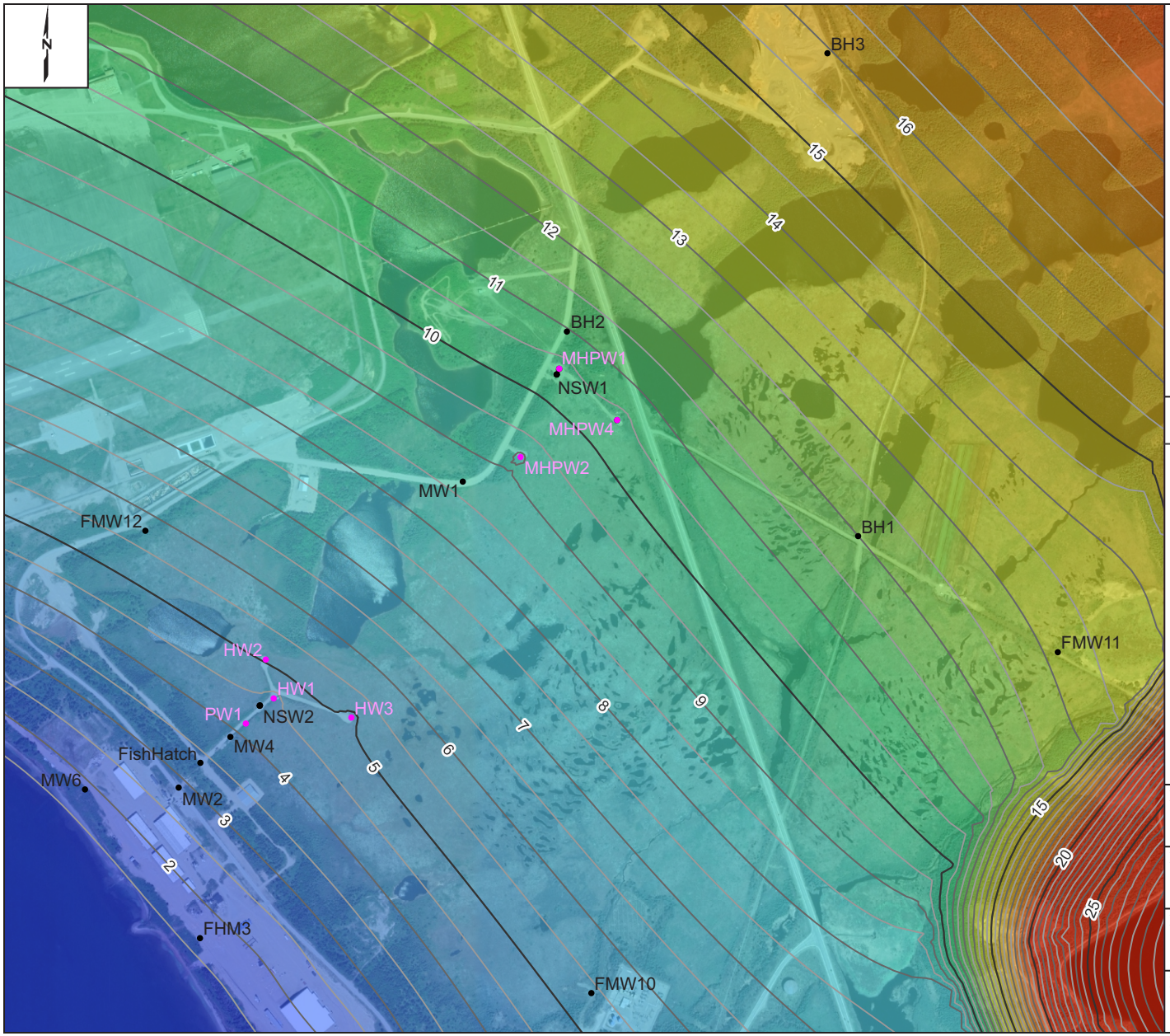

Legend

- Production well location
- Monitoring well location

Legend

Contours, m

1 5 10 15 >20

0 100 200 300 400 500

Scale, m

Note: Base orthorectified image from Google Earth (2022).

Figure 4.26

Contour map of the calculated water elevation (hydraulic head) at the pumping level with the prediction model, *Main 1,* under operation of the five production wells in December 31, 2041.

Document Reference	FFC-NL-3113-057b
Location	Stephenville, NL
Project No.	3113
Date	December 2022

FFC

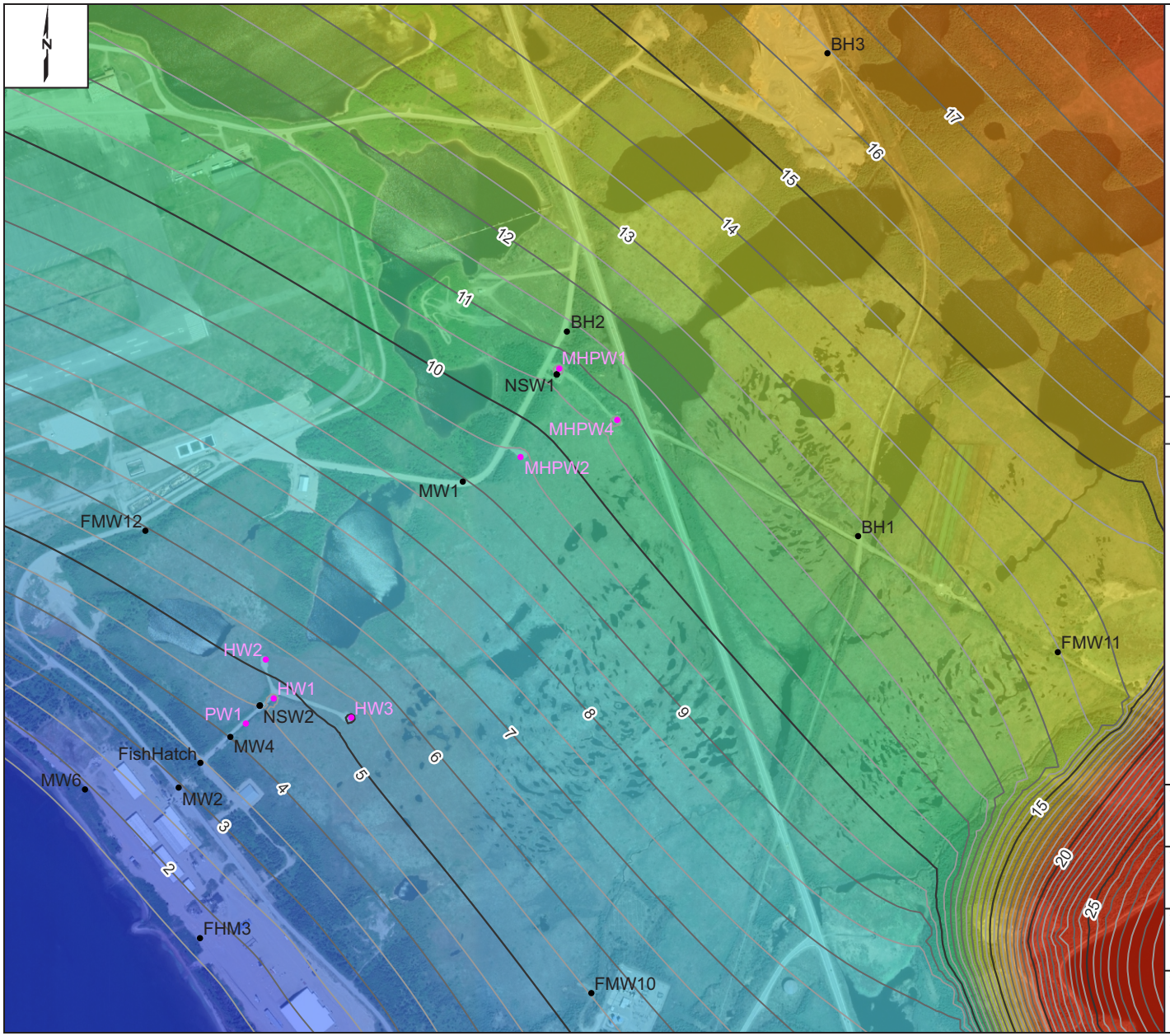

Legend

- Production well location
- Monitoring well location

Legend

Contours, m

1 5 10 15 >20

0 100 200 300 400 500

Scale, m

Note: Base orthorectified image from Google Earth (2022).

Figure 4.27

Contour map of the calculated water elevation (hydraulic head) at the pumping level with the prediction model, *Main 1,* under operation of the five production wells in December 31, 2046.

Document Reference	FFC-NL-3113-057b
Location	Stephenville, NL
Project No.	3113
Date	December 2022

FFC

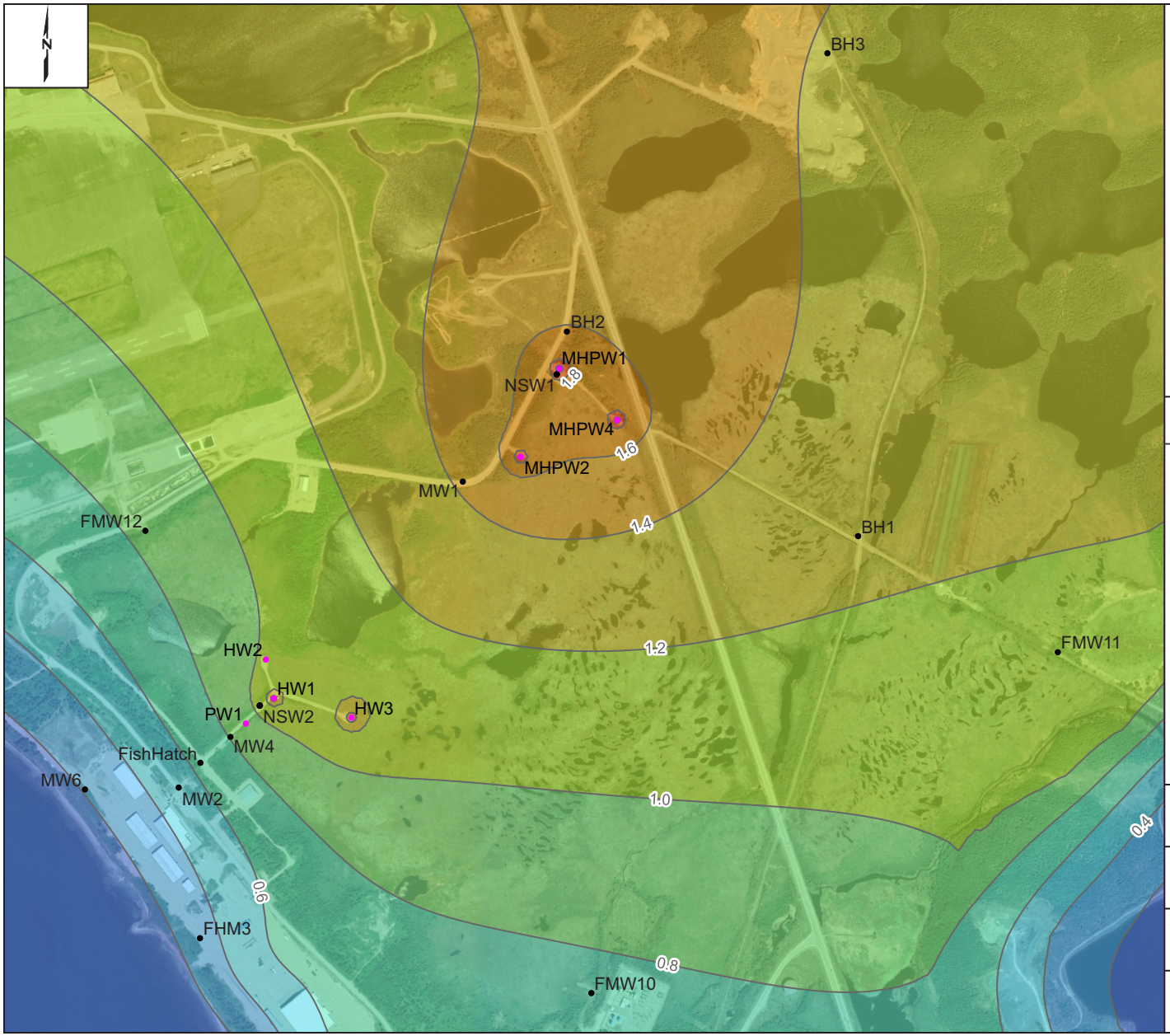

Legend

Production well location

Monitoring well location

Legend

Contours, m

0 0.5 1 1.5 >2

0 100 200 300 400 500

Scale, m

Note: Base orthorectified image from Google Earth (2022).

Figure 4.28

Capture area calculated by the prediction model, *Main 1*, with transient simulation at the pumping level under operation of the five production wells in December 31, 2026.

Document Reference	FFC-NL-3113-057b
Location	Stephenville, NL
Project No.	3113
Date	December 2022

FFC

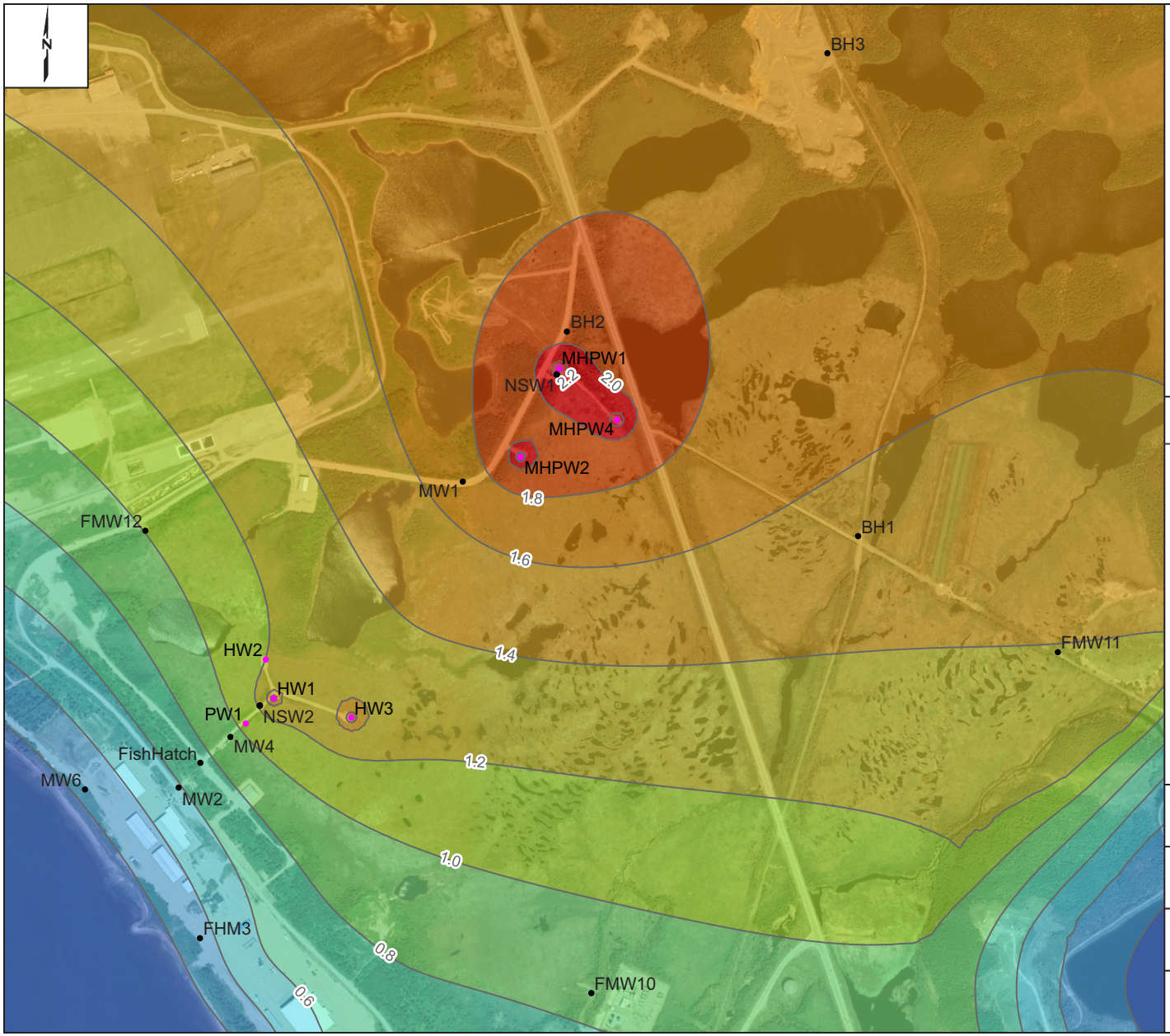

Legend

Production well location

Monitoring well location

Legend

Contours, m

0 0.5 1 1.5 >2

0 100 200 300 400 500

Scale, m

Note: Base orthorectified image from Google Earth (2022).

Figure 4.29

Capture area calculated by the prediction model, *Main 1*, with transient simulation at the pumping level under operation of the five production wells in December 31, 2031.

Document Reference	FFC-NL-3113-057b
Location	Stephenville, NL
Project No.	3113
Date	December 2022

FFC

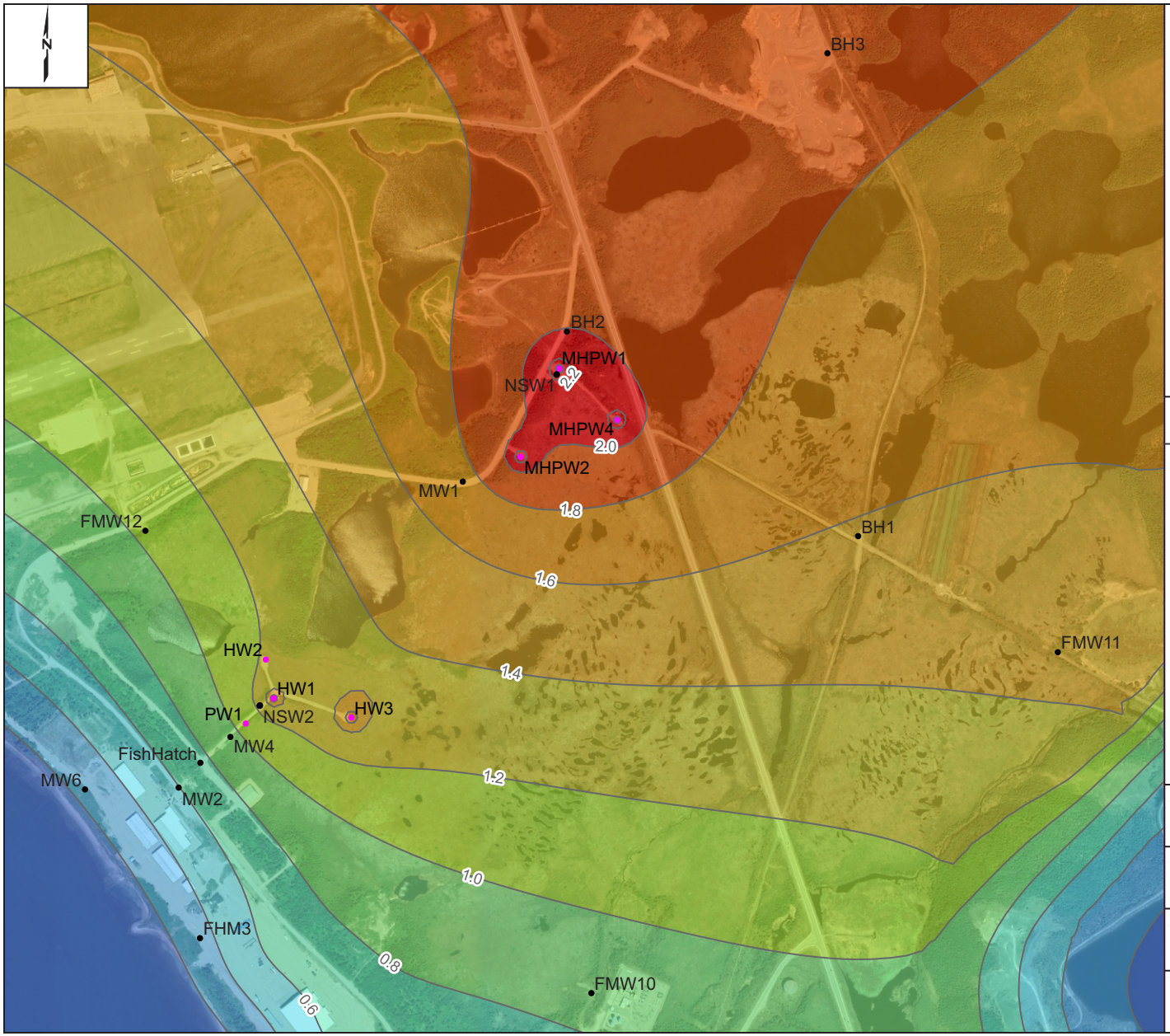

Legend

Production well location

Monitoring well location

Legend

Contours, m

0 0.5 1 1.5 >2

0 100 200 300 400 500

Scale, m

Note: Base orthorectified image from Google Earth (2022).

Figure 4.30

Capture area calculated by the prediction model, *Main 1*, with transient simulation at the pumping level under operation of the five production wells in December 31, 2036.

Document Reference	FFC-NL-3113-057b
Location	Stephenville, NL
Project No.	3113
Date	December 2022

FFC

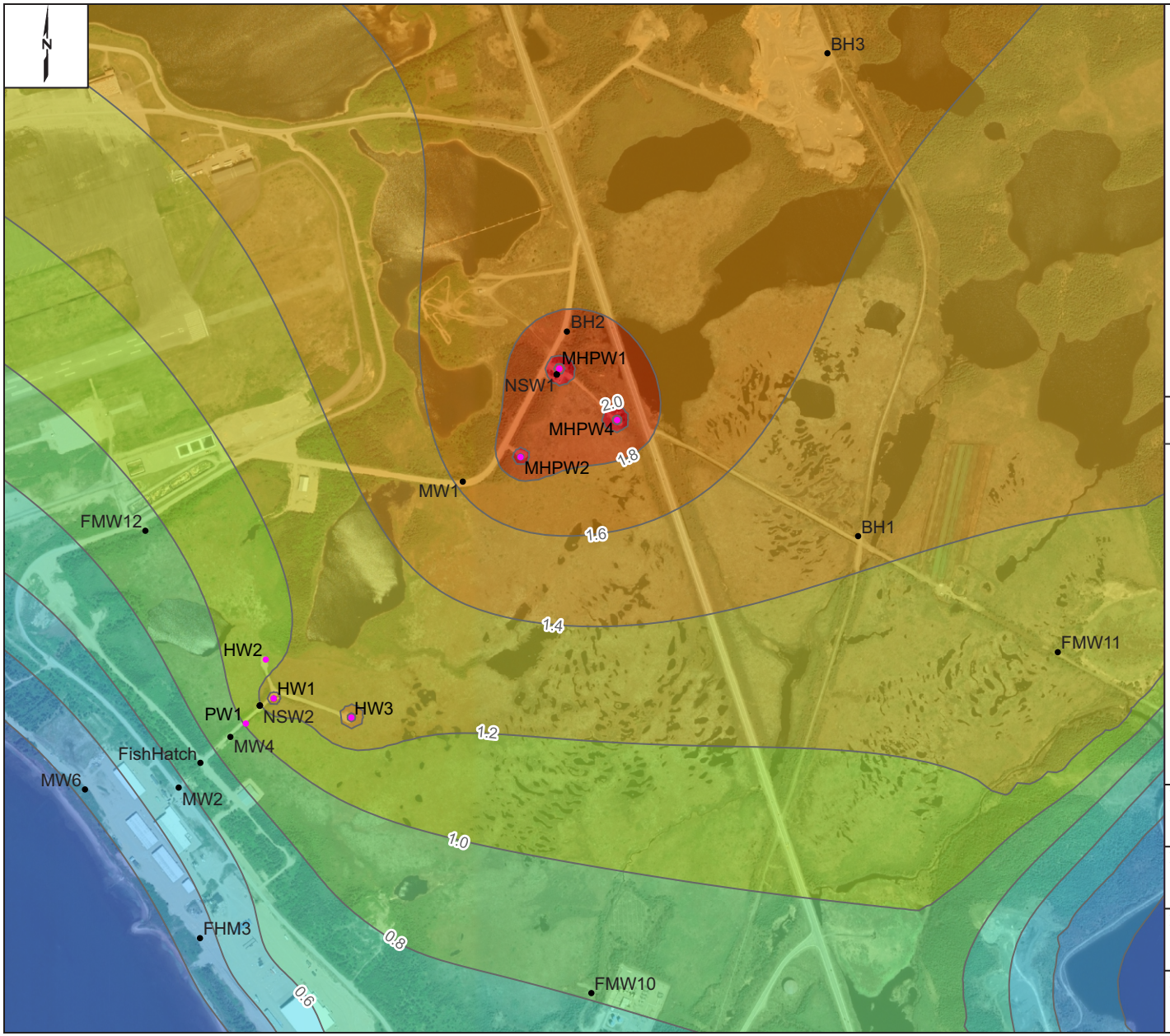

Legend

Production well location

Monitoring well location

Legend

Contours, m

0 0.5 1 1.5 >2

0 100 200 300 400 500

Scale, m

Note: Base orthorectified image from Google Earth (2022).

Figure 4.31

Capture area calculated by the prediction model, *Main 1*, with transient simulation at the pumping level under operation of the five production wells in December 31, 2041.

Document Reference	FFC-NL-3113-057b
Location	Stephenville, NL
Project No.	3113
Date	December 2022

FFC

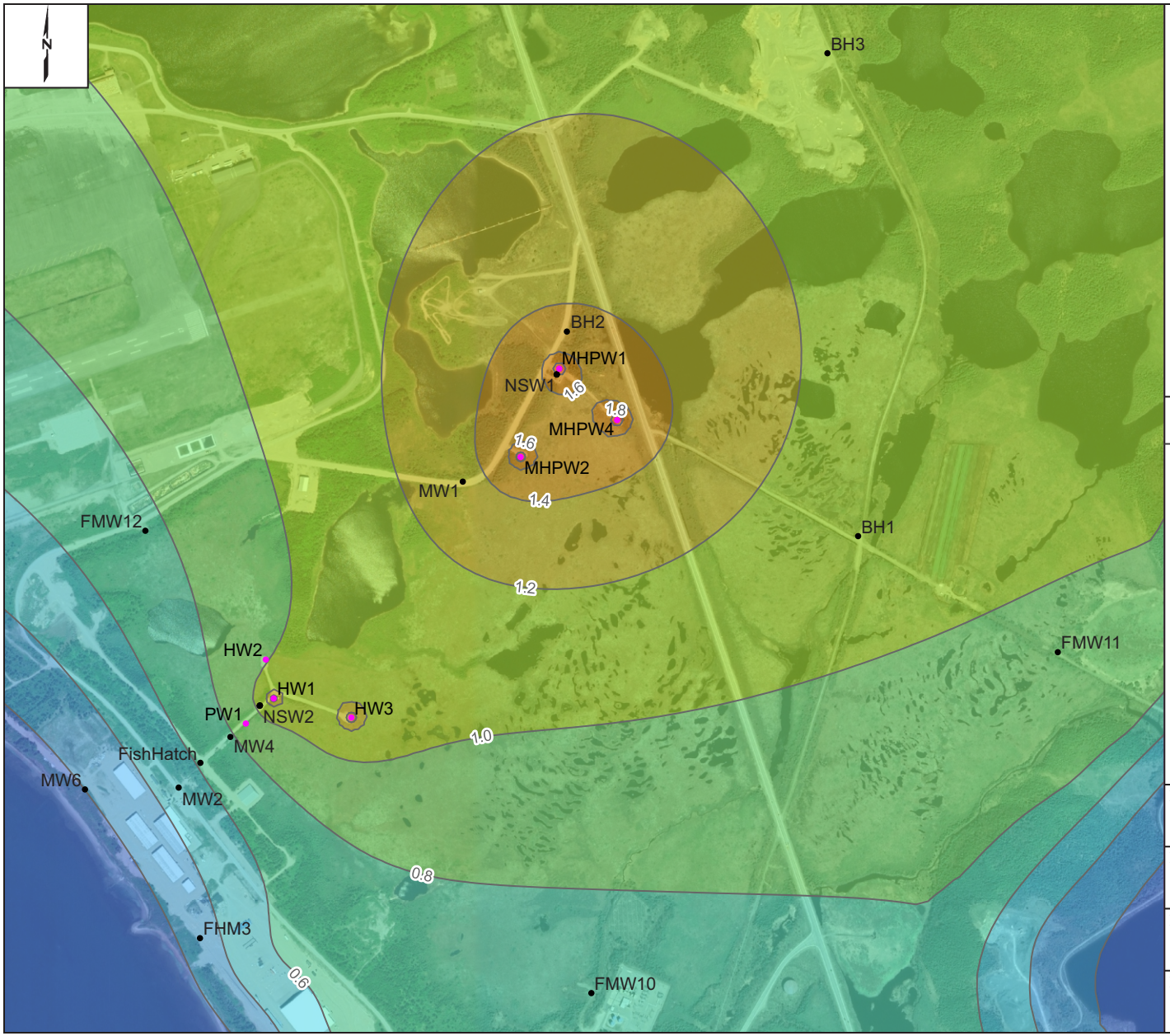

Legend

Production well location

Monitoring well location

Legend

Contours, m

0 0.5 1 1.5 >2

0 100 200 300 400 500

Scale, m

Note: Base orthorectified image from Google Earth (2022).

Figure 4.32

Capture area calculated by the prediction model, *Main 1*, with transient simulation at the pumping level under operation of the five production wells in December 31, 2046.

Document Reference	FFC-NL-3113-057b
Location	Stephenville, NL
Project No.	3113
Date	December 2022

FFC

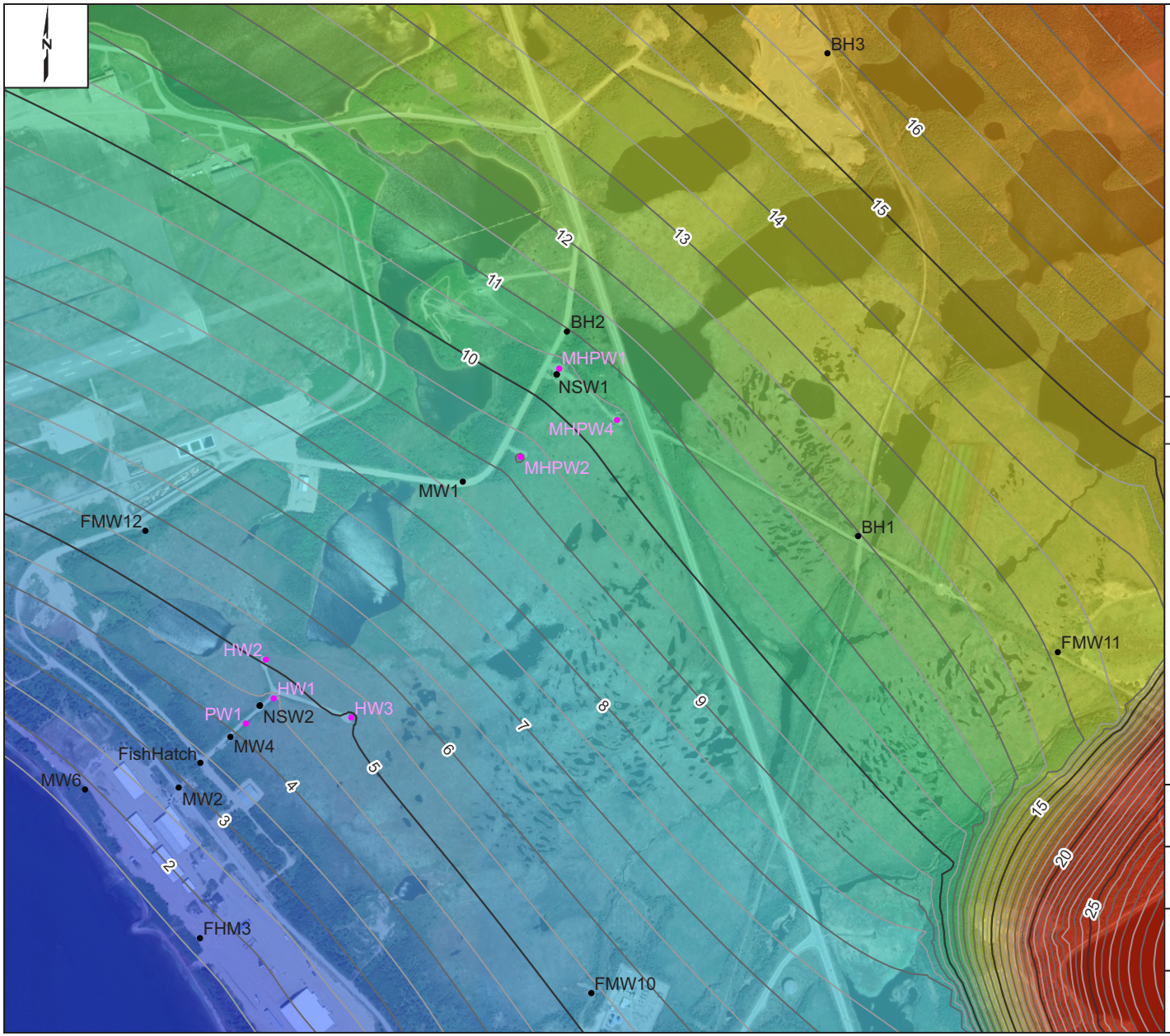

Legend

Production well location

Monitoring well location

Legend

Contours, m

1 5 10 15 >20

0 100 200 300 400 500

Scale, m

Note: Base orthorectified image from Google Earth (2022).

Figure 4.33

Contour map of the calculated water elevation (hydraulic head) at the pumping level with the prediction model, *Main 2,* under operation of the five production wells in December 31, 2026.

Document Reference

FFC-NL-3113-057b

Location

Stephenville, NL

Project No.

3113

Date

December 2022

FFC

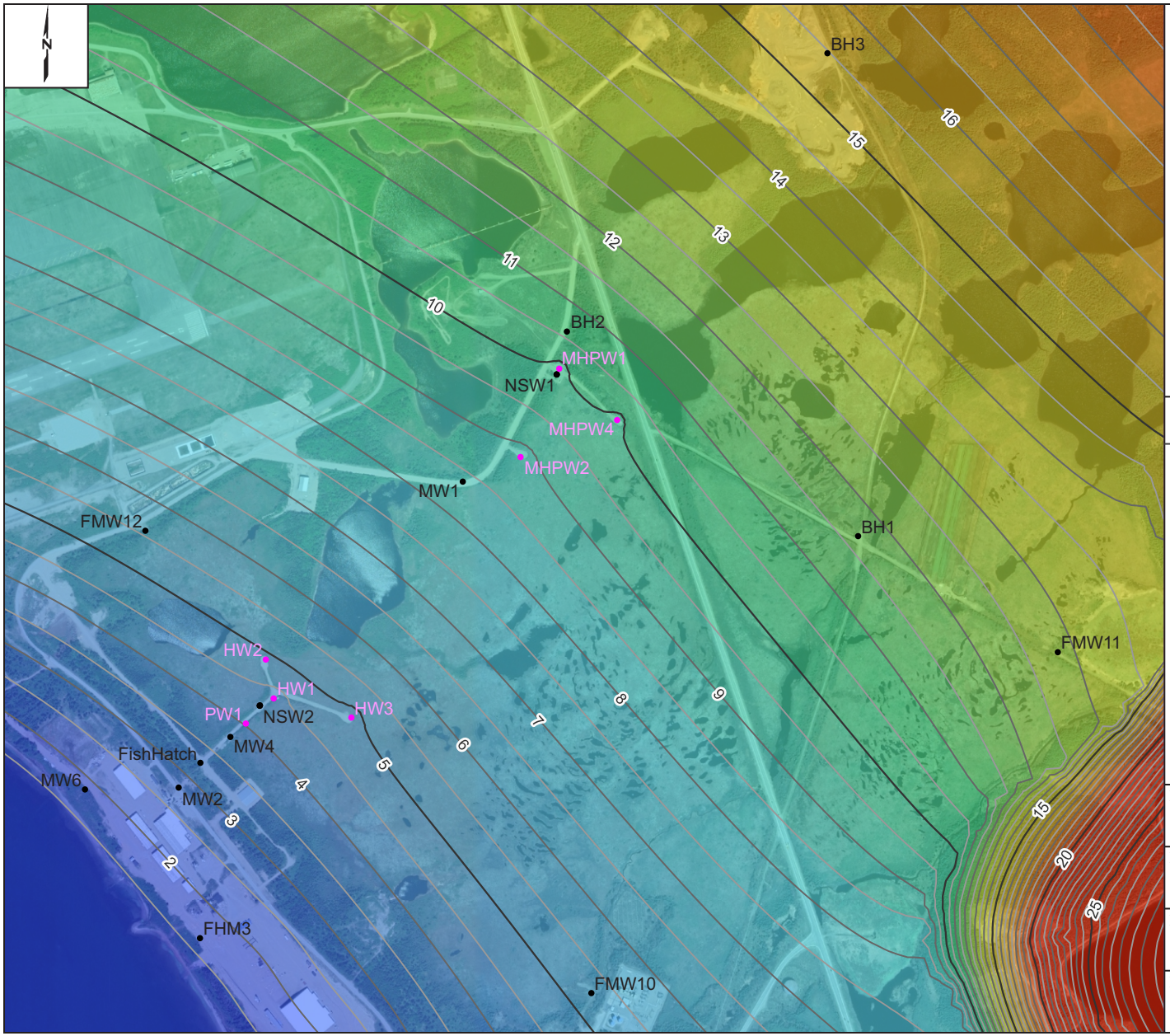

Legend

- Production well location
- Monitoring well location

Legend

Contours, m

1 5 10 15 >20

0 100 200 300 400 500

Scale, m

Note: Base orthorectified image from Google Earth (2022).

Figure 4.34

Contour map of the calculated water elevation (hydraulic head) at the pumping level with the prediction model, *Main 2,* under operation of the five production wells in December 31, 2031.

Document Reference	FFC-NL-3113-057b
Location	Stephenville, NL
Project No.	3113
Date	December 2022

FFC

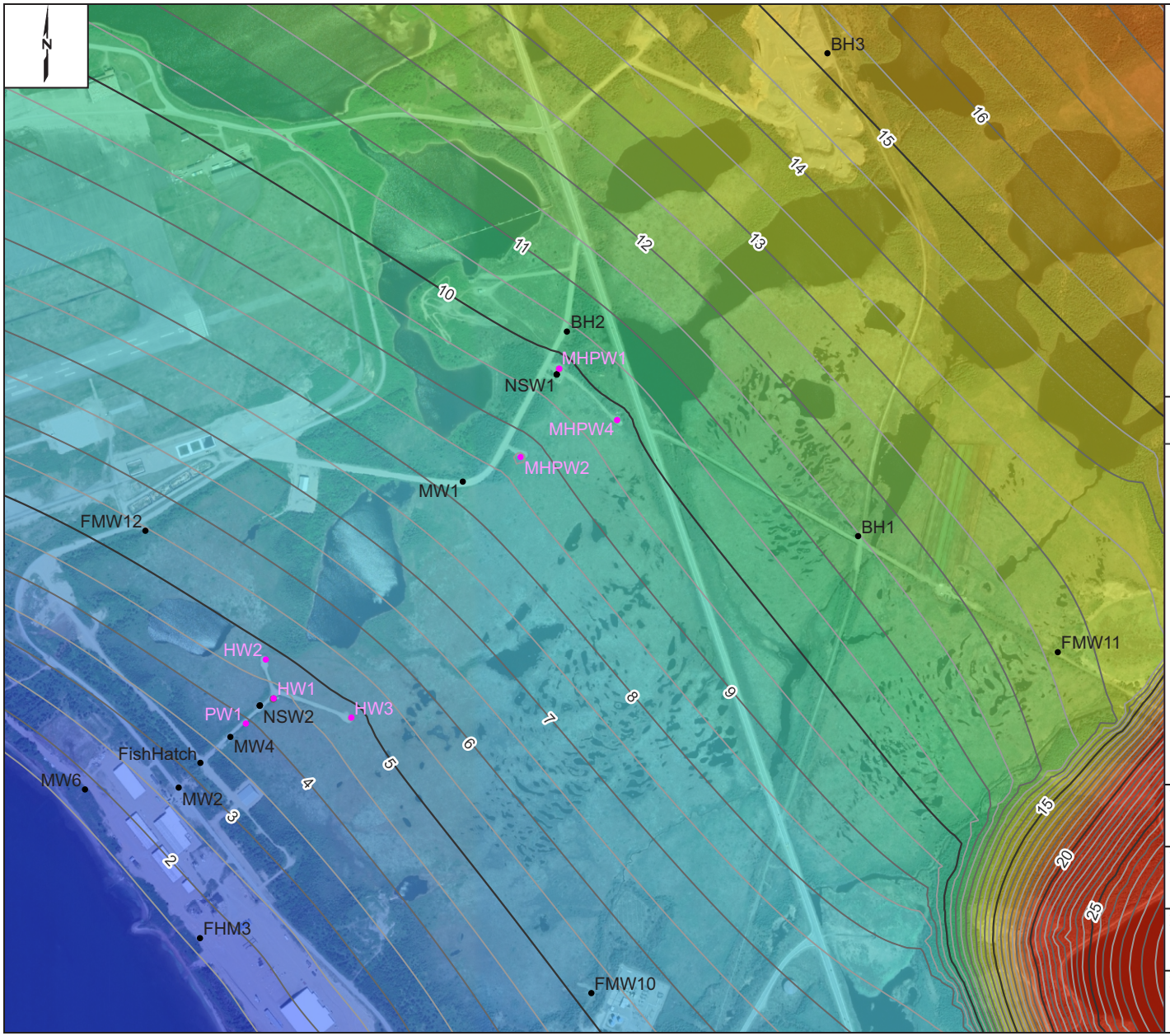

Legend

- Production well location
- Monitoring well location

Legend

Contours, m

1 5 10 15 >20

0 100 200 300 400 500

Scale, m

Note: Base orthorectified image from Google Earth (2022).

Figure 4.35

Contour map of the calculated water elevation (hydraulic head) at the pumping level with the prediction model, *Main 2,* under operation of the five production wells in December 31, 2036.

Document Reference	FFC-NL-3113-057b
Location	Stephenville, NL
Project No.	3113
Date	December 2022

FFC

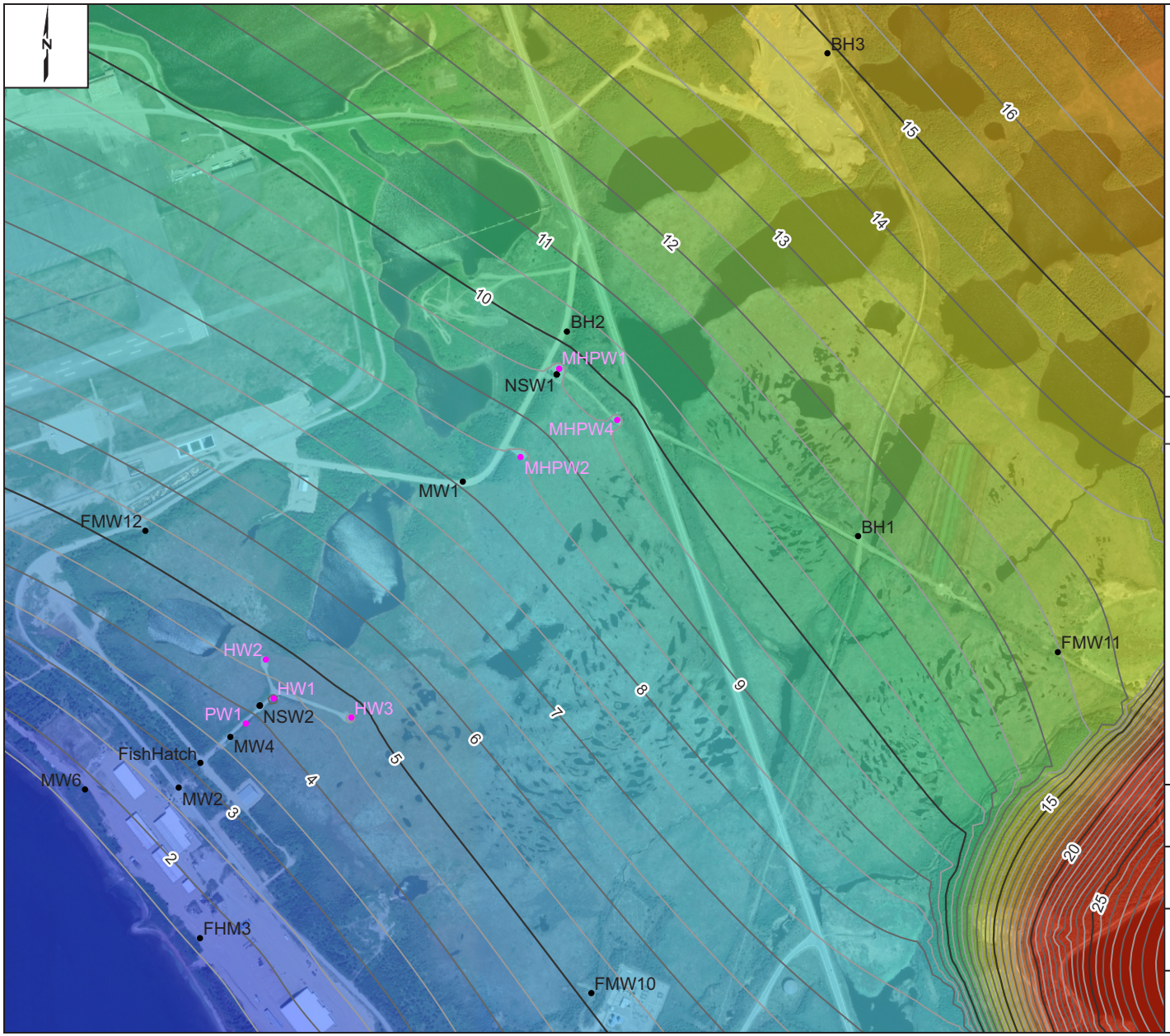

Legend

- Production well location
- Monitoring well location

Legend

Contours, m

1 5 10 15 >20

0 100 200 300 400 500

Scale, m

Note: Base orthorectified image from Google Earth (2022).

Figure 4.36

Contour map of the calculated water elevation (hydraulic head) at the pumping level with the prediction model, *Main 2,* under operation of the five production wells in December 31, 2041.

Document Reference	FFC-NL-3113-057b
Location	Stephenville, NL
Project No.	3113
Date	December 2022

FFC

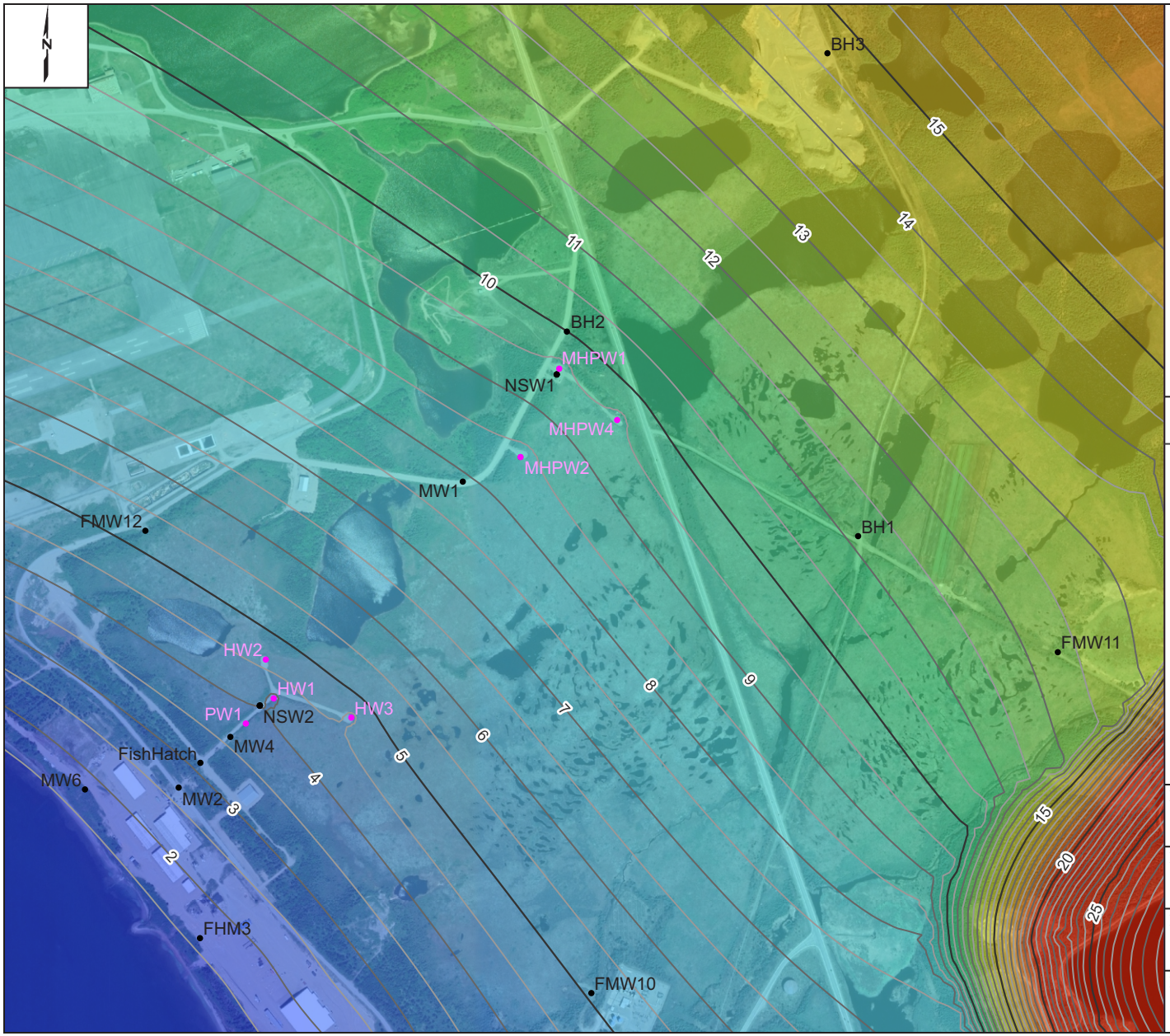

Legend

- Production well location
- Monitoring well location

Legend

Contours, m

1 5 10 15 >20

0 100 200 300 400 500

Scale, m

Note: Base orthorectified image from Google Earth (2022).

Figure 4.37

Contour map of the calculated water elevation (hydraulic head) at the pumping level with the prediction model, *Main 2,* under operation of the five production wells in December 31, 2046.

Document Reference	FFC-NL-3113-057b
Location	Stephenville, NL
Project No.	3113
Date	December 2022

FFC

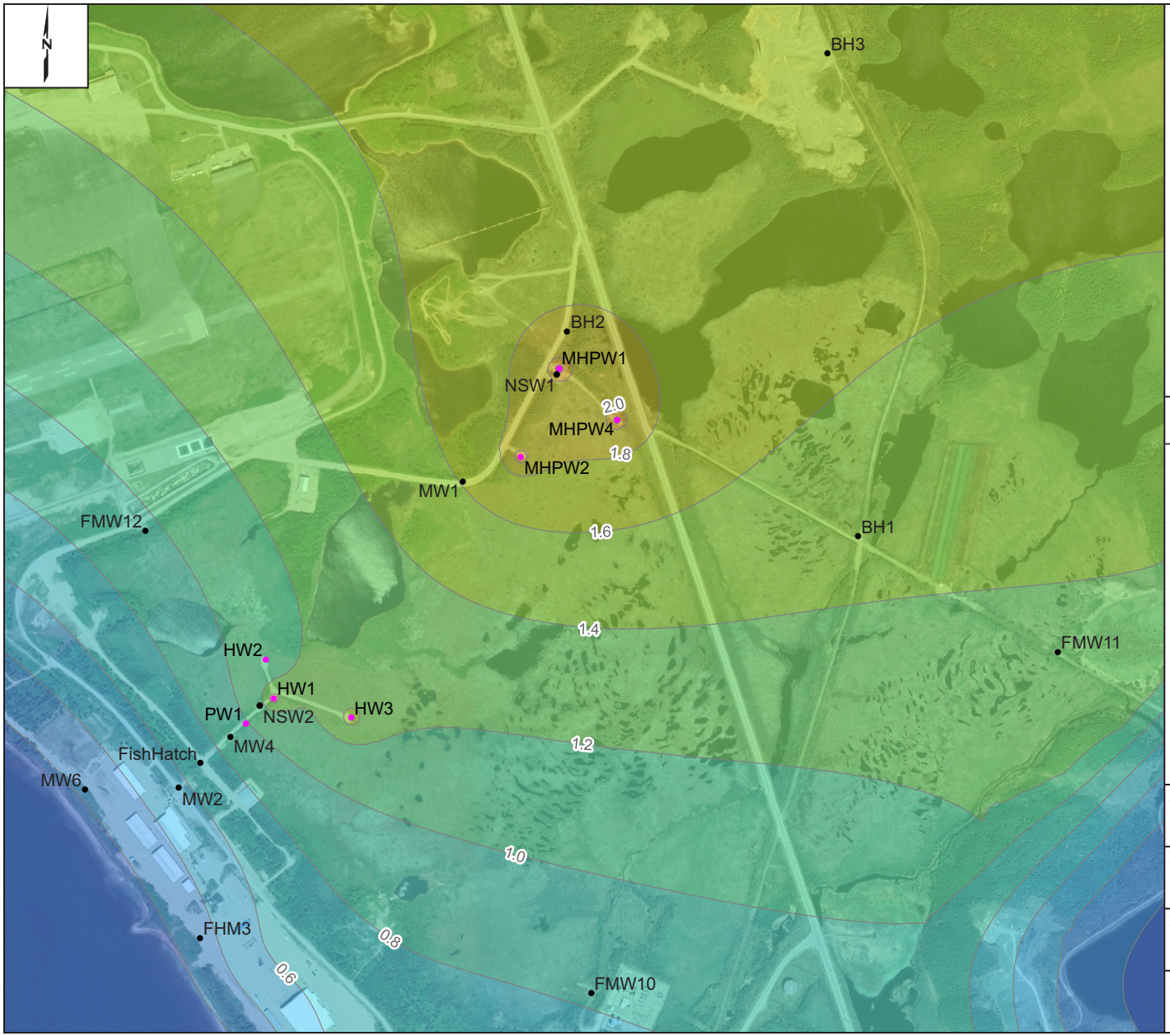

Legend

- Production well location
- Monitoring well location

Legend

Contours, m

0 1 2 >3

0 100 200 300 400 500

Scale, m

Note: Base orthorectified image from Google Earth (2022).

Figure 4.38

Capture area calculated by the prediction model, *Main 2*, with transient simulation at the pumping level under operation of the five production wells in December 31, 2026.

Document Reference	FFC-NL-3113-057b
Location	Stephenville, NL
Project No.	3113
Date	December 2022

FFC

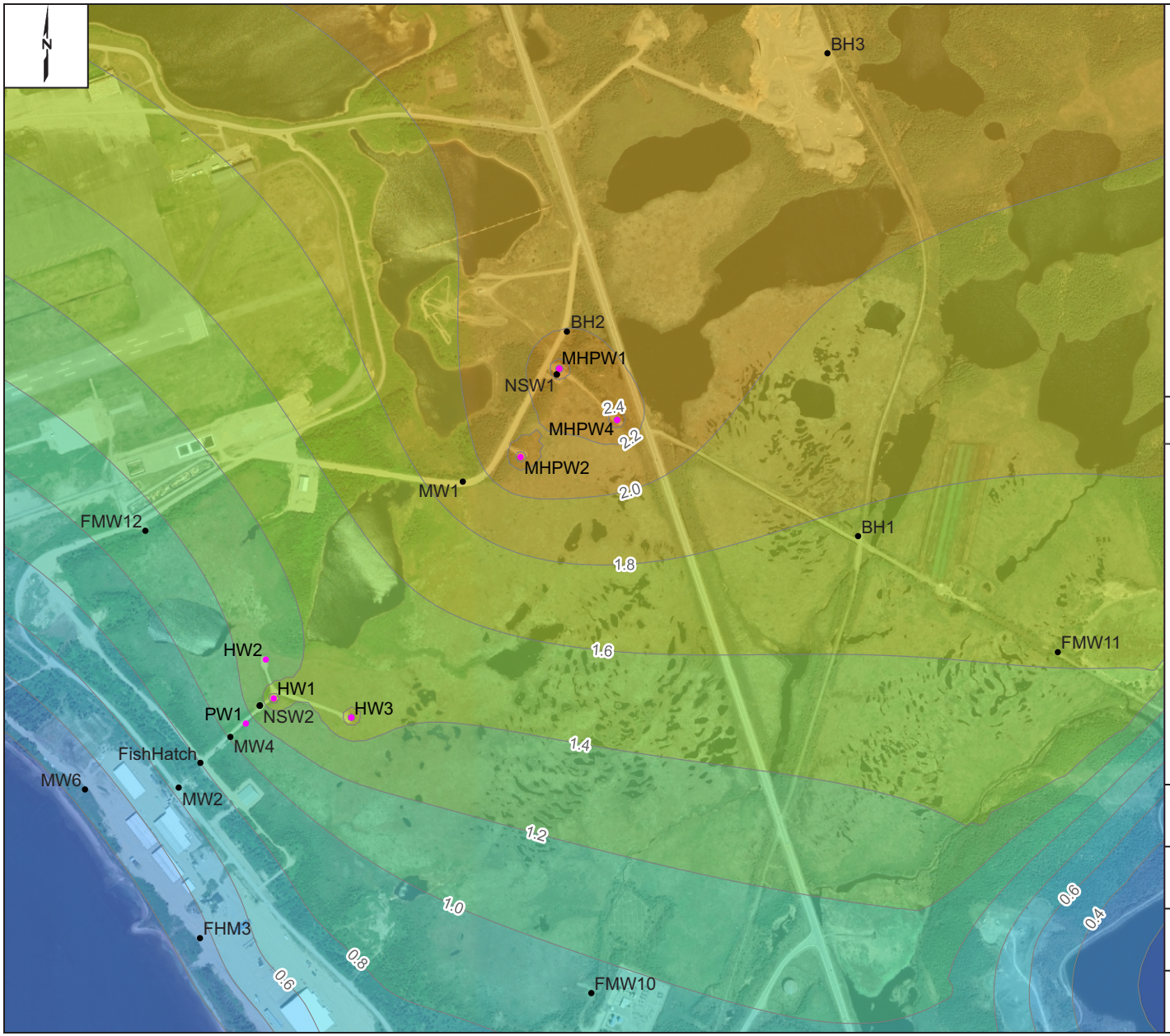

Legend

- Production well location
- Monitoring well location

Legend

Contours, m

0 1 2 >3

0 100 200 300 400 500

Scale, m

Note: Base orthorectified image from Google Earth (2022).

Figure 4.39

Capture area calculated by the prediction model, *Main 2*, with transient simulation at the pumping level under operation of the five production wells in December 31, 2031.

Document Reference	FFC-NL-3113-057b
Location	Stephenville, NL
Project No.	3113
Date	December 2022

FFC

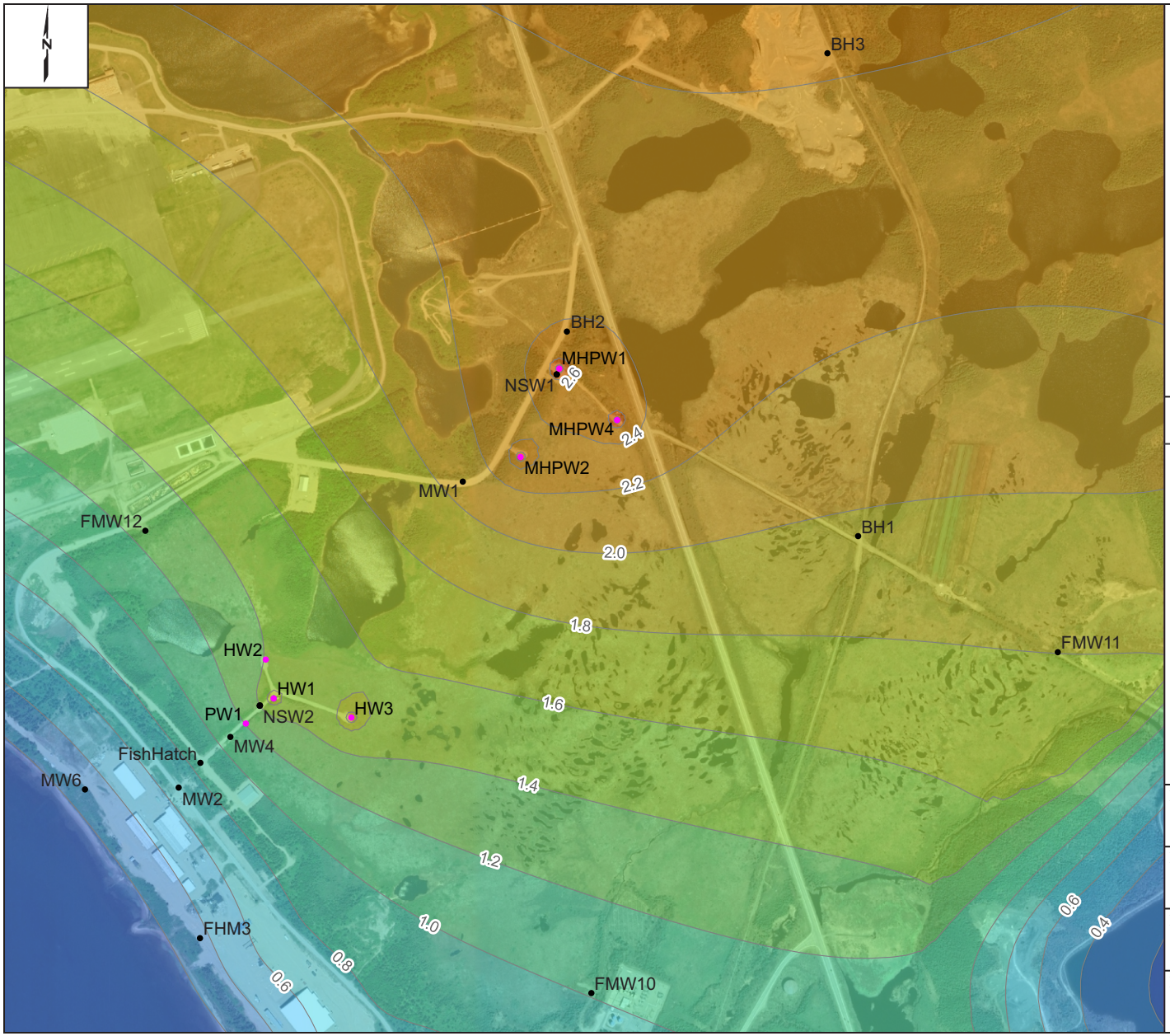

Legend

- Production well location
- Monitoring well location

Legend

Contours, m

0 1 2 >3

0 100 200 300 400 500

Scale, m

Note: Base orthorectified image from Google Earth (2022).

Figure 4.40

Capture area calculated by the prediction model, *Main 2*, with transient simulation at the pumping level under operation of the five production wells in December 31, 2036.

Document Reference	FFC-NL-3113-057b
Location	Stephenville, NL
Project No.	3113
Date	December 2022

FFC

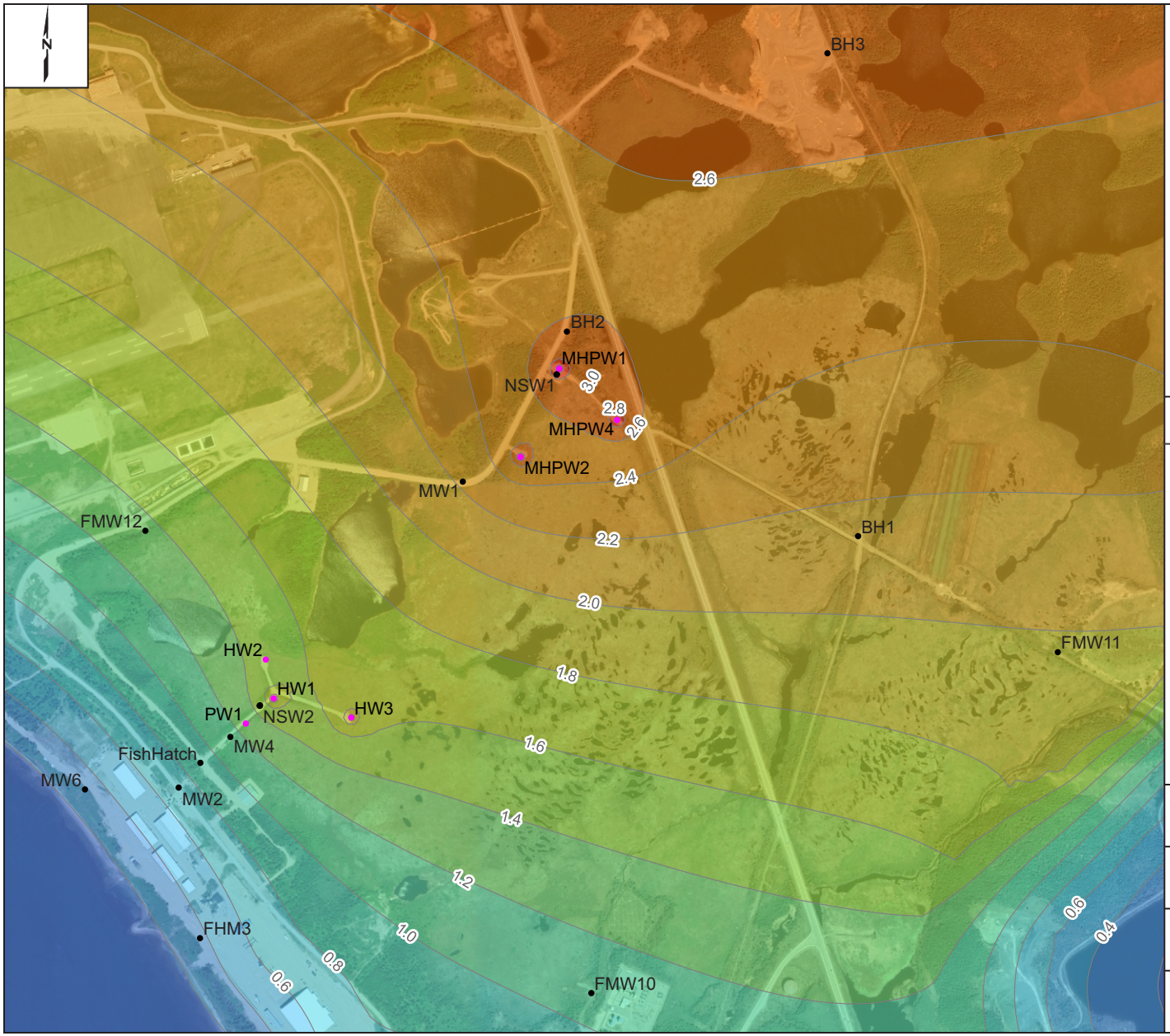

Legend

Production well location

Monitoring well location

Legend

Contours, m

0 1 2 >3

0 100 200 300 400 500

Scale, m

Note: Base orthorectified image from Google Earth (2022).

Figure 4.41

Capture area calculated by the prediction model, *Main 2*, with transient simulation at the pumping level under operation of the five production wells in December 31, 2041.

Document Reference	FFC-NL-3113-057b
Location	Stephenville, NL
Project No.	3113
Date	December 2022

FFC

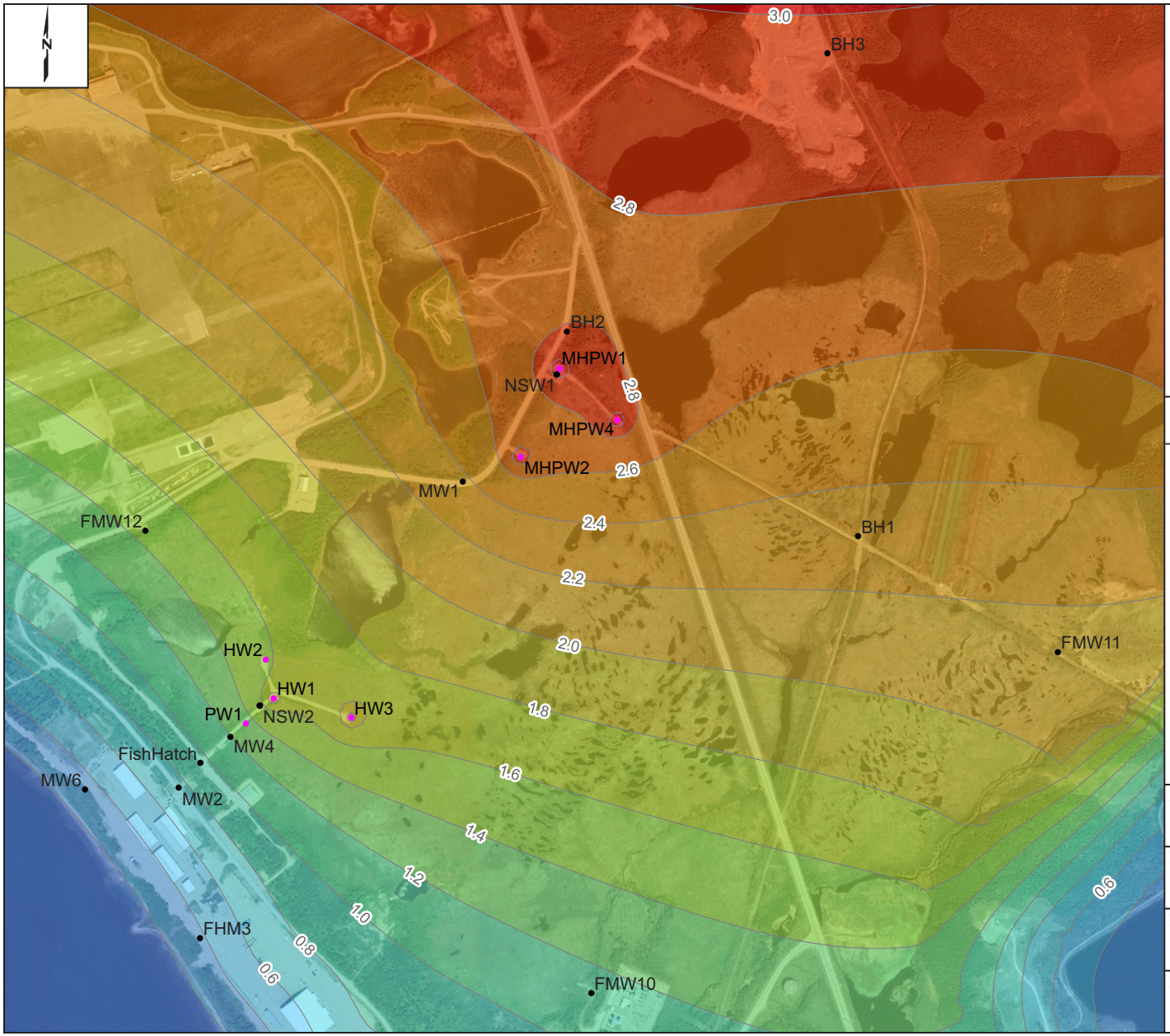

Legend

- Production well location
- Monitoring well location

Legend

Contours, m

0 1 2 >3

0 100 200 300 400 500

Scale, m

Note: Base orthorectified image from Google Earth (2022).

Figure 4.42

Capture area calculated by the prediction model, *Main 2*, with transient simulation at the pumping level under operation of the five production wells in December 31, 2046.

Document Reference	FFC-NL-3113-057b
Location	Stephenville, NL
Project No.	3113
Date	December 2022

FFC

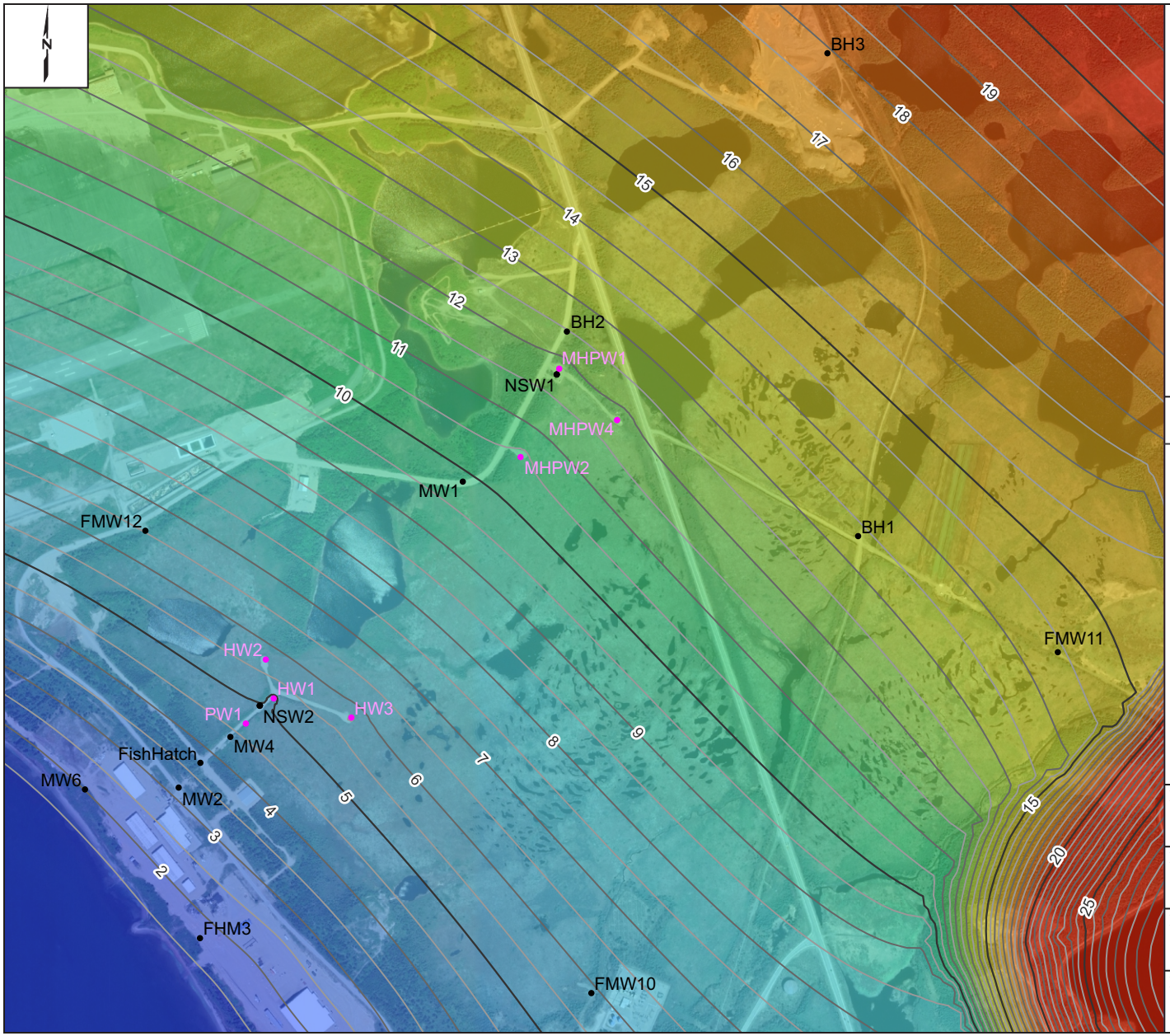

Legend

Production well location

Monitoring well location

Legend

Contours, m

1 5 10 15 >20

0 100 200 300 400 500

Scale, m

Note: Base orthorectified image from Google Earth (2022).

Figure 4.43

Contour map of the calculated water elevation (hydraulic head) at the pumping level with the prediction model, *Upper Limit 1*, under operation of the five production wells in December 31, 2026.

Document Reference
FFC-NL-3113-057b

Location
Stephenville, NL

Project No.
3113

Date
December 2022

FFC

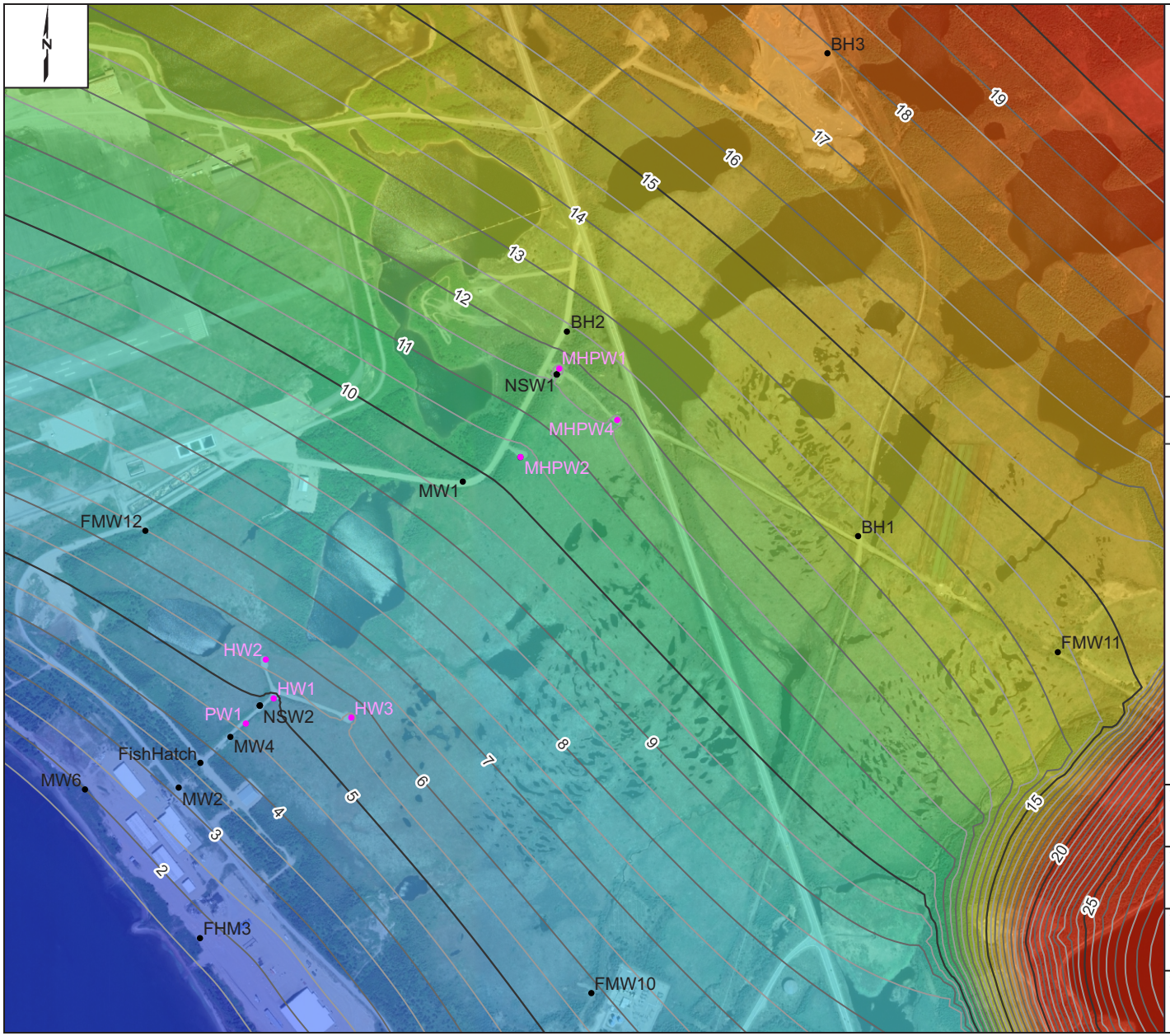

Legend

Production well location

Monitoring well location

Legend

Contours, m

1 5 10 15 >20

0 100 200 300 400 500

Scale, m

Note: Base orthorectified image from Google Earth (2022).

Figure 4.44

Contour map of the calculated water elevation (hydraulic head) at the pumping level with the prediction model, *Upper Limit 1*, under operation of the five production wells in December 31, 2031.

Document Reference
FFC-NL-3113-057b

Location
Stephenville, NL

Project No.
3113

Date
December 2022

FFC

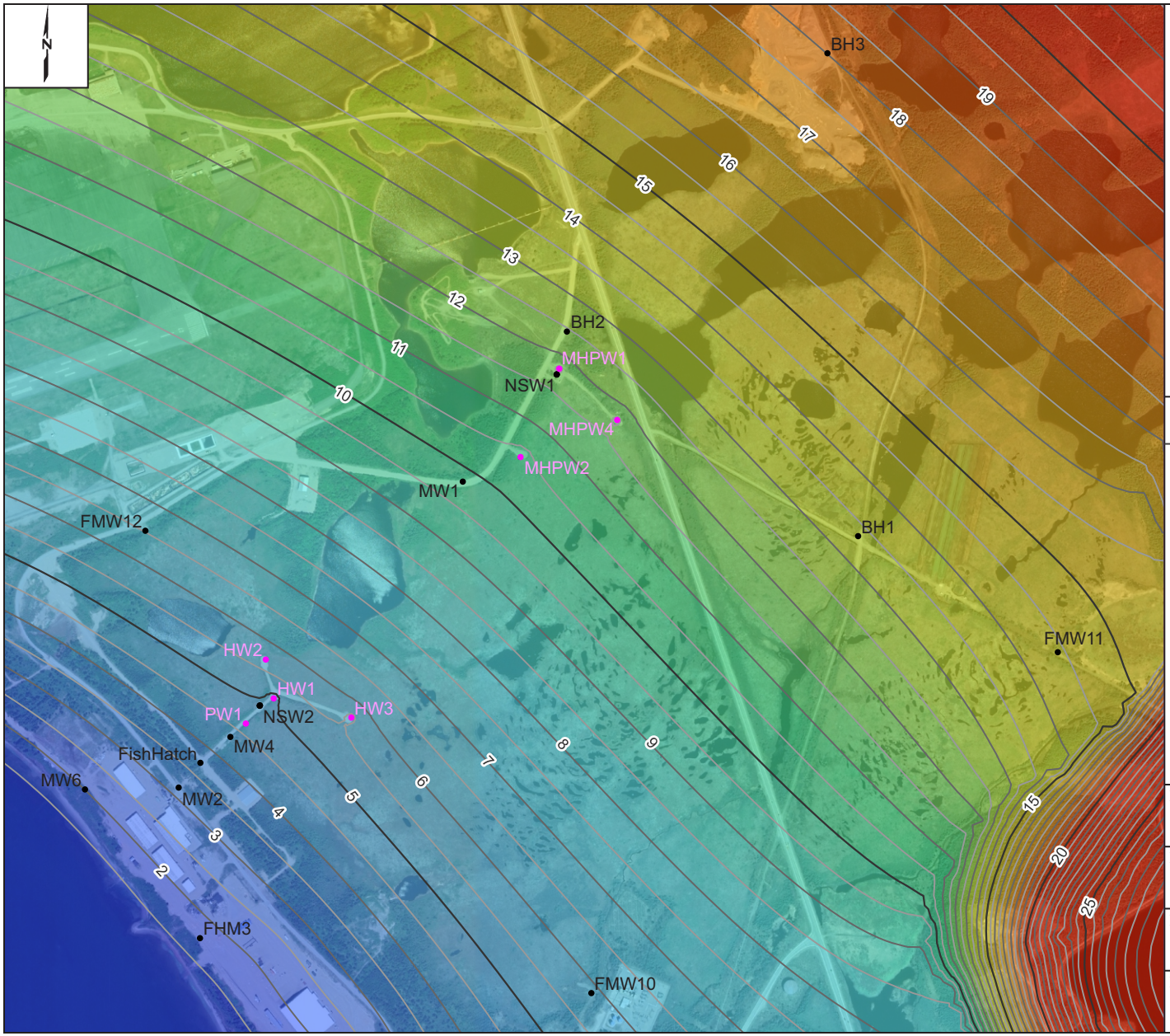

Legend

- Production well location
- Monitoring well location

Legend

Contours, m

1 5 10 15 >20

0 100 200 300 400 500

Scale, m

Note: Base orthorectified image from Google Earth (2022).

Figure 4.45

Contour map of the calculated water elevation (hydraulic head) at the pumping level with the prediction model, *Upper Limit 1,* under operation of the five production wells in December 31, 2036.

Document Reference	FFC-NL-3113-057b
Location	Stephenville, NL
Project No.	3113
Date	December 2022

FFC

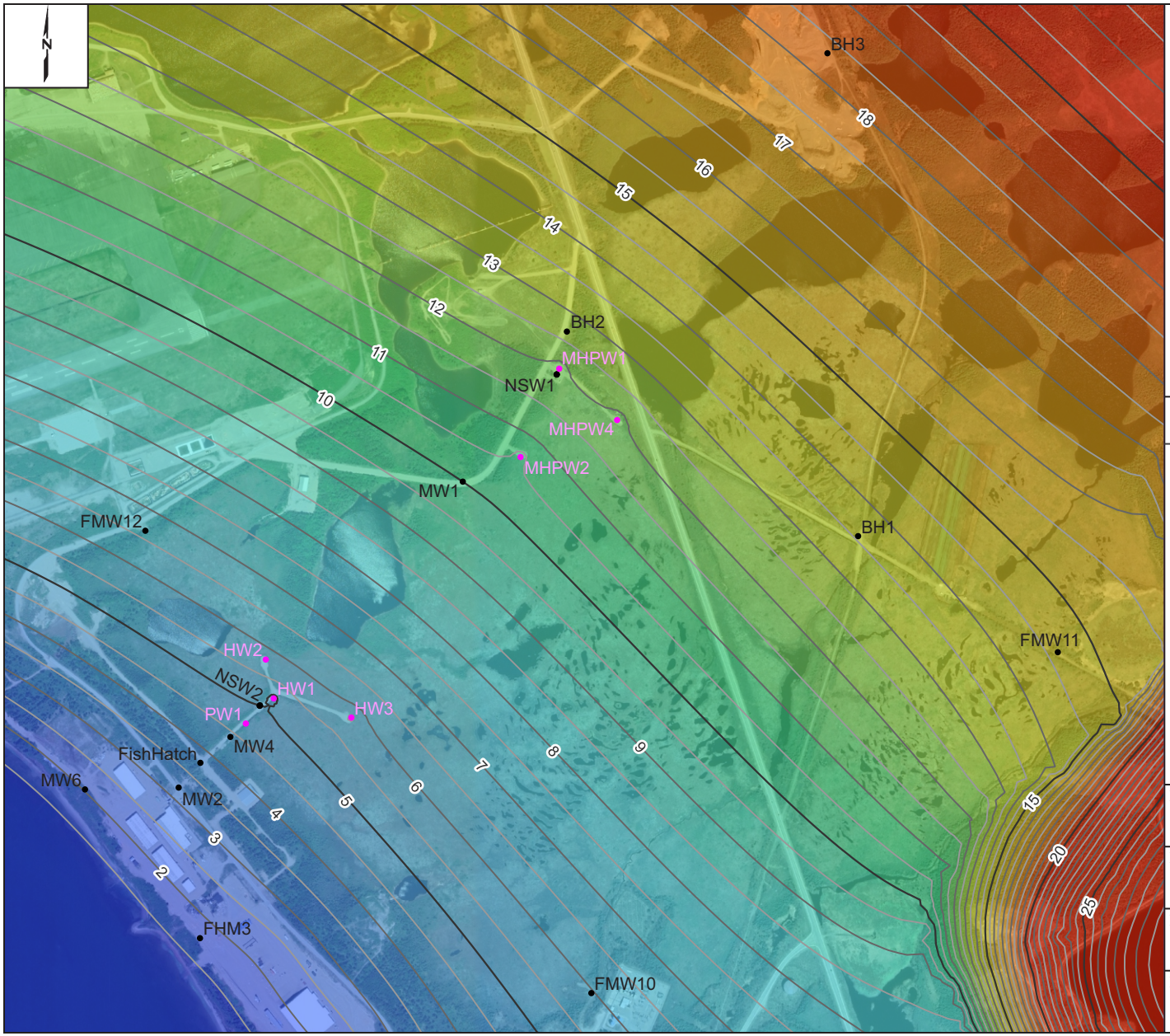

Legend

Production well location

Monitoring well location

Legend

Contours, m

1 5 10 15 >20

0 100 200 300 400 500

Scale, m

Note: Base orthorectified image from Google Earth (2022).

Figure 4.46

Contour map of the calculated water elevation (hydraulic head) at the pumping level with the prediction model, *Upper Limit 1,* under operation of the five production wells in December 31, 2041.

Document Reference	FFC-NL-3113-057b
Location	Stephenville, NL
Project No.	3113
Date	December 2022

FFC

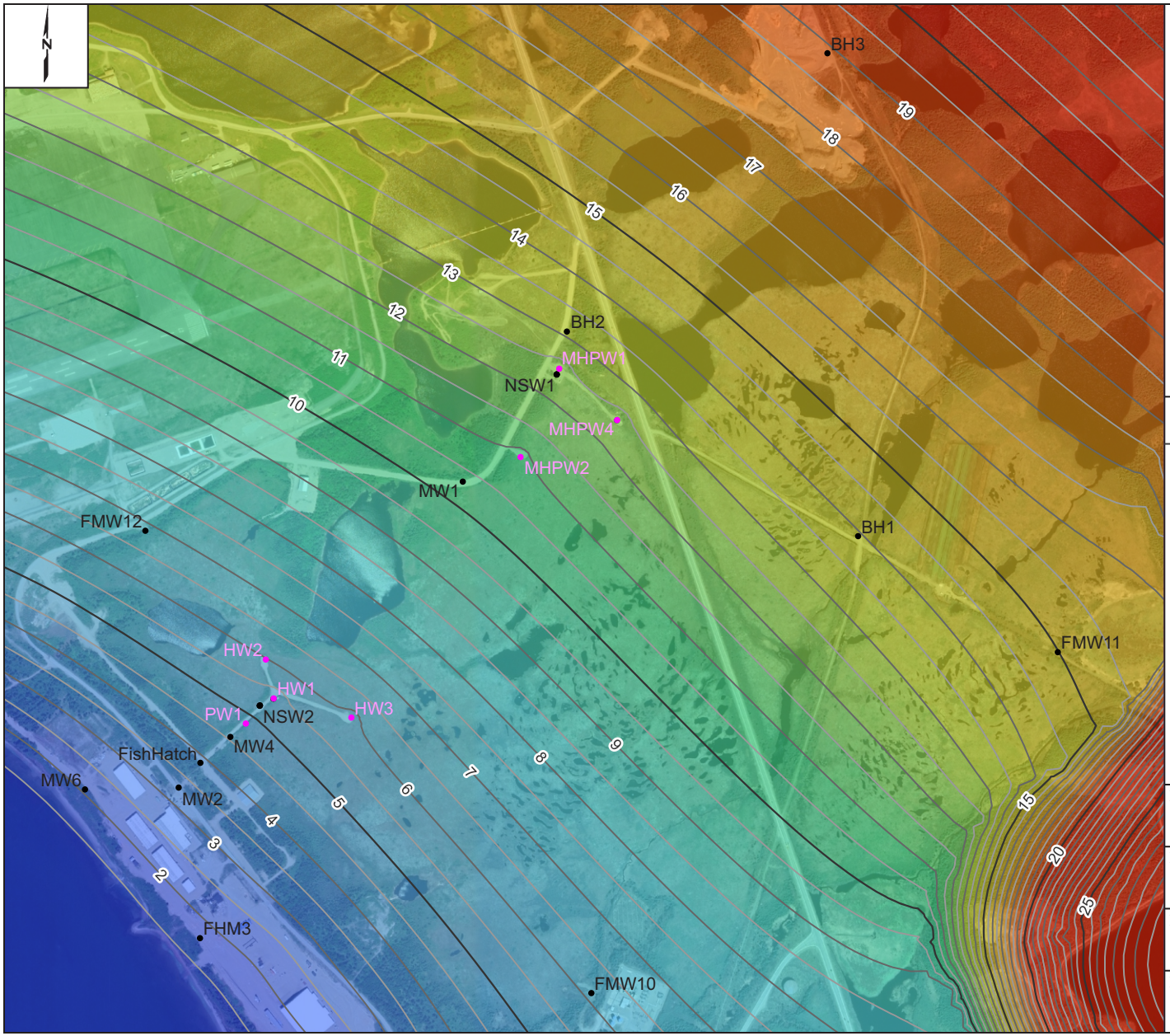

Legend

Production well location

Monitoring well location

Legend

Contours, m

1 5 10 15 >20

0 100 200 300 400 500

Scale, m

Note: Base orthorectified image from Google Earth (2022).

Figure 4.47

Contour map of the calculated water elevation (hydraulic head) at the pumping level with the prediction model, *Upper Limit 1,* under operation of the five production wells in December 31, 2046.

Document Reference	FFC-NL-3113-057b
Location	Stephenville, NL
Project No.	3113
Date	December 2022

FFC

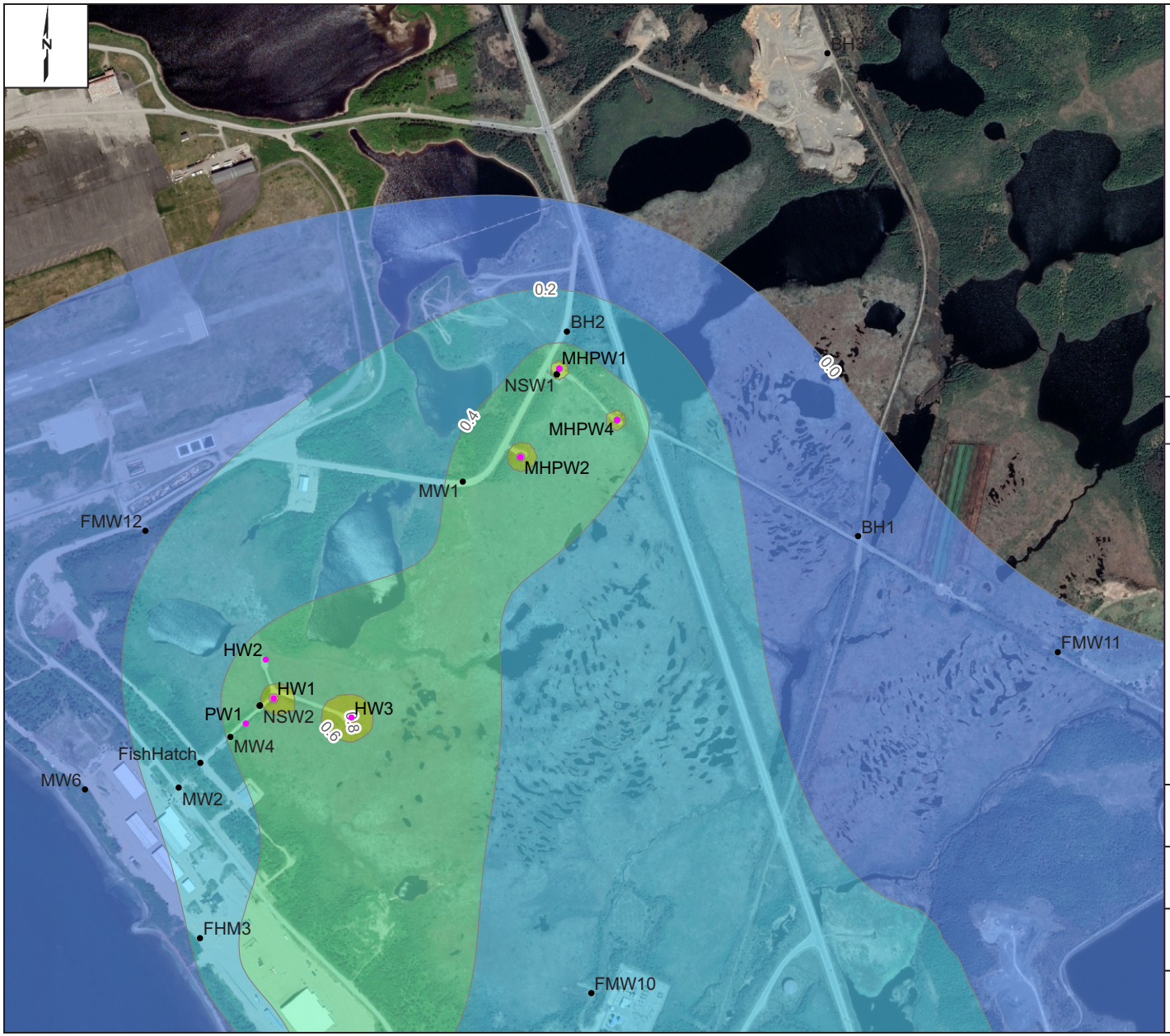

Legend

- Production well location
- Monitoring well location

Legend

Contours, m

0 0.4 0.8 >1.2

0 100 200 300 400 500

Scale, m

Note: Base orthorectified image from Google Earth (2022).

Figure 4.48

Capture area calculated by the prediction model, *Upper Limit 1,* with transient simulation at the pumping level under operation of the five production wells in December 31, 2026.

Document Reference	FFC-NL-3113-057b
Location	Stephenville, NL
Project No.	3113
Date	December 2022

FFC

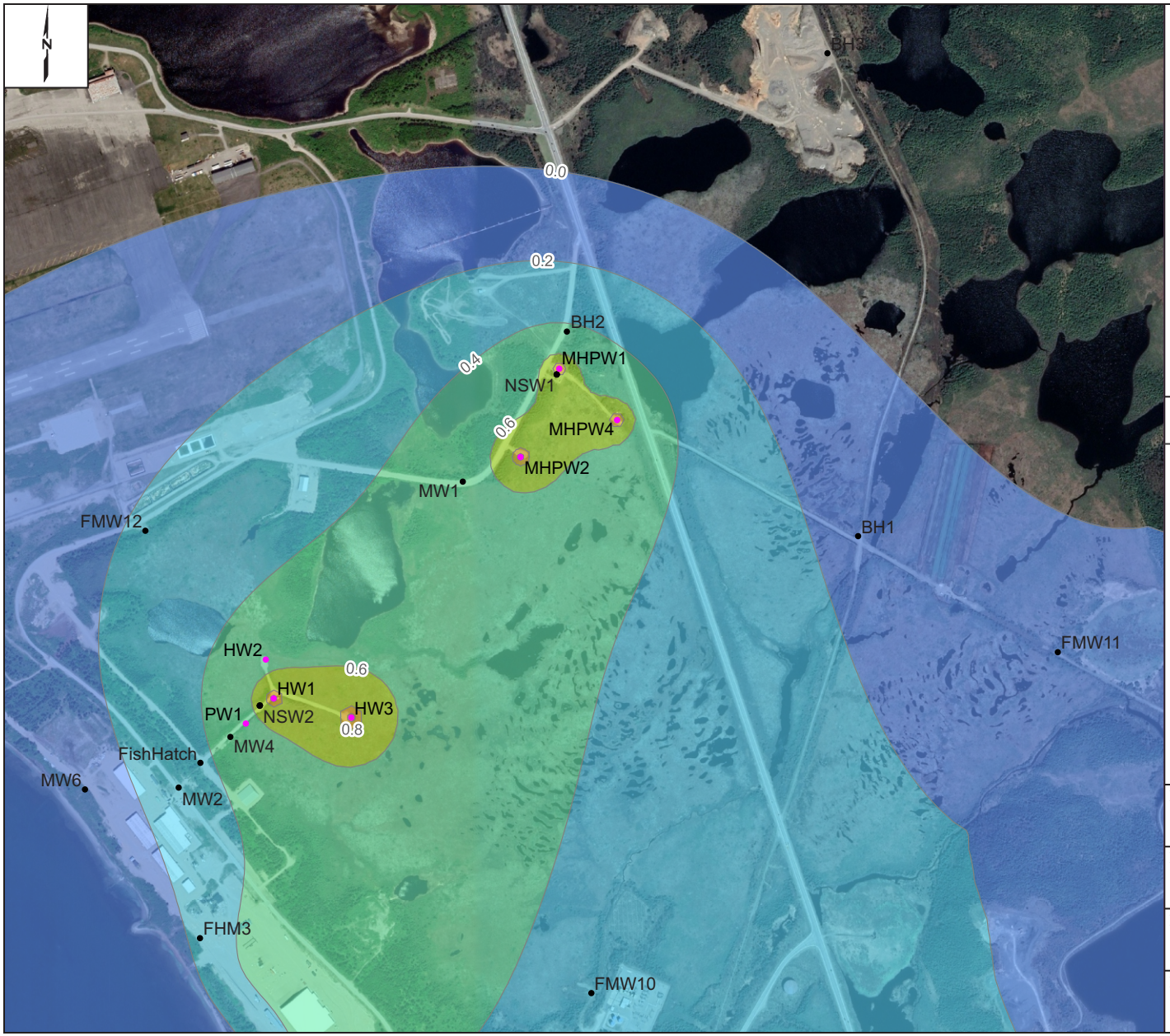

Legend

- Production well location
- Monitoring well location

Legend

Contours, m

0 0,4 0,8 >1,2

0 100 200 300 400 500

Scale, m

Note: Base orthorectified image from Google Earth (2022).

Figure 4.49

Capture area calculated by the prediction model, *Upper Limit 1*, with transient simulation at the pumping level under operation of the five production wells in December 31, 2031.

Document Reference	FFC-NL-3113-057b
Location	Stephenville, NL
Project No.	3113
Date	December 2022

FFC

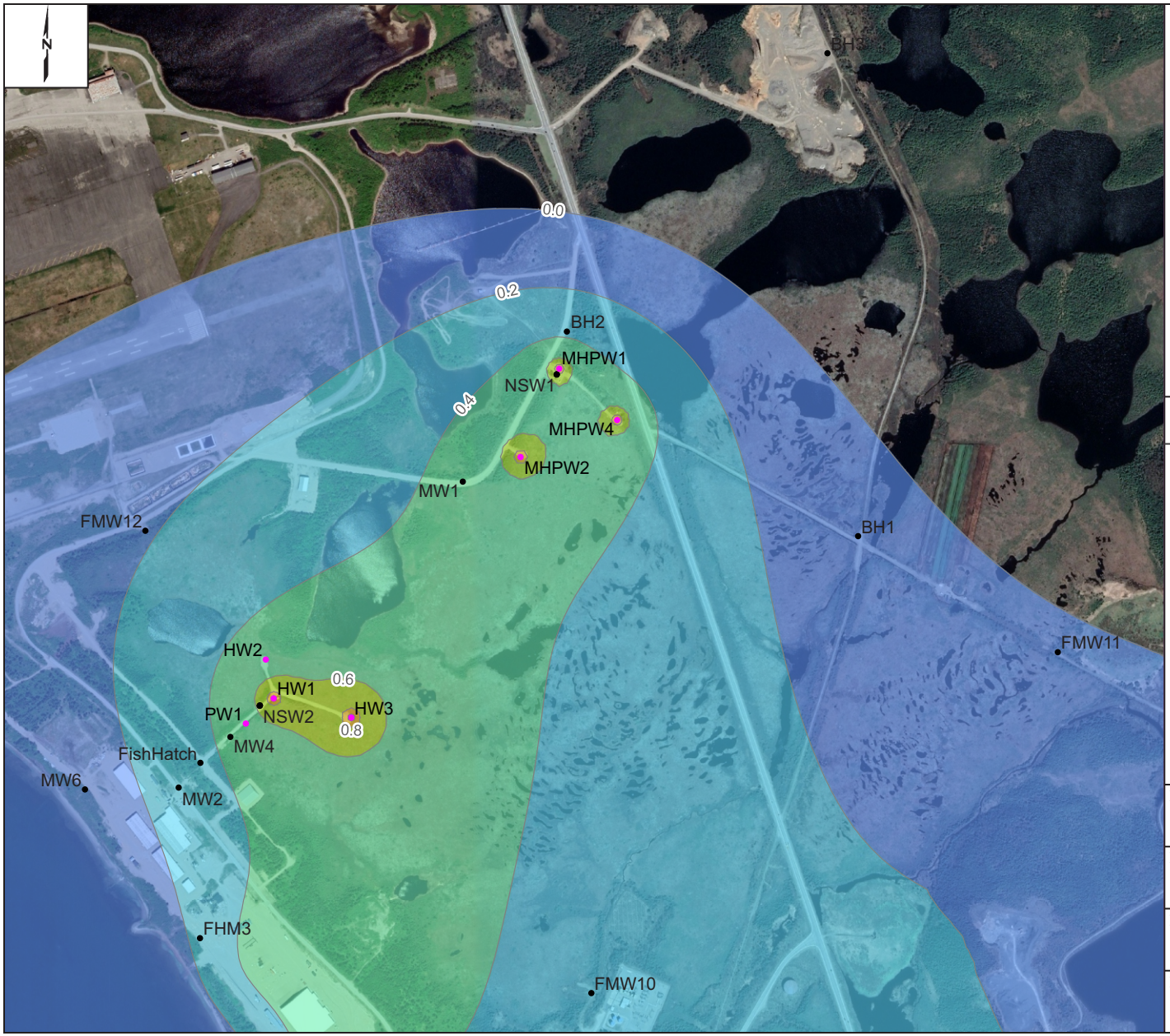

Legend

- Production well location
- Monitoring well location

Legend

Contours, m

0 0.4 0.8 >1.2

0 100 200 300 400 500

Scale, m

Note: Base orthorectified image from Google Earth (2022).

Figure 4.50

Capture area calculated by the prediction model, *Upper Limit 1*, with transient simulation at the pumping level under operation of the five production wells in December 31, 2036.

Document Reference	FFC-NL-3113-057b
Location	Stephenville, NL
Project No.	3113
Date	December 2022

FFC

Legend

- Production well location
- Monitoring well location

Legend

Contours, m

0 0.4 0.8 >1.2

0 100 200 300 400 500

Scale, m

Note: Base orthorectified image from Google Earth (2022).

Figure 4.51

Capture area calculated by the prediction model, *Upper Limit 1*, with transient simulation at the pumping level under operation of the five production wells in December 31, 2041.

Document Reference	FFC-NL-3113-057b
Location	Stephenville, NL
Project No.	3113
Date	December 2022

FFC

Legend

- Production well location
- Monitoring well location

Legend

Contours, m

0 0,4 0,8 >1,2

0 100 200 300 400 500

Scale, m

Note: Base orthorectified image from Google Earth (2022).

Figure 4.52

Capture area calculated by the prediction model, *Upper Limit 1*, with transient simulation at the pumping level under operation of the five production wells in December 31, 2046.

Document Reference	FFC-NL-3113-057b
Location	Stephenville, NL
Project No.	3113
Date	December 2022

FFC

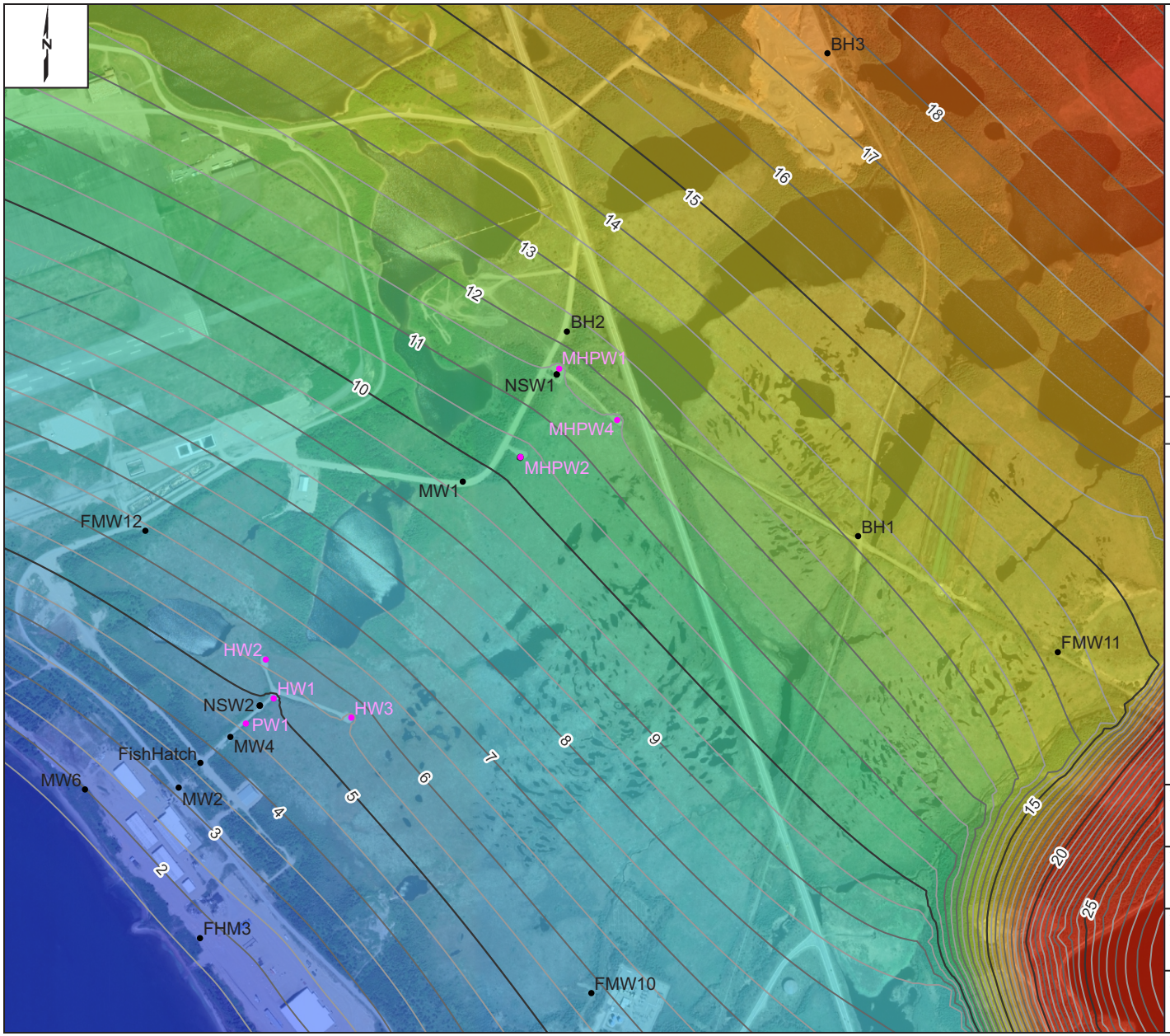

Legend

- Production well location
- Monitoring well location

Legend

Contours, m

1 5 10 15 >20

0 100 200 300 400 500

Scale, m

Note: Base orthorectified image from Google Earth (2022).

Figure 4.53

Contour map of the calculated water elevation (hydraulic head) at the pumping level with the prediction model, *Upper Limit 2,* under operation of the five production wells in December 31, 2026.

Document Reference	FFC-NL-3113-057b
Location	Stephenville, NL
Project No.	3113
Date	December 2022

FFC

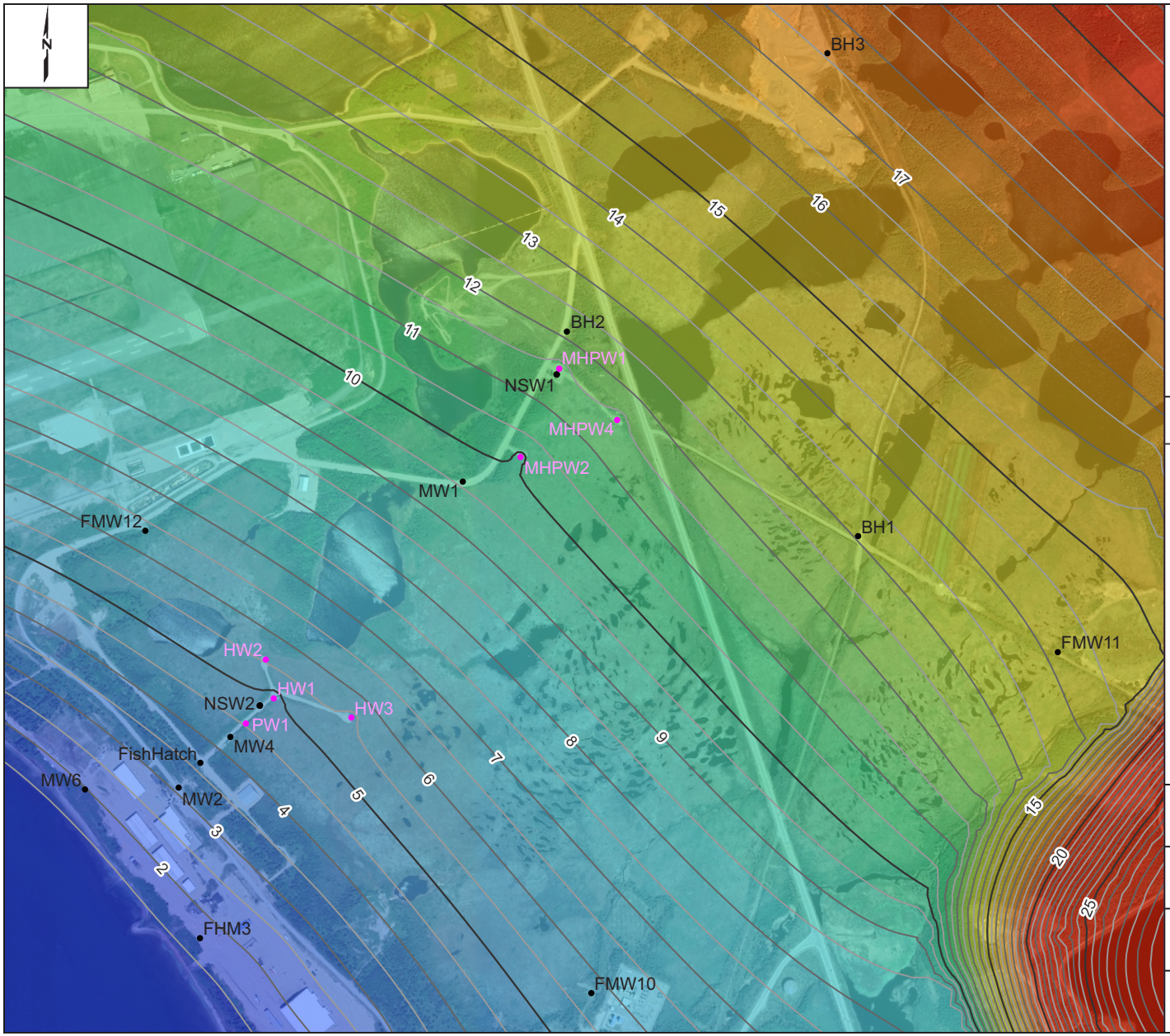

Legend

- Production well location
- Monitoring well location

Legend

Contours, m

1 5 10 15 >20

0 100 200 300 400 500

Scale, m

Note: Base orthorectified image from Google Earth (2022).

Figure 4.54

Contour map of the calculated water elevation (hydraulic head) at the pumping level with the prediction model, *Upper Limit 2,* under operation of the five production wells in December 31, 2031.

Document Reference	FFC-NL-3113-057b
Location	Stephenville, NL
Project No.	3113
Date	December 2022

FFC

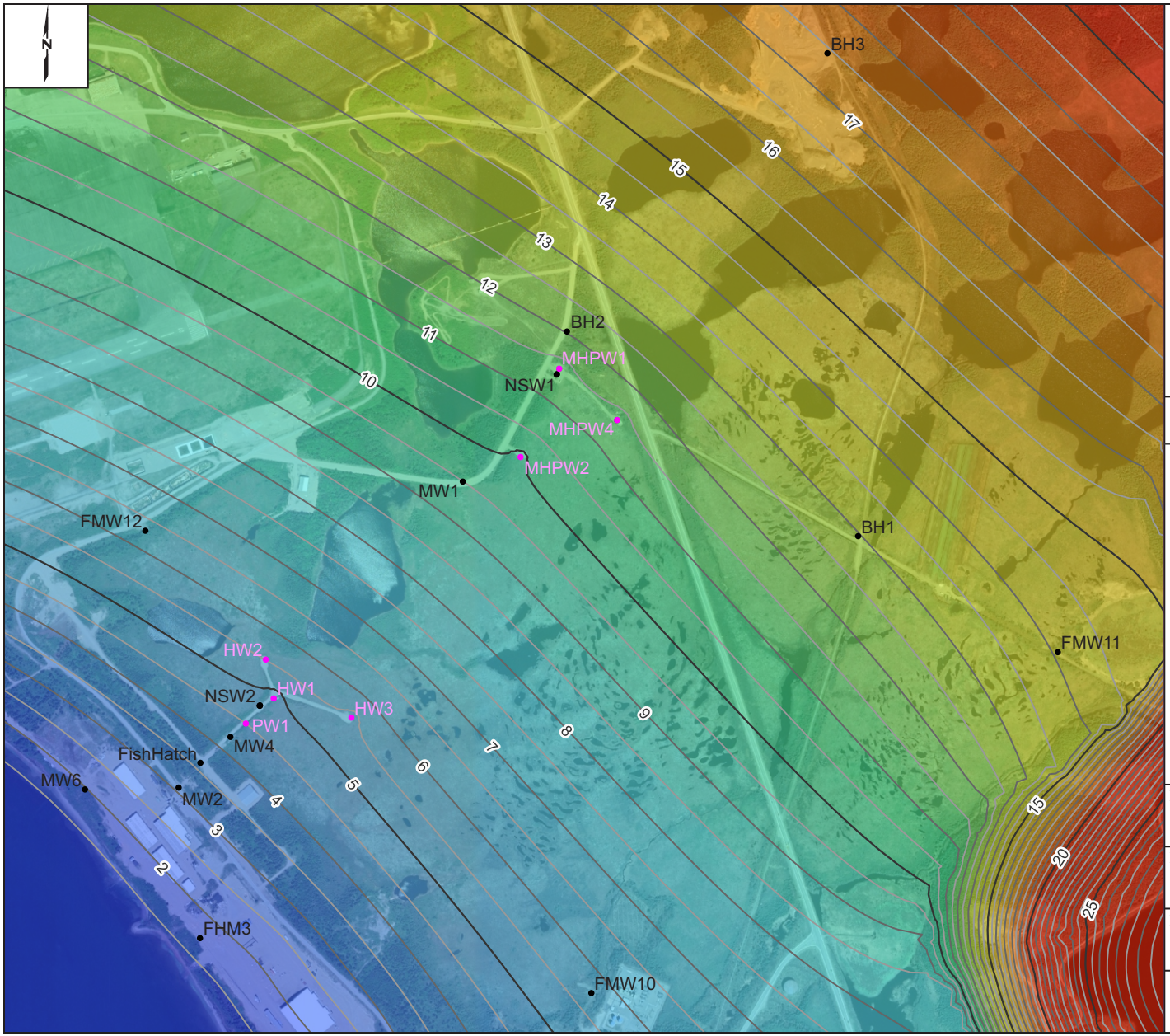

Legend

Production well location

Monitoring well location

Legend

Contours, m

1 5 10 15 >20

0 100 200 300 400 500

Scale, m

Note: Base orthorectified image from Google Earth (2022).

Figure 4.55

Contour map of the calculated water elevation (hydraulic head) at the pumping level with the prediction model, *Upper Limit 2,* under operation of the five production wells in December 31, 2036.

Document Reference	FFC-NL-3113-057b
Location	Stephenville, NL
Project No.	3113
Date	December 2022

FFC

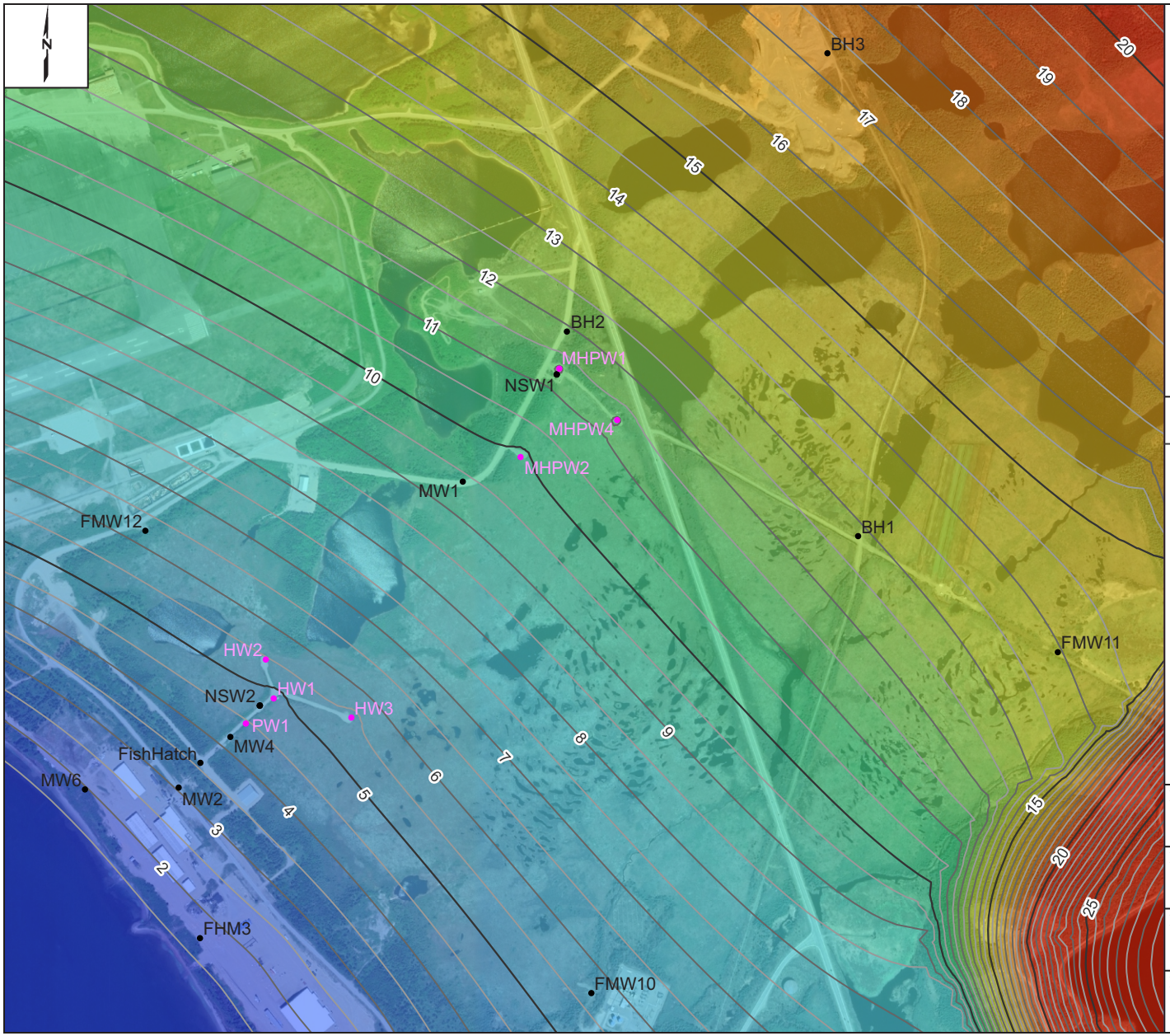

Legend

Production well location

Monitoring well location

Legend

Contours, m

1 5 10 15 >20

0 100 200 300 400 500

Scale, m

Note: Base orthorectified image from Google Earth (2022).

Figure 4.56

Contour map of the calculated water elevation (hydraulic head) at the pumping level with the prediction model, *Upper Limit 2,* under operation of the five production wells in December 31, 2041.

Document Reference
FFC-NL-3113-057b

Location
Stephenville, NL

Project No.
3113

Date
December 2022

FFC

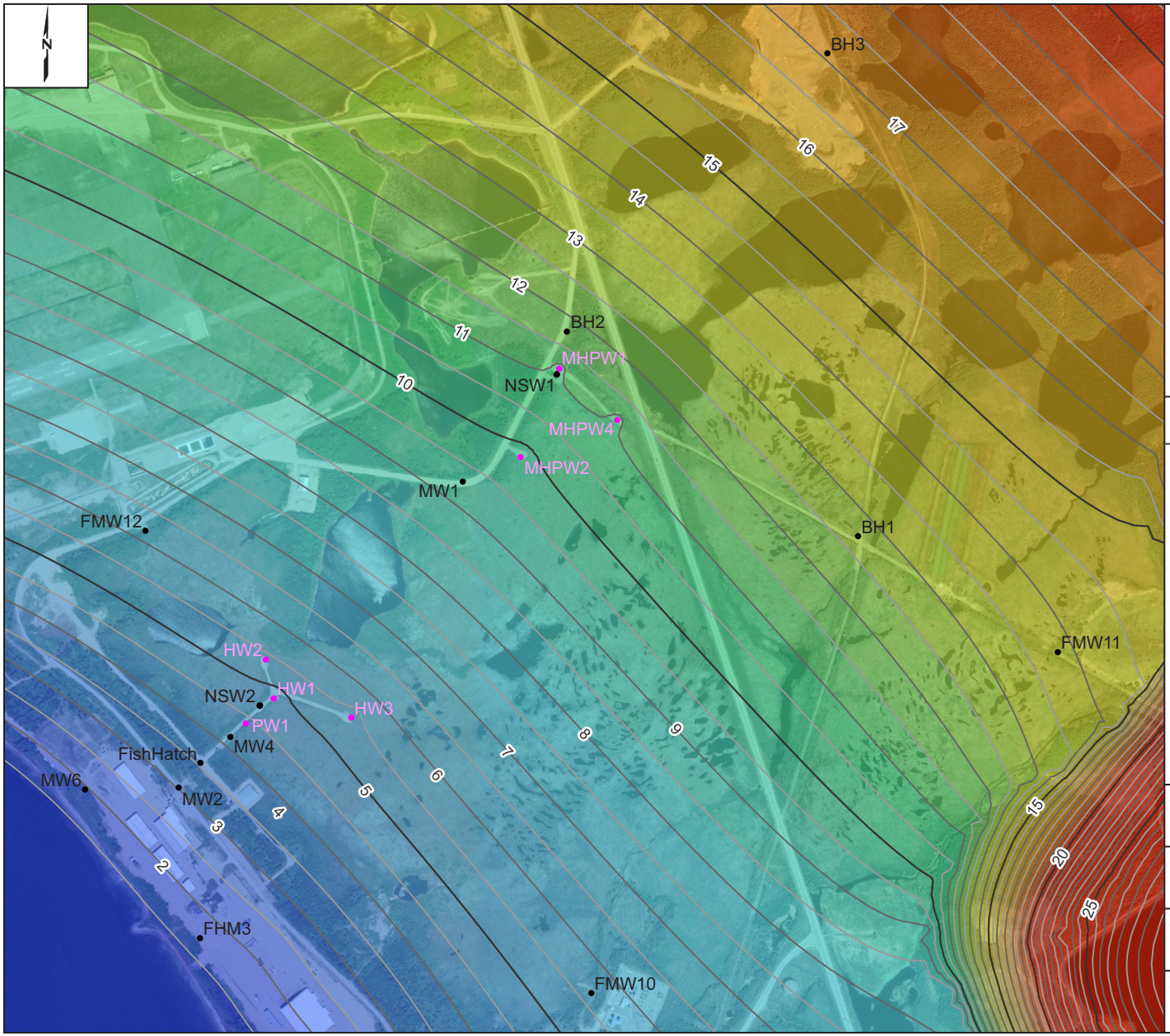

Legend

- Production well location
- Monitoring well location

Legend

Contours, m

1 5 10 15 >20

0 100 200 300 400 500

Scale, m

Note: Base orthorectified image from Google Earth (2022).

Figure 4.57

Contour map of the calculated water elevation (hydraulic head) at the pumping level with the prediction model, *Upper Limit 2,* under operation of the five production wells in December 31, 2046.

Document Reference	FFC-NL-3113-057b
Location	Stephenville, NL
Project No.	3113
Date	December 2022

FFC

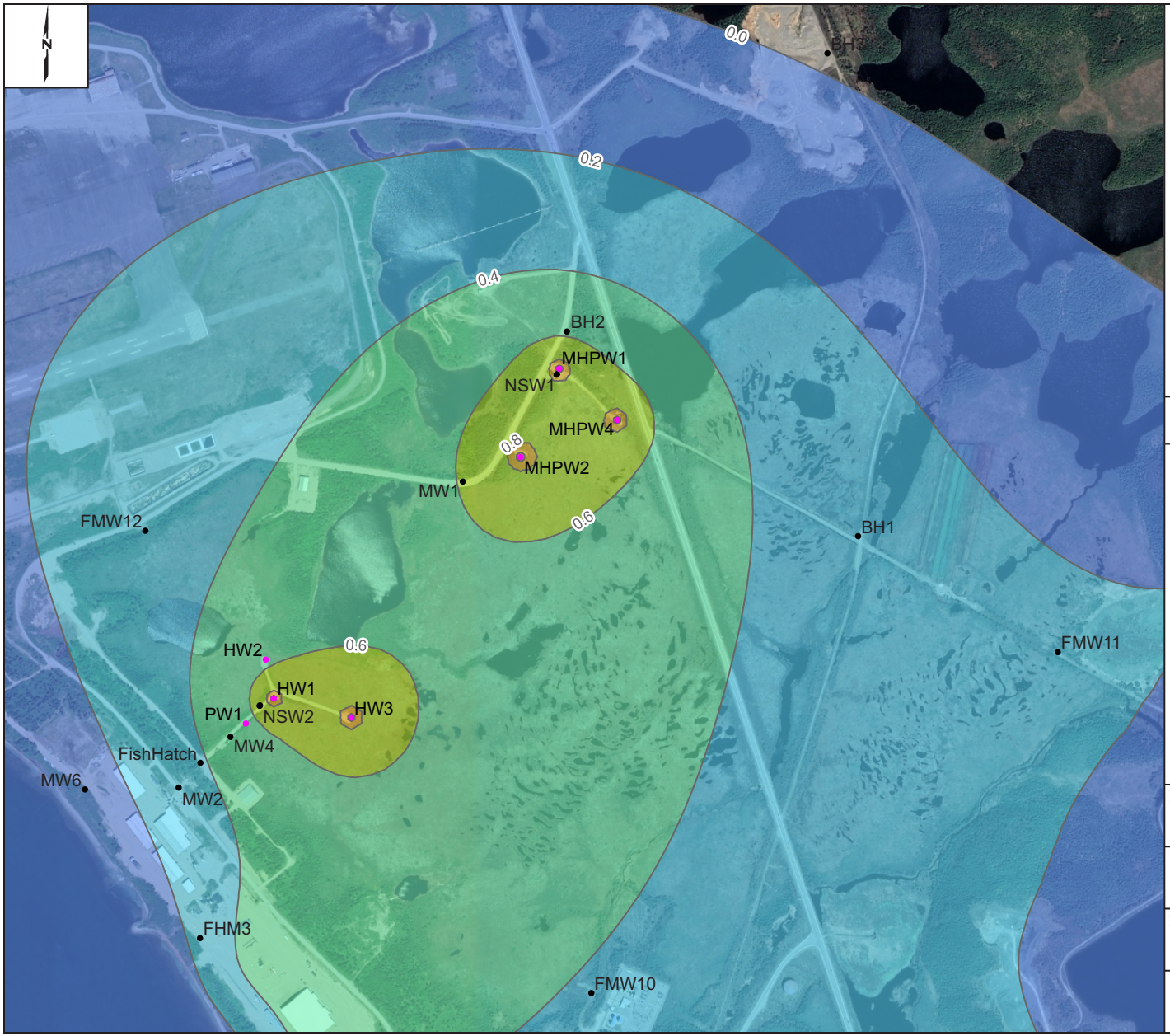

Legend

- Production well location
- Monitoring well location

Legend

Contours, m

0 0.4 0.8 >1.2

0 100 200 300 400 500

Scale, m

Note: Base orthorectified image from Google Earth (2022).

Figure 4.58

Capture area calculated by the prediction model, *Upper Limit 2*, with transient simulation at the pumping level under operation of the five production wells in December 31, 2026.

Document Reference	FFC-NL-3113-057b
Location	Stephenville, NL
Project No.	3113
Date	December 2022

FFC

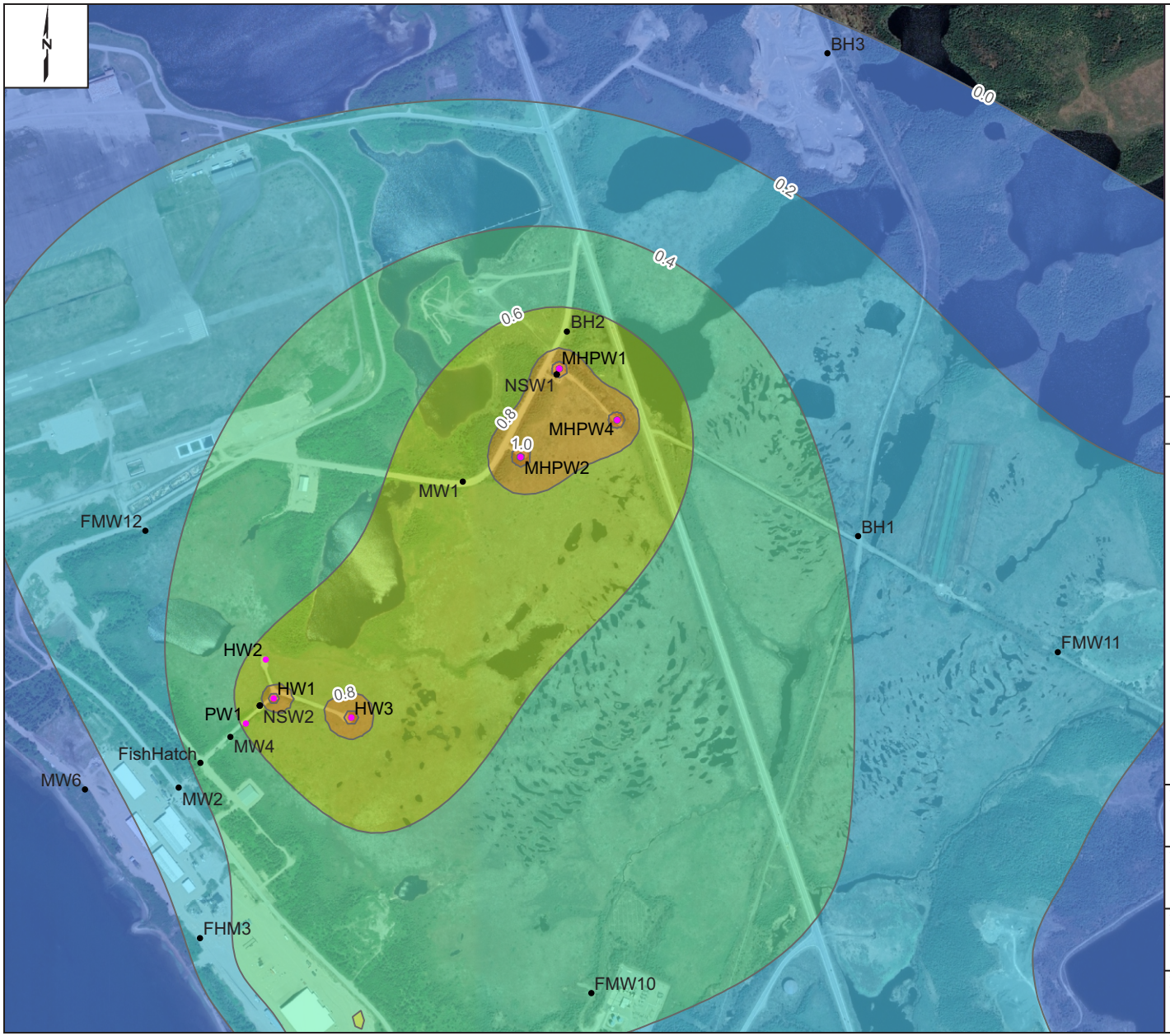

Legend

- Production well location
- Monitoring well location

Legend

Contours, m

0 0.4 0.8 >1.2

0 100 200 300 400 500

Scale, m

Note: Base orthorectified image from Google Earth (2022).

Figure 4.59

Capture area calculated by the prediction model, *Upper Limit 2*, with transient simulation at the pumping level under operation of the five production wells in December 31, 2031.

Document Reference	FFC-NL-3113-057b
Location	Stephenville, NL
Project No.	3113
Date	December 2022

FFC

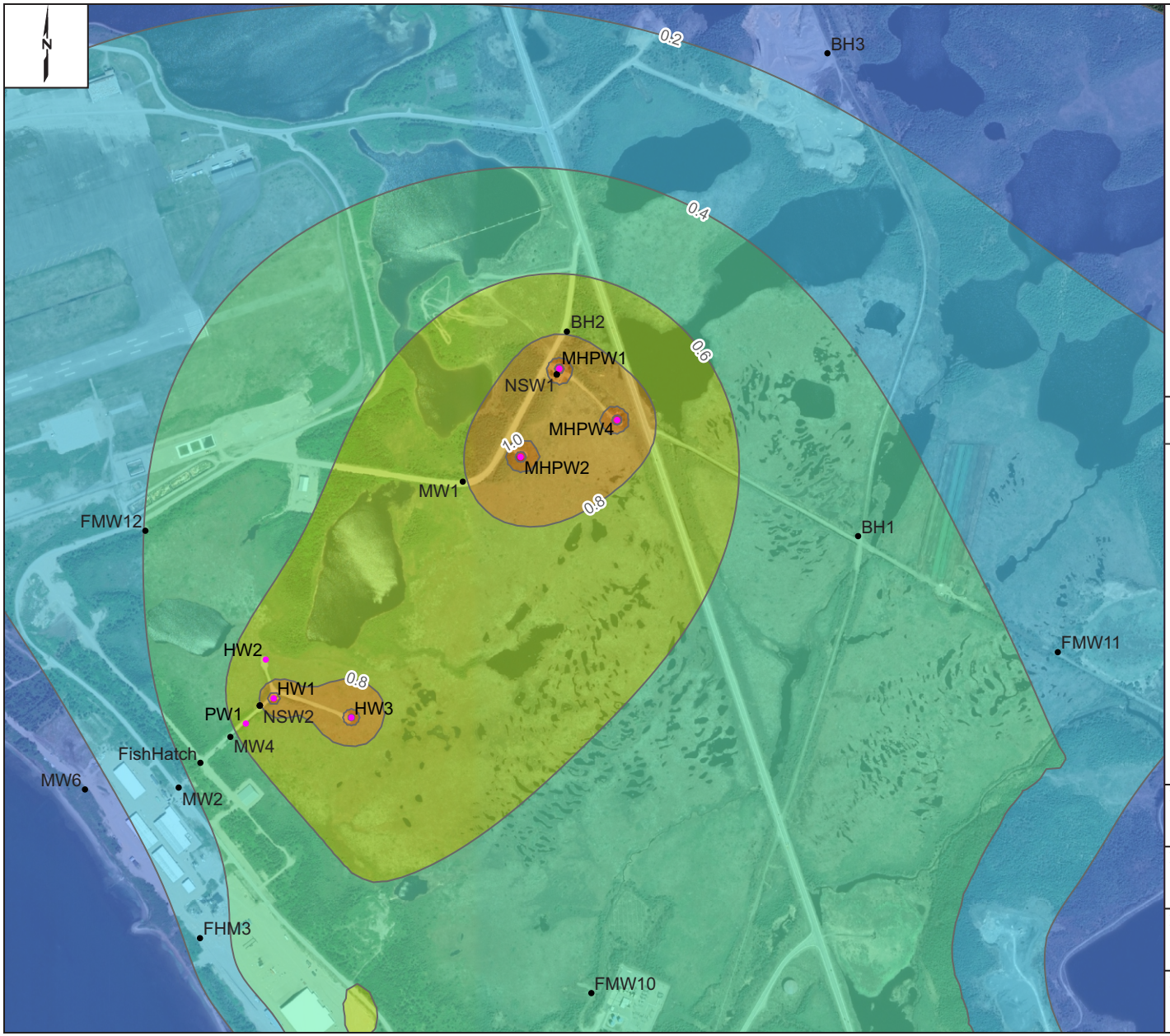

Legend

Production well location

Monitoring well location

Legend

Contours, m

0 0.4 0.8 >1.2

0 100 200 300 400 500

Scale, m

Note: Base orthorectified image from Google Earth (2022).

Figure 4.60

Capture area calculated by the prediction model, *Upper Limit 2*, with transient simulation at the pumping level under operation of the five production wells in December 31, 2036.

Document Reference	FFC-NL-3113-057b
Location	Stephenville, NL
Project No.	3113
Date	December 2022

FFC

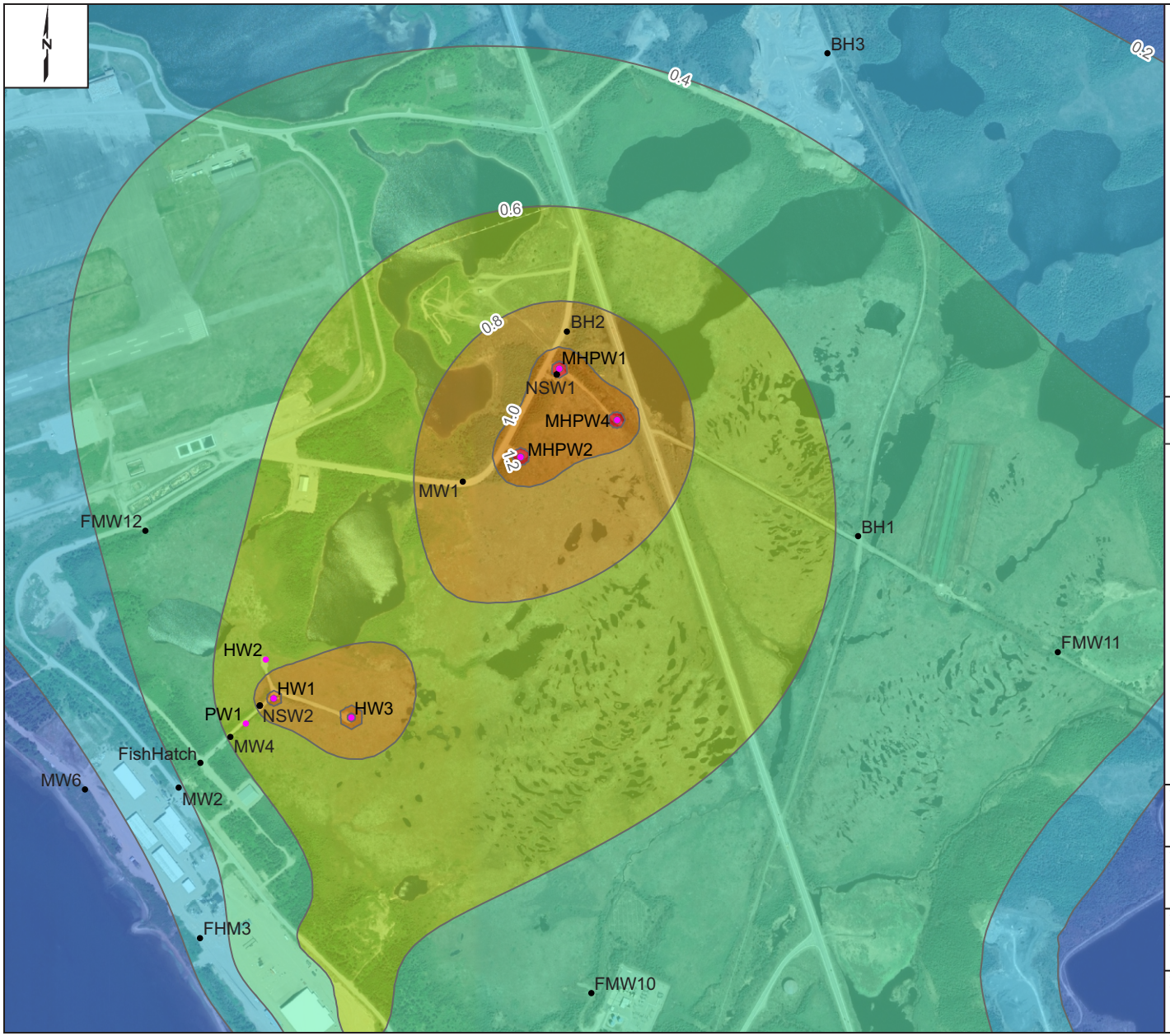

Legend

Production well location

Monitoring well location

Legend

Contours, m

0 0.4 0.8 >1.2

0 100 200 300 400 500

Scale, m

Note: Base orthorectified image from Google Earth (2022).

Figure 4.61

Capture area calculated by the prediction model, *Upper Limit 2*, with transient simulation at the pumping level under operation of the five production wells in December 31, 2041.

Document Reference	FFC-NL-3113-057b
Location	Stephenville, NL
Project No.	3113
Date	December 2022

FFC

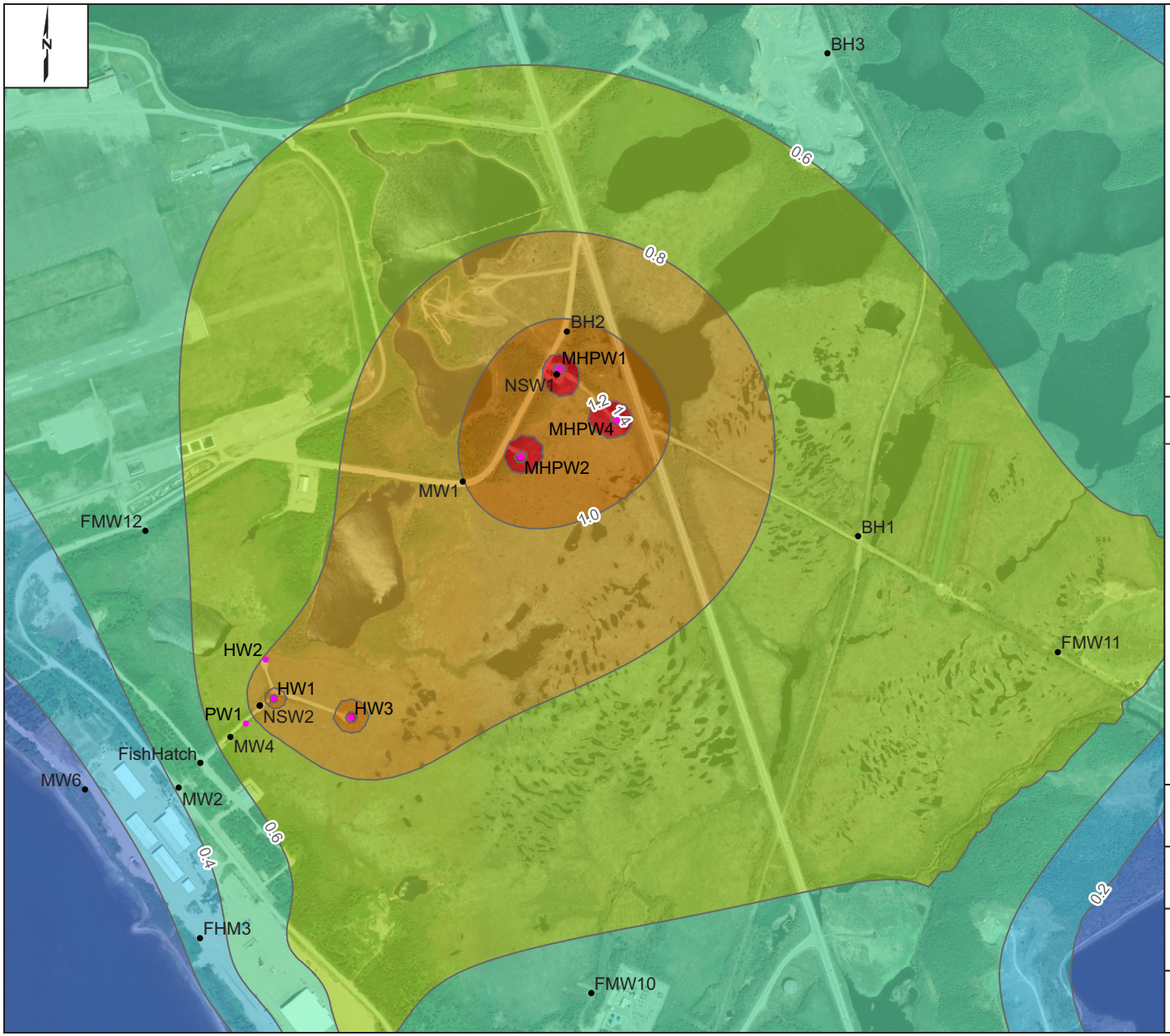

Legend

- Production well location
- Monitoring well location

Legend

Contours, m

0 0.4 0.8 >1.2

0 100 200 300 400 500

Scale, m

Note: Base orthorectified image from Google Earth (2022).

Figure 4.62

Capture area calculated by the prediction model, *Upper Limit 2*, with transient simulation at the pumping level under operation of the five production wells in December 31, 2046.

Document Reference	FFC-NL-3113-057b
Location	Stephenville, NL
Project No.	3113
Date	December 2022

FFC

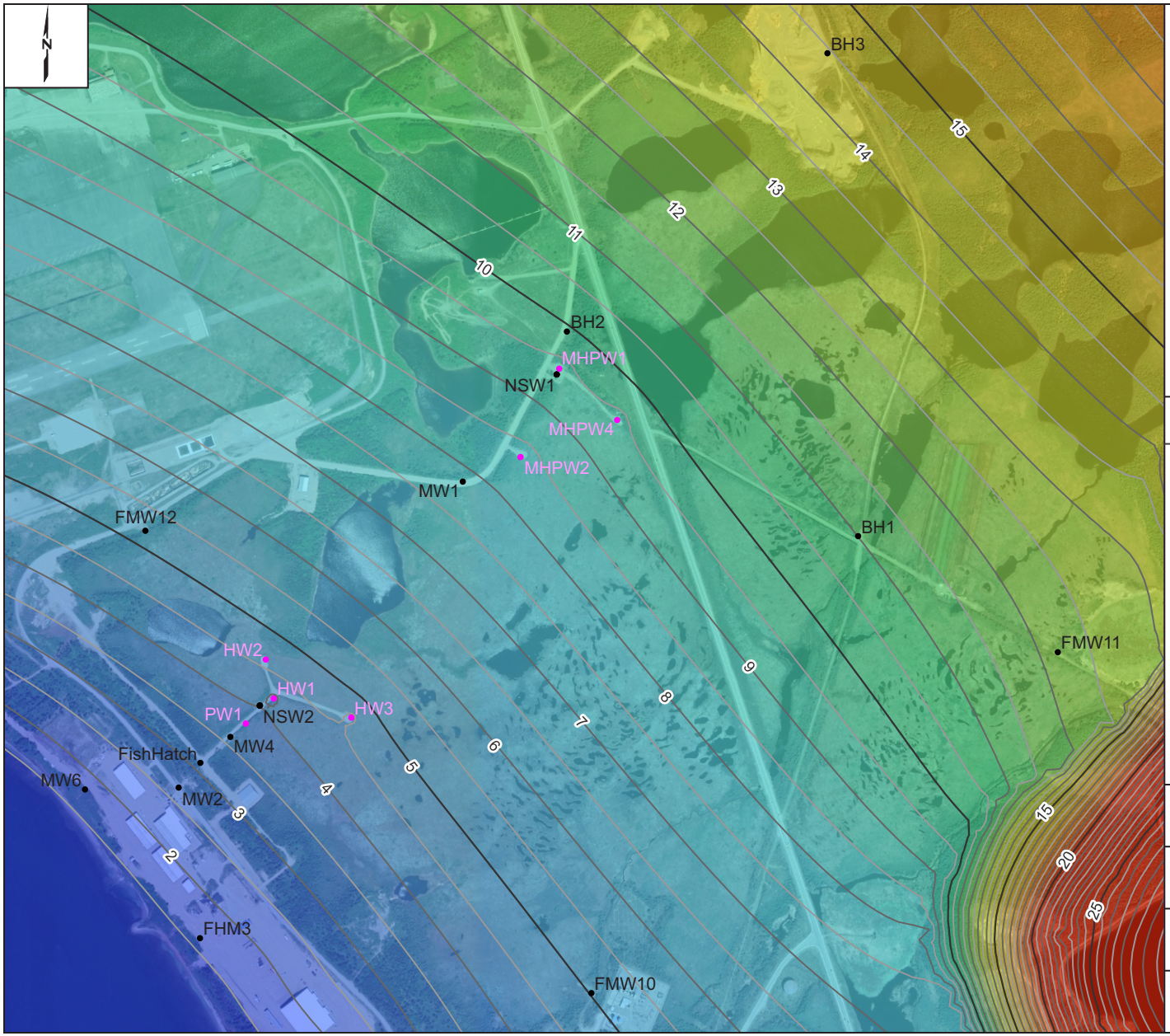

Legend

Production well location

Monitoring well location

Legend

Contours, m

1 5 10 15 >20

0 100 200 300 400 500

Scale, m

Note: Base orthorectified image from Google Earth (2022).

Figure 4.63

Contour map of the calculated water elevation (hydraulic head) at the pumping level with the prediction model, *Lower Limit 1,* under operation of the five production wells in December 31, 2026.

Document Reference
FFC-NL-3113-057b

Location
Stephenville, NL

Project No.
3113

Date
December 2022

FFC

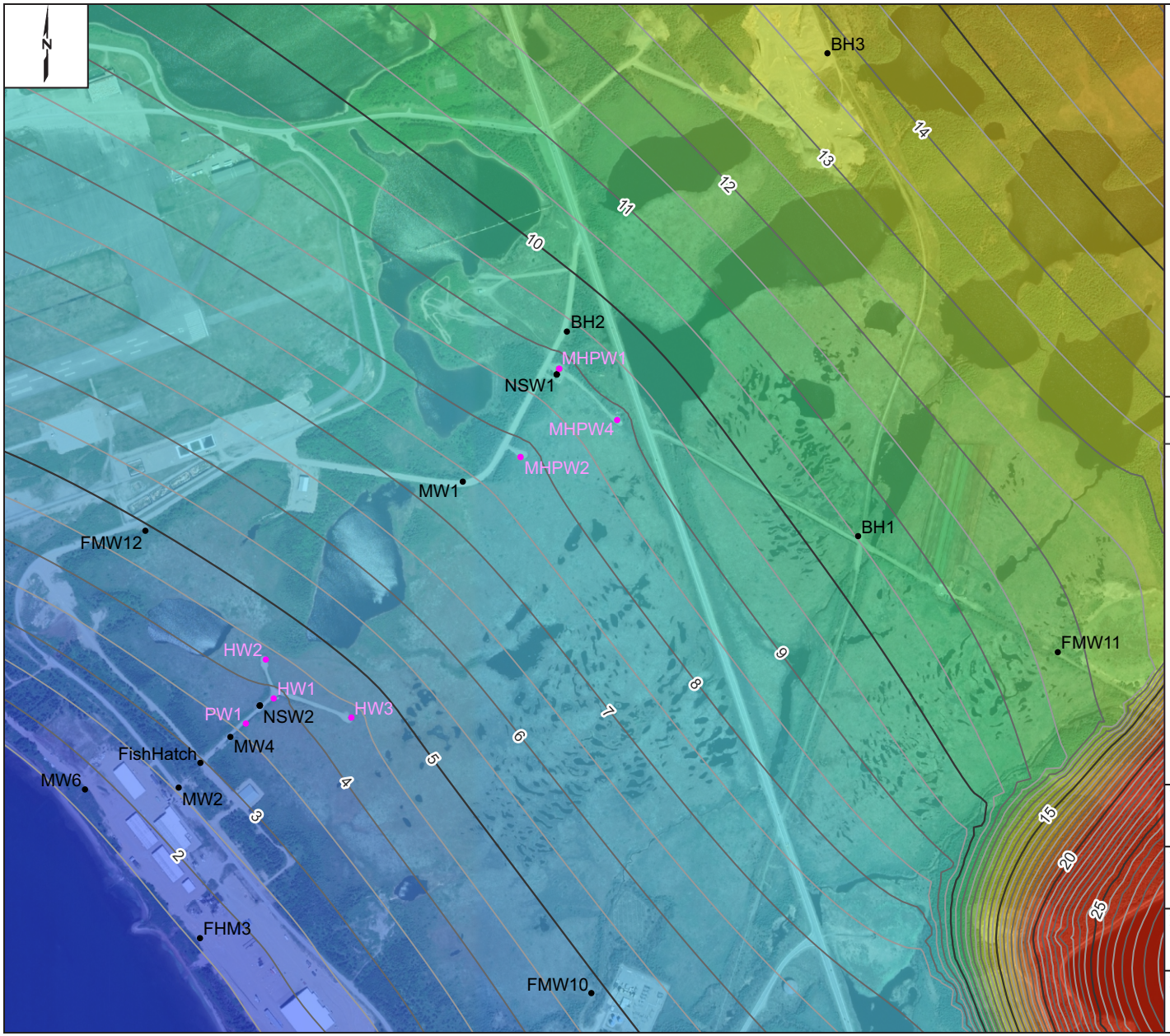

Legend

- Production well location
- Monitoring well location

Legend

Contours, m

1 5 10 15 >20

0 100 200 300 400 500

Scale, m

Note: Base orthorectified image from Google Earth (2022).

Figure 4.64

Contour map of the calculated water elevation (hydraulic head) at the pumping level with the prediction model, *Lower Limit 1,* under operation of the five production wells in December 31, 2031.

Document Reference	FFC-NL-3113-057b
Location	Stephenville, NL
Project No.	3113
Date	December 2022

FFC

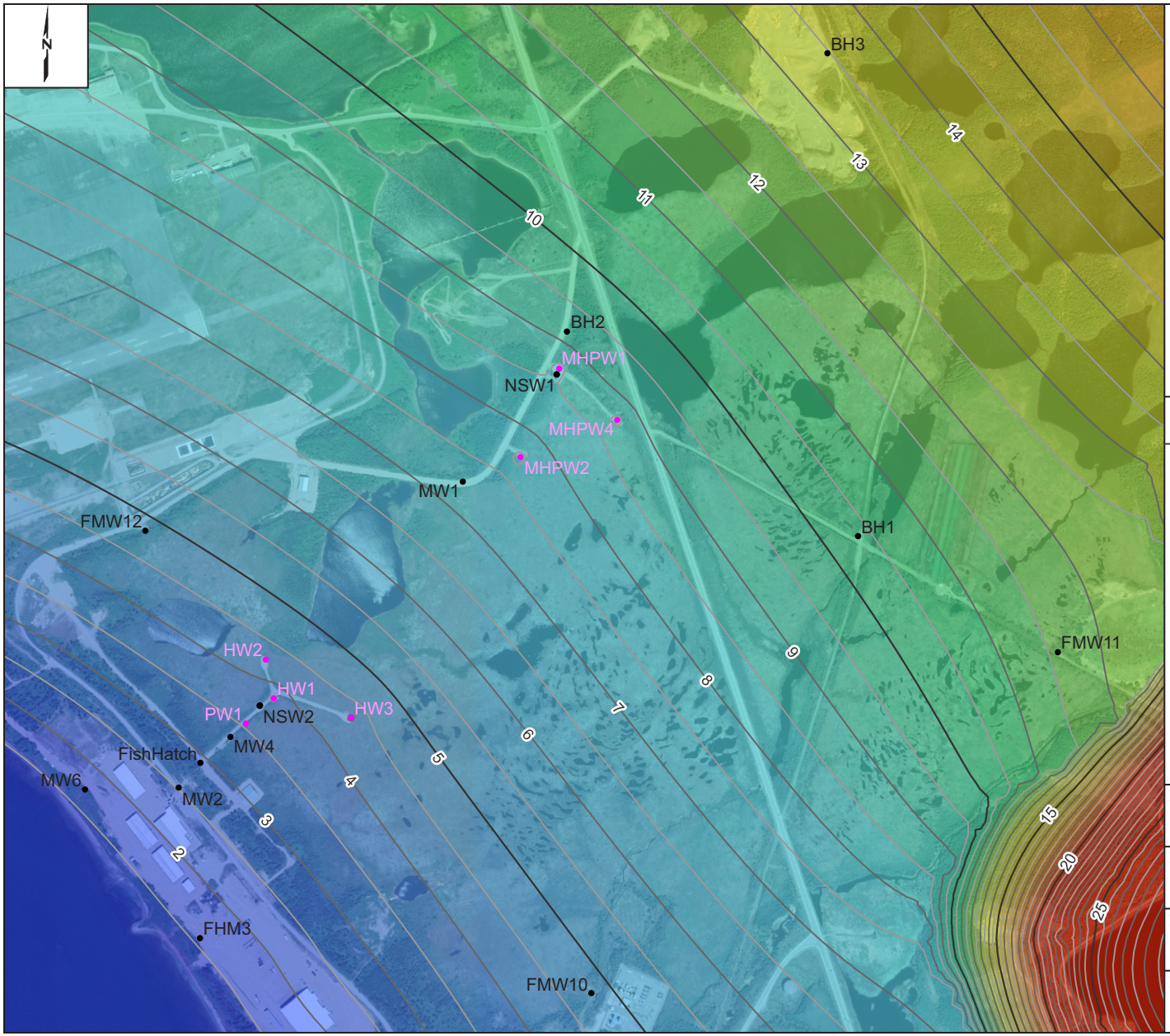

Legend

Production well location

Monitoring well location

Legend

Contours, m

1 5 10 15 >20

0 100 200 300 400 500

Scale, m

Note: Base orthorectified image from Google Earth (2022).

Figure 4.65

Contour map of the calculated water elevation (hydraulic head) at the pumping level with the prediction model, *Lower Limit 1,* under operation of the five production wells in December 31, 2036.

Document Reference
FFC-NL-3113-057b

Location
Stephenville, NL

Project No.
3113

Date
December 2022

FFC

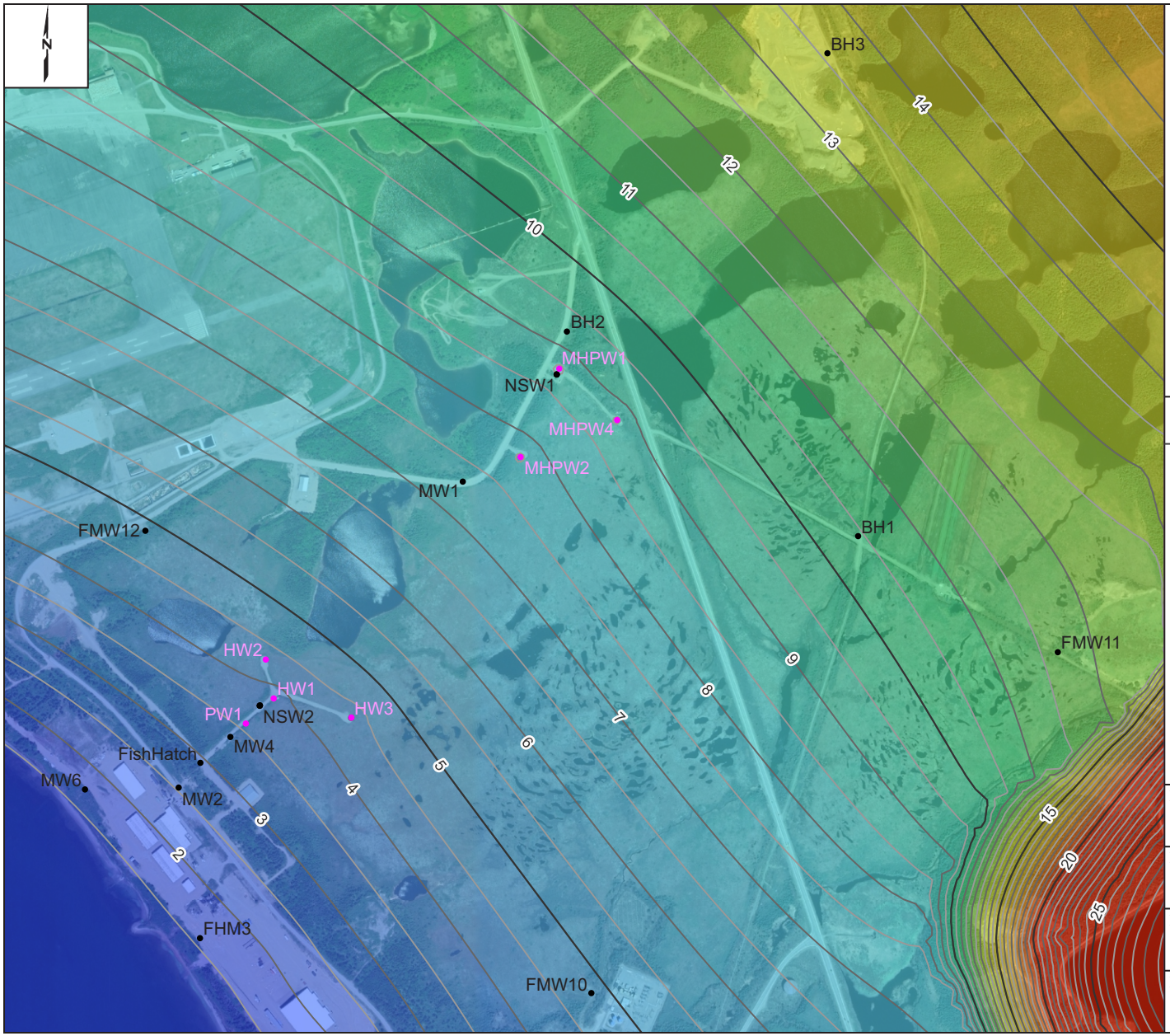

Legend

Production well location

Monitoring well location

Legend

Contours, m

1 5 10 15 >20

0 100 200 300 400 500

Scale, m

Note: Base orthorectified image from Google Earth (2022).

Figure 4.66

Contour map of the calculated water elevation (hydraulic head) at the pumping level with the prediction model, *Lower Limit 1,* under operation of the five production wells in December 31, 2041.

Document Reference	FFC-NL-3113-057b
Location	Stephenville, NL
Project No.	3113
Date	December 2022

FFC

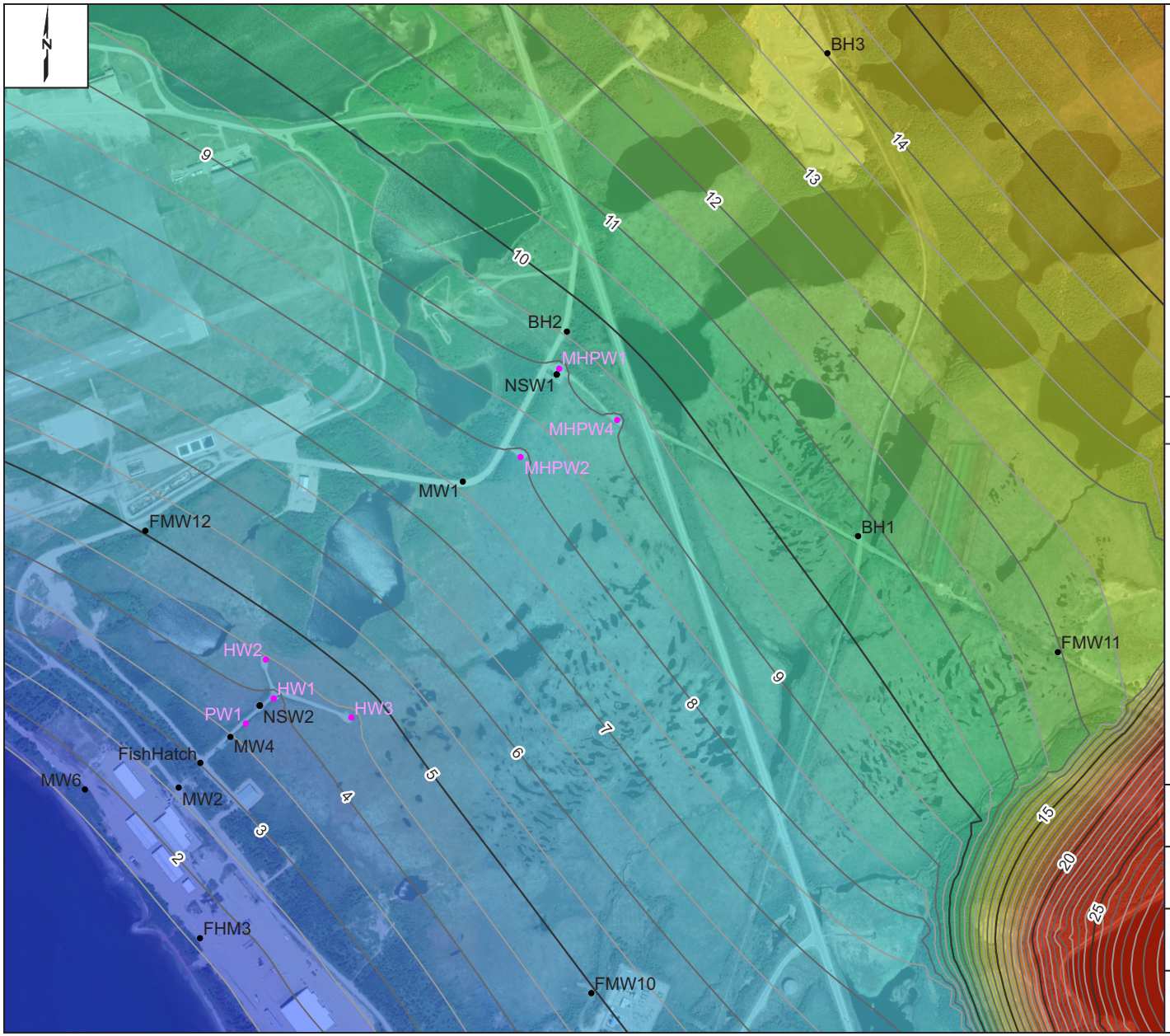

Legend

Production well location

Monitoring well location

Legend

Contours, m

1 5 10 15 >20

0 100 200 300 400 500

Scale, m

Note: Base orthorectified image from Google Earth (2022).

Figure 4.67

Contour map of the calculated water elevation (hydraulic head) at the pumping level with the prediction model, *Lower Limit 1,* under operation of the five production wells in December 31, 2046.

Document Reference
FFC-NL-3113-057b

Location
Stephenville, NL

Project No.
3113

Date
December 2022

FFC

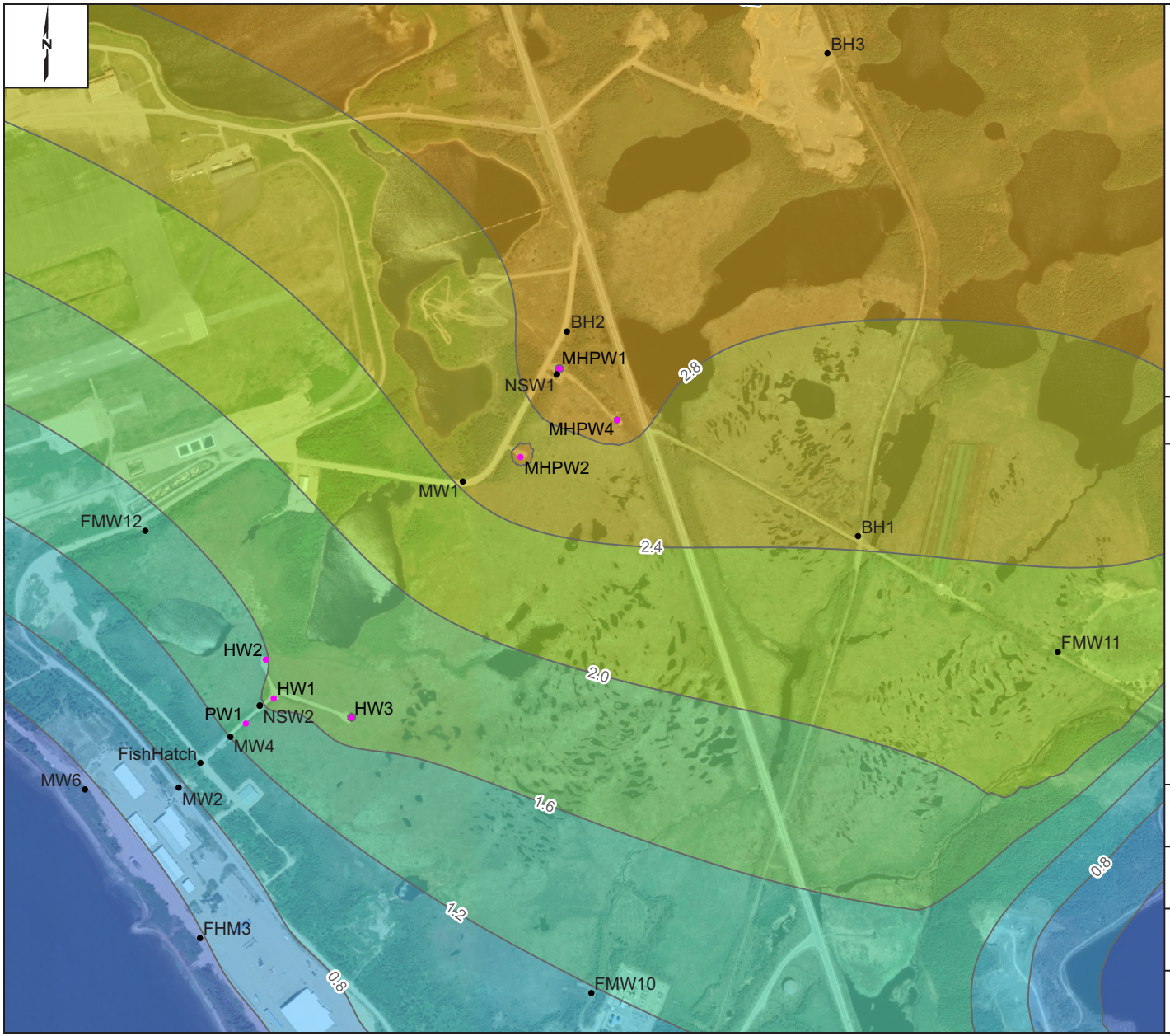

Legend

Production well location

Monitoring well location

Legend

Contours, m

0 1 2 3 >4

0 100 200 300 400 500

Scale, m

Note: Base orthorectified image from Google Earth (2022).

Figure 4.68

Capture area calculated by the prediction model, *Lower Limit 1*, with transient simulation at the pumping level under operation of the five production wells in December 31, 2026.

Document Reference	FFC-NL-3113-057b
Location	Stephenville, NL
Project No.	3113
Date	December 2022

FFC

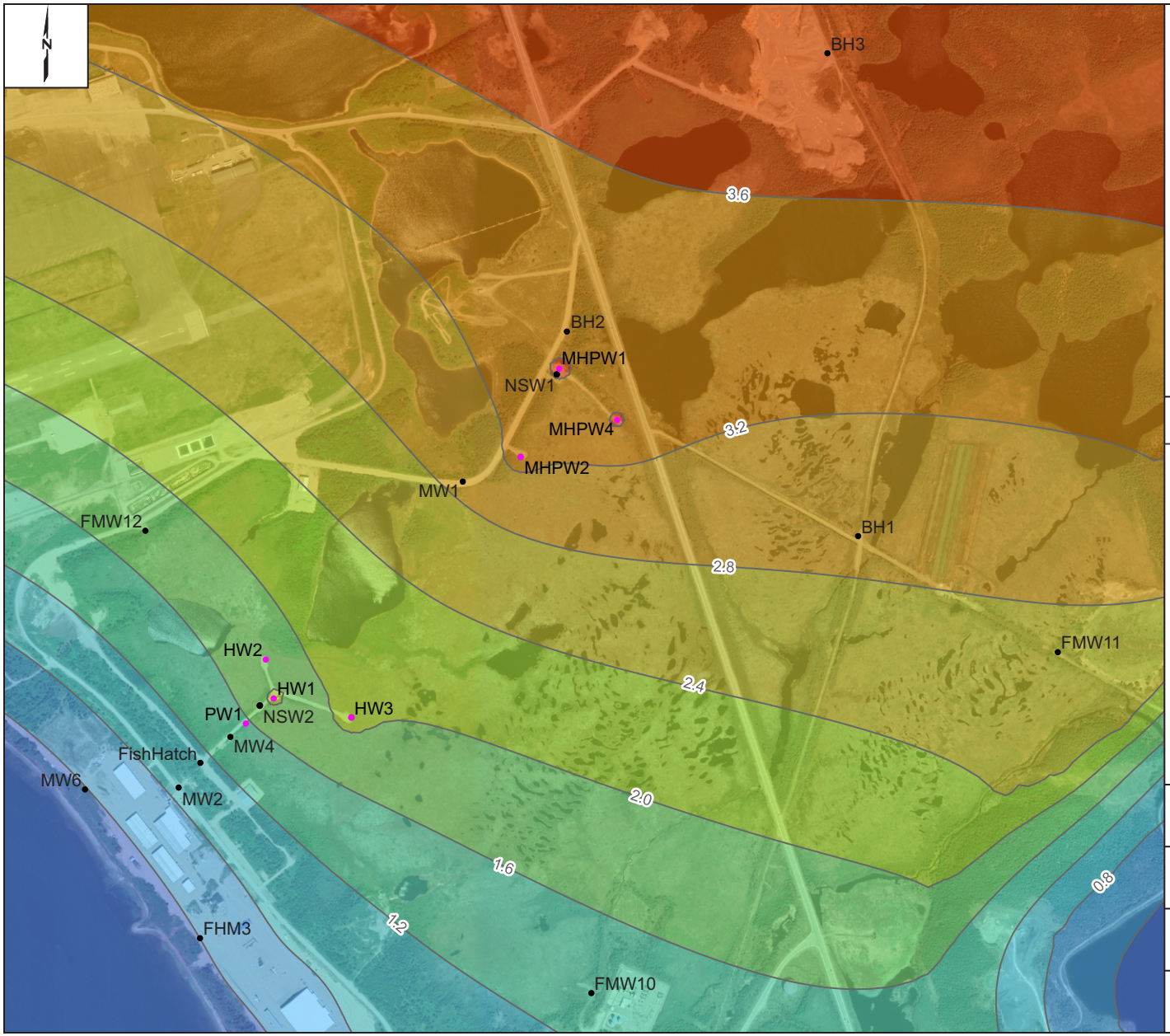

Legend

Production well location

Monitoring well location

Legend

Contours, m

0 1 2 3 >4

0 100 200 300 400 500

Scale, m

Note: Base orthorectified image from Google Earth (2022).

Figure 4.69

Capture area calculated by the prediction model, *Lower Limit 1*, with transient simulation at the pumping level under operation of the five production wells in December 31, 2031.

Document Reference	FFC-NL-3113-057b
Location	Stephenville, NL
Project No.	3113
Date	December 2022

FFC

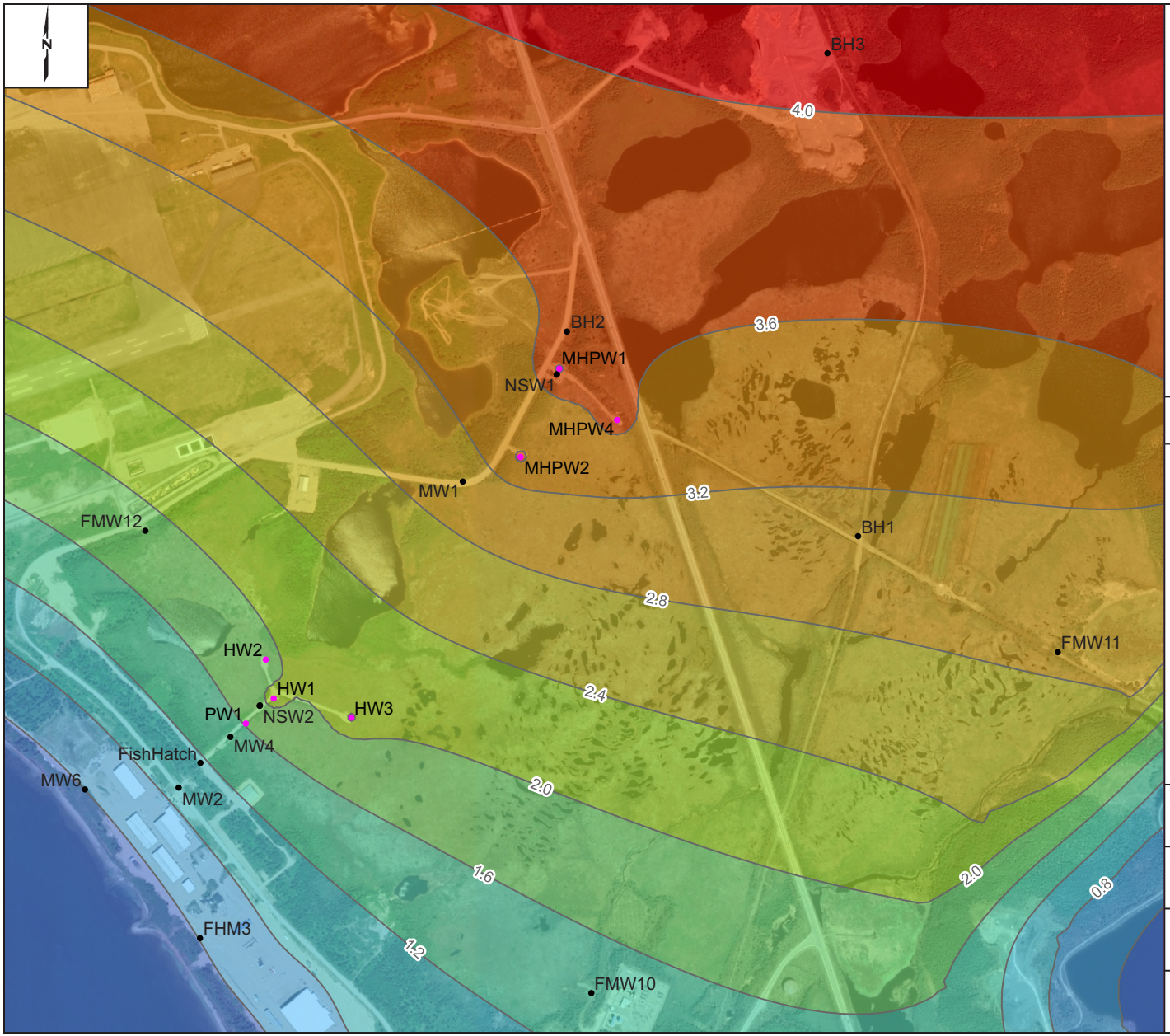

Legend

Production well location

Monitoring well location

Legend

Contours, m

0 1 2 3 >4

0 100 200 300 400 500

Scale, m

Note: Base orthorectified image from Google Earth (2022).

Figure 4.70

Capture area calculated by the prediction model, *Lower Limit 1*, with transient simulation at the pumping level under operation of the five production wells in December 31, 2036.

Document Reference	FFC-NL-3113-057b
Location	Stephenville, NL
Project No.	3113
Date	December 2022

FFC

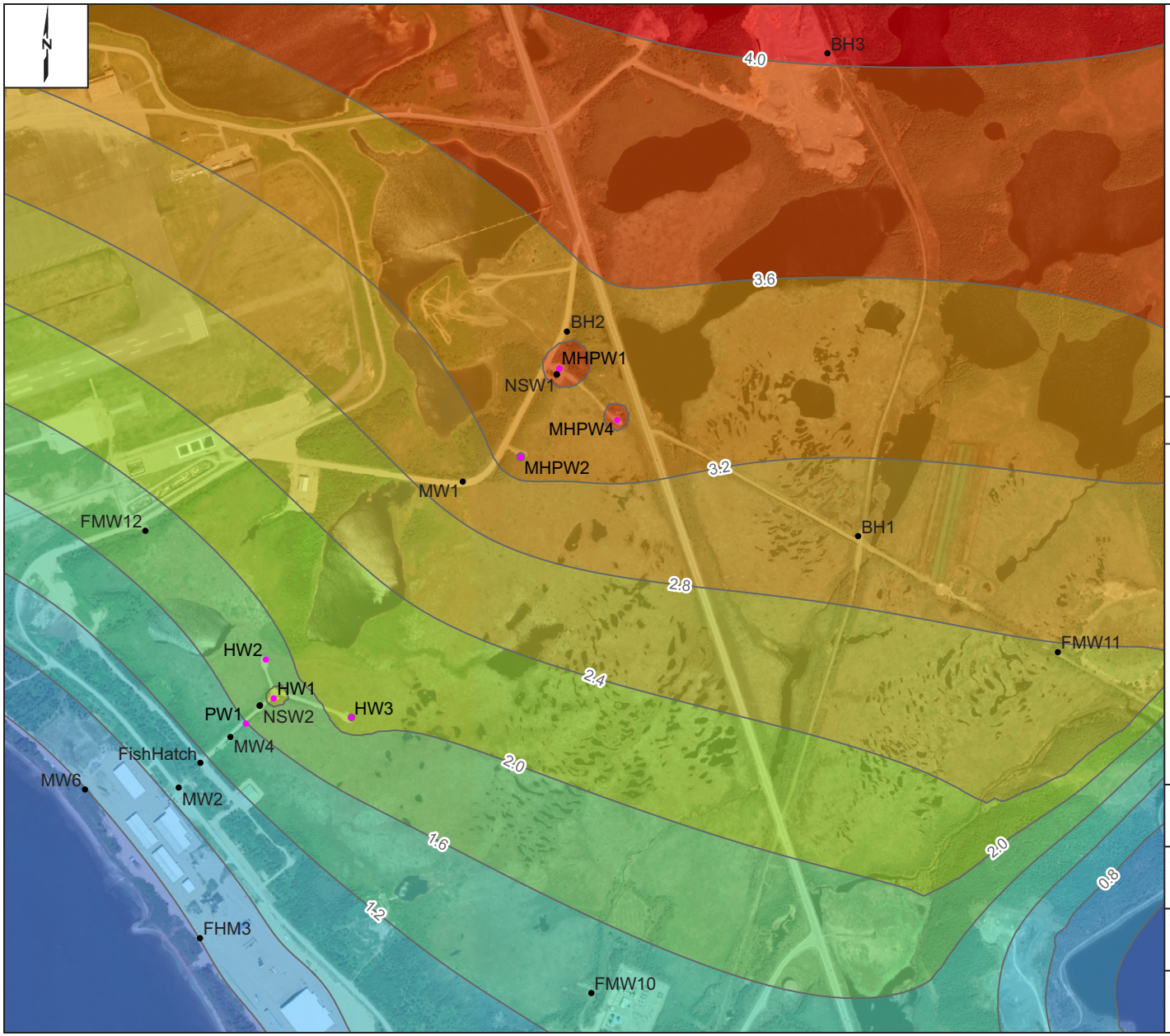

Legend

- Production well location
- Monitoring well location

Legend

Contours, m

0 1 2 3 >4

0 100 200 300 400 500

Scale, m

Note: Base orthorectified image from Google Earth (2022).

Figure 4.71

Capture area calculated by the prediction model, *Lower Limit 1*, with transient simulation at the pumping level under operation of the five production wells in December 31, 2041.

Document Reference	FFC-NL-3113-057b
Location	Stephenville, NL
Project No.	3113
Date	December 2022

FFC

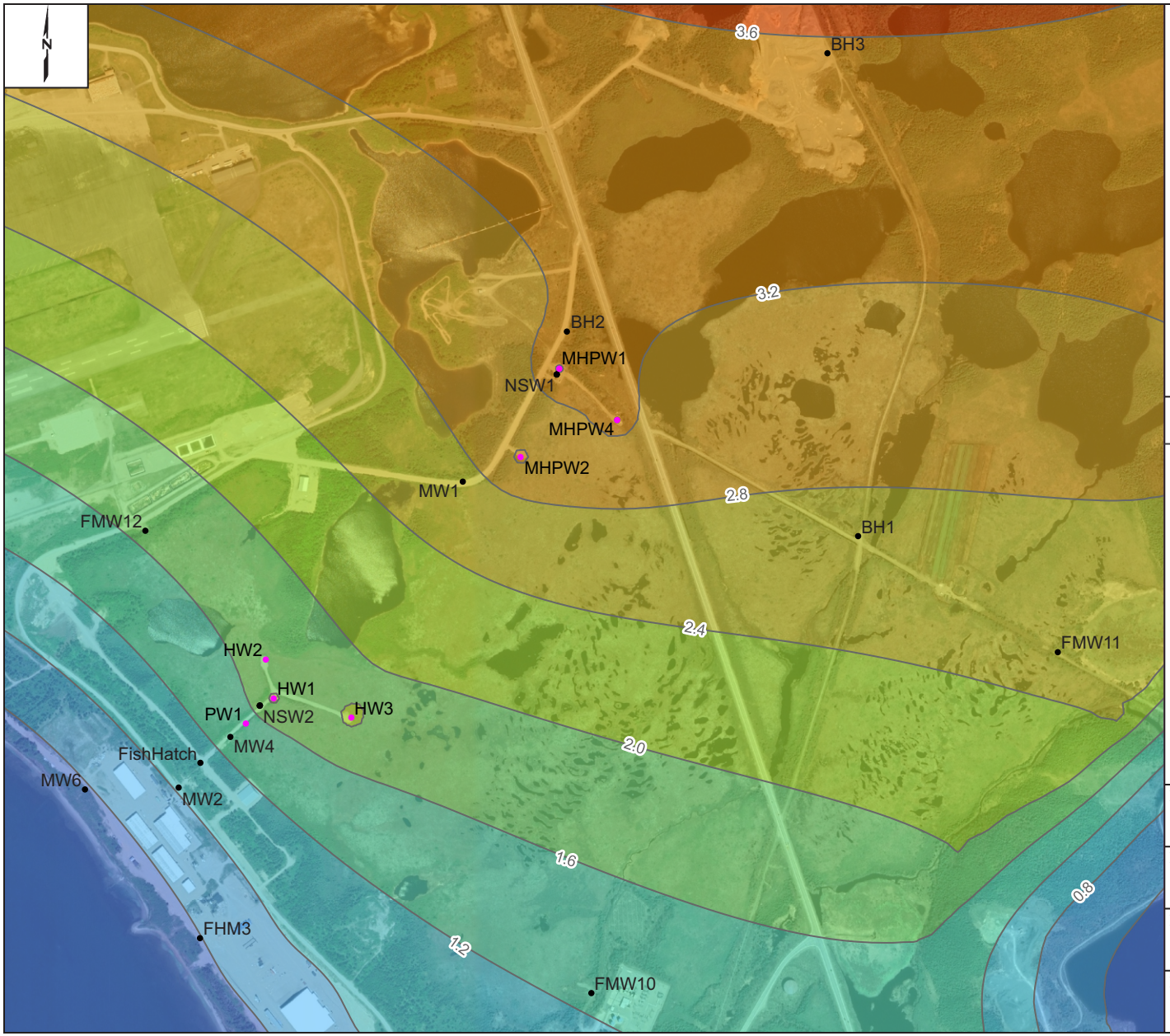

Legend

- Production well location
- Monitoring well location

Legend

Contours, m

0 1 2 3 >4

0 100 200 300 400 500

Scale, m

Note: Base orthorectified image from Google Earth (2022).

Figure 4.72

Capture area calculated by the prediction model, *Lower Limit 1*, with transient simulation at the pumping level under operation of the five production wells in December 31, 2046.

Document Reference	FFC-NL-3113-057b
Location	Stephenville, NL
Project No.	3113
Date	December 2022

FFC

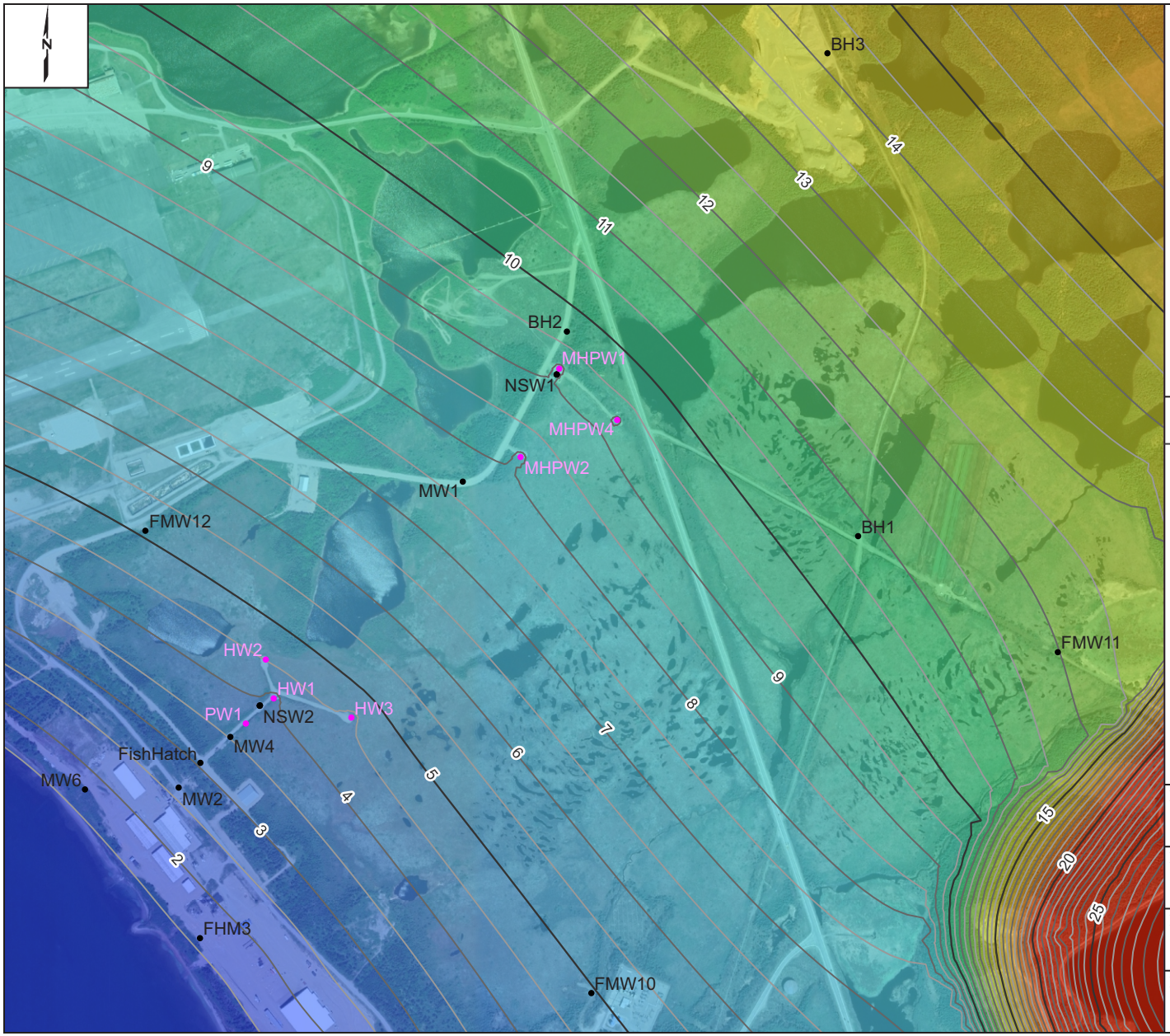

Legend

Production well location

Monitoring well location

Legend

Contours, m

1 5 10 15 >20

0 100 200 300 400 500

Scale, m

Note: Base orthorectified image from Google Earth (2022).

Figure 4.73

Contour map of the calculated water elevation (hydraulic head) at the pumping level with the prediction model, *Lower Limit 2,* under operation of the five production wells in December 31, 2026.

Document Reference
FFC-NL-3113-057b

Location
Stephenville, NL

Project No.
3113

Date
December 2022

FFC

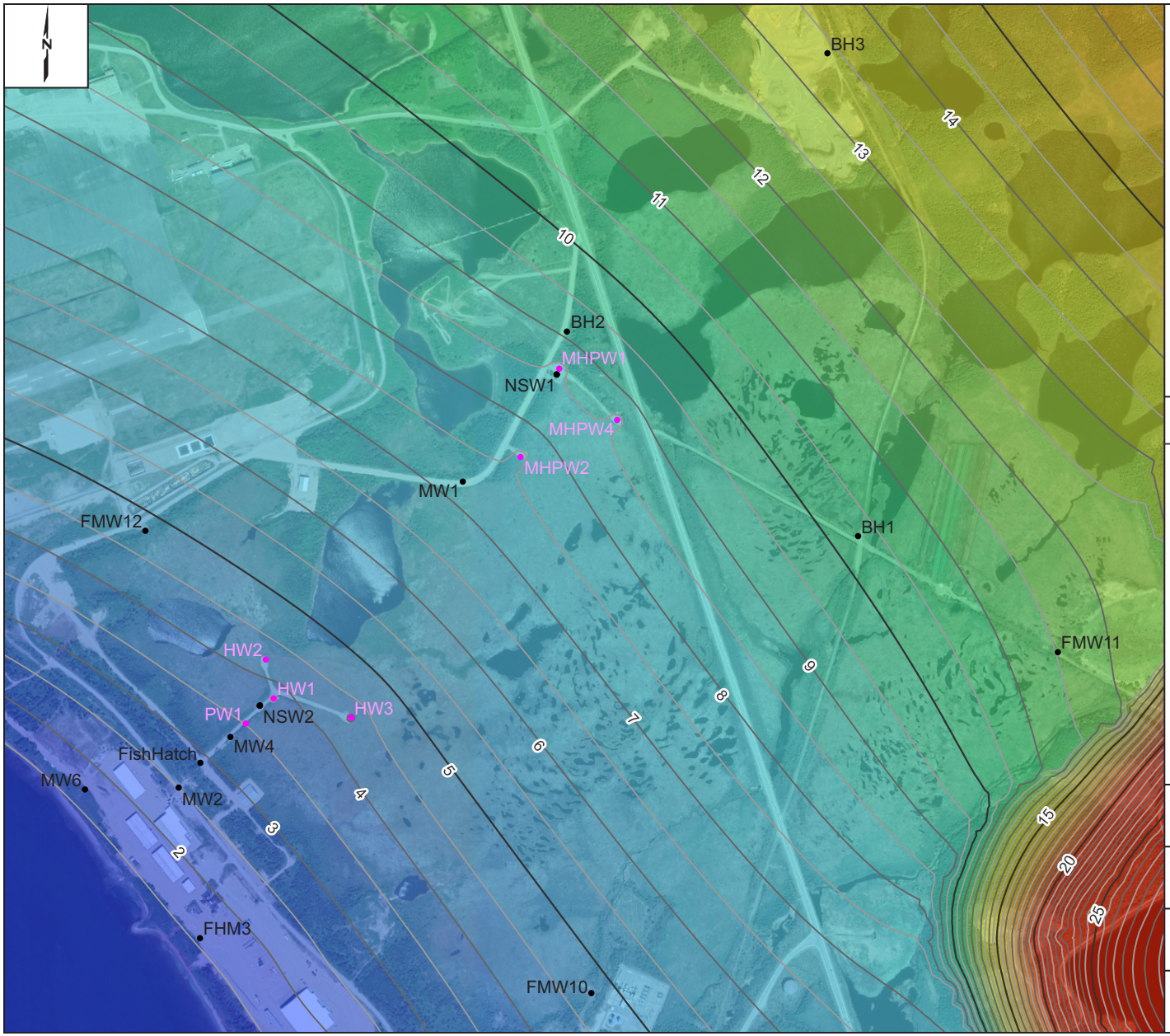

Legend

- Production well location
- Monitoring well location

Legend

Contours, m

1 5 10 15 >20

0 100 200 300 400 500

Scale, m

Note: Base orthorectified image from Google Earth (2022).

Figure 4.74

Contour map of the calculated water elevation (hydraulic head) at the pumping level with the prediction model, *Lower Limit 2,* under operation of the five production wells in December 31, 2031.

Document Reference	FFC-NL-3113-057b
Location	Stephenville, NL
Project No.	3113
Date	December 2022

FFC

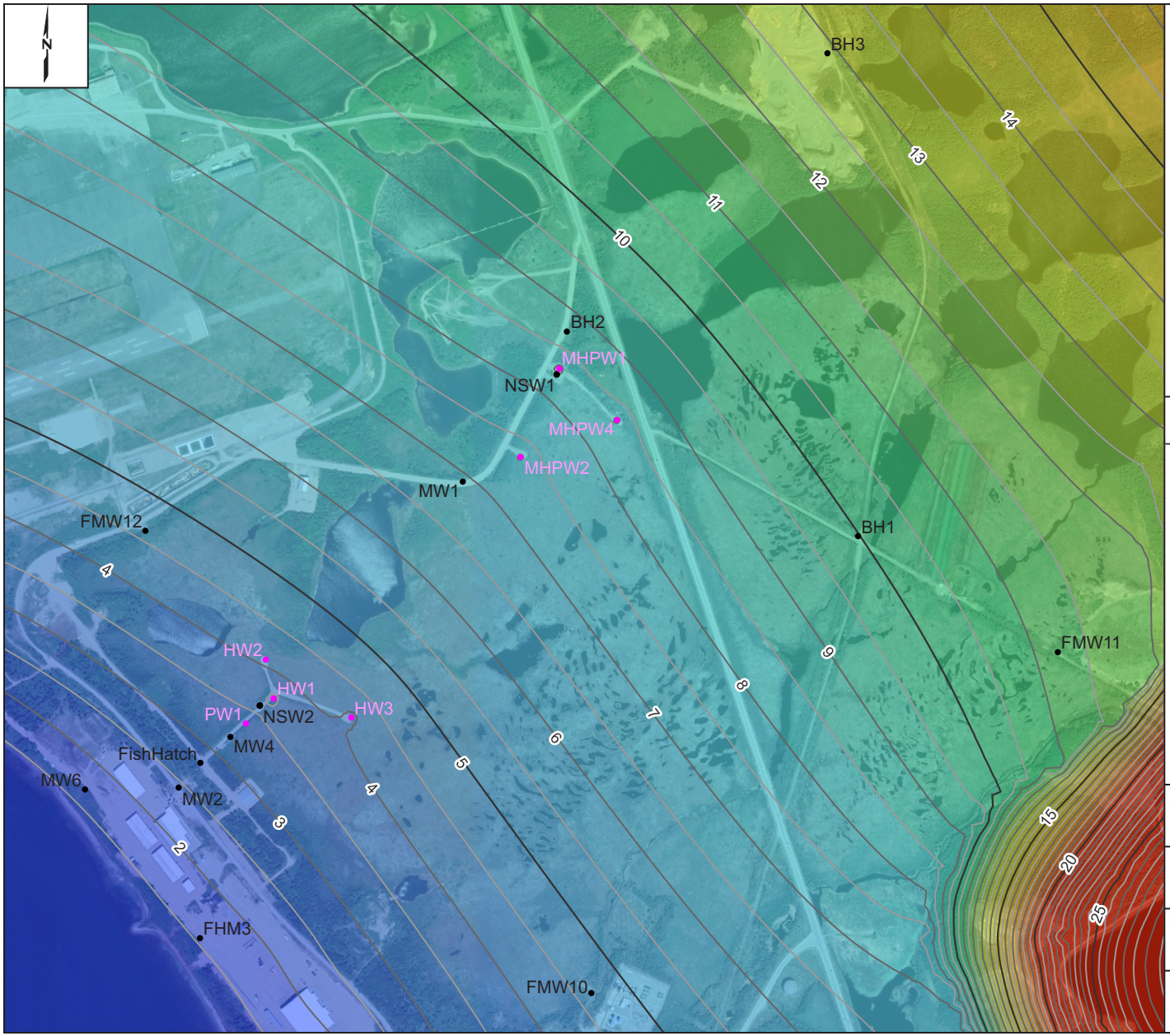

Legend

Production well location

Monitoring well location

Legend

Contours, m

1 5 10 15 >20

0 100 200 300 400 500

Scale, m

Note: Base orthorectified image from Google Earth (2022).

Figure 4.75

Contour map of the calculated water elevation (hydraulic head) at the pumping level with the prediction model, *Lower Limit 2,* under operation of the five production wells in December 31, 2036.

Document Reference	FFC-NL-3113-057b
Location	Stephenville, NL
Project No.	3113
Date	December 2022

FFC

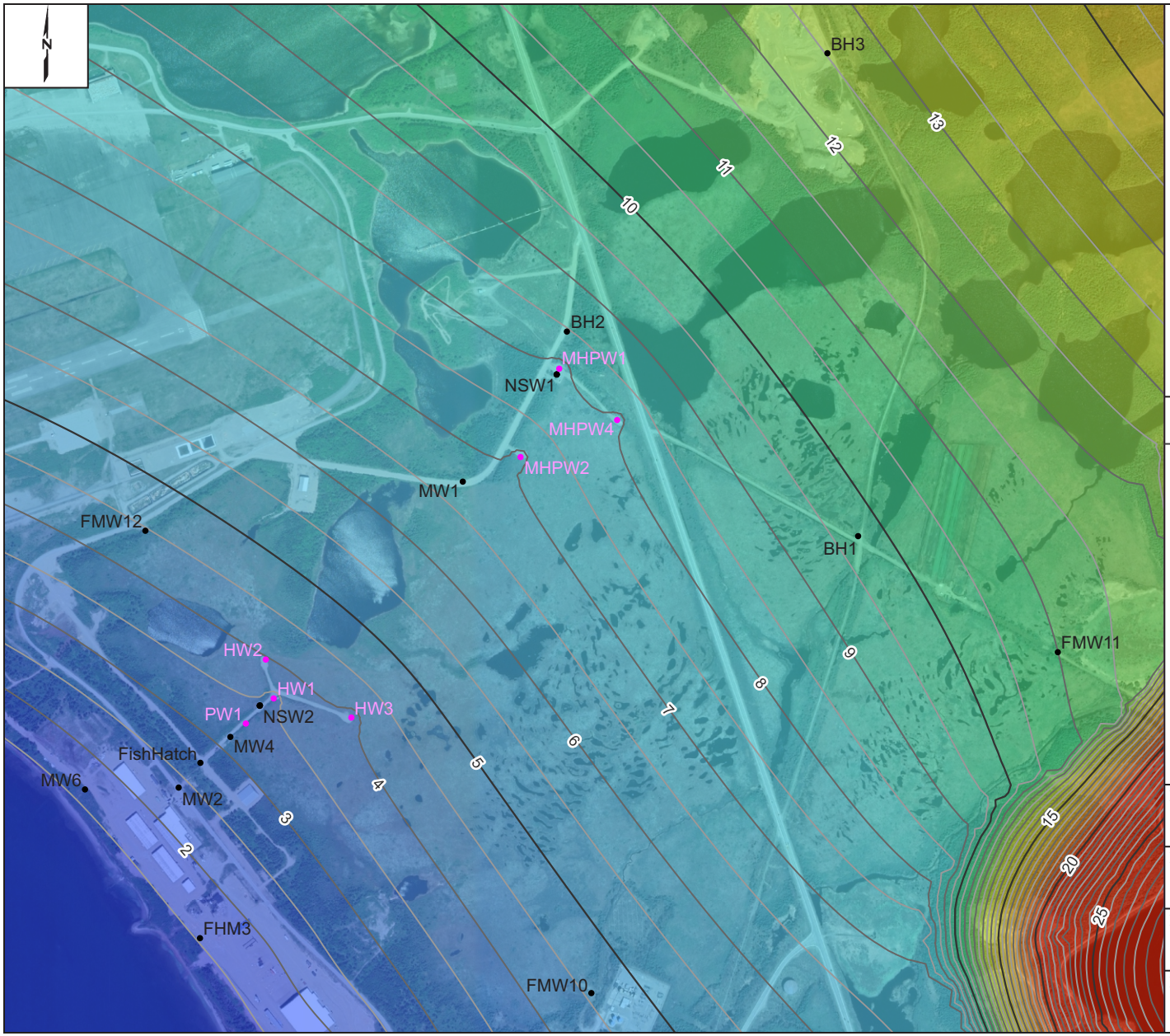

Legend

Production well location

Monitoring well location

Legend

Contours, m

1 5 10 15 >20

0 100 200 300 400 500

Scale, m

Note: Base orthorectified image from Google Earth (2022).

Figure 4.76

Contour map of the calculated water elevation (hydraulic head) at the pumping level with the prediction model, *Lower Limit 2,* under operation of the five production wells in December 31, 2041.

Document Reference	FFC-NL-3113-057b
Location	Stephenville, NL
Project No.	3113
Date	December 2022

FFC

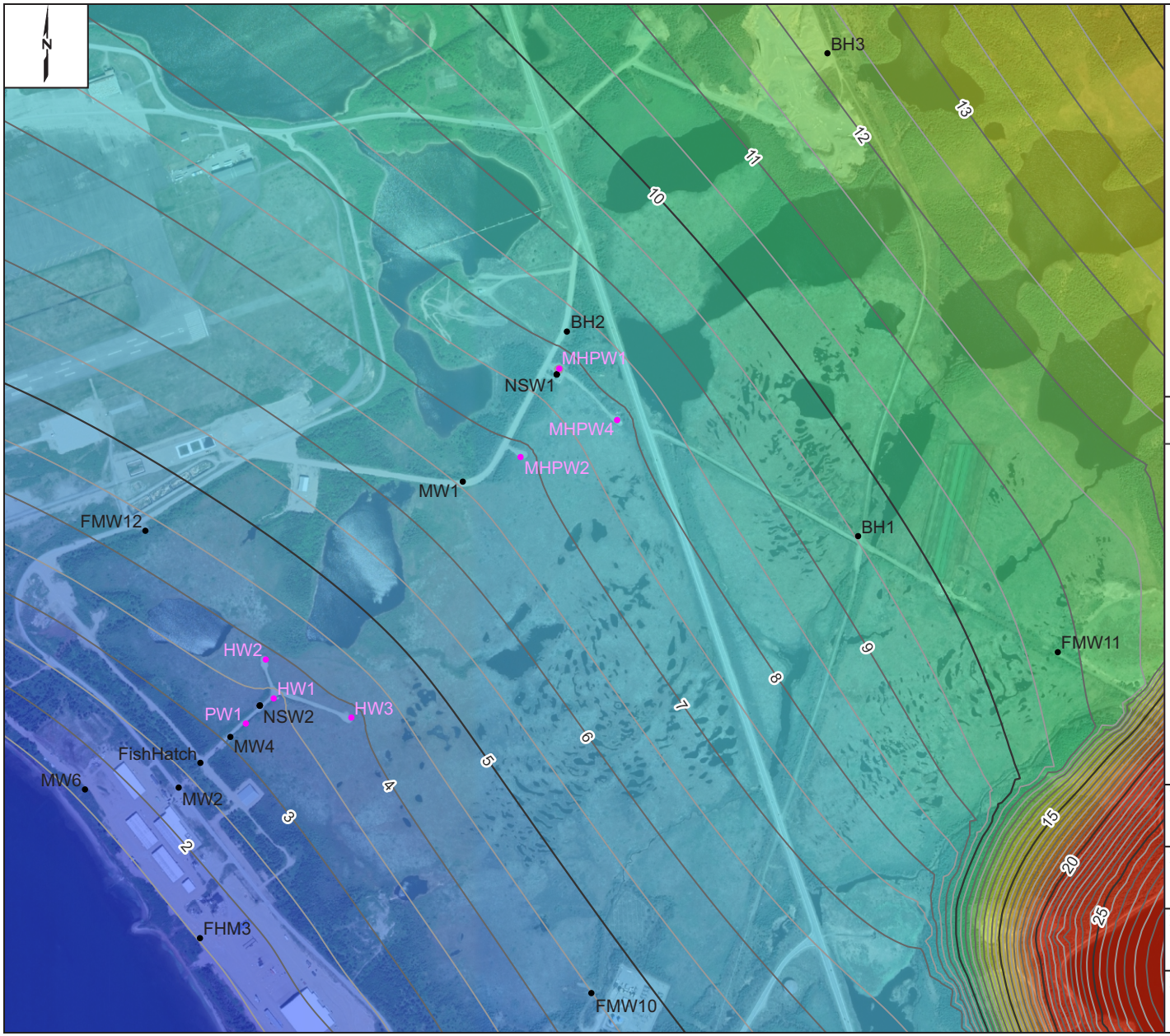

Legend

Production well location

Monitoring well location

Legend

Contours, m

1 5 10 15 >20

0 100 200 300 400 500

Scale, m

Note: Base orthorectified image from Google Earth (2022).

Figure 4.77

Contour map of the calculated water elevation (hydraulic head) at the pumping level with the prediction model, *Lower Limit 2,* under operation of the five production wells in December 31, 2046.

Document Reference	FFC-NL-3113-057b
Location	Stephenville, NL
Project No.	3113
Date	December 2022

FFC

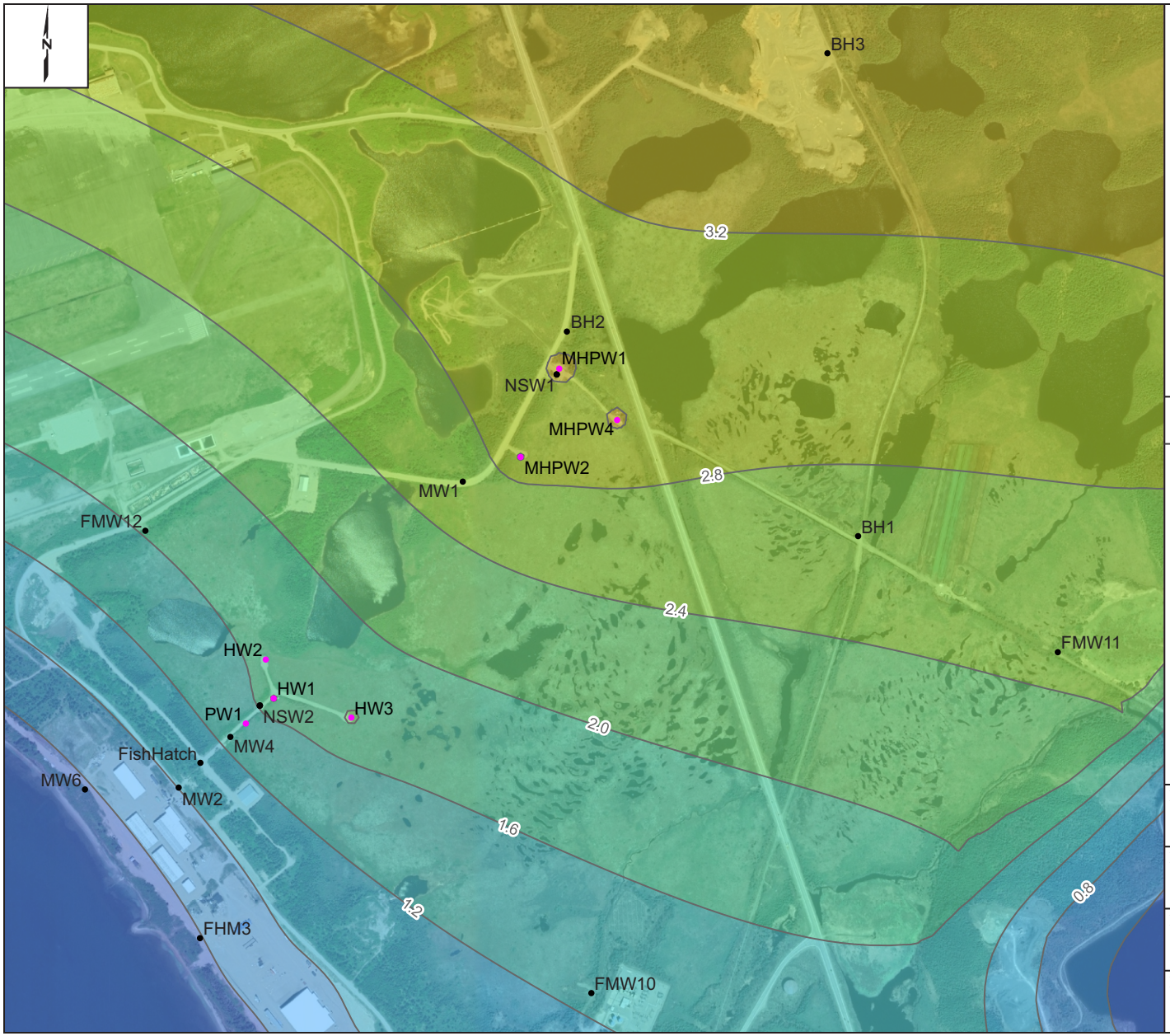

Legend

- Production well location
- Monitoring well location

Legend

Contours, m

0 2.6 >5.2

0 100 200 300 400 500

Scale, m

Note: Base orthorectified image from Google Earth (2022).

Figure 4.78

Capture area calculated by the prediction model, *Lower Limit 2*, with transient simulation at the pumping level under operation of the five production wells in December 31, 2026.

Document Reference	FFC-NL-3113-057b
Location	Stephenville, NL
Project No.	3113
Date	December 2022

FFC

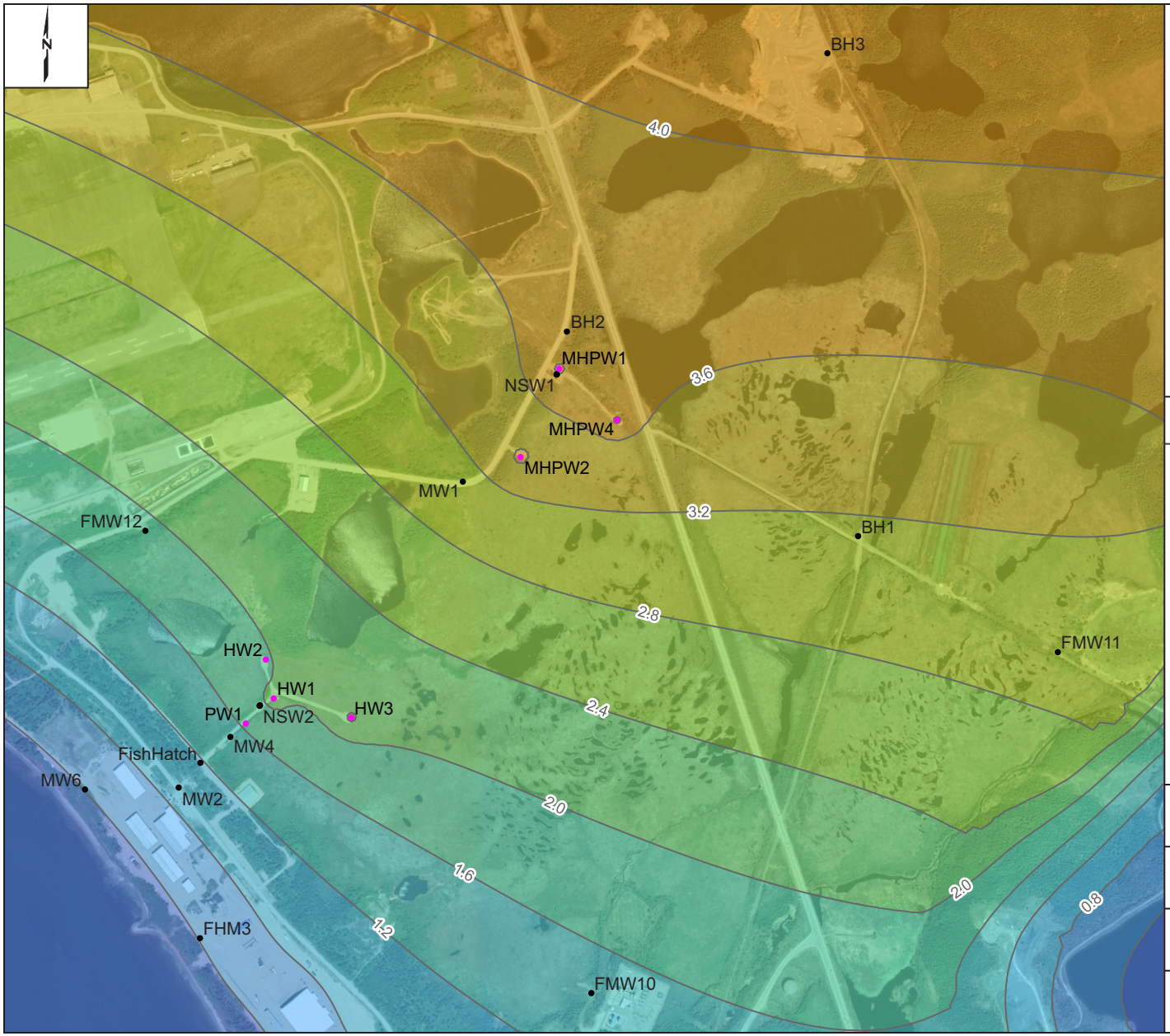

Legend

- Production well location
- Monitoring well location

Legend

Contours, m

0 2,6 >5.2

0 100 200 300 400 500

Scale, m

Note: Base orthorectified image from Google Earth (2022).

Figure 4.79

Capture area calculated by the prediction model, *Lower Limit 2*, with transient simulation at the pumping level under operation of the five production wells in December 31, 2031.

Document Reference	FFC-NL-3113-057b
Location	Stephenville, NL
Project No.	3113
Date	December 2022

FFC

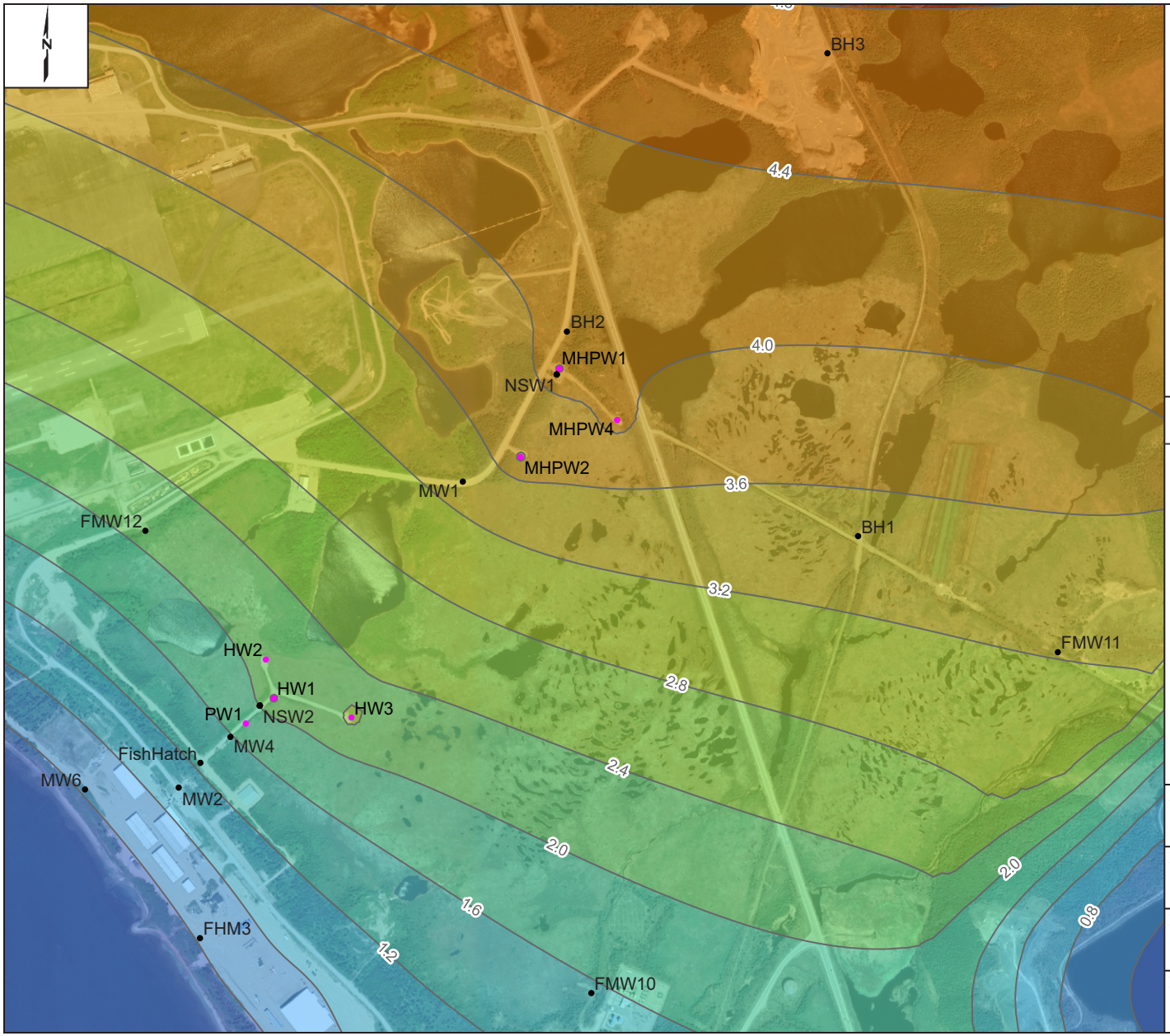

Legend

- Production well location
- Monitoring well location

Legend

Contours, m

0 2,6 >5.2

0 100 200 300 400 500

Scale, m

Note: Base orthorectified image from Google Earth (2022).

Figure 4.80

Capture area calculated by the prediction model, *Lower Limit 2*, with transient simulation at the pumping level under operation of the five production wells in December 31, 2036.

Document Reference	FFC-NL-3113-057b
Location	Stephenville, NL
Project No.	3113
Date	December 2022

FFC

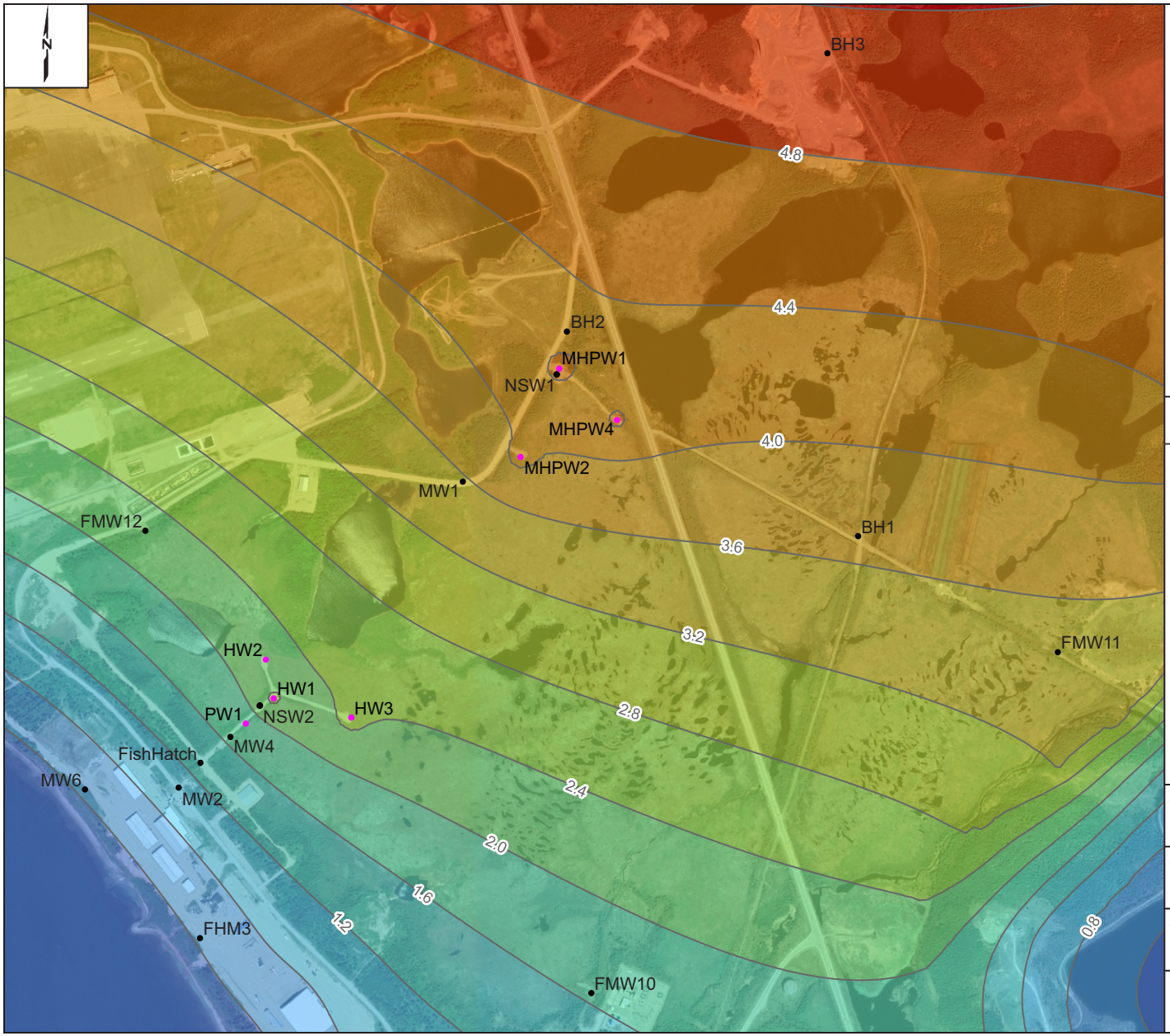

Legend

- Production well location
- Monitoring well location

Legend

Contours, m

0 2,6 >5.2

0 100 200 300 400 500

Scale, m

Note: Base orthorectified image from Google Earth (2022).

Figure 4.81

Capture area calculated by the prediction model, *Lower Limit 2*, with transient simulation at the pumping level under operation of the five production wells in December 31, 2041.

Document Reference	FFC-NL-3113-057b
Location	Stephenville, NL
Project No.	3113
Date	December 2022

FFC

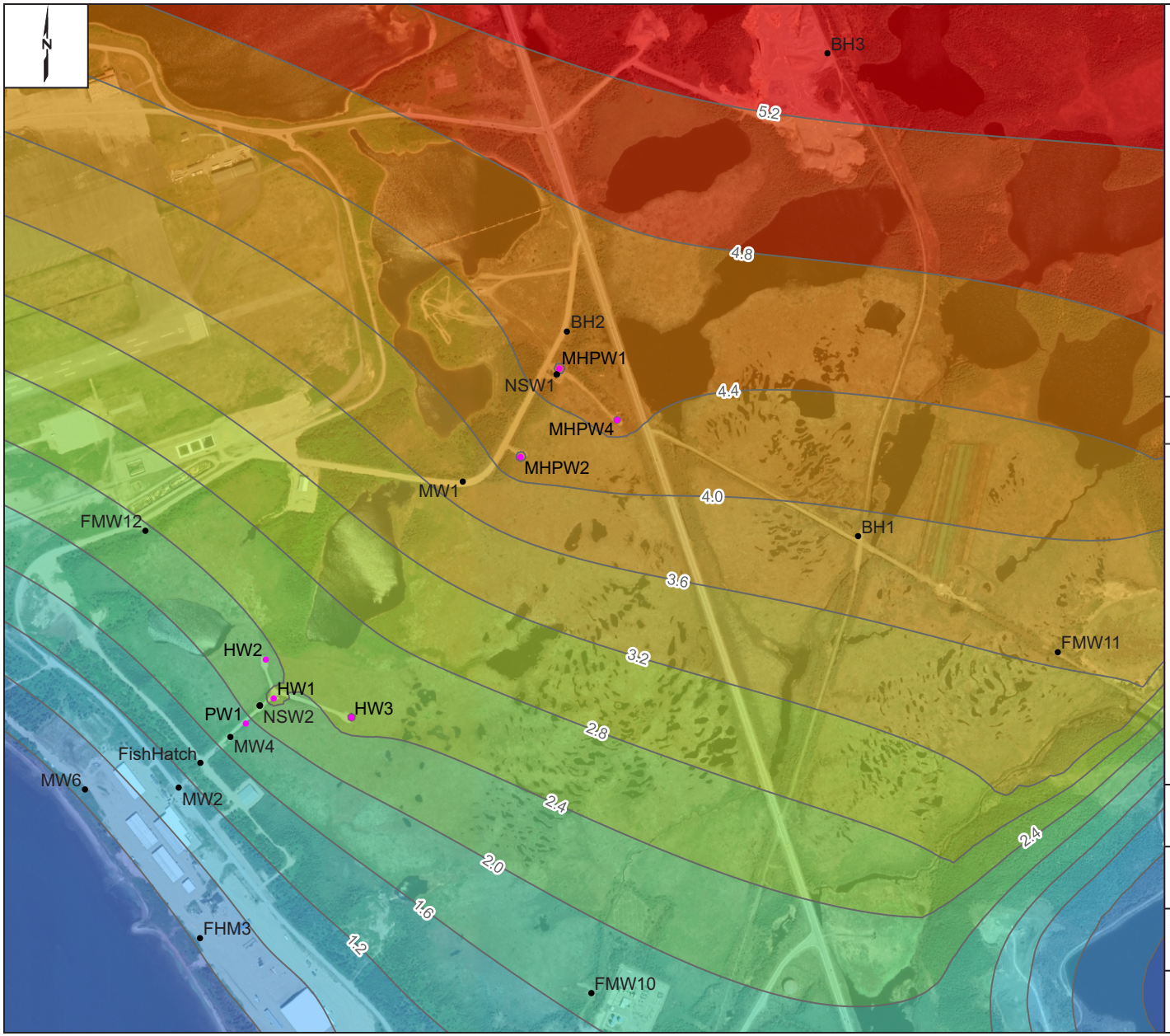

Legend

- Production well location
- Monitoring well location

Legend

Contours, m

0 2,6 >5.2

0 100 200 300 400 500

Scale, m

Note: Base orthorectified image from Google Earth (2022).

Figure 4.82

Capture area calculated by the prediction model, *Lower Limit 2*, with transient simulation at the pumping level under operation of the five production wells in December 31, 2046.

Document Reference	FFC-NL-3113-057b
Location	Stephenville, NL
Project No.	3113
Date	December 2022

FFC

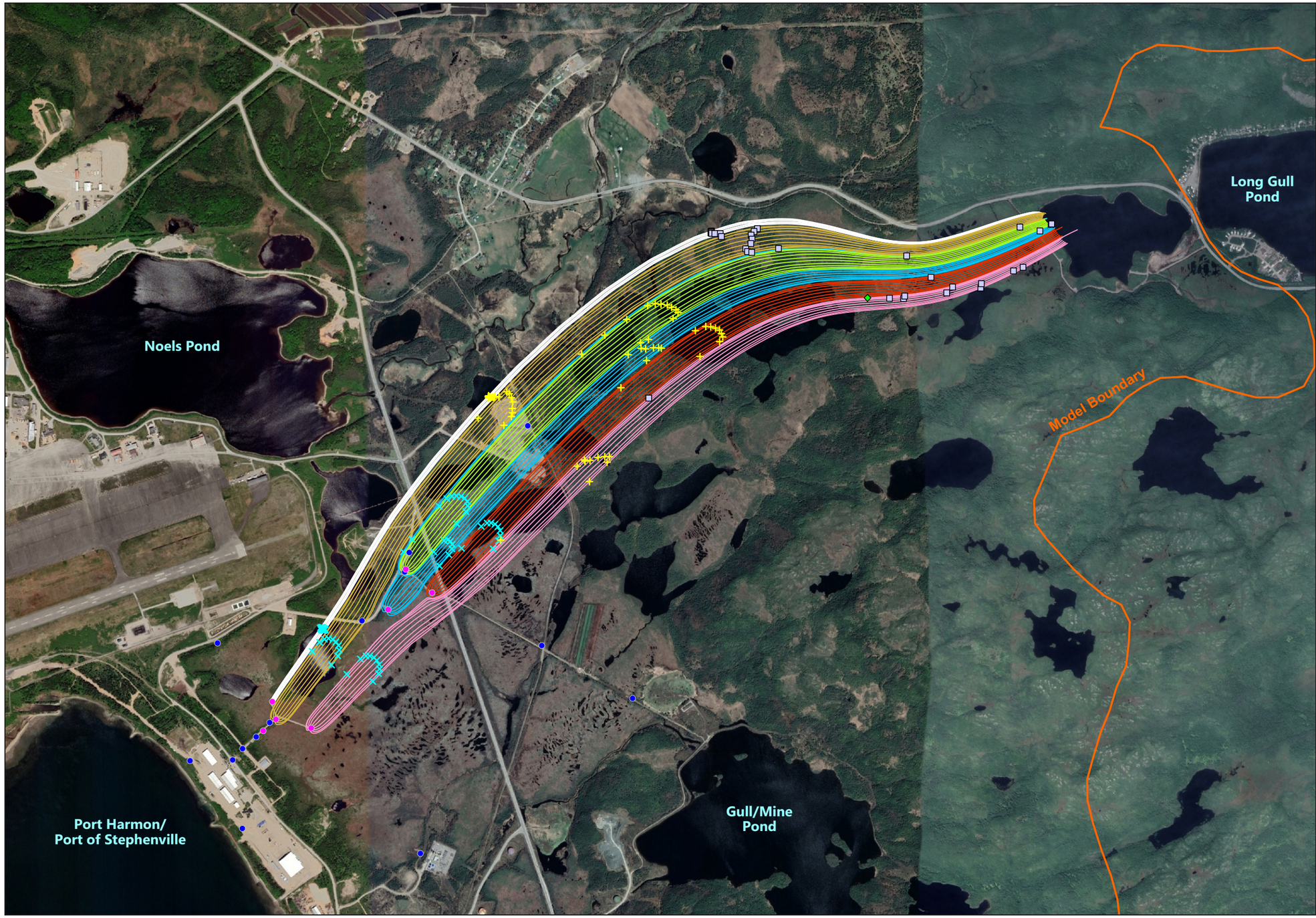

N

Legend

Production well location
Monitoring well location

Marker

1 year
5 years
10 years
15 years
20 years
25 years

0 200 400 600 800

Scale, m

Note: Base orthorectified image from Google Earth (2023).

Figure 4.83

Reverse particle tracks showing selected pathways with markers for distance travelled between 1 year and 25 years for the prediction model, *Main 1*, with transient simulation under operation of the five production wells between 2022 and 2046.

Document Reference.
FFC-NL-3113-057b

Location
Stephenville, NL

Project No
3113

Date
January 2023

FFC

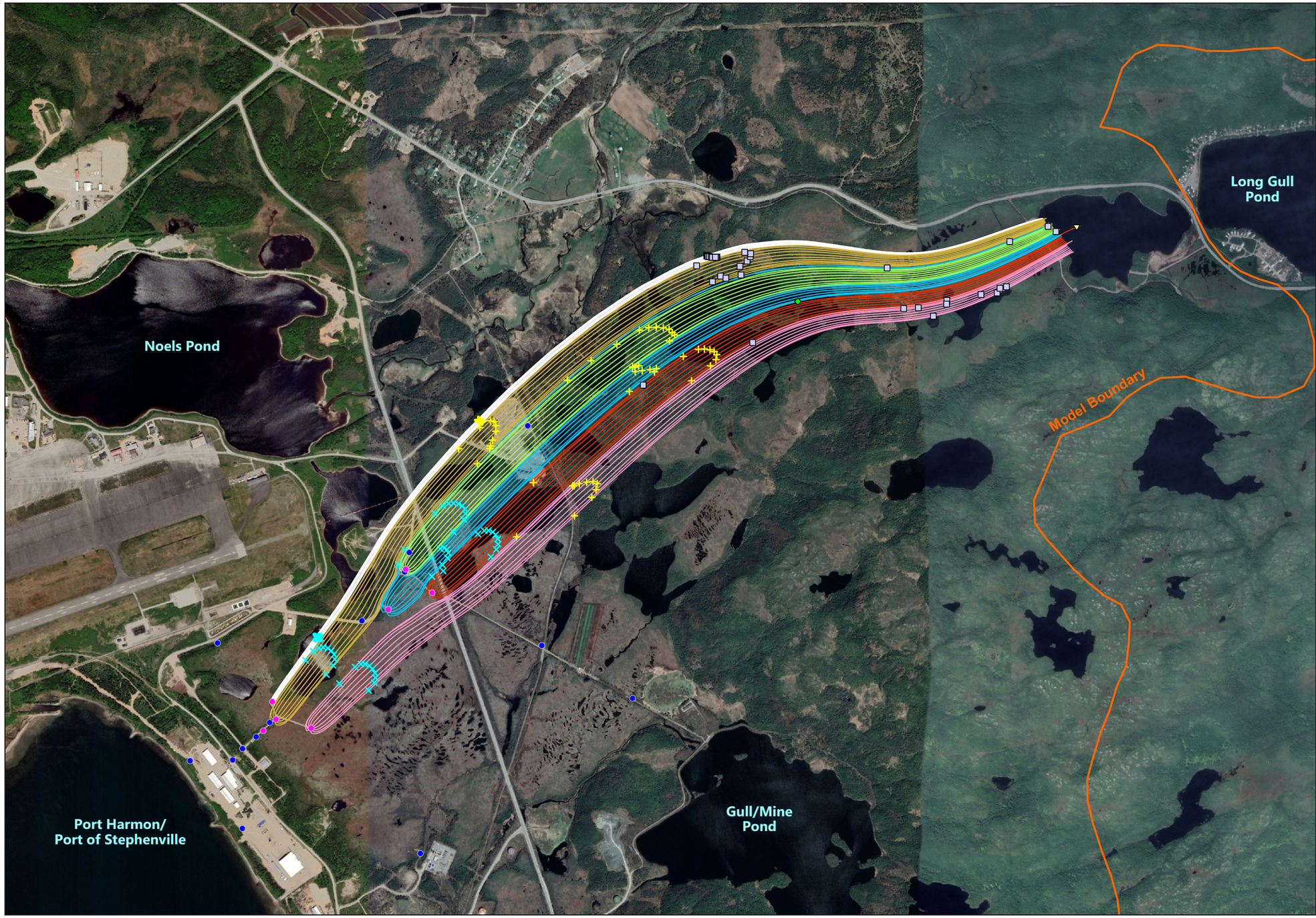

N

Legend

Production well location
Monitoring well location

Marker

1 year
5 years
10 years
15 years
20 years
25 years

0 200 400 600 800

Scale, m

Note: Base orthorectified image from Google Earth (2023).

Figure 4.84

Reverse particle tracks showing selected pathways with markers for distance travelled between 1 year and 25 years for the prediction model, *Main 2*, with transient simulation under operation of the five production wells between 2022 and 2046.

Document Reference.
FFC-NL-3113-057b

Location
Stephenville, NL

Project No
3113

Date
January 2023

FFC

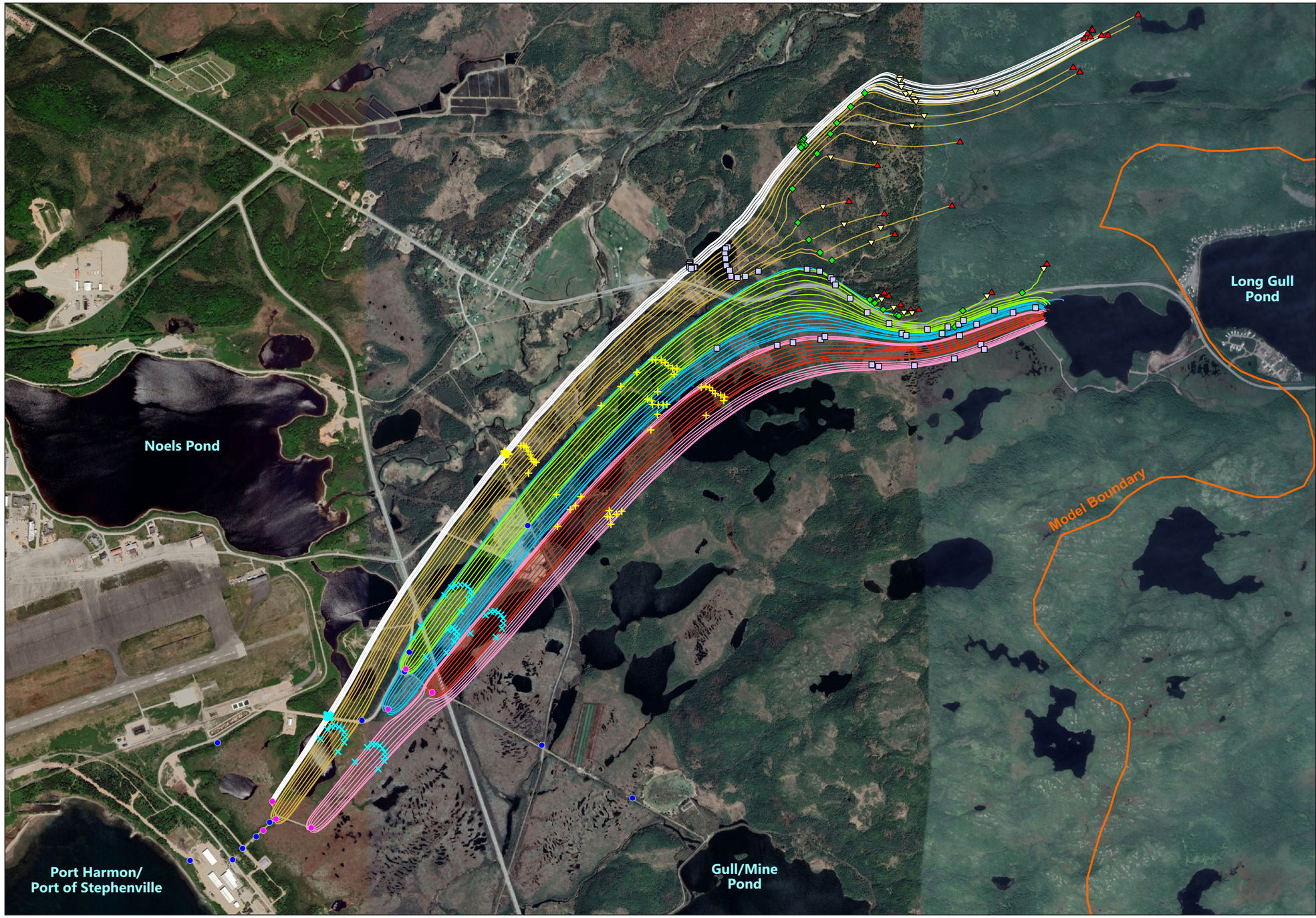

N

Legend

Production well location
Monitoring well location

Marker

1 year
5 years
10 years
15 years
20 years
25 years

0 200 400 600 800

Scale, m

Note: Base orthorectified image from Google Earth (2023).

Figure 4.85

Reverse particle tracks showing selected pathways with markers for distance travelled between 1 year and 25 years for the prediction model, *Upper Limit 1*, with transient simulation under operation of the five production wells between 2022 and 2046.

Document Reference.
FFC-NL-3113-057b

Location
Stephenville, NL

Project No
3113

Date
January 2023

FFC

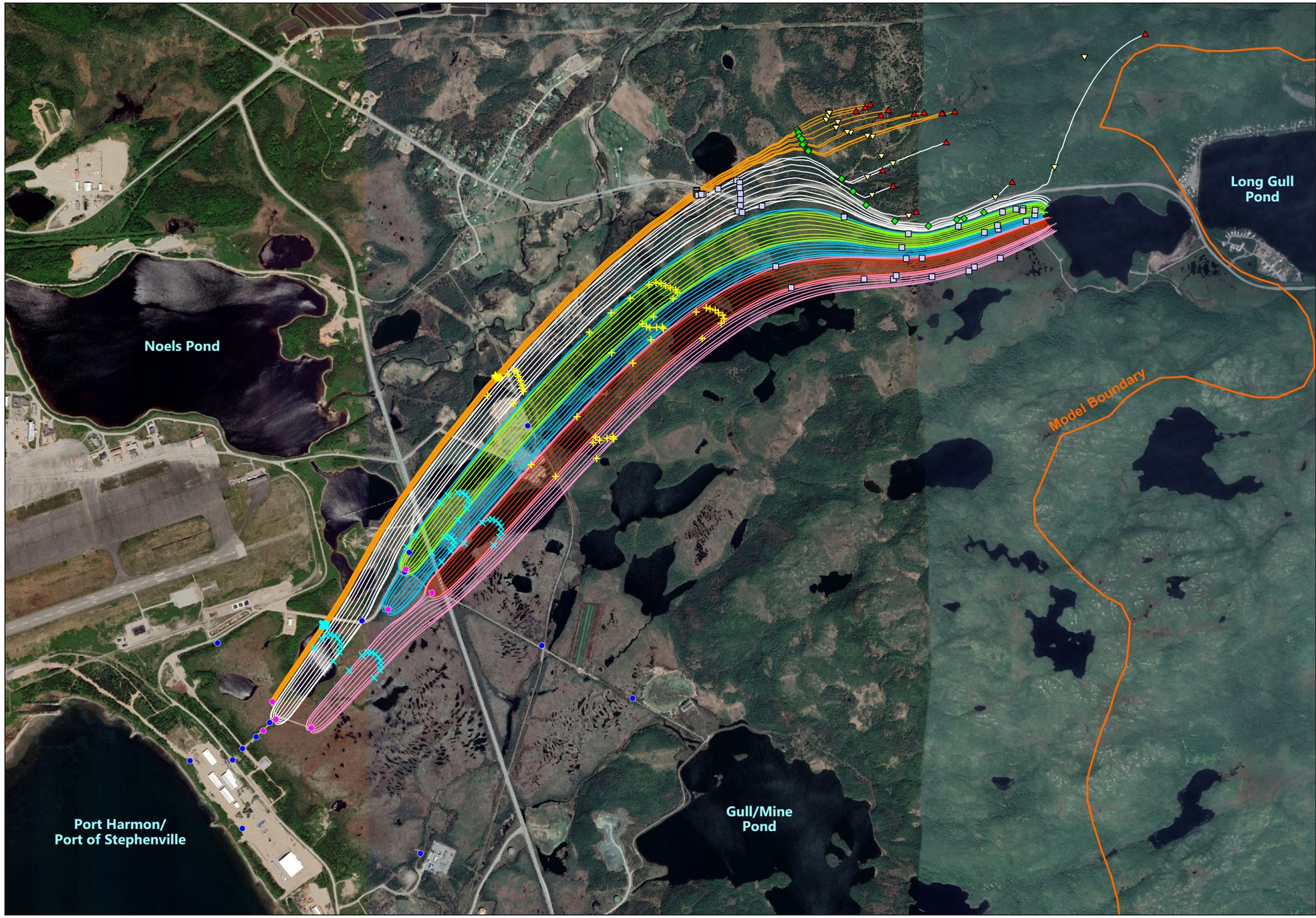

Note: Base orthorectified image from Google Earth (2023).

Figure 4.86

Reverse particle tracks showing selected pathways with markers for distance travelled between 1 year and 25 years for the prediction model, *Upper Limit 2*, with transient simulation under operation of the five production wells between 2022 and 2046.

Document Reference.	FFC-NL-3113-057b
Location	Stephenville, NL
Project No	3113
Date	January 2023

FFC

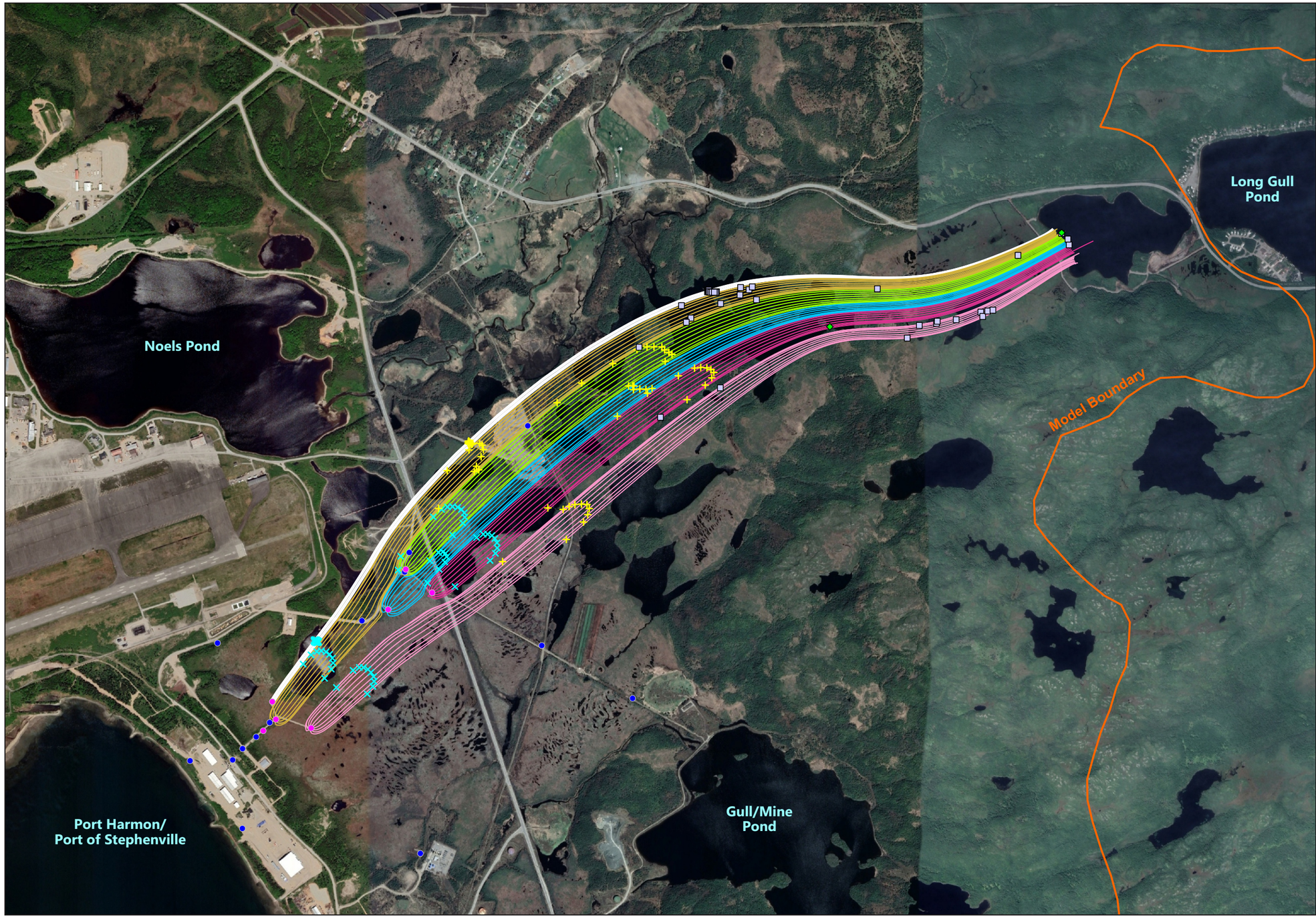

N

Legend

Production well location
Monitoring well location

Marker

1 year
5 years
10 years
15 years
20 years
25 years

0 200 400 600 800

Scale, m

Note: Base orthorectified image from Google Earth (2023).

Figure 4.87

Reverse particle tracks showing selected pathways with markers for distance travelled between 1 year and 25 years for the prediction model, *Lower Limit 1*, with transient simulation under operation of the five production wells between 2022 and 2046.

Document Reference.
FFC-NL-3113-057b

Location
Stephenville, NL

Project No
3113

Date
January 2023

FFC

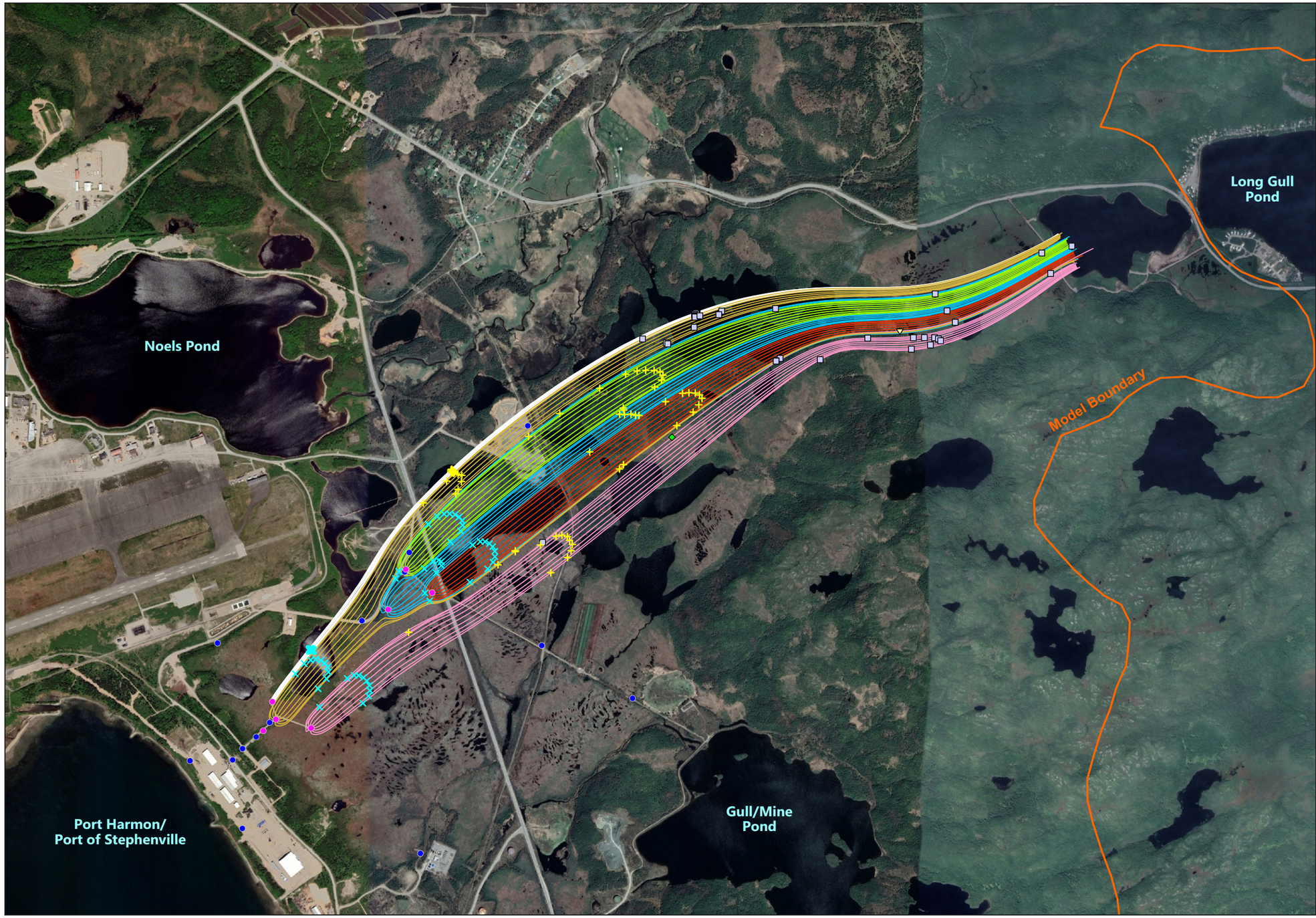

N

Legend

Production well location
Monitoring well location

Marker

1 year
5 years
10 years
15 years
20 years
25 years

0 200 400 600 800

Scale, m

Note: Base orthorectified image from Google Earth (2023).

Figure 4.88

Reverse particle tracks showing selected pathways with markers for distance travelled between 1 year and 25 years for the prediction model, *Lower Limit 2*, with transient simulation under operation of the five production wells between 2022 and 2046.

Document Reference.
FFC-NL-3113-057b

Location
Stephenville, NL

Project No
3113

Date
January 2023

FFC

5.0 CONCLUSIONS AND RECOMMENDATIONS

5.1 Observations and Conclusions

The water elevations were highly correlated with the recharge rate to the aquifer system in the model area. Based on the simulations using the two 25-year precipitation/recharge data sets, the drawdown increased when the recharge values were decreased and the drawdown decreased or the capture area decreased when the recharge increased. This observation was more obvious for the data set with continuous reduction in recharge (*Data Set 2*). With no recovery to the aquifer system, the depletion of the aquifer continued throughout the 25-year simulation period. However, when the recharge increased after a period of decrease as shown in *Data Set 1*, the two well fields responded to the increasing recharge, so the water elevations recovered and en the capture area decreased.

The decreased water elevations (drawdowns) for the current simulations were attributed not only to the pumping of the production wells but also to the reduced recharge values. With the recharge and withdrawal rates changing at the same time, it is difficult to identify which was the controlling factor for the drawdown in the aquifer system. When the withdrawal rates are the main factor in the change of the water elevations and the recharge rates oscillate around their average values with time, the drawdown contours form circular shapes as shown in the results from the *Current Model*. However, when the water elevation changes are mainly due to the changes in recharge rates over the area, the drawdown contours form lines as shown in the contour maps from the *Lower Limit* models. The impacts of the withdrawal rates in those models were shown as bent contour lines around the production wells. The most extreme case among the six sub-data sets was *Lower Limit 2*, showing a drawdown of approximately 5.4 m at the far-field area around BH3. However, the general drawdowns in the two well fields were 2.4 m at the existing well field and 4.4 m at the new well field. The larger drawdowns in the far-field area than those in the near well fields indicate that the drawdowns in the far-field were largely affected by the changes in the overall recharge values. Using the bent contour lines, the drawdowns due to the withdrawals could be extracted from the overall drawdowns. For example, for the worse case of the *Lower Limit 2* model in 2046 (**Figure 4.82**), the general drawdown at the well fields due to the pumping in the production wells would be minimum of 0.4 to 0.6 m. The drawdown would be greater near each production well.

In an in-situ condition, a low permeable layer(s) of silt and clay, was(were) found in a discontinued pattern during the drilling program. However, the 3D numerical model was constructed based on a semi-confined aquifer system with no continuous confining layer throughout the modeled area but a low permeable layer above the main aquifer. Therefore, the simulation of the models showed regional variation in the simulation results. For example, the computed hydraulic heads were lower than the measured heads in the wells at the existing wells, but the computed heads in the wells at the new well field were higher than the measured heads. This indicates that the permeability of the geological layer at the new well field could be less permeable than those at the existing well field, or the recharge rates could be higher in the

existing well field. In addition, the differences in the computed and measured heads were increasing in the area with higher ground elevations. Since replicating the fine details of the in-situ conditions in the 3D numerical model is not possible, during calibration procedures, simulations which provided a better match and less errors in the computed versus measure hydraulic heads were chosen. When a choice needs to be made, the simulation with the calculated heads that were lower than the measured heads was chosen to be consistent as the Worst Case Scenario model simulations.

Due to lack of field data, at the time of model calibration, most of the ponds/lakes were considered to be perched and were not considered to be or assigned as constant head sources. Recent work on several ponds has shown that the water depth in some ponds can be up to 24 m deep and connect directly to the deep water table. If any of the ponds in the capture or recharge areas for the two well fields do not have a low permeability bottom layer of organic pond sediments, recharge from those ponds could reduce the aerial extent of the drawdown cone for each well field.

5.2 Recommendations

The model simulations predict a range of computed responses (essentially a limited probability assessment) for the proposed/predicted future climatic conditions and expected groundwater withdrawals. Therefore, Fracflow proposes that if the measured aquifer drawdowns in 2026 fall within the range predicted by the six prediction models for the 2026 time period (**Table 5.1**), then there would be no need to conduct additional 3D model simulations at that time since this would confirm that the model predictions area a reasonable prediction of the future aquifer responses to pumping/production of the two well fields. For the purposes of comparing measured and computed changes in water levels and determining if the 2026 model simulations match the measured drawdowns, Fracflow proposes that this comparison be based on the two nested deep piezometers in each well field and the two adjacent shallow piezometers for each well field – five reference points (**Table 5.1**) for each well field with the comparison being based on the average precipitation data for both 2025 and 2026 and the recorded withdrawal rates for that two year period that most closely match the precipitation and climate data that were used for the relevant model input data.

Table 5.1 Calculated drawdown for the six prediction models at the water table level and the pumping level in 2026.

			Drawdown at Water Table Level (m)					
Hole ID	**Model X**	**Model Y**	***Main 1***	***Main 2***	***Upper Limit 1***	***Upper Limit 2***	***Lower Limit 1***	***Lower Limit 2***
NSW2-S	302678.9	5378093.4	1.00	1.09	0.52	0.61	1.48	1.57
FishHatch	302549.8	5377969.1	0.65	0.71	0.33	0.39	0.98	1.04
MW2	302502.7	5377915.4	0.52	0.57	0.27	0.32	0.78	0.83
NSW1-S	303322.2	5378810.7	1.70	1.92	0.48	0.71	2.91	3.14
BH2	303344.2	5378903.6	1.61	1.84	0.33	0.57	2.89	3.12
MW1	303118.6	5378578.4	1.42	1.61	0.42	0.61	2.43	2.61

			Drawdown at Pumping Level (m)					
Hole ID	**Model X**	**Model Y**	***Main 1***	***Main 2***	***Upper Limit 1***	***Upper Limit 2***	***Lower Limit 1***	***Lower Limit 2***
NSW2-I	302678.9	5378093.4	1.06	1.15	0.58	0.67	1.54	1.63
FishHatch	302549.8	5377969.1	0.64	0.70	0.32	0.38	0.96	1.02
MW2	302502.7	5377915.4	0.51	0.56	0.26	0.31	0.76	0.81
NSW1-I	303322.2	5378810.7	1.87	2.09	0.65	0.88	3.08	3.30
BH2	303344.2	5378903.6	1.62	1.85	0.34	0.58	2.90	3.13
MW1	303118.6	5378578.4	1.43	1.61	0.42	0.61	2.43	2.61

6.0 REFERENCES

Diersch, H. -J. G., 2005. FEFLOW 5.3 Finite Element - Subsurface Flow and Transport Simulation System. WASY GnbH, Institute for Water Resources Planning and Systems Research, Berlin, Germany.

Environment Canada (ECCC), 2022. Climate Data Online: Stephenville Airport Bulk Data 1942 - 2021, Environment Canada, Ottawa, Canada, www.climate.weather.gc.ca.